AD_____

Award Number: DAMD17-99-1-9352

TITLE: University of Pittsburgh Graduate Training Program in Breast Cancer Biology and Therapy

PRINCIPAL INVESTIGATOR: Olivera J. Finn, Ph.D.

CONTRACTING ORGANIZATION: University of Pittsburgh
Pittsburgh, Pennsylvania 15260

REPORT DATE: September 2001

TYPE OF REPORT: Annual Summary

PREPARED FOR: U.S. Army Medical Research and Materiel Command
Fort Detrick, Maryland 21702-5012

DISTRIBUTION STATEMENT: Approved for Public Release;
Distribution Unlimited

REPORT DOCUMENTATION PAGE

Form Approved
OMB No. 074-0188

1. AGENCY USE ONLY (Leave blank)	2. REPORT DATE	3. REPORT TYPE AND DATES COVERED
	September 2001	Annual (1 Sep 00 - 31 Aug 01)

4. TITLE AND SUBTITLE
University of Pittsburgh Graduate Training Program in Breast Cancer Biology and Therapy

5. FUNDING NUMBERS
DAMD17-99-1-9352

6. AUTHOR(S)
Olivera J. Finn, Ph.D.

7. PERFORMING ORGANIZATION NAME(S) AND ADDRESS(ES)
University of Pittsburgh
Pittsburgh, Pennsylvania 15260

E-Mail: ojfinn@pitt.edu

8. PERFORMING ORGANIZATION REPORT NUMBER

9. SPONSORING / MONITORING AGENCY NAME(S) AND ADDRESS(ES)
U.S. Army Medical Research and Materiel Command
Fort Detrick, Maryland 21702-5012

10. SPONSORING / MONITORING AGENCY REPORT NUMBER

11. SUPPLEMENTARY NOTES

12a. DISTRIBUTION / AVAILABILITY STATEMENT
Approved for Public Release; Distribution Unlimited

12b. DISTRIBUTION CODE

13. Abstract *(Maximum 200 Words)* *(abstract should contain no proprietary or confidential information)*

Our **Graduate Training Program in Breast Cancer Biology and Therapy** is a multidisciplinary approach focused on an important disease. The overall philosophy of our training program is to identify qualified graduate students in the existing discipline-based training programs and to interest and educate them in the unsolved problems in breast cancer.

The specific goals of our Program are: **a)** To recruit qualified predoctoral students to breast cancer related research; **b)** To educate students in the fundamental principles of breast cancer pathobiology and therapy; **c)** To monitor and evaluate the progress of the enrolled students and mentor them in their future career choices; **d)** To organize program activities, such as Seminar Series and Journal Clubs, for increased interaction of the student trainees with postdoctoral fellows and faculty interested in breast cancer.

We have completed the second year of the training program in which we have closely followed our specific goals. Eight students were trained in the second year. Four students have graduated and obtained their PhD degrees, three students are anticipating graduation soon and will be supported through other funds during the writing of their thesies. Five new students were selected and started their fellowships on September 1, 2001.

14. SUBJECT TERMS
Graduate students, doctoral thesis, breast cancer, genetics

15. NUMBER OF PAGES
148

16. PRICE CODE

17. SECURITY CLASSIFICATION OF REPORT	18. SECURITY CLASSIFICATION OF THIS PAGE	19. SECURITY CLASSIFICATION OF ABSTRACT	20. LIMITATION OF ABSTRACT
Unclassified	Unclassified	Unclassified	Unlimited

TABLE OF CONTENTS

INTRODUCTION

Our **Graduate Training Program in Breast Cancer Biology and Therapy** is a multidisciplinary approach focused on an important disease. The overall philosophy of our training program is to identify qualified graduate students in the existing discipline-based training programs and to interest and educate them in the unsolved problems in breast cancer. By raising their interest and providing them with financial help, we encourage them to apply the tools of their individual disciplines in search of solutions to breast cancer-related problems. Our Training Program intends to expand the existing pool of investigators studying breast cancer. The Program also strives to encourage many of our faculty members, by including them into the list of Program Faculty and by providing support for their graduate students, to focus their research effort at least in part on breast cancer. This is an important programmatic by-product because it takes ongoing interdisciplinary research effort by an array of well-funded investigators and directs it towards the problems of breast cancer.

The specific goals of our Program are:

a) To recruit qualified predoctoral students to breast cancer related research.

b) To educate students in the fundamental principles of breast cancer pathobiology and therapy.

c) To monitor and evaluate the progress of the enrolled students and mentor them in their future career choices.

d) To organize program activities, such as Seminar Series and Journal Clubs, for increased interaction of the student trainees with postdoctoral fellows and faculty interested in breast cancer.

We have completed the second year of the training program in which we have closely followed our specific goals.

BODY (ANNUAL SUMMARY)

Progress in Trainee Recruitment

In the first two years of the grant we trained a total of seven students. Six were initially appointed and when two graduated in mid-year, several months earlier than expected, we funded one additional student for the last few months of his work before graduation, and awarded support to a new trainee. Of the total of eight trainees funded during the time covered by this progress report, 5 have obtained their PhD degrees, one is currently on the grant and two are continuing in their last year but funded by other sources. In the early spring, in anticipation of early graduations, and again in June, July and August, we carried out nomination, competition and selection for the second group of trainees to be funded in the last two years of the grant. All training faculty, as well as the community at large, received an electronically transmitted letter informing them of the program and requesting trainee nominations. Applications were submitted also electronically and evaluated by the **Breast Cancer Training Grant Executive Committee**. The current committee members are Drs. Finn, Lazo, Morris and Latimer. Applicants were judged based on their performance in the first and second year of graduate school, faculty comments, and a brief written statement of their research interest as related to breast cancer. An effort was made to ensure equitable distribution of fellowships among multiple disciplines and areas of research. Five new students were selected to receive funding, four starting September 1, 2001 and the fifth January 1, 2002.

Progress in Trainee Education and Monitoring of Progress:

Inasmuch as the students supported by this training grant belong to various graduate programs, the formal course work requirements and credits of dissertation research are

determined by their individual programs. **The Training Program in Breast Cancer Biology and Therapy** requires that the students complete an Ethics course offered by the University and attend the weekly conference on Breast Cancer Biology and Therapy organized every Thursday afternoon by Dr. Jean Latimer. Each student is required to present a seminar in this series at least once during the two year period of support under the training grant..The Program Director, Dr. Finn, monitors all seminars campus wide and alerts the trainees to those of special interest to breast cancer.

Progress in Organizing Program Activities

In addition to several established seminar series that our trainees attend, .in the Spring 2001, the Magee Research Institute of the University of Pittsburgh and the University of Pittsburgh Cancer Institute Breast Program organized a series of monthly Debates on Breast Cancer Care (see Appendix), attendance to which was required of the trainees..

Research Accomplishments from 9/1/2000 until 8/31/2001

Ying Jiang (Dr. Joseph Glorioso III, advisor), Department of Human Genetics, Graduate Program in Molecular Biology. Herpes simplex virus (HSV) represents a promising vector for gene therapy for breast cancer and other solid tumors. The focus of this study is on the promoter region of a promiscuous HSV transactivator, ICP0. 5'- truncation mutants covering -1 to -564 of the ICP0 promoter have been constructed preceding the LacZ reporter gene. This panel of ICP0 promoter reporter vectors also contains the HCMV IE promoter driving GFP in the ICP27 locus that serves as an internal control. In vivo experiments are now underway to investigate the long term effects of the deletions in the promoter region on the expression of ICP0.

No publication has been submitted. Even though progress appears satisfactory, because of lack of publications a decision was made not to extend funding of this trainee beyond the intial two-year committment.

Michael Forlenza (Dr. Andrew Baum, advisor), Department of Psychiatry, Division of Behavioral Medicine and Oncology. Previous research had shown that lymphocytes of high-distress patients have reduced DNA repair. Deficits in repair are associated with an increased risk of cancer. Using and academic stress model, it was hypothesized that students would exhibit lower levels of Nucleotide Excision Repair (NER) during a stressful exam period when compared to a lower stress period. Contrary to prediction, mean values for NER significantly increased during the higher stress period relative to the lower stress period. Furthermore, lymphocytes had significantly increased repair of endogenous damage during the higher stress period. Stress appears to directly increase DNA repair. Additionally, stress may increase DNA repair indirectly by increasing damage to DNA. A study is in progress testing whether stress experienced by breast cancer patients may directly affect DNA repair and treatment outcome.

Published and in press articles or chapters (author or co-author) during the second grant year:

1. Nazir T., Flowers L., Forlenza M., Dimsdale J., Kanbour-Shakir A., Grant S.G., Latimer J.J. Tissue specificity of DNA repair capacity in normal human breast and ovarian epithelium. *The Breast Journal (submitted)*

2. Forlenza, M. J., & Baum, A. (*in press*). Psychoneuroimmunology in (Eds.) Handbook of Health Psychology, Volume 1. APA, Washington, DC.

3. Forlenza, M. J. (*2001*). Aging, Immunity, and Cancer. Cancer Control: Journal of the Moffitt Cancer Center, 8 (3), 288-289.

4. Forlenza, M. J., & Baum, A. (2000). Psychosocial Influences on Cancer Progression: Alternative Cellular and Molecular Mechanisms. Current Opinions in Psychiatry, 13 (6), 639-645.

5. Forlenza, M. J., Latimer, J. J. & Baum, A. (2000). The Effects of Stress on DNA Repair. Psychology and Health: An International Journal, 15, 881-981.

Presentations (author or co-author) during this academic year:

1. Biobehavioral Influences on Cancer: Alternative Cellular & Molecular Mechanisms: Poster presented at the 13th Annual Scientific Retreat

2. Psychoneuroimmunology in Cancer Prevention: Invited talk for Psychosocial Approaches to Cancer Prevention Conference sponsored by Fox Chase Cancer Center

This student was also awarded Directors Award for Scientific Excellence & Potential – UPCI Scientific Retreat, June 2001.

Michael Forlenza's fellowship ends 12/31/2001..

Nina Joshi (Dr. Jeanne Latimer and Dr. Steven Grant, co-advisors), Department of Epidemiology, Program in Molecular Toxicology. Ms. Joshi continues to identify a model to examine the mitogen/mutagen hypothesis. She has extended her analysis to include cell stimulation and mutagenic effects from tamoxifen and its metabolites. This research holds a special relevance to breast cancer. The cause of the increase in endometrial cancer observed in breast cancer patients treated with tamoxifen is currently under debate. To determine the mutagenic effect of tamoxifen and its metabolites both the TK-6, a lymphoblastoid cell line, and the Ishikawa, an endometrial cell line, were employed. Tamoxifen exposure in TK6 and Ishikawa cells to concentrations of 0.01 μM to 1 μM, did not increase the mutational frequency at the HPRT locus. However, exposure to 4-hydroxy tamoxifen statistically significantly increased ($p=0.001$) the mutation frequency in TK-6 cells over controls at a concentration of 10 μM. There was no indication that 4 hydroxy tamoxifen increased cell proliferation, suggesting a direct mutagenic effect. These results have important implications for breast cancer patients and more importantly for women at high risk of developing breast cancer that have most recently been placed on tamoxifen treatment.

Abstracts

Grant, S., **Joshi, N.** (2001). Variable hypermutability in chromosomally unstable endometrial and breast tumor cell lines. *Proceedings from the American Association for Cancer Research.* 42: 904.

Joshi, N, Grant, S. (2001). Mutagenic potential of 4-hydroxytamoxifen, an activated metabolite of tamoxifen, in human lymphoblast and endometrial tumor cell lines. *Proceedings from the American Association for Cancer Research.* 42:471.

Joshi, N., Grant, S., Kisin, E., Draper, D., Latimer, J. (1999). Generation and characterization of primary endometrial explant cultures. *The 50th Anniversary Symposium of the Graduate School of Public Health*, University of Pittsburgh, PA.

Joshi, N., Grant, S., Kisin, E., Draper, D., Latimer, J. (1999). Establishment of primary endometrial explant cultures. *University of Pittsburgh Cancer Institute Symposium*, Johnstown, PA

Even though progress has been judged superior, due to lack of publications Ms. Joshi's funding was not extended beyond 8/31/2001.

Melina Soares (Dr. Olivera Finn, advisor), Department of Molecular Genetics and Biochemistry, Graduate Immunology Program. Epithelial cell mucin (MUC1) is expressed on ductal epithelial surfaces of breast, pancreatic, colon and several other tissues and on tumors arising from these tissues. In the MUC1 Tg. mouse, human MUC1 is expressed under the control of endogenous promoter and its tissue distribution is similar to that seen in humans. This project investigated whether tumor responses elicited by immunization result in autoimmune destruction of MUC1-expressing tissues. Tumor rejection correlated with the induction of MUC1-specific CD8+ T cells and did not result in autoimmunity. When mice were immunized with MUC1-peptide PLGA microspheres, both MUC1-specific CD4+ and CD8+ T cells were elicited. No autoimmunity was detected. This shows that MUC1 tumor vaccine is both safe and effective.

Dr. Soares successfully defended her thesis on April 16, 2001. Her present position is as a Postdoctoral Research Fellow, Simmons Cancer Center, UT Southwestern Medical Center, Dallas, TX.

Published and in press articles or chapters (author or co-author) during the second grant year:

1. Soares M., Mehta V., and Finn OJ. Three Different Vaccines Based on the 140-Amino Acid MUC1 Peptide with Seven Tandemly Repeated Tumor-Specific Epitopes Elicit Distinct Immune Effector Mechanisms in Wild-Type Versus MUC1-Transgenic Mice with Different Potential for Tumor Rejection . *J Immunol* 166: 6555-6563 (2001).
2. Soares M. Hanisch FG. **Finn** OJ. Ciborowski P. Recombinant human tumor antigen MUC1 expressed in insect cells:structure and immunogenicity. *Protein Expression & Purification. 22(1):92-100 (2001).*
3. Soares, M. Immunogenecity, Tumor Rejection Potential and Safety of MUC1 Cancer Vaccines in Transgenic Mouse Models., Ph.D. Thesis, 2001.

Oral presentations:

Annual Meeting of the American Association of Immunologists, Orlando, FL, April 2001.

Pao-Hsiu (Tracy) Chen (Dr. Billy Day, advisor), Program in Molecular Toxicology. Previous research has shown that components from marine algae could be protective or used as treatments against human tumors. Curacin A is an antimitotic agent with unique properties that has previously been determined to act at the colchicine site of tubulin. In one component of a multiparameter high content screening (HCS) technique, Curacin A's unique effects on the microtubule (MT) cytoskeleton were revealed. HCS also showed that curacin A modulated the normal regulation of kinase-mediated stress pathways and nuclear morphology within the same population of cells. Curacin A caused concentration-dependent increases in the activation of three MAPK pathways measured as increased phosphorylation of three key pathway intermediates, RSK1, p38MAPK and c-Jun. The results show that MEK1 inhibition combined with a colchicine site MT perturbing agent lead to triggering of calpain and caspase actions and suggest potential apoptosis-enhancing combination therapies.

Dr. Chen successfully defended her Ph.D thesis June 15. She is currently a Research Associate in the Department of Surgery, University of Pittsburgh School of Medicine.

Published and in press articles or chapters (author or co-author) during the second grant year:

1. Chen, P.-H., Guiliano, K.A., Grant, S.G., Day, B.W., Panetta, C.J. A mathematical model of in vitro cancer cell growth and treatment with the antimitotic agent curacin A. Math. Biosci. 170:1-16, 2001.
2. Chen, P.-H., Guiliano, K.A., Vogt, A., Wipf, P., Day, B.W. Moecular and morphological effects of curacin A on PC-3 human prostate carcinoma cells-MEK1 inhibition enhances caspase/calpain actions. Submitted.

Henry Kao (Dr. Olivera J. Finn, advisor), Graduate Program in Immunology. Successful immunotherapy of tumors relies in part on the identification of tumor antigens. This project designed and tested a new method for tumor antigen discovery. It involved extracting peptides from tumor HLA class I molecules, fractionating by RP-HPLC and loading onto dendritic cells to prime naive CD8+ T cells. Fractions that supported growth of tumor-specific CTLs were sequenced by electrospray ionization tandem mass spectrometry. One fraction yielded six peptides homologous to the human cyclin B1. These results illustrate a) a novel approach to tumor antigen discovery based on the in vitro priming of naive T cells with dendritic cells, and b) the identification of cyclin B1 as a shared tumor-associated antigen.

Dr. Kao successfully defended his Ph.D. thesis in March 2001. He is currently a Research Associate in the Department of Pathology, Washington University School of Medicine, St. Louis, MS.

Published and in press articles or chapters (author or co-author) during the second grant year:

1. Kao, H., Amoscato, A.A., Ciborowski, P., and Finn, O.J. 2001. A New Strategy for Tumor Antigen Discovery Based on In Vitro Priming of Naive T Cells with Dendritic Cells. *Clinical Cancer Research* 7 (Suppl):773s-780s
2. Kao, H., Marto, J.A., Hoffman, T.K., Shabanowitz, J., Finkelstein, S.D., Whiteside, T.L., Hunt, D.F., Finn, O.J. Identification of cyclin B1 as a shared human epithelial tumor-associated antigen recognized by T cells. In press.

Poster presentations:

Annual Meeting of the American Association of Immunologists, Orlando, FL, April 2001.

Patent Application:

"Anticancer vaccine and diagnostic methods and reagents", filed 9/25/2001.

Michel Gray (Dr. Sidney Morris, advisor), Molecular Biology Program. This student was reviewed in the first round of nominations. When Vivian Liu graduated a year earlier than expected, we awarded the fellowship to Michael, starting 5/1/2001

...

Yadi Tan (Dr. Leif Huang, advisor), Molecular Pharmacology Program. This student was reviewed in the first round of nominations. When Henry Kao graduated five months earlier than expected, we awarded the remainder to Yadi for the last five months of her research in gene therapy of cancer. Yadi defended her Ph.D. thesis in August 2001.

APPENDIX TO THE SUMMARY

1) Key research accomplishments:

- Further progress was made on the generation of a Herpes Virus (HSV) vector for use in gene therapy.
- Anew study was initiated in breast cancer patients to evaluate if stress increases rather than decreases DNA repair.
- Tamoxifen and its metaboloites were evaluated for their mutagenic effects and found to be risk factors for development of cancer.
- MUC1 based breast cancer vaccines were found to be safe and effective in transgenic mouse models with relevance to human situation.
- A component from marine algae was evaluated in the laboratory as treatment against breast cancer and its action was determined to be through induction of apoptosis of tumor cells.
- Methods were developed to use non-viral vectors for delivery of therapeutic genes into tumors without causing inflammation.
- A new tumor antigen was discovered, cyclin B1, and a whole family of cyclins was implicated in eliciting tumor specific immunity

2) Reportable outcomes

- Four trainees obtained their Ph.D. degrees in 2001 and obtained academic research positions.
- Seven papers were published, authored or co-authored by the trainees.
- Four Ph.D. theses were published.
- Two papers are in press.
- A patent application "Anticancer Vaccine and Diagnostic Methods and Reagents" was filed September 23, 2001.

3) Three copies of the above published and in press manuscripts are included.

Debates in Breast Cancer Care

Sponsored by the

Magee/UPCI Breast Program
of
Magee-Womens Hospital and
University of Pittsburgh Cancer Institute
and
University of Pittsburgh Center for
Continuing Education in the Heath Sciences

PROGRAM INTENT:
Debaters will vigorously defend a position with support from the literature. After both presenters have completed their brief presentation the floor is open for rebuttal and discussion. The goal is not to solve the dilemma, but to understand the rationale behind the different positions. At the close of the program, participants should be able to describe opposing perspectives in breast cancer management issues.

LOCATION:
The *Debates in Breast Cancer Care* is held at 4:00 PM on the first Thursday of each month, following the Breast Care Consultation Center conference, in the Magee-Womens Hospital Clinic Conference Room. Interested health care professionals are invited to attend the Magee/UPCI weekly breast cancer multidisciplinary conference at 3:00 PM in addition to the Debates in Breast Cancer Care Program.

WHO SHOULD ATTEND
This program is designed for healthcare professionals interested in the management of breast cancer. ©We encourage participation by all individuals. If you have a disability, advance notification of any special needs will help us serve you. Please notify us of your needs at least two weeks in advance of the program.

REGISTRATION INFORMATION
The program is offered at no cost to all interested healthcare professionals. Pre-registration is not required.

CONTINUING EDUCATION CREDITS
The University of Pittsburgh School of Medicine, as part of the Consortium for Academic Continuing Medical Education, is accredited by the Accreditation Council for Continuing Medical Education to sponsor continuing medical education for physicians.

The Center for Continuing Education in the Health Sciences designates this continuing medical education activity for a maximum of 1.0 hours of Category 1 credit toward the AMA Physician's Recognition Award. Each physician should claim only those hours of credit that he/she actually spent in the educational activity.

Other healthcare professionals are awarded 0.1 continuing education units (CEU's).

COURSE DIRECTOR
Ronald R. Johnson, MD
Magee-Womens Surgical Associates
Magee-Womens Hospital
300 Halket Street, Pittsburgh, PA 15213-3180
Phone: 412-641-1400
email: rjohnson@magee.edu

FACULTY
The course director and program faculty are affiliated with the University of Pittsburgh School of Medicine, unless indicated otherwise.

In accordance with Accreditation Council for Continuing Medical Education requirements on disclosure, information about relationships of presenters with commercial interests (if any) will be included in materials distributed at the time of the conference.

CALENDAR:

March 1, 2001 Screening Mammography
- The case for annual screening in women under age 50 ... *L. Hardesty, MD*
- Unproven survival benefits in pre-menopausal women ... *M. Ganott, MD*

April 5, 2001 Surgery
- Operations for breast cancer should be timed to a patient's menstrual cycle ... *J. Kelley, MD*
- This job is hard enough without timing operations for unproven benefits ... *M. Bonaventura, MD*

June 14, 2001 Survival Improvements
- Early detection accounts for the majority of the improvement in breast cancer survival ... *W. Poller, MD*
- Treatment is getting better. The case for the impact of systemic therapies ... *A. Brufsky, MD, PhD*

July 12, 2001 Neoadjuvant Chemotherapy
- A "diamond in the rough" which is losing its luster ... *R. Johnson, MD*
- A vitally important strategy in the care of Stage II breast cancer patients ... *J. Kelley, MD*

August 2, 2001 DCIS
- Total mastectomy is the preferred treatment for all but a select subset ... *D. Keenan, MD, PhD*
- BCT is appropriate for the majority of cases ... *R. Johnson, MD*

September -- cancelled

October 4, 2001 Mediocolegal Aspects
- Predicting metastases is a function of time...and delay in diagnosis hurts ... V. Vogel, MD, MHS
- "No harm ... No Foul" Minor delay in diagnosis affect prognosis only in some circumstances ... K McCarty, MD, PhD

November 1, 2001 Sequencing Treatment
- Chemoendocrine interventions should precede RT in the majority of cases ... *J. Baar, MD, PhD*
- Optimizing local control. The case for early delivery of RT ... *D. Herron, MD*

December 6, 2001 Breast Cancer in the Elderly
- Non-surgical management of the elderly or "let it be" ... *V. Vogel, MD, MHS*
- Non-surgical therapy of elderly patients is denying potentially curative treatment ... *J. Falk, MD*

January 3, 2002 Chemotherapy
- Dose-intensity Chemotherapy ... *B. Lembersky, MD*
- Dose-density Chemotherapy ... *A. Brufsky, MD, PhD*

February 7, 2002 Sentinel Lymphatic Mapping
- "Sentinel" is the first node, not the first six, seven or eight ... *G. Trucco, MD*
- The importance of identifying all sentinel nodes in the prevention of false negative results ... *H. Edington, MD, MBA*

March 7, 2002 Occult Breast Cancer
- "The prognosis of patients with Stage N1a disease is similar to that of patients with Stage pN0 disease" AJCC ... *S. Silver, MD, PhD*
- Microscopic nodal disease identifies a subset of node positive patients whose prognosis is between that of pN0 and pN1 ... *to be announced*

April 4, 2002 Biostatistics
- "Meta-analysis" allows small but significant improvements in patient care to be available ... *B. Lembersky, MD*
- Focus on mediocrity. How metanalyses hurt breast cancer care ... *R. Johnson, MD*

May 2, 2002 Breast Cancer Risk
- Therapeutic and spontaneous abortion contribute significantly to breast cancer risk ... *Surgical Oncology Fellow*
- Liars, worse liars, and statisticians — the evidence is unclear and the clinical relevance is negligible ... *Medical Oncology Fellow*

June 6, 2002 Diagnosis
- Identifying breast cancer without X-rays...the future of early diagnosis ... *J. Sumkin, DO*
- From the HIP study to the present ... mammography remains the only proven screening method for breast cancer ... *W. Poller, MD*

Teach

Get Acrobat Reader

Workshops: Monthly Workshops at the University of Pittsburgh

- General information
- Registration Form PDF / HTML

SCHEDULE FOR 2001-2002

The following is a listing of the monthly workshops we will offer at the University of Pittsburgh in 2001-2002.

FALL 2001

SEPTEMBER 15: Training for Success!

The topics addressed in this workshop include taking charge of your own training: developing a training plan, selecting a research project, finding mentors, and managing time and stress. Special break-out sessions will focus on issues specific to graduate students (e.g., comprehensive exam, thesis) and postdoctoral fellows (i.e., moving toward an independent position).

OCTOBER 6: Making Oral Presentations

Participants will learn about the standard organization of a research seminar, then be provided with a step-by-step plan for developing a presentation. Techniques of delivery will be covered, including information on dealing with stage fright and strategies for non-native speakers of English. Also covered will be the design and use of visual aids, and other types of oral presentations, including poster presentations and "job talks." Individuals will have the option of participating in a mini-practicum on oral presentations.

NOVEMBER 3: Teaching

Participants will learn about the process of developing and teaching a course, from start to finish. Issues of course design to be covered include selecting a text book, developing a syllabus, establishing a grading policy and ground rules, and designing exams. Individuals will also hear about strategies for lecturing and leading discussions, accommodating individual differences in the classroom, and balancing teaching and research.

DECEMBER 1: Advancing in Your Career

This workshop will cover the basics of getting promoted in both academia and industry, and will discuss the critical variables for success. Learn about hiring, supervising, and mentoring staff and students. Participants may attend break-out sessions on conflict management and a mock tenure review.

SPRING 2002

JANUARY 12: Writing Research Articles

This workshop will provide information on the anatomy of a research article, as well as a step-by-step method for moving from the conception of an idea through to the printed research article. Strategies for dealing with common problems - such as writer's block - will be covered. Breakout sessions will allow participants to gain experience in editing text or designing effective tables and figures.

FEBRUARY 9: Grantspersonship : FREE

The morning plenary session will cover the essentials of writing grant applications including topics such as identifying funding sources, components of successful grant applications, the process of writing and submitting and application, and responding to reviewers' criticisms. The afternoon is comprised of a series of break-out sessions providing information specific to a given funding agency. Sessions will be led by individuals who have experience serving as reviewers for organizations including the National Institutes of Health, National Science Foundation, Department of Defense, private foundations, and more.

MARCH 16: Job Hunting

This workshop will provide an overview of the process of job hunting, covering topics including doing a personal skills inventory, targeting the job market, developing the essential skill of networking, designing an "employment package" (curriculum vita or resume, statement of interests, and supporting materials), getting good letters of recommendation, and interviewing for a position. Individuals at all stages of their career are encouraged to attend, including persons who may be years away from finishing their training, since the information provided can help you tailor your training for success in the position you desire. Participants of this workshop may also find it beneficial to attend the workshop on career options.

April 6: Career Options

Learn about a broad range of career options available to individuals receiving training in research. Outside speakers will present information on a large number of options, including research in industry, college teaching, science law, publishing, and administration, any many other types of positions. The modular format of this workshop will allow participants to tailor the event to fit their specific interests. Participants of this workshop may also find it beneficial to attend the workshop on job hunting.

ELSEVIER

Mathematical Biosciences 170 (2001) 1–16

Mathematical Biosciences

www.elsevier.com/locate/mbs

A mathematical model of in vitro cancer cell growth and treatment with the antimitotic agent curacin A

Frank Kozusko [a], Pao-Hsiu Chen [b], Stephen G. Grant [b,c,d], Billy W. Day [b,d,e,1], John Carl Panetta [f,*,2]

[a] *Department of Mathematics, Hampton University, Hampton, VA 23668, USA*
[b] *Department of Environmental & Occupational Health, University of Pittsburgh, Pittsburgh PA 15238, USA*
[c] *Department of Obstetrics Gynecology & Reproductive Sciences of the Magee-Womens Research Institute, University of Pittsburgh, Pittsburgh, PA 15238, USA*
[d] *University of Pittsburgh Cancer Institute, University of Pittsburgh, Pittsburgh, PA 15238, USA*
[e] *Department of Pharmaceutical Sciences, University of Pittsburgh, Pittsburgh, PA 15238, USA*
[f] *Pharmaceutical Sciences Department, St. Jude Children's Research Hospital, 332 North Lauderdale St., Memphis, TN 38105-2794, USA*

Received 9 June 2000; received in revised form 5 December 2000; accepted 6 December 2000

Abstract

A mathematical model of cancer cell growth and response to treatment with the experimental antimitotic agent curacin A is presented. Rate parameters for the untreated growth of MCF-7/LY2 breast cancer and A2780 ovarian cell lines are determined from in vitro growth studies. Subsequent growth studies following treatments with 2.5, 25 and 50 nanomolar (nM), concentrations of curacin A are used to determine effects on the cell cycle and cell viability. The model's system of ordinary differential equations yields an approximate analytical solution which predicts the minimum concentration necessary to prevent growth. The model shows that cell growth is arrested when the apoptotic rate is greater than the mitotic rate and that the S-phase transition rate acts to amplify this effect. Analysis of the data suggests that curacin A is rapidly absorbed into both cell lines causing an increase in the S-phase transition and a decrease in the M-phase transition. The model also indicates that the rate of apoptosis remains virtually constant for MCF-7/LY2 while that of A2780 increases 38% at 2.5 nM and 59% at 50 nM as compared to the untreated apoptotic rate.

Keywords: Cell cycle phase-specific chemotherapy; Curacin A; Pharmacodynamic models; Antimitotic drugs; Apoptosis

* Corresponding author. Tel.: +1-901 495 3172; fax: +1-901 525 6869.
E-mail address: carl.panetta@stjude.org (J.C. Panetta).

[1] Supported by NIH grant CA78039.
[2] Supported by Cancer Center CORE Grant CA21765, a Center of Excellence grant from the State of Tennessee, and the American Lebanese Syrian Associated Charities (ALSAC).

PII: S0025-5564(00)00065-1

1. Introduction

A consistent mathematical model of in vitro cancer cell growth and response to chemotherapeutic drugs can be beneficial in two ways. First, it can be used to extend and interpret in vitro studies. Second, it can be the foundation of the pharmacodynamic modeling of drug response in the body. Therefore, we develop a mathematical model of the effects of the cell cycle phase-specific agent curacin A (a new experimental agent currently under investigation) in vitro. We then use this model to help understand and describe the dynamics of curacin A.

First, to understand the effects of cell cycle phase-specific agents we need to have an understanding of the cell cycle. Fig. 1 gives a basic diagram of the cell cycle where the phases of the cell cycle are described as follows. In G1-phase (the first gap phase), the cell prepares for DNA synthesis. In S-phase, the DNA is synthesized. In G2-phase (the second gap phase), the cell prepares for mitosis. In M-phase (the mitotic phase) the cell splits into two daughter cells. This cycle, $G1 \rightarrow S \rightarrow G2 \rightarrow M \rightarrow G1$, represents the active growth phase while the G0-phase represents the resting stage where the cells are viable but not actively transiting the cell cycle. Several models have been developed to describe the effects of chemotherapeutic drugs on the active portion of the cell cycle [1–3] as well as the drug's effects on both the active and the resting phase [4,5].

As noted above, curacin A is an experimental agent currently under investigation for potential activity via in vitro studies. This first required step in drug development is qualitatively different from later in vivo steps. These differences include the fact that in vitro studies are designed so that the cell lines grow in log phase (exponentially) and therefore do not have a large G0-phase since the growth media has ample nutrition and oxygen. Future in vivo studies drop the assumption of exponential growth and non-linear growth patterns such as Gompertz growth or models described in [4,5] are implemented.

Here, we specifically model the antimitotic (M-phase) agent curacin A which interferes with the cells' microtubule dynamics and prevents completion of mitosis. This results in an accumulation of cells in the M-phase. Examples of other M-phase agents include the drugs paclitaxel and vinblastine, of which we have previously modeled the effects of paclitaxel on breast and ovarian cancer [6]. In the present modeling process we quantitatively describe the effects curacin A has in vitro on the cell cycle including how the agent affects the cell cycle and apoptosis. The model is also used to mechanistically describe the pharmacodynamics of the agent on two different cell

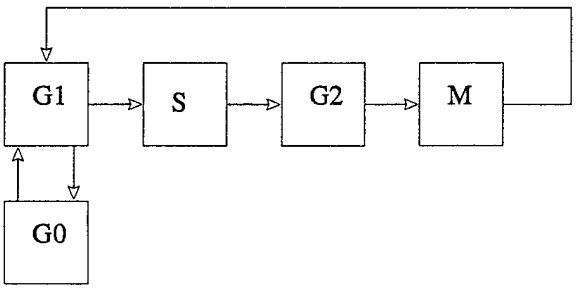

Fig. 1. The cell cycle.

lines including calculations of 50% growth inhibitory concentrations (IC_{50}) and maximal effective dose.

2. The model

The model presented here is a modification and extension of our previous work [5,6]. First, we describe in vitro growth and then add terms that indicate the drug effects. Terms in the model are derived from either known mechanisms of the cell cycle or are hypothesized from experimentally observed results.

2.1. Model of in vitro cell growth

We make several assumptions in the development of the model. (1) The in vitro growth medium is constant. This allows us to assume that the phase transition rate coefficients are constant and thus the cells are growing at a fixed rate. (2) There are no G0-phase cells. This assumption is based on the fact that in the in vitro setting there is an abundance of nutrient to keep the cells in the active growth phase. (3) The model groups the G1- and S-phases into one compartment and the G2- and M-phases into a second compartment. These groupings are based on the fact that we collected data on the flow cytometer, which determines the cell-cycle distribution, in a way that groups G2- and M-phase together. Also, the grouping of G1- and S-phases is for simplicity, though separating them does not qualitatively change the model.

The in vitro growth model is depicted in Fig. 2. s and m represents the population of cells in the G1/S and the G2/M compartments, with initial values s_0 and m_0, respectively. The transition rate coefficients are: α, the rate of s-phase cells transitioning to m-phase cells; β, the rate of m-phase cells dividing to form two s-phase cells; and, η, the rate of m-phase cells transitioning through apoptosis – programmed cell death. The model equations are

$$\dot{s} = -\alpha s + 2\beta m, \quad s(0) = s_0, \tag{1}$$

$$\dot{m} = \alpha s - (\beta + \eta)m, \quad m(0) = m_0 \tag{2}$$

with analytic solutions

$$s = A_s e^{\lambda_- t} + B_s e^{\lambda_+ t}, \tag{3}$$

$$m = A_m e^{\lambda_- t} + B_m e^{\lambda_+ t}, \tag{4}$$

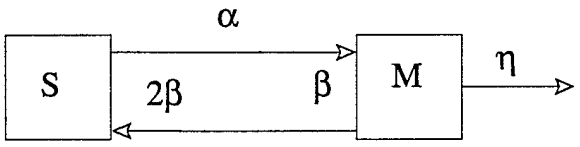

Fig. 2. Model of cell growth.

where

$$\lambda_{\pm} = \frac{-(\alpha+\beta+\eta) \pm \sqrt{(\alpha+\beta+\eta)^2 + 4\alpha(\beta-\eta)}}{2} \tag{5}$$

and

$$\begin{aligned} &A_s = 2\beta m_0 - (\lambda_+ + \alpha)s_0/(\lambda_- - \lambda_+), \quad B_s = (\lambda_- + \alpha)s_0 - 2\beta m_0/(\lambda_- - \lambda_+), \\ &A_m = (\lambda_- + \alpha)/2\beta A_s, \quad B_m = (\lambda_+ + \alpha)/2\beta B_s. \end{aligned} \tag{6}$$

Sign analysis of Eqs. (5) and (6) shows $B_s > 0$, $B_m > 0$ and, for $\beta > \eta$, $\lambda_+ > 0$ yielding a positive growth term. Parameter estimates which follow in Table 1 show that the values of α, β and η produce a $\lambda_- \ll 0$. Then even for small values of t, the $e^{\lambda_- t}$ term decays rapidly, and the phases approximate simple exponential growth.

$$s \approx B_s e^{\lambda_+ t}, \quad m \approx B_m e^{\lambda_+ t}. \tag{7}$$

2.2. Model of drug treatment

Antimitotic agents interfere with mitosis preventing the cells from successfully dividing. Affected cells remain in the G2/M-phase longer as indicated by the subsequent G2/M-phase population increase and G1/S phase decrease. These blocked cells will either eventually die via apoptosis, overcome the drug effects due to some type of resistance, e.g. a repair mechanism, or go through aberrant mitosis and become hyperploid. We observe this block experimentally (Section 4, Figs. 4 and 5) and describe it mathematically by curacin A concentration dependent functional changes in the rate transition parameters α, β, and η ((13)–(15)).

In modifying the model the following definitions are used: m_f and s_f, respectively, G_2/M- and G_1/S-phase cells that are free of absorbed drug; m_b and s_b, respectively G_2/M- and G_1/S-phase cells that are bound to the drug by absorption; α_f, β_f and η_f, the phase transition rates of the drug free cells (the same value as α, β and η for the untreated case); α_b, β_b and η_b, the phase transition rates of the cells with absorbed drug which, unlike those in the drug free cells, are not necessarily constant and can be functions of dose (see Eqs. (13)–(15)); ψ_s and ψ_m are the irreversible

Table 1
Drug free (0.0 nM) and curacin A (2.5, 25 and 50 nM) treated phase growth rate coefficients (α, β and η) and drug absorption coefficient (ψ) for cancer cell lines A2780 and MCF-7/LY2.[a]

A2780 (nM)	α_f	β_f	η_f		MCF-7/ LY2 (nM)	α_f	β_f	η_f	
0.0	1.593	2.685	0.9413		0.0	1.879	2.137	1.262	
	α_b	β_b	η_b	ψ		α_b	β_b	η_b	ψ
2.5	1.592	2.690	0.8982	16.6	2.5	1.896	2.116	1.378	16.6
25.0	2.488	1.672	1.2230	16.6	25.0	6.071	1.197	1.254	16.6
50.0	9.450	1.118	1.4660	16.6	50.0	6.718	1.175	1.266	16.6

[a] All units are h^{-1}.

drug absorption/binding rate coefficients which is consistent with the strong binding and slow disassociation of curacin A reported in [7,8]; γ_s and γ_m represent drug absorption and unit conversion; δ_d represents any nonabsorption loss of drug concentration; and, D represents the drug concentration in the in vitro medium external to the cells. The values $s_f(0)$, $m_f(0)$, $s_b(0)$, $m_b(0)$, and $D(0)$ are the initial values (time = 0) of the respective variables. The model is depicted in Fig. 3 and the model equations are

$$\dot{s}_f = -\alpha_f s_f + 2\beta_f m_f - \psi_s D s_f, \quad s_f(0) = s_0, \tag{8}$$

$$\dot{m}_f = \alpha_f s_f - (\beta_f + \eta_f + \psi_m D) m_f, \quad m_f(0) = m_0, \tag{9}$$

$$\dot{s}_b = -\alpha_b s_b + \psi_s D s_f + 2\beta_b m_b, \quad s_b(0) = 0, \tag{10}$$

$$\dot{m}_b = \alpha_b s_b + \psi_m D m_f - (\beta_b + \eta_b)\dot{m}_b, \quad m_b(0) = 0, \tag{11}$$

$$\dot{D} = -\gamma_s \psi_s D s_f - \gamma_m \psi_m D m_f - \delta_d D, \quad D(0) = D_0, \tag{12}$$

where

$$\alpha_b = \alpha_f + \frac{V_\alpha D^{n_\alpha}}{K_\alpha^{n_\alpha} + D^{n_\alpha}}, \tag{13}$$

$$\beta_b = \beta_f - \frac{V_\beta D^{n_\beta}}{K_\beta^{n_\beta} + D^{n_\beta}}, \tag{14}$$

$$\eta_b = \eta_f + \frac{V_\eta D^{n_\eta}}{K_\eta^{n_\eta} + D^{n_\eta}}. \tag{15}$$

The functional forms of Eqs. (13)–(15) were derived from the experimental data and represent the saturated changes observed in the transition rate parameters (see Figs. 8 and 9). V is the maximum change at large values of D, K is the half-saturation parameter, and n is the constant that determines the rate of saturation. Eq. (13) is an increasing function of dose implying that as dose increases the S-phase transition rate increases. The justification for this functional form comes from both the experimental data given here as well as from the many other experimental studies of tubulin polymerization inhibitory agents (e.g. [9]). When cells in G1/S experience an effective concentration of agents such as curacin A, their microtubule lattices dissolve. In the

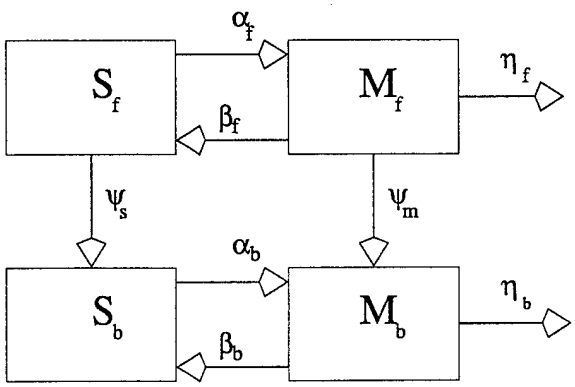

Fig. 3. Model of antimitotic drug treated cell cycle.

normal (antimitotic agent-untreated) cell cycle, microtubule dissolution is tightly associated with completion of duplication of the genome (i.e., DNA synthesis) and entry into G2/M. Thus, agents like curacin A 'trick' cells into thinking that they should be entering mitosis and, if a cell that has yet to complete genome duplication experiences this microtubule dissolution, it increases its rate of DNA synthesis to match the cytoskeletal changes. Eq. (14) is a decreasing function of dose describing the decrease in the mitotic rate as dose is increased and Eq. (15) is an increasing function of dose which implies that dose may increase the apoptotic rate. These three equations result in an increased block on the G2/M-phase with increased concentration of curacin A.

2.3. Approximating an analytic solution of drug treatment

We assume the dose is a constant of time or $\dot{D} \approx 0$. This is based on the fact that the cell sample size was small (0.03–0.15 ml) compared to the drug medium volume (7.0–12.0 ml) therefore, the average drug concentration in the medium was assume to be nearly constant. The remaining set of drug treatment equations has the analytic solution:

$$s_f = A_{s_f} e^{\lambda_{f-} t} + B_{s_f} e^{\lambda_{f+} t}, \tag{16}$$

$$s_b = A_{s_b} e^{\lambda_{f-} t} + B_{s_b} e^{\lambda_{f+} t} + C_{s_b} e^{\lambda_{b-} t} + B_{s_b} e^{\lambda_{b+} t}, \tag{17}$$

$$m_f = A_{m_f} e^{\lambda_{f-} t} + B_{m_f} e^{\lambda_{f+} t}, \tag{18}$$

$$m_b = A_{m_b} e^{\lambda_{f-} t} + B_{m_b} e^{\lambda_{f+} t} + C_{m_b} e^{\lambda_{b-} t} + B_{m_b} e^{\lambda_{b+} t} \tag{19}$$

with

$$\lambda_{f_\pm} = \frac{-(\alpha_f + \beta_f + \eta_f + \psi_m D + \psi_s D)}{2} \pm \frac{\sqrt{(\alpha_f + \beta_f + \eta_f + \psi_m D + \psi_s D)^2 + 4(2\alpha_f \beta_f - (\beta_f + \eta_f + \psi_m D)(\alpha_f + \psi_s D))}}{2} \tag{20}$$

and

$$\lambda_{b_\pm} = \frac{-(\alpha_b + \beta_b + \eta_b) \pm \sqrt{(\alpha_b + \beta_b + \eta_b)^2 + 4\alpha_b(\eta_b - \beta_b)}}{2}. \tag{21}$$

λ_{b^-} and λ_{f^-} are decay terms. λ_{b^+} and λ_{f^+} change from growth to decay when the dose dependence of the parameters renders the last term in each radical equal to 0:

$$\alpha_b(\eta_b - \beta_b) = 0 \tag{22}$$

and

$$2\alpha_f \beta_f - (\beta_f + \eta_f + \psi_m D)(\alpha_f + \psi_s D) = 0. \tag{23}$$

This determines the minimum dose required to arrest growth.

3. Applying the model to in vitro growth data

Next, we use the model to aid in the understanding of the dynamics of the antimitotic agent curacin A on the breast carcinoma cell line MCF-7/LY2 and the ovarian carcinoma cell line A2780.

3.1. Experimental procedures

(+)-Curacin A, a gift from Professor Peter Wipf (Univ. Pittsburgh) [10], was dissolved in DMSO (dimethyl sulfoxide) as a 1 mM stock solution, which was diluted into growth medium to give the final exposure concentrations. Control cultures contained vehicle equivalent to that in drug-treated cultures.

3.1.1. Cell lines and culture conditions

MCF-7/LY2 cells were from Dr Marc E. Lippman (Lombardi Cancer Center). The A2780 cell line was a gift from Dr Thomas Hamilton (Fox Chase Cancer Center). MCF-7/LY2 cells were cultured in DMEM and the A2780 cells in RPMI-1640, each containing 10% fetal bovine serum, at 37°C in a 5% CO_2, humidified incubator.

3.1.2. Growth inhibition assay

Cells were plated at a density of 2×10^5/dish in 5 ml of growth medium for 72 h to allow attachment, then in the absence or presence of increasing concentrations of (+)-curacin A in triplicate. At 24 h increments, medium from three dishes per treatment group with nonadherent cells was removed and adherent cells were dispersed with trypsin/ethylenediamine tetraacetic acid. The cells were combined, centrifuged, resuspended in Hank's balanced salts solution (HBSS), and an aliquot was mixed with an equal volume of 0.08% Trypan blue in HBSS. After a 10 min. period to allow for dye uptake in nonviable cells, cell counts were made on dye-excluding viable cells microscopically on a hemacytometer in blinded triplicate.

3.1.3. Flow cytometry

Cellular DNA content was quantified by propidium iodide (PI) flow cytometry. Combined adherent and nonadherent cells were fixed in 70% ethanol (4°C, 30 min), pelleted by centrifugation, washed with HBSS, pelleted by centrifugation, and RNA was digested by the addition of 10 μg of RNase A. PI (10 μg) was added, the cells were incubated for 30 min at 37°C, then stored in the dark at 4°C until analyzed (at least 24 h). DNA content was determined on a Becton–Dickinson FACScan flow cytometer equipped with a 488 nm argon laser by measuring forward versus orthogonal light scatter and peak versus area red fluorescence. DNA histograms gave cell cycle distributions, and cell cycle populations were quantified from a standard count of 5000–10 000 cells using the Becton–Dickinson Lysis II program.

3.2. Parameter estimation procedures

First, the parameters α, β and η were estimated for the untreated model equations (1) and (2). Next, the parameters α_b, β_b, η_b, ψ_s and ψ_m for the treated model equations (8)–(12) were

determined independently at each drug concentration level (2.5 nanomolar (nM), 25.0 nM and 50.0 nM) with $\alpha_f = \alpha$, $\beta_f = \beta$ and $\eta_f = \eta$ fixed at the estimates determined in the untreated case. In all cases the maximum likelihood estimation technique via ADAPT II [11] was used to estimate the parameters.

Table 2
Curacin A-dependent phase transition rate (α_b, β_b and η_b) saturation parameters[a]

	A2780	CV%	MCF-7/LY2	CV%
V_α	7.97	12.4	4.93	15.8
K_α	31.4	4.4	14.6	45.7
n_α	9.0	Fixed	3.25	Fixed
V_β	1.58	7.0	0.96	9.6
K_β	23.0	6.3	8.11	169.0
n_β	7.0	Fixed	3.25	Fixed
V_η	0.55	27.2	0.0	NA
K_η	24.2	13.7	NA	NA
n_η	7.0	Fixed	NA	NA

[a] See Eqs. (13)–(15). CV%: coefficient of variation. Units: V – h^{-1}, K – nM, n – unitless. NA – not applicable.

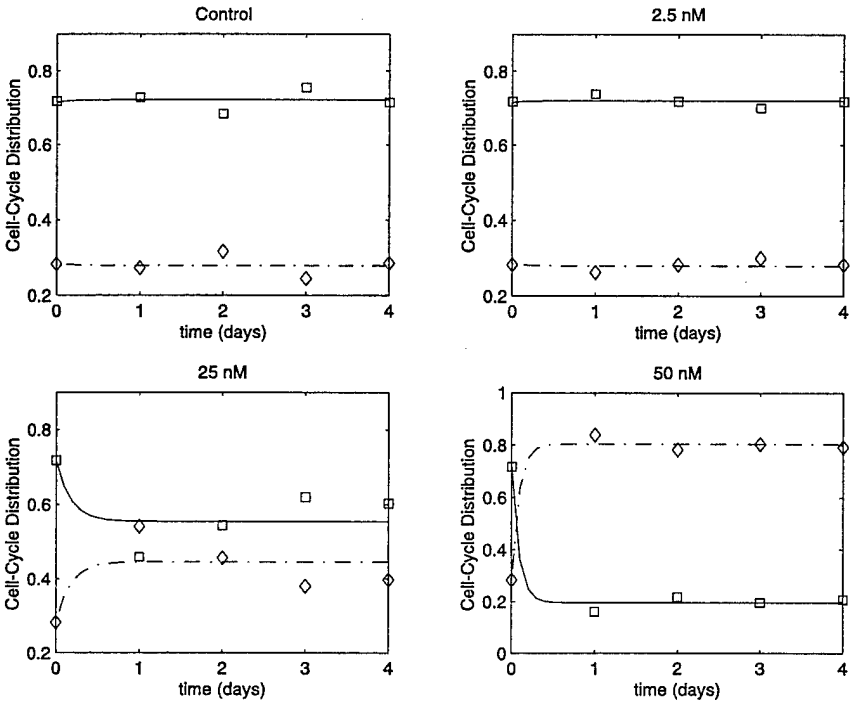

Fig. 4. A2780 cell cycle distribution versus time for control cell growth and cell growth with 2.5, 25 and 50 nM curacin A; G1/S-phase fraction for model (solid) and data (□) and G2/M-phase fraction for model (dash) and data (◇).

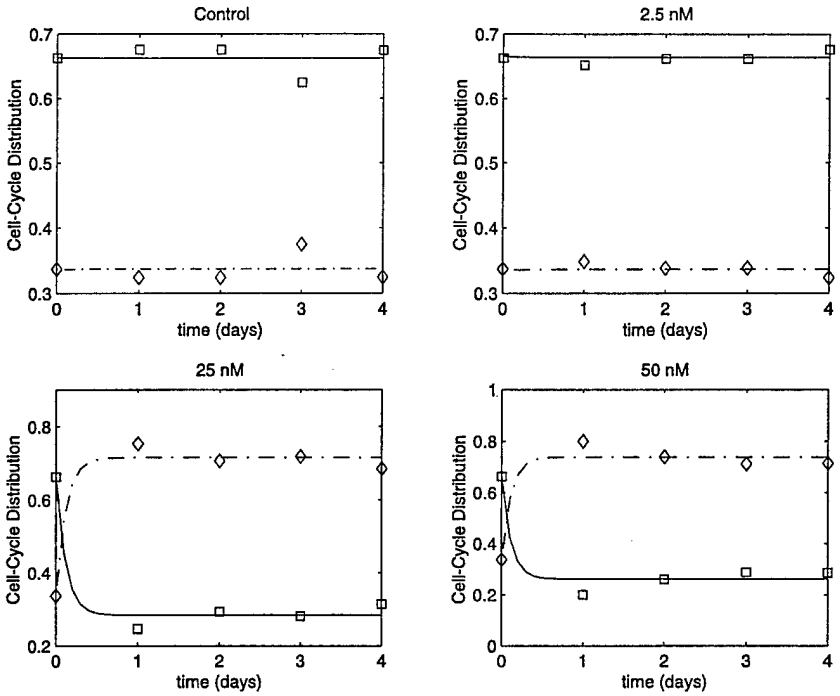

Fig. 5. MCF-7/LY2 cell cycle distribution versus time for control cell growth and cell growth with 2.5, 25 and 50 nM curacin A; G1/S-phase fraction for model (solid) and data (□) and G2/M-phase fraction for model (dash) and data (◇).

To uniquely determine the values of α, β and η, the cell cycle time is needed. The cell cycle time was observed to be approximately one day in the two cell-lines that are considered. Therefore, the average time for S phase transition plus the average time for M phase transition was set to one day (Eq. 24).

$$\frac{1}{\alpha}+\frac{1}{\beta}=1 \text{ (day)}. \tag{24}$$

We note that η affects the number of cells completing the cell cycle, but it does not affect the cell cycle time for those that do.

The precise values of ψ_s and ψ_m could not be determined because the cells free of curacin A and those bound by it were not distinguishable and no absorption data was available. But, large values of ψ_m and ψ_s gave a better description of the data compared to small values and large values were consistent with the known rapid interaction of curacin A with tubulin [7].

Once the values of α_b, β_b and η_b were determined at each dose level, the functional dependences could be determined by fitting these estimates to Eqs. (13)–(15). This was accomplished by fixing α_f, β_f and η_f at the control levels, fixing n at the values given in Table 2, and estimating V and K. The parameter n was fixed since it cannot be accurately determined with only the four concentrations available.

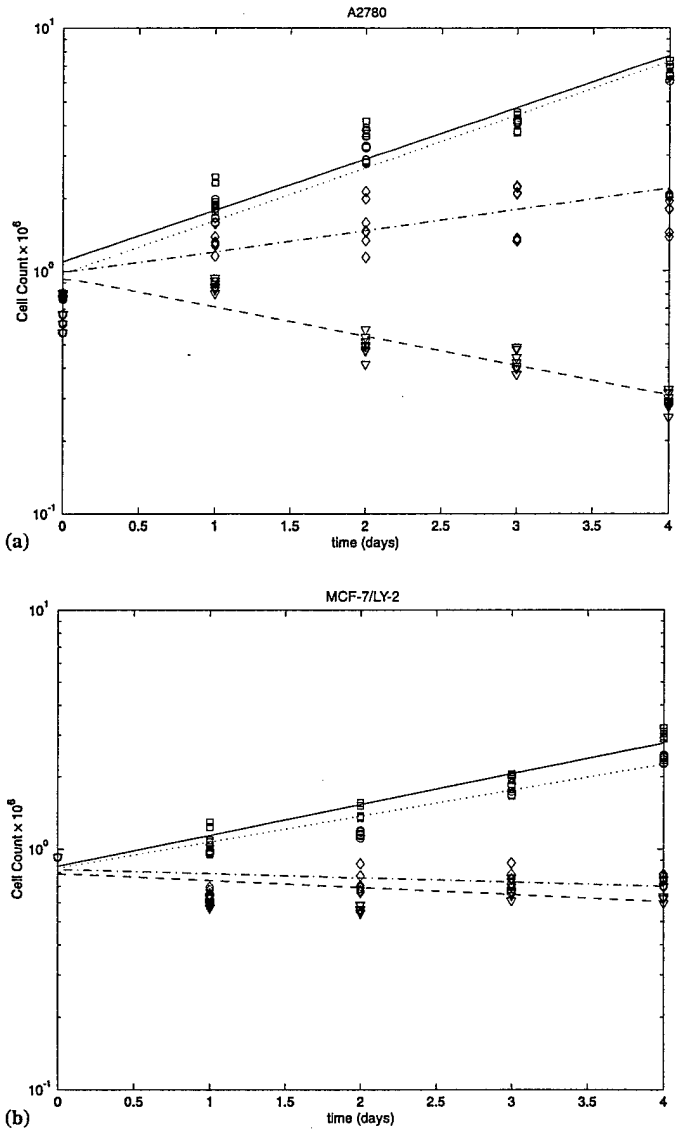

Fig. 6. (a) A2780 total cell counts vs time. (b) MCF-7/LY2 total cell counts vs time. The symbols represent the experimental data at various concentrations of curacin A and the lines represent the model description of the data. untreated: model —, data □. curacin A 2.5 nM: model ···, data ○. 25 nM: model —·—·—, data ◇. 50 nM: model ——, data △.

4. Results

Figs. 4 and 5 show the model fit to the cell cycle distribution for A2780 and MCF-7/LY2, respectively, and Fig. 6 shows the subsequent model fits to the total cell count. The estimated model parameters are given in Tables 1 and 2.

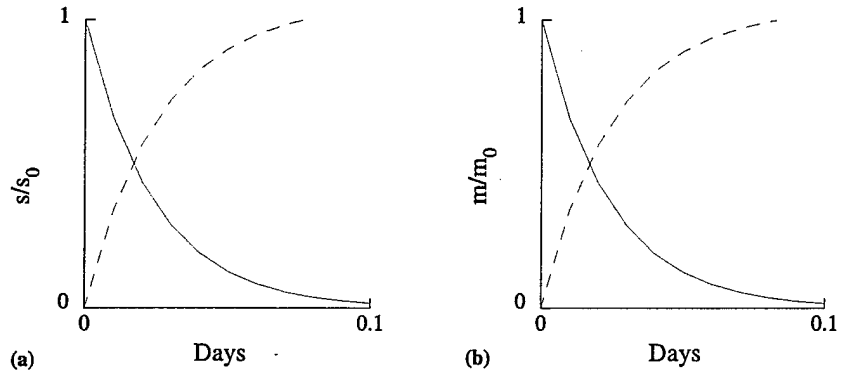

Fig. 7. (a) s_f/s_0 (solid) and s_b/s_0 (dashed) versus time for 2.5 nM curacin A, (b) m_f/m_0 (solid) and m_b/m_0 (dashed) versus time for 2.5 nM curacin A, where m_0 and s_0 are the initial values of the m and s phases, respectively.

4.1. Rapid binding of curacin A

The binding of curacin A was found to be rapid and since no specific influx data was available, (i.e. intra- and extra-cellular curacin A concentrations) the two parameters were assumed to be equal ($\psi = \psi_s = \psi_m$). Fig. 7 shows the calculated values of s_f, s_b, m_f, m_b (normalized to the initial values s_0 and m_0) versus time for A2780 in a dose concentration of 2.5 nM, indicating that all cells had absorbed the agent after approximately 2.4 h. The absorption times for 25 and 50 nM were on the order of 10–15 min. Evaluating the solutions for s_f and m_f in Eqs. (16)–(19) shows that for large values of ψ, s_f and $m_f \approx e^{-\psi t}$. Similar results were obtained for MCF-7/LY2.

4.2. Drug dependence of the phase transition rates

As noted in Eqs. (13)–(15), the transition rates between the different phases of the cell cycle may be functions of curacin A concentration. Figs. 8 and 9 show this for the two cell lines and Table 2 shows the parameter estimates for the equations. Eq. (24) indicates that a theoretical maximum block of the M-phase transition occurs when $\beta_b = 1$, which is nearly reached for both cell lines. For MCF-7/LY2, the 99% maximal block is reached at 31 nM (see Fig. 8) and in a similar manner for A2780, the 99% maximal block is reached at 47 nM (see Fig. 9). The apoptotic rate, η_b, for the MCF-7/LY2 cell line, did not significantly change with respect to curacin A concentration (see Table 1) and therefore V_η was defined to be 0. This indicates that for this cell line the agent only blocks the cell cycle but does *not* increase the rate of cell death. Very different dynamics are observed for the A2780 cell line. Here η_b is an increasing function of curacin A concentration indicating that not only is the agent blocking the cell cycle (by a decrease in β_b) but it is also increasing the rate of cell death. Specifically, when compared to the control there is a 38% increase in η_b at the minimum concentration of 2.5 nM and 59% increase at 50 nM.

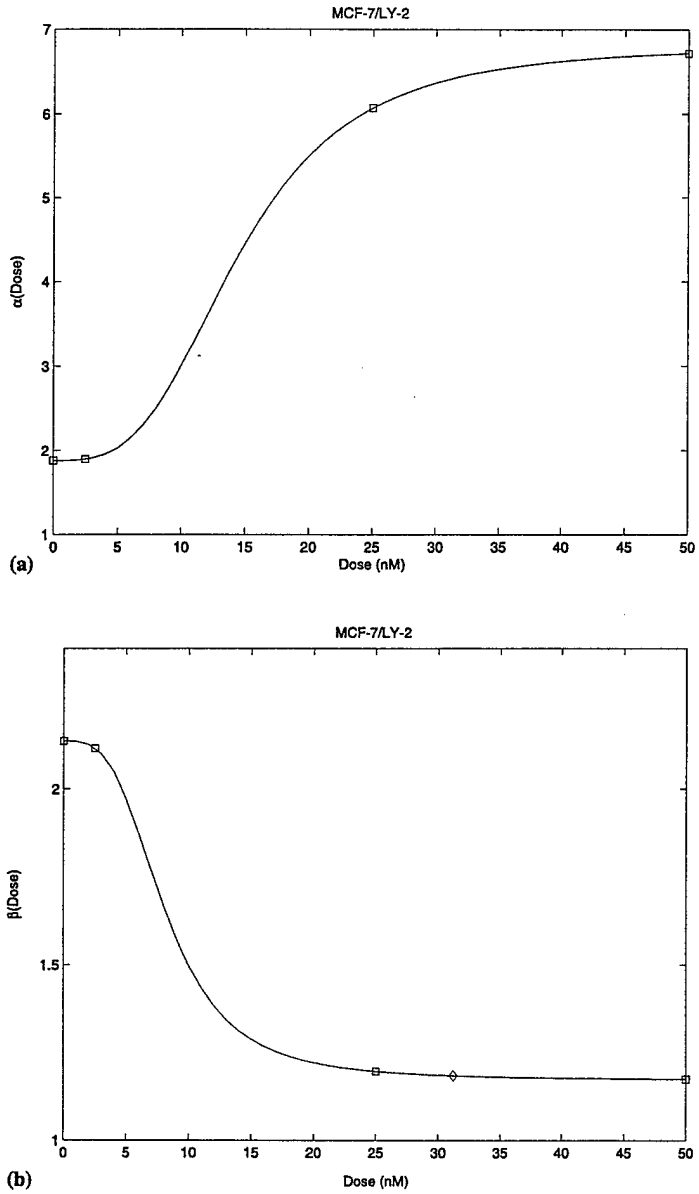

Fig. 8. Phase transition of MCF-7/LY2 cells versus curacin A concentration for α and β ((a)–(b)) for model (solid) and data (□). The 99% maximal block is indicated by (◇) in the lower graph.

4.3. Minimum dose to arrest growth

Eqs. (22) and (23) predicted the relationship necessary to stop growth in the curacin A free and bound cells, respectively. The large value of ψ indicates that very small concentrations are effective in controlling the growth of the curacin A free cells. Eq. (22) indicates that cell growth will be

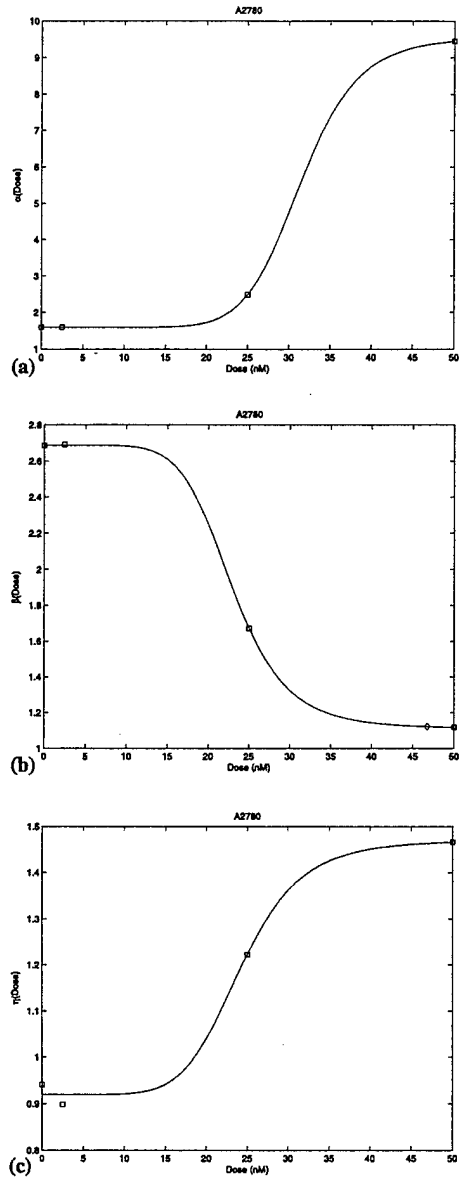

Fig. 9. Phase transition of A2780 cells versus curacin A concentration for α, β and η ((a)–(c)) for model (solid) and data (□). The 99% maximal block is indicated by (◇) in the middle graph.

arrested when η_b is greater than β_b; that is, when the apoptotic rate is greater than the mitotic rate. Solving Eq. (22) using the functional forms for η_b and β_b from Eqs. (13)–(15) and parameters in Table 2, we calculate the minimum concentration for stopping growth to be 29.1 nM for A2780 and 16.5 nM for MCF-7/LY2. From the experimental data (shown in Fig. 6) the concentration needed to stop growth was observed to be between 25 and 50 nM for A2780 and 2.5 and 25 nM for MCF-7/LY2. The model estimates for each cell line fall in these ranges.

4.4. Time response and saturation

Eqs. (20) and (21) for growth/decay constants show that λ_- is always negative while the sign of λ_+ depends on $\beta - \eta$. While $\beta > \eta$ causes λ_+ to be positive (growth) and $\beta < \eta$ causes λ_+ to be negative (decay), the difference is enhanced by the G1/S-phase transition rate, α, as seen in the $\alpha(\beta - \eta)$ term. Fig. 10(a) shows the product $\alpha(\beta - \eta)$ for A2780 (solid) and MCF-7/LY2 (dashed) cells versus curacin A concentration calculated using values from Tables 1 and 2. MCF-7/LY2 reach the concentration where $\alpha(\beta - \eta) = 0$ sooner than A2780, but the maximum rate of decay for MCF-7/LY2 is much smaller than that for A2780. These effects are further demonstrated in Figs. 10(b) and (c).

4.5. IC_{50} and 48 h responses

Fig. 11 shows the IC_{50} concentration with respect to time. We observe that the IC_{50} is unobtainable for approximately the first 1/2 day in A2780 and 1.25 days in MCF-7/LY2 indicating that it takes more time to be able to obtain a 50% reduced number of new cells with respect to controls in MCF-7/LY2 compared to A2780. Next, we observe that for times greater than about 1.25 days, more curacin A is required to obtain the IC_{50} in A2780 cells as compared to MCF-7/LY2 cells. Also, as noted in Section 4.3, the minimum concentration to arrest growth is also lower for MCF-7/LY2 compared to A2780. But, as observed in Section 4.4, MCF-7/LY2 cells are saturated at a lower concentration compared to A2780. It should be noted that curacin A concentrations below the minimum for arresting growth produce the indicated IC_{50} responses at the indicated times, but still permit total cell count growth for longer time intervals.

The concentration response and saturation comparisons are also observed in Fig. 12 which shows the normalized (with respect to control) total cell counts along with the G2/M-phase fraction at 48 h. The graphs indicate a greater block of the G2/M-phase, a greater reduction in the total cell count for A2780, and an earlier saturation point of approximately 25 nM for MCF-7/LY2 compared to approximately 40 nM for A2780.

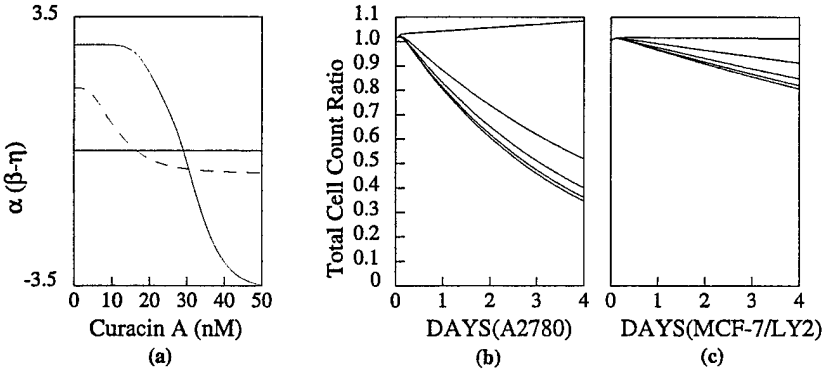

Fig. 10. (a) $\alpha(\beta - \eta)$ for A2780 (solid) and MCF-7/LY2 (dashed) cells versus curacin A concentration. (b) and (c) show the modeled total cell count ratio, $(s + m)/(s_0 + m_0)$, versus time for curacin A concentrations: (b) A2780 (29.1, 35, 40, 45 and 50 nM) (top to bottom) and (c) MCF-7/LY2 (16.5, 20, 25, 30 and 35 nM) (top to bottom).

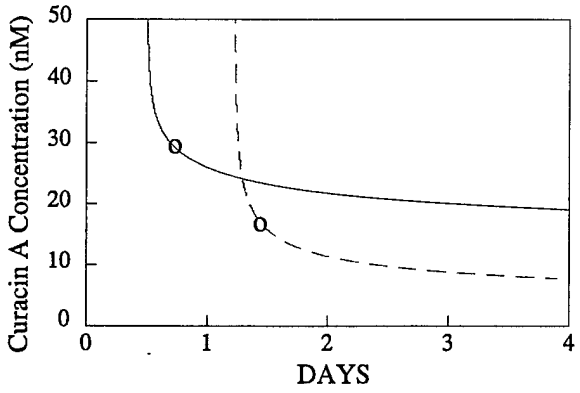

Fig. 11. Model IC_{50} Concentration Response; Concentration versus time to reduce the total cell count to 50% of the control growth level for A2780 (solid) and MCF-7/LY2 (dashed). 'o' locates the calculated minimum dose for arresting growth.

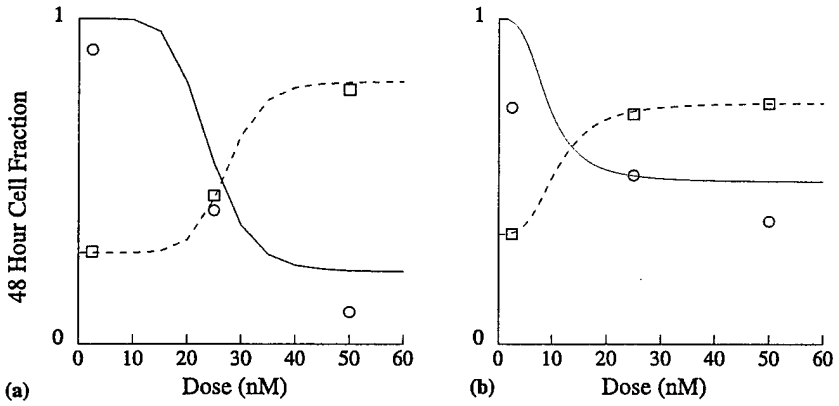

Fig. 12. 48 h cell fraction versus curacin A concentration for A2780 (a) and MCF-7/LY2 (b) cell lines. The values are determined 48 h after the indicated concentration of curacin A is applied. Displayed are: (1) 48 h total cell count fraction (dose level/control level) generated by the model (solid) and data (○) and (2) G2/M-phase fraction (G2/M-phase cell count)/(total cell count) generated by the model (dash) and the data (□).

5. Conclusion

A model of in vitro cancer cell growth and antimitotic drug interaction has been presented and adapted to the growth and treatment of cancer cell lines A2780 and MCF-7/LY2 with the experimental chemotherapeutic agent curacin A. Specifically, the model predicts that the A2780 cell line will react with a concentration-dependent increase in the S-phase transition, decrease in the mitotic rate, and increase in the apoptotic rate. In the MCF-7/LY2 cell line, however, the model predicts that the cells will react with a concentration-dependent increase in the S-phase transition, decrease in the mitotic rate, but a constant apoptotic rate. The model calculates the minimum

curacin A concentration to arrest growth, which is lower for MCF-7/LY2 with a quickly saturated response and higher for A2780 but with a slower saturation rate.

In general, the model predicts that curacin A will be quickly absorbed into all cell phases. The cells will respond with an increase in the rate of DNA synthesis, a decrease in the rate of mitosis/cytokinesis and possibly an increase in the rate of apoptosis. The drug will be more effective if the concentration increases the apoptotic rate, since the agent effectiveness is determined by differences in the mitotic and apoptotic rates. If the cells do not respond with an increase in apoptosis, the agent effectiveness will saturate quickly as the limit of mitotic decrease is reached.

References

[1] Z. Agur, The effect of drug schedule on responsiveness to chemotherapy, Ann. N.Y. Acad. Sci. 504 (1986) 274.
[2] Z. Agur, R. Arnon, B. Schechter, Reduction of cytotoxicity to normal tissues by new regimens of cell-cycle phase-specific drugs, Math. Biosci. 92 (1988) 1.
[3] L. Cojocaru, Z. Agur, A theoretical analysis of interval drug dosing for cell-cycle-phase-specific drugs, Math. Biosci. 109 (1992) 85.
[4] G.F. Webb, A cell population model of periodic chemotherapy treatment, in: Biomedical Modeling and Simulation, Elsevier, Amsterdam, 1992, p. 83.
[5] J.C. Panetta, J.A. Adam, A mathematical model of cycle-specific chemotherapy, Math. Comput. Modelling 22 (1995) 67.
[6] J.C. Panetta, A mathematical model of breast and ovarian cancer treated with paclitaxel, Math. Biosci. 146 (1997) 89.
[7] P. Verdier-Pinard, N. Sitachitta, J.V. Rossi, D.L. Sackett, W.H. Gerwick, E. Hamel, Biosynthesis of radiolabeled curacin A and its rapid and apparent irreversible binding to the colchicine site of tubulin, Arch. Biochem. Biophys. 370 (1999) 51.
[8] A.V. Blokhin, H.D. Yoo, R.S. Geralds, D.G. Nagle, W.H. Gerwick, E. Hamel, Characterization of the interaction of the marine cyanobacterial natural product curacin A with the colchicine site of tubulin and the initial structure-activity studies with analogues, Molec. Pharmacol. 48 (1995) 523.
[9] R. Balachandran, E. ter Haar, M.J. Welsh, J.C. Yalowich, S.G. Grant, B.W. Day, Induction of human breast cancer cell apoptosis from G2/M preceded by stimulation into the cell cycle by *Z*-1,1-dichloro-2,3-diphenylcyclopropane, Biochem. Pharmacol. 57 (1999) 97.
[10] P. Wipf, W. Xu, Total synthesis of the antimitotic marine natural product (+)-curacin A, J. Org. Chem. 61 (1996) 6556.
[11] D.Z. D'Argenio, A. Schumitzky. ADAPT II User's Guide: Pharmacokinetic/Pharmacodynamic Systems Analysis Software, Biomedical Simulations Resource, Los Angeles, 1997.

Molecular and Morphological Effects of Curacin A on PC-3 Human Prostate Carcinoma Cells – MEK1 Inhibition Enhances Caspase/Calpain Actions*

Pao-Hsiu Chen‡ §, Kenneth A. Giuliano¶, Andreas Vogt §§, Peter Wipf‖, and Billy W. Day‡ ‡‡ §§ ****

*Departments of ‡Environmental & Occupational Health, ‖Chemistry, **Pharmacology and ‡‡Pharmaceutical Sciences and the §§University of Pittsburgh Cancer Institute, University of Pittsburgh, Pittsburgh, Pennsylvania 15238, 15260 and 15261, and ¶Cellomics, Inc., Pittsburgh, Pennsylvania 15238*

*Supported in part by USPHS grants CA78039 from the National Cancer Institute and GM55433 from the National Institute of General Medical Sciences, and by United States Army Medical Research and Materiel Command Predoctoral Fellowship DAMD17-99-1-9352 (to P.-H.C).

§ Partial fulfillment of the requirements for the Ph.D. degree. University of Pittsburgh, Dept. of Environmental & Occupational Health.

**To whom correspondence should be addressed at Departments of Pharmaceutical Sciences and of Environmental & Occupational Health, University of Pittsburgh, 728 Salk Hall, 3501 Terrace Street, Pittsburgh, PA 15261, Phone: 1-412-648-9706. Fax: 1-412-624-1020. E-mail: bday@pitt.edu

Running title: PD098059 enhances curacin A-induced cell death

SUMMARY

Curacin A is an antimitotic agent with unique properties that has previously been determined to act at the colchicine site of tubulin. In one component of a multiparameter high content screening (HCS) technique, curacin A's unique effects on the microtubule (MT) cytoskeleton were revealed. At near its GI_{100} concentration, curacin A caused changes in MT arrays intermediate to those found in cells treated with the MT-perturbing drugs, paclitaxel (PTX) and vinblastine (VBL). Higher concentrations of curacin A resulted in the formation of wispy MT bundles in the cytoplasm and rings of bundled MTs around the nuclei of treated cells. HCS also showed that curacin A modulated the normal regulation of kinase-mediated stress pathways and nuclear morphology within the same population of cells. Curacin A caused concentration-dependent increases in the activation of three MAPK pathways measured as increased phosphorylation of three key pathway intermediates, RSK1, p38MAPK and c-Jun. The levels of the phosphorylated forms of these targets induced by curacin A was comparable to those caused by PTX and VBL. To further dissect the mechanism of curacin A action, the MEK1 inhibitor PD098059 was used to investigate mechanisms of cell death in non-synchronized human PC-3 prostate carcinoma cells. Curacin A alone caused Bcl-2 and Raf-1 phosphorylation, Raf-1 and PARP fragmentation, and $p21^{CIP1/WAF1}$ induction. PD098059 alone had little effect on proliferation, caused no cell cycle changes nor effects on markers of apoptosis, but did inhibit ERK-1 phosphorylation. Pretreatment of cells with PD098059 for 1h followed by treatment with curacin A caused decreased Bcl-2, Bax and stathmin levels and enhanced curacin A-induced phosphorylation of Raf-1, its fragmentation, PARP fragmentation and $p21^{CIP1/WAF1}$ levels over that caused by curacin A alone. The results show that MEK1 inhibition combined with a colchicine site MT perturbing agent lead to triggering of calpain and caspase actions and suggest potential apoptosis-enhancing combination therapies.

FOOTNOTES

[1] The abbreviations used are: DMSO, dimethyl sulfoxide; ERK, extracellular signal-regulated kinase; FBS, fetal bovine serum; HCS, multiparameter high content screening; HRP, horseradish peroxidase; JNK, c-Jun N-terminal kinase; MAP, microtubule-associated protein; MAPK, mitogen-activated protein kinase; MEK, MAPK/ERK kinase; MSK, MAPK and stress-activated kinase; MT, microtubule; PARP, poly(ADPribose) polymerase; PD098059, 2'-amino-3'-methoxyflavone; PTX, paclitaxel; RSK, ribosomal S6 kinase; SAPK, stress-activated protein kinase; VBL, vinblastine

INTRODUCTION

Curacin A (Fig. 1) is a structurally novel antimitotic natural product. It was originally derived from the lipid fraction of the marine cyanobacterium *Lyngbya majuscula* obtained near Curaçao (1), but has since been prepared by total synthesis (2). In assays with isolated bovine brain tubulin, low concentrations of curacin A inhibit glutamate/GTP-induced assembly of the protein, but higher concentrations lead to the formation of complex abnormal polymers that resemble twisted cables of fine spiral filaments (3). Curacin A avidly binds the colchicine site of tubulin with unprecedented high affinity (4-6), but does not fit the classical structure-activity requirements of colchicine site agents. This interesting agent is antiproliferative at low nanomolar concentrations, causes G_2/M arrest, and leads to differing levels of hypodiploidy (a measure of apoptosis) in human breast, prostate and ovarian carcinoma cell lines (5,7,8).

Microtubules (MT)[1] are polar hollow structures composed of alternating α- and β-tubulin heterodimers, with a fast elongating (plus) end and a more slowly shrinking (minus) end. Alternating growth and shrinkage of MTs has been termed dynamics, which plays an important role in supporting cell structure, intracellular vesicle transport and chromosome segregation. The dynamic instability of MTs contributes to the dramatic changes in cellular arrays of MTs during the cell cycle. For instance, interphase MTs are stable and usually form a large array radiating from the periphery of the nucleus out to all parts of the cytoplasm and cell membrane. As cells reach mitosis, their MTs become quite dynamic: interphase MT arrays disappear and reassemble only in the region around the now duplicated and assembled chromosomes (9), forming the complex structure termed the mitotic spindle. The driving forces for these highly regulated events include two major factors: MT-stabilizing [i.e., MT-associated proteins (MAPs)] and -destabilizing proteins (i.e., stathmin). The functions of these proteins are determined by their

phosphorylation status; i.e., phosphorylation of MAPs 2 and 4 decreases their MT-affinity and –stabilizing functions, and phosphorylation of stathmin abrogates its MT-destabilizing ability (10,11). In the mitotic spindle, condensed chromosomes locally stabilize spindle MTs, perhaps through kinetochore capture, and the newly duplicated centrosomes also stabilize MTs by local dephosphorylation of MAPs and phosphorylation of stathmin (9,12,13). How these complicated controlling systems operate is incompletely elucidated, but present models point to the relationships between signal transduction pathways and MTs (14).

In the transfer of stimuli from the plasma membrane into the cytoskeleton, nucleus, and other subcellular targets, several molecular pathways play pivotal roles in the orchestrated regulation of ions, metabolites, macromolecules, and organelles that mediate signal transduction. One class of these pathways involves mitogen-activated protein kinases (MAPKs) and it is comprised of at least three different subgroups: ERKs (extracellular signal-regulated kinases), p38MAPK kinase, and JNK/SAPK (c-Jun N-terminal kinase/stress-activated protein kinase). A high proportion of ERK, also known as p44/42 MAPK, which is two steps downstream of Raf-1, is distributed along MTs and can phosphorylate MAPs 2 and 4 (15,16) allowing MT depolymerization. Thus, activated ERK is poised to regulate MT dynamics, leading to the reorganization of the MT cytoskeleton and cell rounding, normal events on the path to mitosis. Furthermore, MT drugs have been shown activate kinases involved in stress pathway regulation (17,18). 2'-Amino-3'-methoxyflavone (PD098059; Fig. 1) is a synthetic agent that specifically blocks a kinase that activates ERK, MEK1 by binding to the inactive form of the protein, inhibiting the kinase by an allosteric effect (19,20). Through use of PD098059, it has been shown that activated MEK, which is the kinase activated by Raf-1, is required for cell cycle progression through G_2/M (21,22). In addition, it has been reported that activated Raf-1 can regulate ERKs

and affect MTs dynamics through stathmin (23).

Recent studies show that some G_2/M-phase specific drugs, e.g. MT-perturbing agents, cause Bcl-2 phosphorylation and apoptosis, while drug with other activities, e.g., DNA-damaging drugs, antimetabolites and alkylating agents, do not (24). Bcl-2 is an apoptosis repressor and its ability to dimerize with proapoptotic proteins acts to suppress cell death (25,26). Bcl-2 and the pro-apoptotic protein Bax can be substrates of caspases (27) and calpain(28,29), respectively. These two proteolytic processes are parts of apoptosis cascades. Analysis by selected mutation shows that the loop region of Bcl-2, which contains serines susceptible to phosphorylation, is important in paclitaxel(PTX)-induced apoptosis (30). Overexpressed Bcl-2 can protect against PTX-induced MT alterations probably through mediation of the post-translational modification of tubulin (31). Bcl-2 overexpression can provide another escape pathway after G_2/M arrest by causing multi-nucleation (32). Some studies suggest that Bcl-2 phosphorylation is mitosis related but not an apoptosis determinant (33,34). In addition, some reports indicate that Bcl-2 also can interact with proteins outside of its family, i.e., Raf-1 (35). The nature and implications of interaction between these two proteins is still unclear.

Raf-1 is a 74 kDa protein kinase component of the intracellular Ras signaling cascade that participates in the regulation of cell proliferation, differentiation, transformation, and apoptosis (36). It has been implicated in MT perturbing agent-induced apoptosis, but its role in this process remains enigmatic. One model shows that hyperphosphorylation of Raf-1 can negatively regulate its membrane binding ability (37). Cytosolic c-Raf-1 activation could be an important upstream regulator in PTX-induced $p21^{CIP1/WAF1}$ expression and apoptosis. The induction of $p21^{CIP1/WAF1}$, a cyclin dependent kinase inhibitor that causes G_1 cell cycle arrest, can be p53-independent (38,39). On the other hand, highly expressed Raf-1 kinase activity has been

reported to be protective against PTX-induced apoptosis (40). The possible Raf-1 activation model has been reported (41). Raf-1 also becomes phosphorylated in response to MT-perturbing agents (24). Perturbation of MT dynamics could very well be an integral part of the mechanism by which signal transduction changes occur. To summarize, there are several factors which could be used to interpret Raf kinase's diversity in regulatory mechanisms, such as stimulation conditions, cell type-specificity, subcellular location, different phosphorylation sites, proteolytic events, feedback regulation and different Raf family proteins.

We have noted that one prostate carcinoma cell line, PC-3, although sensitive to the antiproliferative and G_2/M blocking activity of curacin A, developed few to no hypodiploid cells in short term ($\leq$ 48 h) response to the agent (7,8). To further dissect the mechanisms of action of curacin A on these cells, we used flow cytometry, Western blotting, and multiparameter high content screening (HCS) (42) technology to measure changes in MT cytoskeleton morphology and the phosphorylation of signal transduction proteins [RSK (ribosomal S6 kinase), c-Jun, histone H3 (40,41) and p38MAPK] after curacin A and other MT-perturbing agents [PTX and vinblastine(VBL)] treatments. In addition, intrigued by the possibility that Bcl-2 and Raf-1 pathways interact via MT-mediated events, we used PD098059 to block MEK1 in unsynchronized PC-3 cells and then determined its effects in combination with curacin A. The results show the possible mechanism of curacin A's cell death-inducing effects and provide its cytotoxic synergy with the combination with PD098059, and suggest possible means to enhance the antitumor actions of MT perturbing drugs.

EXPERIMENTAL PROCEDURES

Materials – Curacin A, synthesized as previously described (2), and PD098059, from New England Biolabs, were dissolved in dimethyl sulfoxide (DMSO) as 1 mM and 20 mM stock solutions, respectively, and stored frozen until used. PC-3 cells were from Prof. Candace Johnson (Univ. Pittsburgh). Ca^{2+}- and Mg^{2+}-free Hank's balanced salt solution (HBSS) was from either GIBCO/BRL-Life Technologies or BioWhittaker. Fetal bovine serum (FBS) was from Hyclone. RPMI-1640 culture medium, Trypan blue dye and trypsin/EDTA were obtained from GIBCO/BRL-Life Technologies. Formaldehyde was from Polysciences (Warrington, PA). Primary antibodies for ERK1/2 and their phosphorylated forms were from New England Biolabs. Anti-stathmin antibody was from Calbiochem. Anti-phosphorylated c-Jun was from Cell Signaling Technology (Beverly, MA) and anti-phosphorylated p38MAPK was from Promega (Madison, WI). Anti- phosphorylated histone H3 and anti- phosphorylated RSK1 (RSK90[S363]) were from Upstate Biotechnology (Lake Placid, NY). Anti-α-tubulin antibody was from Sigma Chemical Company. The secondary Abs used in HCS were from Jackson ImmunoResearch; (West Grove, PA). The ArrayScan® II HCS system was from Cellomics®, Inc. (Pittsburgh, PA). All other primary antibodies were from Santa Cruz Biotechnology. Complete™ protease inhibitor cocktail tablets were from Boehringer Mannheim GmbH. The ECL chemiluminescence kit and secondary, horseradish peroxidase (HRP)-conjugated anti-rabbit or -mouse IgG antibodies were from Amersham Life Sciences. X-OMAT AR film was from Kodak. The Transblot-SD Semi-Dry transfer cell used for electroblotting, the DC protein assay kit, and the Multi-Analyst/PC® Image Analysis system were purchased from BioRad. Flow cytometric analysis and cell cycle quantitation were performed with a FACScan flow cytometer and the Lysis II program from Becton-Dickinson. All other materials were from Sigma Chemical

Co.

Cell Culture for Flow Cytometry and Western Blotting – Cells were grown in RPMI-1640 medium containing 10% FBS at 37°C in a 5% CO_2, humidified incubator. Two completely independent experiments were performed wherein all of the endpoints in this manuscript were examined; results from the two experiments were essentially identical. PD098059 was diluted in complete medium and added to cultures 1h before adding curacin A. Control samples contained vehicle equivalent to that in drug-treated cultures. At 0, 1, 24 and 48 h of curacin A treatment, medium was removed, adherent cells were detached with trypsin/EDTA, combined with floating cells in the medium, pelleted by centrifugation, and resuspended in HBSS. An aliquot was used to determine cell number microscopically by counting in a field of Trypan blue in HBSS on a hemacytometer.

Flow Cytometry – Combined attached and floating cells were fixed in 70% aqueous ethanol at 4°C for at least 1 h, pelleted by centrifugation, washed with HBSS, pelleted, and treated with 100 μg of RNase A and 5 μg of propidium iodide in a final volume of 1.1 ml of HBSS. Samples were incubated at 37°C for 30 min, then stored in the dark for at least 24 h at 4°C. Samples were analyzed by flow cytometry using 488 nm Ar laser excitation and measurement of forward and orthogonal light scatter and peak and area red fluorescence. Cell cycle populations were quantified from a standard count of 10,000 cells.

Western Blots – Cold HBSS-washed and pelleted (combined attached and floating) cells were lysed in 50 mM Tris, pH 7.5, containing 2 mM EDTA, 100 mM NaCl, 2 mM Na_3VO_4, 100 mM NaF, 10 μg/ml leupeptin, 10 μg/ml aprotinin, 1% NP40, 10% glycerol, 0.5% sodium deoxycholate and Complete™ cocktail (one tablet/10 ml) on ice for 30 min. Debris was removed by centrifugation. Protein concentrations were determined and equal amounts of proteins were

loaded and separated by SDS-PAGE. Bands were electroblotted onto nitrocellulose (1h, 15 V) in Bjerrum and Schafer-Nielsen transfer buffer (48 mM Tris, pH 7.5, containing 39 mM glycine, and 20% CH_3OH). The filter was blocked with a 10% non-fat dry milk powder solution overnight and then incubated for 1h with primary antibody. After several washes in 100 mM Tris, pH 7.5, with 150 mM NaCl, 0.5 mM EDTA and 0.02% Tween 20, the membrane was incubated with HRP-conjugated secondary antibody. Immunorecognized bands on the blot were determined by chemiluminescence detection followed by exposure of the blot to x-ray film. Band densities were estimated either directly from the gels or from the films on a BioRad MultiFluor-S imaging system. Membranes were washed and re-probed with anti-β-actin antibody to confirm equal loading of lanes.

HCS Assays for Morphological Changes and Molecular Pathway Activation – Logarithmically growing PC-3 cells were plated at 7000 cells per well in collagen I-coated 384-well microplates and allowed to attach for 3-8 h before being treated with drugs for 14.5 h. After treatment, cells were fixed and their nuclei fluorescently labeled by incubating them for 30 min at room temperature in 4% (v/v) aqueous formaldehyde and 10 μg/ml Hoechst 33342 in HBSS. Wells were then rinsed once with HBSS before incubating the cells in 0.5% (w/w) Triton X-100 detergent for 5 min at room temperature. After rinsing with HBSS, the cells were incubated with primary antibody solution for 1h at room temperature. This solution consisted of rabbit polyclonal antibodies directed against either phosphorylated c-Jun (1:200), phosphorylated p38MAPK (1:200), or phosphorylated histone H3 (1:1000) diluted in an HBSS solution containing polyclonal sheep antibodies directed against phosphorylated RSK90[S363] (1:1000) and monoclonal mouse antibodies directed against α-tubulin (1:2500). After rinsing with HBSS, all wells in the microplate were incubated for 1h in an HBSS solution containing a mixture of the

following fluorescently labeled secondary antibodies. FITC-labeled donkey anti-mouse IgG (1:250), Cy3-labeled donkey anti-rabbit IgG (1:250), and Cy5-labeled donkey anti-sheep IgG (1:250). After the incubation, cells were rinsed once with HBSS and stored at 4°C in HBSS for up to two weeks before being analyzed. This protocol yielded cells labeled with four distinct fluorophores in 384-well microplates ready for HCS.

HCS microplates were analyzed with the ArrayScan® II using the general screening application. Within the screening application, multiple fields in each well were imaged at four different wavelengths each (42). Proprietary algorithms provided both morphological information (*e.g.,* nuclear condensation) or, because primary antibodies directed against the phosphorylated (activated) form of several signaling kinase substrates were used, a population distribution of cells containing a range of activated kinases. To visualize the cell population distribution changes, an activation ratio value was defined as the quotient of the number of cells within a treated population of cells containing activated kinases and the number of cells containing unstimulated kinases. For example, the nuclear condensation ratio was defined as the number of cells in a well exceeding a threshold criterion value (*e.g.,* average nuclear intensity) divided by the number of cells in the same well exhibiting criterion values below the threshold. HCS data are presented here in graphical form using the same y-axis spanning values for each activation ratio so the effects of drugs can be directly compared.

RESULTS

Effects on Cell Proliferation – Non-synchronous cultures of PC-3 cells were treated with a series of concentrations (25, 50, 75 and 100 μM) of the MEK1 inhibitor PD098059 or with an equivalent volume of vehicle for 1 h, then with 100 nM curacin A or vehicle. Cells were examined for effects 0, 1, 24 and 48 h post-curacin A treatment. Fig. 1 shows the effects of the treatment protocols on cell proliferation. PD098059 alone caused a minor but concentration- and time-dependent decrement in cell growth rate. Curacin A as a single agent potently inhibited growth. In the combination treatment, the presence of PD098059 had little effect, positive or negative, on the antiproliferative effect of curacin A.

Cell Cycle Distribution Changes – Flow cytometric analysis showed that curacin A caused a time-dependent increase in G_2/M-arrested cells (Fig. 2*A*). None of the cultures treated with PD098059 as a single agent showed alterations in cell cycle distribution. Neither agent alone nor in combination caused any significant increase in hypodiploid (a.k.a. apoptotic or A_0) cells in the timeframe of these experiments. The combination of the two agents caused a time-dependent increase in cells arrested in mitosis, but PD098059 concentration-dependently antagonized curacin A-induced G_2/M accumulation. The numerated data from flow cytometry shown in Fig. 2*B* give a clear picture of the effects of single and combination treatments.

Alteration of Phospho-ERK1/2 (Phospho-p44/42 MAPK) Levels – Some phospho-ERK1/2 was detectable even at high PD098059 concentrations (Fig. 3*A*, lanes 2-5). Comparison of the ratio of phospho- to total ERK1/2 (Fig. 3*B* and *C*) showed that PD098059 caused a concentration- and time-dependent inhibition of phosphorylation (or, decreased the stability of the phosphorylated form) of both ERK1 and ERK2. The level of phospho-ERK1 was more affected than that of phospho-ERK2 in the presence of the MEK1 inhibitor. Curacin A had no

effect on the ratio of phospho- to total ERK1/2. At the 48 h time point, however, the combination treatment caused a larger decrement in the phosphorylation/stability of ERK1/2 than did exposure to only PD098059.

Changes in Apoptosis-Related Proteins – As a single agent, PD098059 had no effect on the expression levels of Bcl-2, Bax, Raf-1, stathmin, poly(ADP-ribose) polymerase (PARP) or $p21^{CIP1/WAF1}$, on the phosphorylation levels of Bcl-2 or Raf-1, nor on the fragmentation of Raf-1 or PARP (Fig. 4). As has been reported for many MT-perturbing agents, curacin A as a single agent caused Bcl-2 and Raf-1 phosphorylation. Curacin A also caused a slight increase in the cleavage of PARP to an atypical ca. 74 kDa fragment after 24 h of exposure, but this effect disappeared by the 48 h time point. PC-3 cells express barely detectable levels of $p21^{CIP1/WAF1}$; 100 nM curacin A, however, caused a significant increase in the level of this protein.

The combination treatment, on the other hand, substantially changed these markers as compared to the effects from the single agents (Fig. 4). PD098059 decreased the Bcl-2 phosphorylation induced by curacin A, as well as the levels of this protein. PD098059 also reduced curacin A-induced Raf-1 phosphorylation and enhanced curacin A-induced Raf-1 fragmentation. PD098059 increased curacin A-induced formation of the ca. 74 kDa PARP fragment. In addition, at 48h, PD098059 decreased the expression level of Bax and stathmin. Finally, inhibition of MEK1 increased the curacin A-induced expression levels of $p21^{CIP1/WAF1}$.

Simultaneous Determination of Curacin A-Induced Morphological Changes in Nuclei and the Microtubule Cytoskeleton as well as Activation of Stress Pathways – In control cells (Fig. 5*A-D*), most condensed nuclei were accompanied by condensed and rounded MT structures, as well as co-localized pp38MAPK and pRSK1. In cells treated with MT drugs near their GI_{100}, concentrations, a subpopulation of cells exhibited altered and biochemical and

morphological regulation. The PTX (13.5 nM)-treated cells (Fig. 5*E-H*) showed multiple types of condensed nuclei with an increased number of cells blocked at mitosis. Cells appearing to be in interphase had MTs with bundled architecture. Cells blocked at G_2/M as a result of drug action, like normal mitotic cells in control wells, showed condensed and rounded MT structures as well as co-localized pp38MAPK and pRSK1. In addition, the distribution of pp38MAPK and pRSK1 in all cases was more dispersed than in the control group, likely due to the breakdown of the nuclear membrane. Curacin A (116 nM)-treated cells (Fig. 5*I-L*) showed MT structures distinct from those found in cells treated with PTX or VBL. Curacin A at this concentration caused some nuclear condensation, but not different from that seen in control cells. Of note was that some interphase cells had a perinuclear MT ring in concert with wisps of cytoplasmic MT bundles, which became much more significant at higher concentrations of curacin A (Fig. 5*F*). In addition, the intracellular distribution of pp38MAPK and pRSK1 caused by 270 nM curacin A was more dispersed (Fig. 5*S-T*). VBL (1.35 nM)-treated cells (Fig. 5*M-P*) showed altered mitotic cells. One nucleus with apparently segregating chromosomes (arrowhead) had an astral MT structure, suggesting drug-induced alterations in MT organizing centers/centrosomes. Other mitotic-like cells showed either brighter or non-spherical nuclei with collateral condensed/rounded MT structures, which were concurrent with increased levels of pp38MAPK and pRSK1. However, like in PTX-treated cells, VBL treatment caused the distribution of pp38MAPK and pRSK1 to be more dispersed than in control cells. A cell having nearly completed cytokinesis is visible near the middle of the photos (to the right of the arrowhead). Some residual pp38MAPK was evident in the developing daughter nuclei (Fig. 5*O*), but pRSK1 was no longer present at this stage of the cell cycle (Fig. 5*P*).

In contrast to the bundling of MTs induced by PTX and the generalized MT dissolution

and appearance of foci induced by VBL, higher concentrations of curacin A resulted in the formation of wispy MT bundles in the cytoplasm of interphase cells and rings of bundled MTs around the nuclei of treated cells (Fig. 5*R*). Thus, curacin A appeared to both induce the bundling of MTs into unique structures while clearing MTs from most of the cytoplasm. Thus, each drug caused unique effects on cellular MT arrays while inducing similar activation of stress pathway kinases.

Curacin A-Induced G_2/M Arrest – A subpopulation of PC-3 cells treated with curacin A, PTX, and VBL exhibited a nuclear morphology similar to that of cells undergoing normal mitosis (Fig. 5*A*, *E*, *I*, and *M*). However, when the morphology of individual nuclei was quantified with HCS, curacin A treated cells exhibited a mechanism of action more similar to VBL than PTX (Fig. 6). That is, both curacin A and VBL activities resulted in similar increases in the nuclear condensation ratio despite the fact that curacin A was approximately an order of magnitude less potent than VBL. Furthermore, curacin A induced one of the hallmark molecular pathways associated with cells entering mitosis, the hyperphosphorylation of histone H3. Curacin A caused a concentration-dependent increase in the histone H3 activation ratio with a potency less than VBL, but similar to that of PTX (Fig. 7*A*). Thus, several morphological and molecular measures of curacin A activity were consistent with it being a drug that blocks the entry of PC-3 cells as well as MCF-7 cells into mitosis (45).

Curacin A-Activated Cellular Stress Pathways Associated with the Early Events of Normal Mitosis – The multiparameter HCS of drug treated PC-3 cells (Fig. 5) shows not only the effects of drugs on the MT cytoskeleton and nuclear morphology, but also the activation of kinase-mediated stress pathways in the same cells. For example, the cells in Fig. 5 exhibiting nuclear condensation and spindle-like MT morphologies also showed increased levels of

phosphorylated (activated) p38MAPK (Fig. 5 *C*, *G*, *K*, and *O*) and RSK1 (Fig. 5 *D*, *H*, *L*, *P*), a protein substrate of activated ERK. Moreover, the p38MAPK and ERKs can both activate MSK1 (MAPK and stress-activated kinase 1), which is an upstream kinase of histone H3 (46). The data presented in Fig. 7 show that curacin A, PTX, and VBL caused a concentration-dependent increase in the activation of key kinases associated with the p38MAPK, JNK, and ERK signaling pathways. Curacin A and PTX had similar potencies in activating stress pathways while VBL was about an order of magnitude more potent in activating the same pathways.

DISCUSSION

As single agents, both PD098059 and curacin A gave results consistent with their known mechanisms of action. PD098059 alone slowed cell proliferation only slightly and blocked ERK1 phosphorylation without causing cell cycle perturbation or changes in apoptosis markers. Including the expected effects on Bcl-2 and Raf-1, curacin A alone potently inhibited cell growth, blocked cells in G_2/M, caused a slight increase in PARP cleavage after 24 h of exposure and a significant increase in levels of $p21^{CIP1/WAF1}$. As G_2/M accumulation occurred, this suggests that in the single agent treatment, $p21^{CIP1/WAF1}$ was acting in its role as a monitor of mitotic spindle damage and assisted in the mitotic arrest caused by curacin A (47,48).

The combination of MEK1 inhibition with the rapid binding and potent MT perturbing actions of curacin A altered the latter's mitotic-blocking effects. There appeared to be some synergy in this regard, as ERK1 phosphorylation was more inhibited by the combination treatment than by PD098059 alone. Both the increase in curacin A-induced Bcl-2 phosphorylation and the decreased levels of this protein by PD098059 can be considered to be antagonistic to the anti-apoptosis properties of Bcl-2; Bcl-2 phosphorylation has, however, been shown to best correlate with mitotic arrest rather than with apoptosis (33,49). Raf-1 phosphorylation, which has also been suggested to be more associated with mitosis than with apoptosis (50), was enhanced by curacin A alone, but was decreased in the combination treatment. This effect of the combination treatment could have been due to feedback from the MEK1 block, but is more likely due to PD098059's dampening of the rate of curacin A-induced transit of cells into G_2/M and the subsequent lowered level of phosphorylated cytoplasmic mitotic Raf-1, which has been reported to be uncoupled from the MEK/ERK pathway (51). Raf-1 fragmentation is considered also a marker of apoptosis (52). Curacin A alone produced some

Raf-1 fragmentation, but degradation of this protein was enhanced when MEK1 was also inhibited. In addition, the reduced expression levels of Bax and stathmin could possible be the effects of calpain-catalyzed cleavage. Calpains are a family of cytosolic Ca^{+2}-dependent cysteine proteases whose members are expressed either ubiquitously or tissue-specifically. Their activity is determined by Ca^{+2} binding, autolysis, and the level of their endogeneous inhibitor, calpastatin (53). Some studies report that calpains are involved in apoptosis regulation because of the degradation of calpastatin by caspases (29,54). On the other hand, it has been shown that both procaspase-3 and PARP are calpain substrates (55). Bax cleavage is controlled by calpain (28) and this calpain-cleaved Bax is more potent at inducing cell death than is native Bax (56). Caspases are also cysteine proteases. Several studies have discussed the calpains and caspasesand their overlapping substrates, autoproteolytic mechanisms and possiblecontrol of each other (53,57) The interaction between them and their functions are, however, incompletely elucidated.

The data here show that curacin A increases the phosphorylation of RSK1, JNK, p38MAPK, and histone H3, and also enhances nuclear condensation in a concentration-dependent manner. These effects were comparable with two other MT-perturbing agents, PTX and VBL, although potencies differed. It has recently been shown that inhibition of ERK by PD098059 can convert VBL into a non-cell cycle-specific toxin (58). Our flow cytometry data also showed that PD0980589 decreases curacin A's G_2/M arrest effect yet increased curacin A-induced PARP fragmentation. Interestingly, the cleavage did not produce the classical caspase 3-catalyzed ca. 85 kDa and 26 kDa products, but rather an atypical ca. 74 kDa fragment; a similar atypical, apoptosis-related PARP fragment (ca. 60 kDa in MCF-7 cells) has been reported to be the result of a yet to be characterized calcium-dependent, calpain-like cysteine protease (59).

Curacin A alone caused little hypodiploidy in the time frame of these experiments. At time points later than 48 h, however, flow cytometry showed 100 nM curacin A did induce some hypodiploidy (ref. 7, 8; data not shown). Thus, detection of this atypical PARP cleavage product is an earlier, clearer indicator of apoptosis-related events than is flow cytometry in this system.

Co-treatment with PD098059 also increased the curacin A-induced expression levels of $p21^{CIP1/WAF1}$. As PC-3 cells are p53-null, this increase in $p21^{CIP1/WAF1}$ indicates cell cycle arrest via a p53-independent pathway that was enhanced by MEK1 inhibition. Since less G_2/M accumulation occurred in the combination-treated cells than in cells treated with curacin A alone, and an even greater $p21^{CIP1/WAF1}$ induction was seen in the combination treatment, the enhancement of MEK1 inhibition by simultaneous MT perturbation appears to allow $p21^{CIP1/WAF1}$ to monitor MT damage and assist in inducing G_1 arrest (48).

PD098059 also decreased stathmin expression when combined with curacin A. Stathmin (60), also named oncoprotein 18 (Op18) (and p17, p18, p19, 19K, prosolin, and metablastin), is a cytosolic phosphoprotein. In its non-phosphorylated form, stathmin assists in MT destabilization (61-64), either by sequestration of free tubulin heterodimers forming a ternary structure of one stathmin per two tubulin α/β heterodimers (65,66) or by promoting catastrophe on the plus end of MTs and enhancing GTP cap hydrolysis (67). Some studies show that stathmin is overexpressed in tumors (68,69) and overexpression of its non-phosphorylated form causes mitotic and G_2/M phase arrest (9,13,70,71). In contrast, decreased stathmin levels can increase MT polymer in vivo (72). Induction of p53 has been shown to down-regulate expression of stathmin (73,74). This is likely mediated through induction of $p21^{CIP1/WAF1}$. The importance of stathmin in this scenario has been shown in that antisense inhibition of its levels enhances PTX's cell killing effects (75,76).

Taken together, our data can be summarized in a proposed mechanism of cell death induction by combination of pretreatment with PD098059 followed by curacin A in PC-3 cells (Fig. 8). Curacin A's major action is MT perturbation. This action is related to phosphorylation of histone H3 and DNA condensation. Curacin A alone causes G_2/M arrest, Bcl-2 and Raf-1 phosphorylation which may be G_2/M related, and Raf-1 fragmentation which could be linked to caspase activity. [Note that the role of phosphorylated Raf-1 induced by curacin A (shown as Raf-1* in Fig. 8) should be distinguished from the ligand-receptor triggered (e.g., via Ras) phosphorylated Raf-1 (50,51)]. On the other hand, the curacin A-enhanced phosphorylation of MAPK regulators could be part of G_2/M events. Curacin A-induced phosphorylation of histone H3 could be related to its G_2/M arresting effect, or through the regulation of RSKs and p38MAPK (77). PD098059 enhanced curacin A's effects on caspase- and calpain-induced proteolysis of substrates. We suggest this was through increased Raf-1 fragmentation, decreased Bcl-2 and Raf-1 phosphorylation, increased $p21^{CIP1/WAF1}$ expression and the related down-regulation of stathmin, decreased Bax expression and increased PARP fragmentation. The PARP fragmentation occurred most likely via calpain, which also can inhibit cyclin D1 (57) to cause G_1 arrest. The increased $p21^{CIP1/WAF1}$ could be also part of this induction of calpain action.

Because MTs are ubiquitous structures in cells, it is reasonable that they should play important roles not only in support and control of cell shape, sister chromatid segregation and transport of vesicles, but also in signal transduction pathways (14). They are thus pivotal members of cellular biochemistry. Perturbation of MT dynamics is reflected in the most pronounced way at mitosis, the portion of the cell cycle in which cells arrest in response to MT-affecting drugs. The results here concur with those recently reported which support the notion that G_2/M arrest by MT-perturbing agents is dependent on a functional MEK/ERK pathway (22).

They also suggest that perturbation of MT dynamics, when the function of MEK1 is blocked, leads to an increase in the multifunctional effects of the cell cycle inhibitor $p21^{CIP1/WAF1}$ as well as to an enhancement of any apoptosis-inducing effects the MT-perturbing agent has. In summary, the combination treatment leads to an enhancement of curacin A's cytotoxic activity by causing cell cycle arrest at both G_1 and G_2/M, leading to the cascade of effects depicted in Fig. 8.

Acknowledgements – We are indebted to Prof. Richard A. Steinman for insightful commentary on this work and to Dr. Wenjing Xu for the sample of synthetic curacin A.

REFERENCES

1. Gerwick, W. H., Proteau, P. J., Nagle, D. G., Hamel, E., Blokhin, A., and Slate, D. L. (1994) *J. Org. Chem.* **59,** 1243–1245
2. Wipf, P., and Xu, W. (1996) *J. Org. Chem.* **61,** 6556–6562
3. Hamel, E., Blokhin, A. V., Nagle, D. G., Yoo, H.-D., and Gerwick, W. H. (1995) *Drug Dev. Res.* **34,** 110–120
4. Blokhin, A. V., Yoo, H.-D., Geralds, R.-S., Nagle, D. G., Gerwick, W. H., and Hamel, E. (1995) *Mol. Pharmacol.* **48,** 523–531
5. Verdier-Pinard, P., Lai, J.-Y., Yoo, H. D., Yu, J., Marquez, B., Nagle, D. G., Nambu, M., White, J. D., Falck, J. R., Gerwick, W. H., Day, B. W., and Hamel, E. (1998) *Mol. Pharmacol.* **53,** 62–76
6. Verdier-Pinard, P., Sitachitta, N., Rossi, J. V., Sackett, D. L., Gerwick, W. H., and Hamel, E. (1999) *Arch. Biochem. Biophys.* **370,** 51–58
7. Chen, P.-H., Balachandran, R., Grant, S. G., Xu, W., Wipf, P., and Day, B. W. (1998) *Proc. Am. Assoc. Cancer Res.* **39,** 192
8. Chen, P.-H., Balachandran, R., Grant, S. G., Xu, W., Wipf, P., and Day, B. W. (1999) *Proc. Am. Assoc. Cancer Res.* **40,** 286
9. Andersen, S. S. (1999) *Bioessays* **21,** 53–60
10. Di Paolo, G., Antonsson, B., Kassel, D., Riederer, B. M., and Grenningloh, G. (1997) *FEBS Lett.* **416,** 149–152
11. Moreno, F. J., and Avila, J. (1998) *Mol. Cell. Biochem.* **183,** 201–209
12. Rodionov, V., Nadezhdina, E., and Borisy, G. (1999) *Proc. Natl. Acad. Sci. U. S. A.* **96,** 115–120
13. Andersen, S. S., Ashford, A. J., Tournebize, R., Gavet, O., Sobel, A., Hyman, A. A., and Karsenti, E. (1997) *Nature* **389,** 640–643
14. Gunderson, G. G., and Cook, T. A. (1999) *Curr. Opin. Cell Biol.* **11,** 81–94
15. Zecevic, M., Catling, A. D., Eblen, S. T., Renzi, L., Hittle, J. C., Yen, T. J., Gorbsky, G. J., and Weber, M. J. (1998) *J. Cell Biol.* **142,** 1547–1558
16. Reszka, A. A., Seger, R., Diltz, C. D., Krebs, E. G., and Fischer, E. H. (1995) *Proc. Natl. Acad. Sci. U. S. A.* **92,** 8881–8885
17. Okano, J. and Rustgi, A. K. (2001) *J. Biol. Chem.* **276,** 19555–19564
18. Stone, A. A., and Chambers, T. C. (2000) *Exp. Cell Res.* **254,** 110–119.
19. Dudley, D. T., Pang, L., Decker, S. J., Bridges, A. J., and Saltiel, A. R. (1995) *Proc. Natl. Acad. Sci. U. S. A.* **92,** 7686–7689
20. Alessi, D. R., Cuenda, A., Cohen, P., Dudley, D. T., and Saltiel, A. R. (1995) *J. Biol. Chem.* **270,** 27489–27494
21. Wright, J. H., Munar, E., Jameson, D. R., Andreassen, P. R., Margolis, R. L., Seger, R., and Krebs, E. G. (1999) *Proc. Natl. Acad. Sci. U. S. A.* **96,** 11335–11340
22. Hayne, C., Tzivion, G., and Luo, Z. (2000) *J. Biol. Chem.* **275,** 31876–31882
23. Lovric, J., Dammeier, S., Kieser, A., Mischak, H., and Kolch, W. (1998) *J. Biol. Chem.* **273**(35), 22848–22855
24. Blagosklonny, M. V., Giannakakou, P., El-Deiry, W. S., Kinsgton, D. G. I., Higgs, P. I., Neckers, L., and Fojo, T. (1997) *Cancer Res.* **57,** 130–135
25. Reed, J. C. (1994) *J. Biol. Chem.* **124,** 1–6
26. Kroemer, G. (1997) *Nature Med.* **3,** 614–620

27. Yamamoto, A. M., Eloy, L., Bach, J. F., and Garchon, H. J. (1998) *Leukemia* **12,** 1467–1472
28. Wood, D. E., Thomas, A., Devi, L. A., Berman, Y., Beavis, R. C., Reed, J. C., and Newcomb, E. W. (1998) *Oncogene* **17,** 1069–1078
29. Wood, D. E., and Newcomb, E. W. (1999) *J. Biol. Chem.* **274,** 8309–8315
30. Srivastava, R. K., Mi, Q.-S., Hardwick, J. M., and Longo, D. L. (1999 *Proc. Natl. Acad. Sci. U. S. A.* **96,** 3775–3780
31. Nuydens, R., Dispersyn, G., Van Den Kieboom , G., de Jong, M., Connors, R., Ramaekers, F., Borgers, M., and Geerts, H. (2000) *Apoptosis* **5,** 43–51
32. Nuydens, R., Dispersyn, G., Van Den Kieboom , G., de Jong, M., Connors, R., Ramaekers, F., Borgers, M., and Geerts, H. (2000) *Apoptosis* **5,** 335–343
33. Ling, Y.-H., Tornos, C., and Perez-Soler, R. (1998) *J. Biol. Chem.* **273,** 18984–18991
34. Scatena, C. D., Stewart, Z. A., Mays, D., Tang, L. J., Keefer, C. J., Leach, S. D., and A., P. J. (1998) *J. Biol. Chem.* **273,** 30777–30784
35. Wang, H. G., and Reed, J. C. (1998) *Biofactors* **8,** 13–16
36. Magnuson, N. S., Beck, T., Vahidi, H., Hahn, H., Smola, U., and Rapp, U. R. (1994) *Semin. Cancer Biol.* **5,** 247–253
37. Wartmann, M., Hofer, P., Turowski, P., Saltiel, A. R., and Hynes, N. E. (1997) *J. Biol. Chem.* **272,** 3915–3923
38. Woods, D., Parry, D., Cherwinski, H., Bosch, E., Lees, E., and McMahon, M. (1997) *Mol. Cell. Biol.* **17,** 5598–5611
39. Blagosklonny, M. V., Schulte, T., Nguyen, P., Trepel, J., and Neckers, L. M. (1996) *Cancer Res.* **56,** 1851–1854
40. Rasouli-Nia, A., Liu, D., Perdue, S., and Britten, R. A. (1998) *Clin. Cancer Res.* **4,** 1111–1116
41. Morrison, D. K., and Cutler, J. R. E. (1997) *Curr. Opin. Cell Biol.* **9,** 174–179
42. Giuliano, K. A., DeBiasio, R. L., Dunlay, T., Gough, A., M., V. J., Zock, J., Pavlakis, G. N., and Taylor, D. L. (1997) *J. Biomol. Screen.* **2,** 249–259
43. Goto, H., Tomono, Y., Ajiro, K., Kosako, H., Fujita, M., Sakurai, M., Okawa, K., Iwamatsu, A., Okigaki, T., Takahashi, T., and Inagaki, M. (1999) *J. Biol. Chem.* **274,** 25543–25549
44. Sauve, D. M., Anderson, H. J., Ray, J. M., James, W. M., and Roberge, M. (1999) *J. Cell Biol.* **145,** 225–235
45. Wipf, P., Reeves, J.T., Balachandran, R., Giuliano, K.A., Hamel, E., and Day, B.W. (2000) *J. Am. Chem. Soc.* **122,** 9391–9395
46. Thomson, S., Clayton, A. L., Hazzalin, C. A., Rose, S., Barratt, M. J., and Mahadevan, L. C. (1999) *EMBO J.* **18,** 4779–4793
47. Medema, R. H., Klompmaker, R., Smits, V. A., and Rijksen, G. (1998) *Oncogene* **16,** 431–441
48. Duli´c, V., Stein, G. H., Far, D. F., and Reed, S. I. (1998) *Mol. Cell. Biol.* **18,** 546–557
49. Fan, M., Du, L., Stone, A. A., Gilbert, K. M., and Chambers, T. C. (2000) *Cancer Res.* **60,** 6403–6407
50. Laird, A. D., Taylor, S. J., Oberst, M., and Shalloway, D. (1995) *J. Biol. Chemistry* **270,** 26742-26745
51. Ziogas, A., Lorenz I, C., Moelling, K., and Radziwill, G. (1998) *J. Biol. Chem.* **273,** 24108–24114

52. Widmann, C., Gibson, S., and Johnson, G. L. (1998) *J. Biol. Chem.* **273,** 7141–7147
53. Johnson, D. E. (2000) *Leukemia* **14,** 1695–1703
54. Knepper-Nicolai, B., Savill, J., and Brown, S. B. (1998) *J. Biol. Chem.* **273,** 30530-30536
55. McGinnis, K. M., Gnegy, M. E., Park, Y. H., Mukerjee, N., and Wang, K. K. (1999) *Biochem. Biophys. Res. Comm.* **263,** 94–99
56. Wood, D. E., and Newcomb, E. W. (2000) *Exp. Cell Res.* **256,** 375–382
57. Wang, K. K. (2000) *Trends Neurosci.* **23,** 20–26
58. Stadheim, T. A., Xiao, H., and Eastman, A. (2001) *Cancer Res.* **61,** 1533–1540
59. Pink, J. J., S., W.-D., Tagliarino, C., Planchon, S. M., Yang, X., Froelich, C. J., and Boothman, D. A. (2000) *Exp. Cell Res.* **255,** 144–155
60. Mistry, S. J., Li, H. C., and Atweh, G. F. (1998) *Biochem. J.* **334,** 23–29
61. McNally, F. J. (1999) *Curr. Biol.* **9,** R274–R276
62. Lawler, S. (1998) *Curr. Biol.* **8,** R212–R214
63. Steinmetz, M. O., Kammerer, R. A., Jahnke, W., Goldie, K. N., Lustig, A., and van Oostrum, J. (2000) *EMBO J.* **19,** 572–580
64. Wallon, G., Rappsilber, J., Mann, M., and Serrano, L. (2000) *EMBO J.* **19,** 213–222
65. Jourdain, L., Curmi, P., Sobel, A., Pantaloni, D., and Carlier, M. F. (1997) *Biochemistry* **36,** 10817–10821
66. Curmi, P. A., Andersen, S. S., Lachkar, S., Gavet, O., Karsenti, E., Knossow, M., and Sobel, A. (1997) *J. Biol. Chem.* **272,** 25029–25036
67. Belmont, L. D., and Mitchison, T. J. (1996) *Cell* **84,** 623–631
68. Mistry, S. J., and Atweh, G. F. (1999) *Anticancer Res.* **19,** 573–577
69. Curmi, P., Nogues, C., Lachkar, S., Carelle, N., Gonthier, M. P., Sobel, A., Lidereau, R., and Bieche, I. (2000) *Brit. J. Cancer* **82,** 142–150
70. Luo, X. N., Mookerjee, B., Ferrari, A., Mistry, S., and Atweh, G. F. (1994) *J. Biol. Chem.* **269,** 10312–10318
71. Andersen, S. S. (2000) *Trends Cell Biol.* **10,** 261–267
72. Howell, B., Deacon, H., and Cassimeris, L. (1999) *J. Cell Sci.* **112,** 3713–3722
73. Ahn, J., Murphy, M., Kratowicz, S., Wang, A., Levine, A. J., and George, D. L. (1999) *Oncogene* **18,** 5954–5958
74. Johnsen, J. I., Aurelio, O. N., Kwaja, Z., Jörgensen, G. E., Pellegata, N. S., Plattner, R., Stanbridge, E. J., and Cajot, J.-F. (2000) *Int. J. Cancer* **88,** 685–691
75. Iancu, C., Mistry, S. J., Arkin, S., and Atweh, G. F. (2000) *Cancer Res.* **60,** 3537–3541
76. Iancu, C., Mistry, S. J., Arkin, S., Wallenstein, S., and Atweh, G. F. (2001) *J. Cell Sci.* **114,** 909–916
77. Zhong, S. P., Ma, W. Y., and Dong, Z. (2000) *J. Biol. Chem.* **275,** 20980–20984

FIGURE LEGENDS

FIG. 1. **Curacin A inhibits PC-3 cell growth while PD098059 has little to no effect.** Structures of the agents are shown. PD098059 or vehicle was given 1h before addition of curacin A or vehicle to cells. Cells were harvested at 0 and 48h of curacin A treatment. Cell numbers were determined microscopically by counting Trypan blue-excluding cells from a metered aliquot of total cells.

FIG. 2. **PD098059 dampens curacin A-induced G_2/M accumulation.** *A*, Histograms of PC-3 cellular DNA after treatment with vehicle (*treatment 1*), PD098059 only (*treatments 2-5*), curacin A only (*treatment 10*), or combination of the agents (*treatments 6-9*) for 48h as described in the legend of Fig. 1. Numbers above the bars in the histograms give the percentage of cells in that region. *B*, Graphical summaries of hypodiploid (upper) and ratios of G_2M/G_1 (lower) cell subpopulation percentages. ($N = 2$).

FIG. 3. **Effects of PD098059 and/or curacin A on phospho-ERK levels in PC-3 cells.** Western blots for phospho-ERK1/2 (*A*), total ERK1/2 (*B*), and histograms showing the ratios of phospho-ERK1/2 to total ERK1/2 (*C*). Cells were lysed, protein concentrations were determined, equal amounts of proteins were loaded and separated by SDS-PAGE, transferred to nitrocellulose membranes, and probed by Western blotting. Equal loading in lanes was confirmed by Western blot analysis of the same membrane with anti-β-actin (data not shown).

FIG. 4. **Western blots for Bcl-2, Raf-1, PARP, Bax, stathmin, and $p21^{CIP1/WAF1}$ in PC-3 cells at 1 and 48 h of treatment with curacin A after a 1 h pre-treatment with PD098059 or vehicle.** Equal amounts of proteins were separated by SDS-PAGE and analyzed for the proteins as described in the legend of Fig. 3. Pretreatment with PD098059 caused the following effects: decreased the Bcl-2 phosphorylation induced by curacin A and the levels of this protein; reduced curacin A-induced Raf-1 phosphorylation and enhanced curacin A-induced Raf-1 fragmentation; increased curacin A-induced formation of a PARP fragment; decreased the levels of Bax and stathmin, and increased the curacin A-induced expression levels of $p21^{CIP1/WAF1}$.

FIG. 5. **Multiparameter morphological analysis of microtubule-drug-treated PC-3 cells.** Cells were left untreated (*A-D*), or were treated with concentrations near the GI_{100} of paclitaxel (13.5 nM; *E-H*), curacin A (116 nM; *I-L*), or vinblastine (1.35 nM; *M-P*) for 14.5 h. *Q-T*, Cells treated with 270 nM curacin A. Cells were then multiply labeled for nuclei (*A*, *E*, *I*, *J*, *Q*), α-tubulin (*B*, *F*, *J*, *N*, *R*), phosphorylated p38MAPK (*C*, *G*, *K*, *O*, *S*), and phosphorylated RSK1 (*D*, *H*, *L*, *P*, *T*). Arrows, as read across a row of images, indicate the same cells labeled for four different physiological parameters. The images show cytoskeletal and nuclear morphological changes as well as stress pathway activation in mitotic cells (*A-D*) and cells blocked at G_2/M (*E-T*).

FIG. 6. **Microtubule drugs have varied effects on nuclear condensation.** PC-3 cells were treated with microtubule drugs as described in FIG. 5 and the condensation of nuclei determined with HCS. The data were consistent with curacin A and vinblastine producing morphologically similar condensed nuclei. The decreased nuclear condensation ratio and statistically

heterogeneous response at higher drug concentrations was due to the enhanced loss of cells with condensed nuclei (G_2/M blocked) from the substrate.

FIG. 7. **Multiparameter HCS of PC-3 cells responding to microtubule drugs.** Cells were titrated with drugs as in Fig. 5 and labeled for the activation of molecular pathways involved in phosphorylation of histone H3 (*A*), ERK activation (*B*), p38MAPK activation (*C*), and JNK activation (*D*). While there were obvious differences in drug potency, all three drugs activated molecular pathways involved in cellular mitosis and stress to nearly the same extent.

FIG. 8. **Mechanisms of action of curacin A in PC-3 prostate carcinoma cells.** Red-colored portion shows curacin A's effects detected in this study. Blue-colored parts show the changes in combination with PD098059.

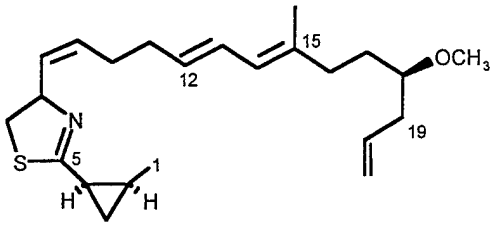

(+)-Curacin A

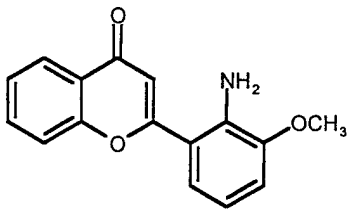

PD098059

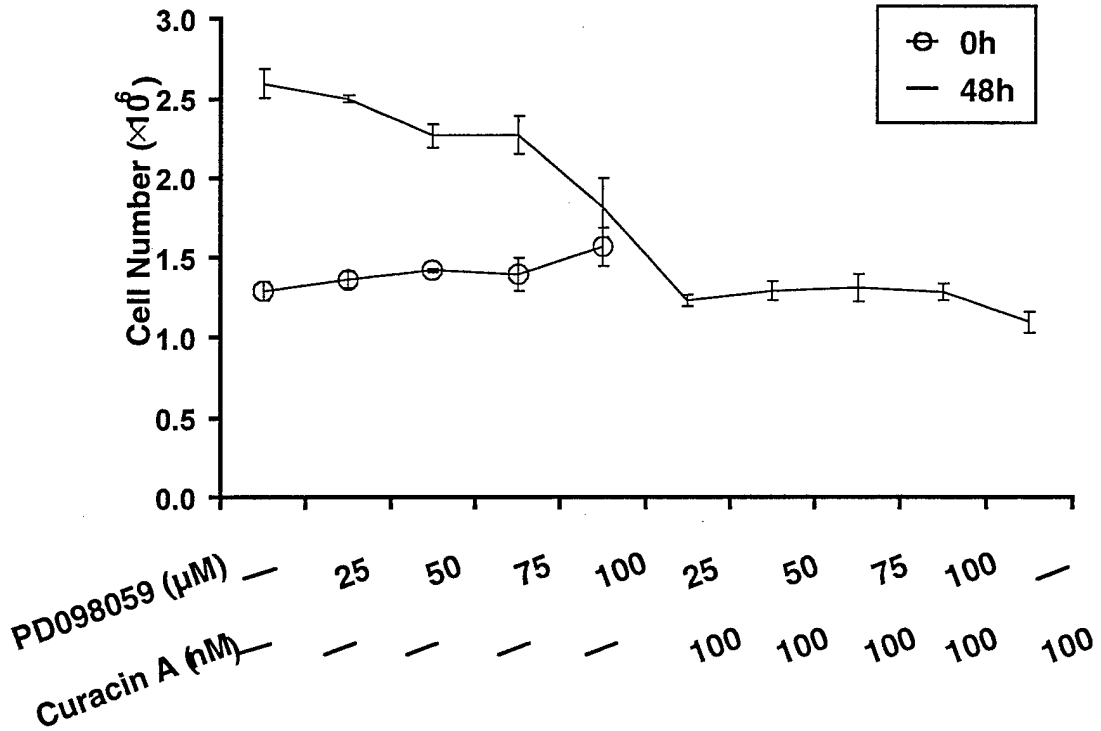

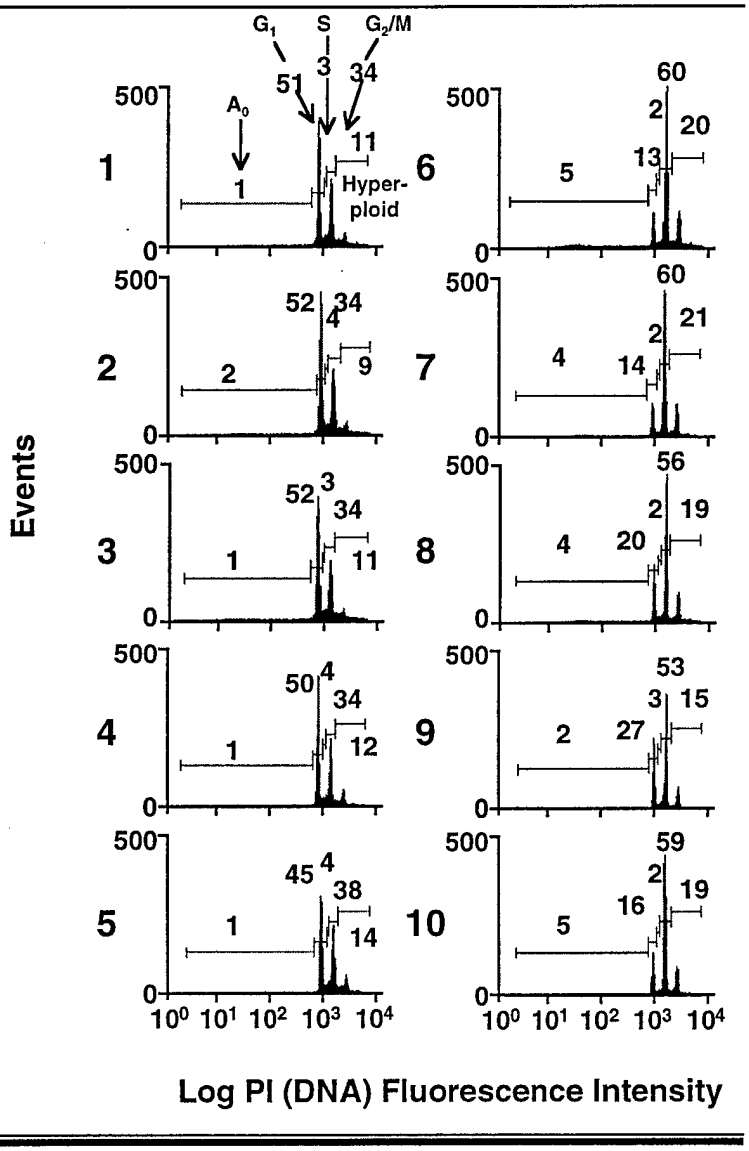
48 h
G1
S
G2/M
A0
Hyper-
ploid
Events
Log PI (DNA) Fluorescence Intensity
500
0
10^0 10^1 10^2 10^3 10^4
1
51
3
34
11
1
6
60
2
20
5
13
2
52
4
34
9
2
7
60
2
21
4
14
3
52
3
34
11
1
8
56
2
19
4
20
4
50
4
34
12
1
9
53
3
15
2
27
5
45
4
38
14
1
10
59
2
19
16
5

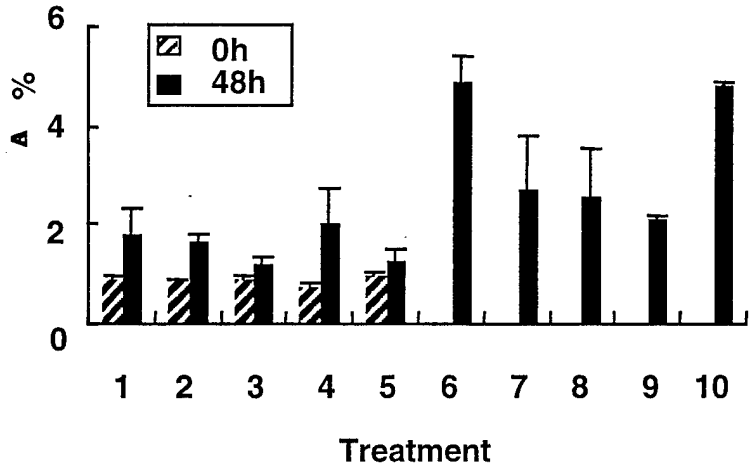

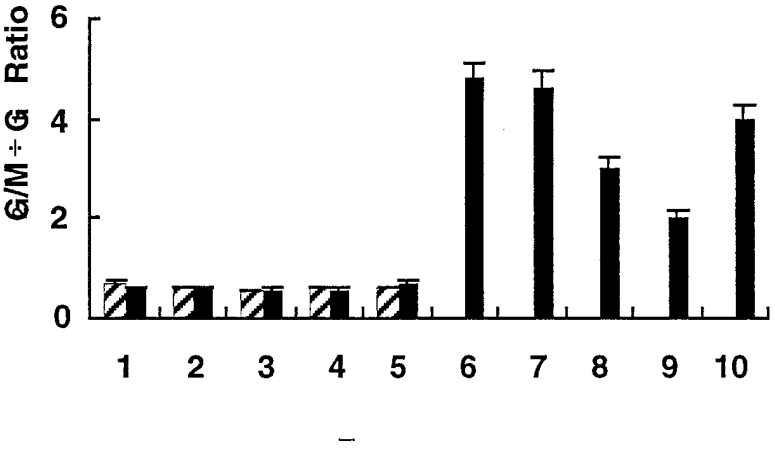

Treatment	1	2	3	4	5	6	7	8	9	10
PD098059 (μM)	—	25	50	75	100	25	50	75	100	—
Curacin A (nM)	—	—	—	—	—	100	100	100	100	100

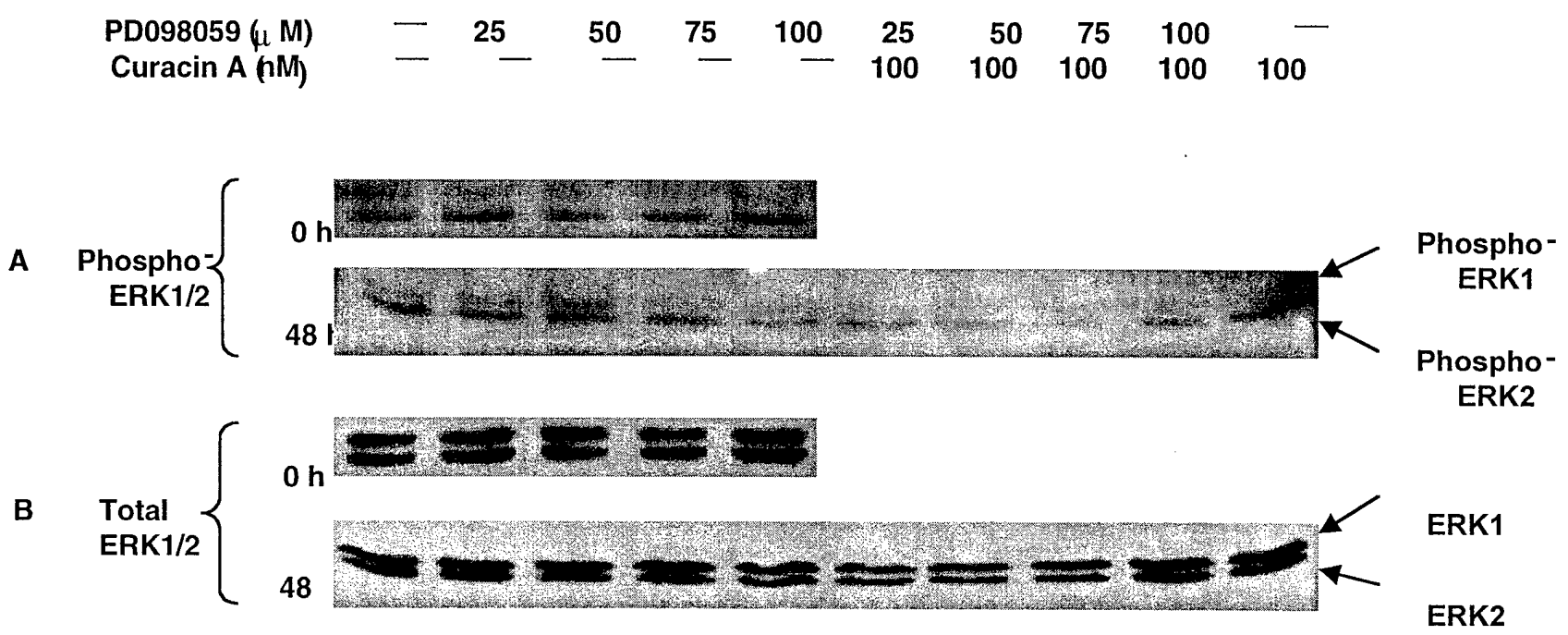
PD098059 (μ M) — 25 50 75 100 25 50 75 100 —
Curacin A (nM) — — — — — 100 100 100 100 100
A
Phospho-ERK1/2
0 h
48 h
Phospho-ERK1
Phospho-ERK2
B
Total ERK1/2
0 h
48
ERK1
ERK2

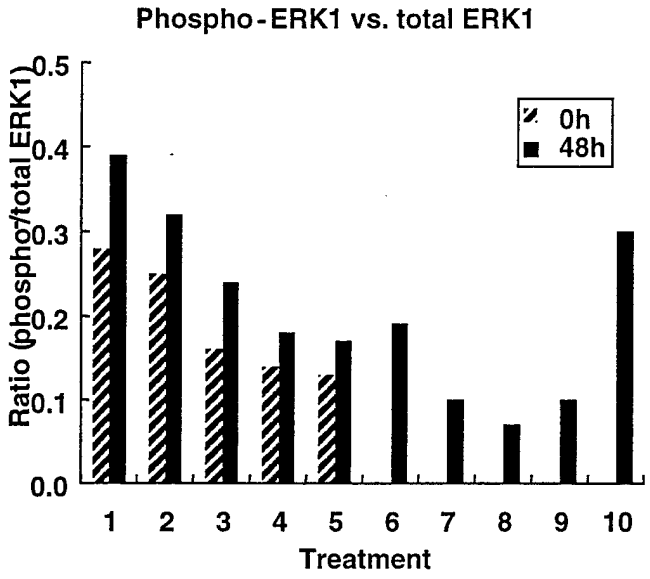
Phospho-ERK1 vs. total ERK1
Ratio (phospho/total ERK1)
0.0
0.1
0.2
0.3
0.4
0.5
0h
48h
1 2 3 4 5 6 7 8 9 10
Treatment

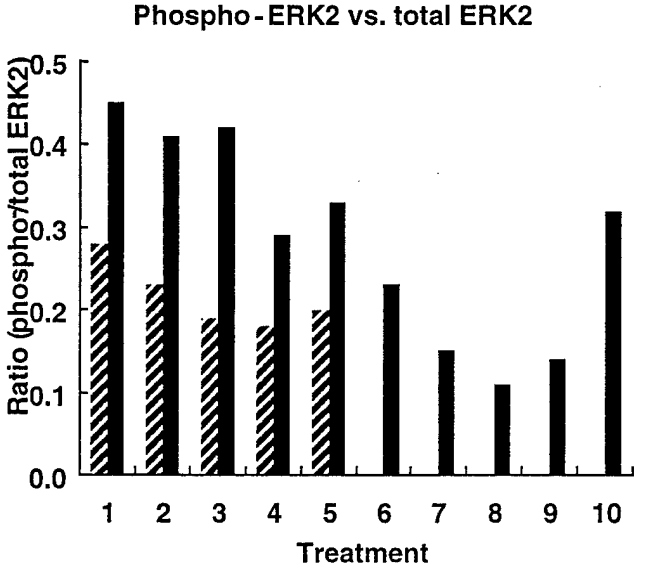
Phospho-ERK2 vs. total ERK2
Ratio (phospho/total ERK2)
0.0
0.1
0.2
0.3
0.4
0.5
1 2 3 4 5 6 7 8 9 10
Treatment

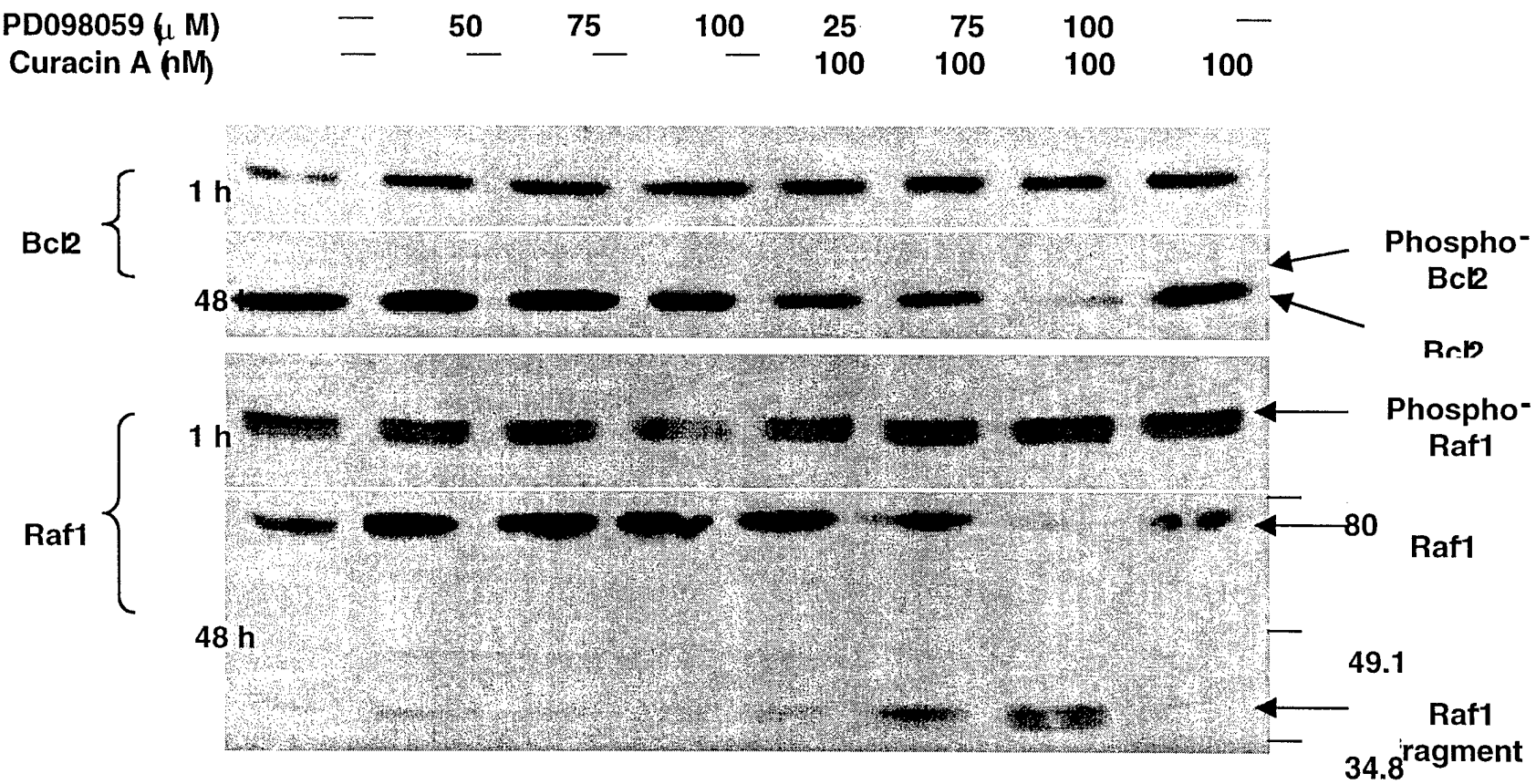
PD098059 (μ M)
—
50
75
100
25
75
100
—
Curacin A (nM)
—
—
—
—
100
100
100
100
Bcl2
1 h
48 h
Phospho-Bcl2
Bcl2
Raf1
1 h
48 h
Phospho-Raf1
80
Raf1
49.1
Raf1 fragment
34.8

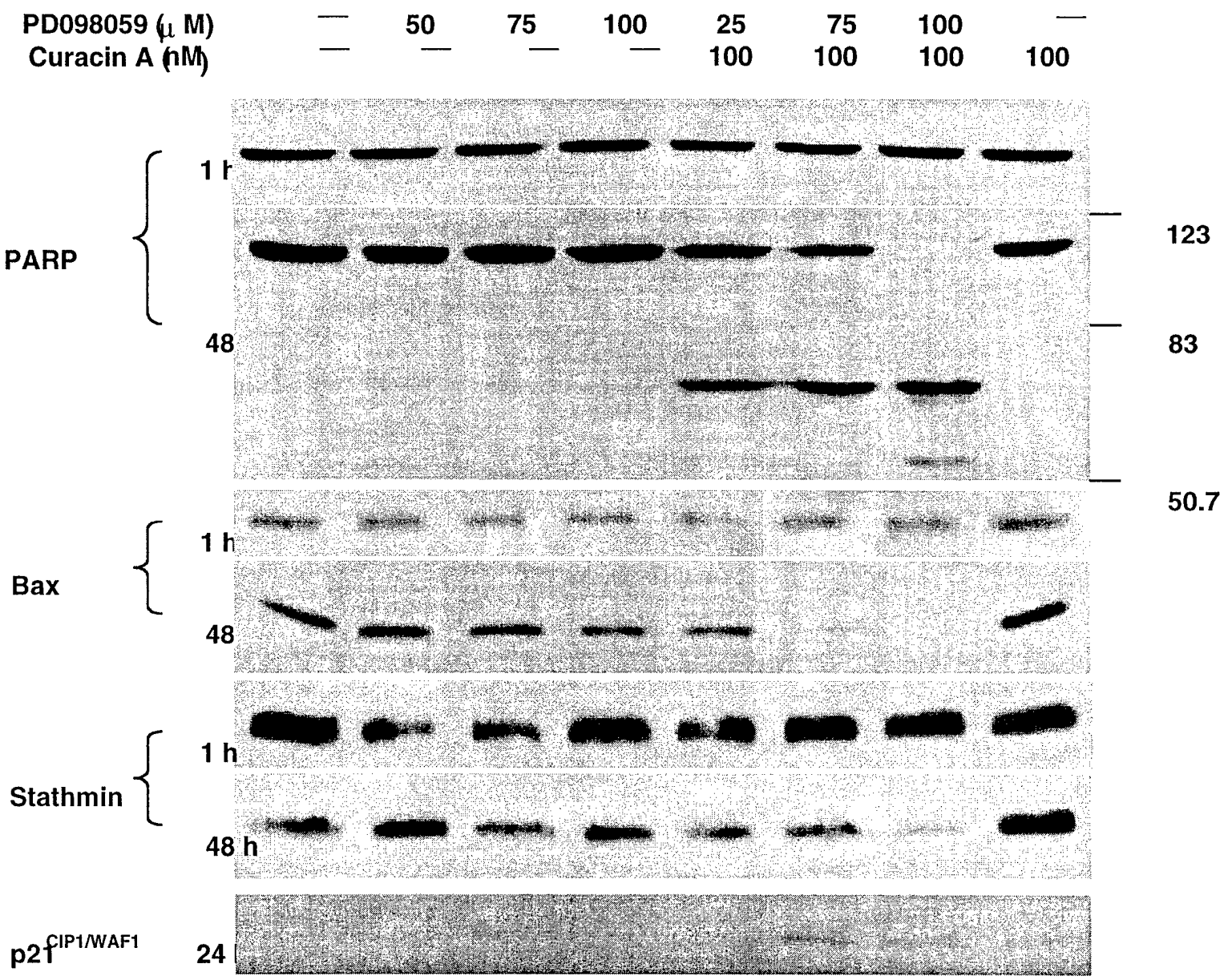
PD098059 (μ M)
— 50 75 100 25 75 100 —
Curacin A (nM)
— — — — 100 100 100 100
PARP
1 h
48
123
83
50.7
Bax
1 h
48
Stathmin
1 h
48 h
p21CIP1/WAF1
24

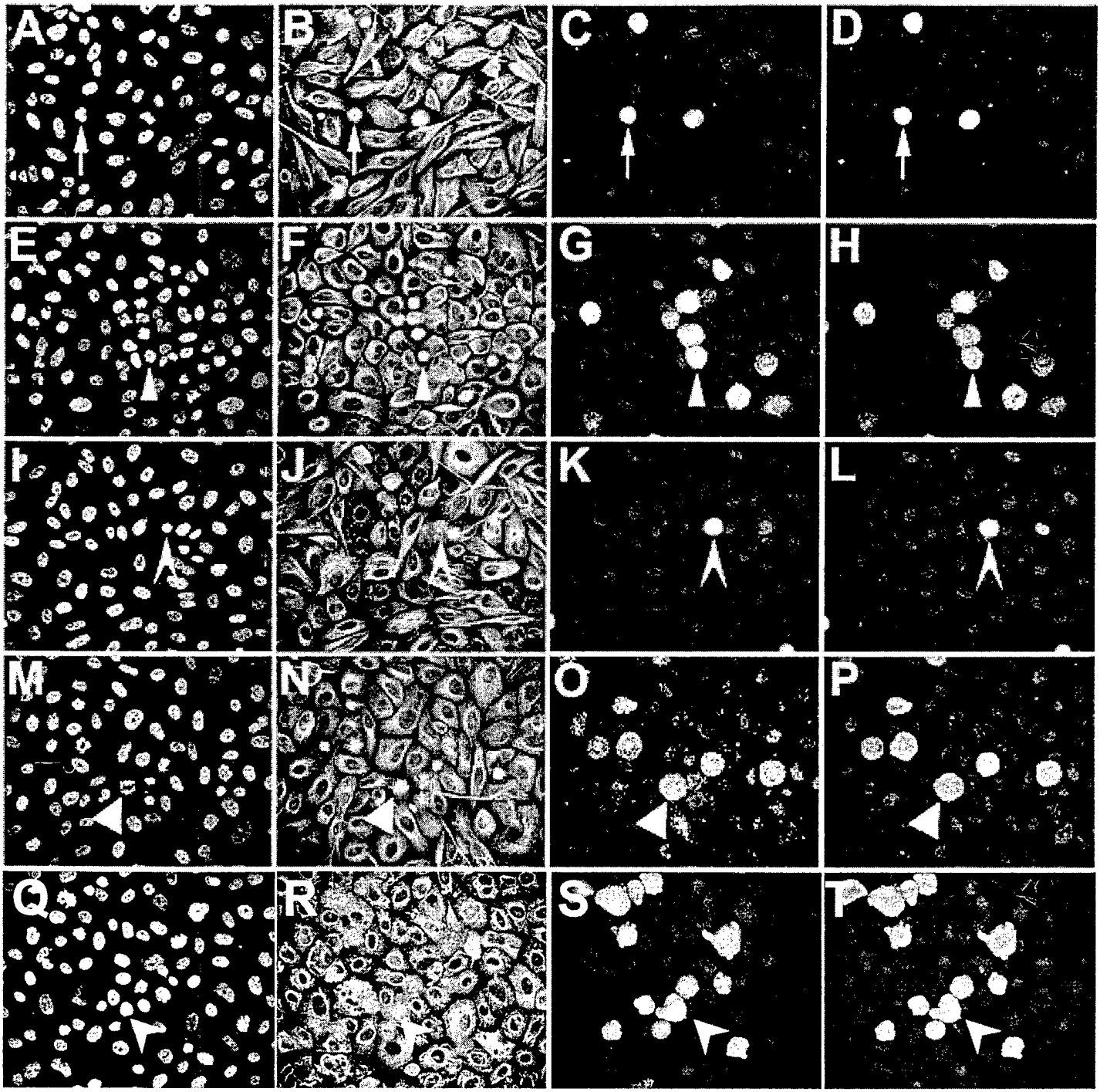
A
B
C
D
E
F
G
H
I
J
K
L
M
N
O
P
Q
R
S
T

Identification of Cyclin B1 as a Shared Human Epithelial Tumor-Associated Antigen Recognized by T Cells

Henry Kao[*], Jarrod A. Marto[¶], Thomas K. Hoffmann[†], Jeffrey Shabanowitz[¶], Sydney D. Finkelstein[‡], Theresa L. Whiteside[†], Donald F. Hunt[¶#], and Olivera J. Finn[*†]

[*]Department of Molecular Genetics & Biochemistry, [†]University of Pittsburgh Cancer Institute, [‡]Department of Pathology, University of Pittsburgh School of Medicine, Pittsburgh, PA 15261, [¶]Department of Chemistry, [#]Department of Pathology, University of Virginia, Charlottesville, VA 22901, USA.

Running Title: Cyclin B1 as a tumor antigen

Keywords: HLA Class I, peptides, ELISPOT, tandem mass spectrometry

Corresponding Address:

To whom requests for reprints should be addressed: Dr. Olivera J. Finn, University of Pittsburgh School of Medicine, Department of Molecular Genetics & Biochemistry, W1142 Biomedical Science Tower, Terrace & DeSoto Streets, Pittsburgh, PA 15261. Tel: (412) 648-9816, Fax: (412) 383-8859, E-mail: ojfinn@pitt.edu.

Total Word Count: 7650

Abstract

We eluted peptides from class I molecules of an HLA-A2.1$^+$ breast adenocarcinoma and loaded RP-HPLC fractions onto DCs to prime CD8$^+$ T cells from a healthy donor. Peptide fractions that supported growth of tumor-specific CTL were sequenced by nano-HPLC micro-ESI tandem mass spectrometry. Six HLA-A2.1-binding peptides, four 9-mers (P1-P4) differing in the C-terminal residue, and two 10-mers (P5-P6) with an additional C-terminal alanine, were identified in one fraction. The peptide sequences were homologous to cyclin B1. We primed CD8$^+$ T cells from another HLA-A2.1$^+$ healthy donor *in vitro* and generated responses to P4. We also detected secondary T cell responses to one or more of the peptides in four of six breast cancer patients and four of five patients with squamous cell carcinomas of the head and neck. Immunohistochemical analysis of the tumor line from which the peptides were derived, a lung adenocarcinoma line and SCCHN tumors showed overexpression of cyclin B1 and its aberrant localization in the cytoplasm instead of the nucleus. Sequencing genomic and cDNA corresponding to P1-P6 region showed that differences in C-terminal residues were not due to mutations in the DNA or mRNA suggesting instead a high error rate in translation of cyclin B1 in tumors.

Introduction

For tumor-specific immunotherapy to be successful, tumor antigens must be identified that are effective in inducing strong immune responses in the host. A number of methods have been described to identify tumor antigens, including transfection of recombinant tumor cDNA libraries and HLA molecules into target cells ("genetic approach") (1, 2), elution of peptides from the binding cleft of tumor HLA molecules ("peptide-elution approach") (3, 4), deduction of peptide sequences from known oncogenes or tumor-associated proteins using known HLA-anchor motifs ("reverse immunology approach") (5, 6), and more recently, serological analysis of recombinant tumor cDNA expression libraries (SEREX) (7). These methods have led to the discovery of a number of tumor antigens, primarily in melanomas (8). These tumor antigens have been classified into five categories: a) cancer testis antigens, such as MAGE (9, 10), BAGE (11), GAGE (12), and more recently, NY-ESO-1 (13); b) differentiation antigens, such as gp100 (14), Melan-A/Mart-1 (2, 15), and tyrosinase (1); c) mutated antigens, such as cdk4 (16), β-catenin (17), and cdc27 (18); d) overexpressed and/or ubiquitous antigens, such as PRAME (19), and p53 (20), and e) viral antigens, such as HPV (21) and EBV (22). Very few tumor-specific antigens have been identified in epithelial tumors, the best known being CEA (23), PSA (24), Her-2/Neu (25) and MUC-1 (26).

We recently described a novel method for tumor antigen discovery whereby we primed naïve $CD8^+$ T cells from healthy donors to *in vitro* generated dendritic cells loaded with peptides eluted from HLA Class I molecules of a breast cancer cell line (27). We identified several tumor peptide fractions that supported growth of tumor-specific CTL, suggesting that these fractions contained peptides that could potentially be tumor antigens. In this paper we report that one of these tumor peptide fractions contained peptides derived from cyclin B1, a checkpoint protein

that regulates the transition from the G2 to M phase of the cell cycle (28). Staining of the tumor cell line with anti-cyclin B1 antibody revealed that this protein was greatly overexpressed and found mostly in the cytoplasm rather than in its normal location, the nucleus. We were able to prime naive $CD8^+$ T cells from another healthy donor using synthetic peptides and detect T cell responses to one of the peptides via the IFN-γ ELISPOT[1] assay. We also detected secondary T cell responses to one or more of these peptides in breast cancer patients and patients with squamous cell carcinomas of the head and neck head (SCCHN). Where we were able to evaluate, these T cell responses correlated with the overexpression of cyclin B1 protein in the patients' tumors. In the fresh tumor samples as well, the overexpressed protein was found predominantly in the cytoplasm instead of the nucleus. We propose that this aberrant overexpression of cyclin B1 in the cytoplasm leads to over abundance of cyclin B1-derived peptides on tumor HLA Class I molecules, which can now play a role of tumor antigens recognized by T cells.

[1] Abbreviations used in this paper: ELISPOT, enzyme-linked immunospot; SCCHN, squamous cell carcinoma of the head and neck.

Materials and Methods

Cells and Tumor Cell lines. MS-A2 is an HLA-A*0201$^+$ transfected tumor cell line derived from a breast adenocarcinoma cell line, MS, characterized in our laboratory (27, 29). The lung tumor cell line, 201T, was obtained from Dr. Jill Siegfried, University of Pittsburgh School of Medicine. The head and neck tumor cell line, PCI-13, was also established by us (30). T cells, dendritic cells (DCs), and macrophages were derived from the peripheral blood of HLA-A*0201$^+$ healthy donor and cancer patients under an IRB approved protocol and with signed informed consent.

Peptide Synthesis. All peptides used in this study were synthesized with F-moc chemistry using the 432A Synergy Peptide Synthesizer (Applied Biosystems, Foster City, CA). Peptides were purified by RP-HPLC to greater than 85% purity, and dissolved in DMSO and frozen until further use.

Antibodies. MA2.1, a mouse anti-human HLA-A2.1 antibody, was produced by the MA2.1 hybridoma; W6/32, a mouse anti-human MHC Class I antibody, was produced by the W6/32 hybridoma; both were obtained from the American Tissue Culture Collection (ATCC, Manasas, VA). GNS-1, a mouse anti-human cyclin B1 antibody, was purchased from BD Pharmingen, Franklin Lakes, NJ.

Mass spectrometry (MS) Data Acquisition. Active first-dimension HPLC fractions were screened for peptide content on a home-built Fourier transform mass spectrometer (FTMS),

equipped with a nano-flow high performance liquid chromatography micro-electrospray ionization (nano-HPLC micro-ESI) interface (31). Nano-HPLC columns were constructed from 50 μm I.D. fused silica capillaries and packed with an 8 cm bed length of 5 μm diameter reversed phase beads. An integrated microESI emitter tip (~2 μm diameter) was located a few mm from the column bed. Typically, ~0.75 μL (corresponding to ~2.3 x 10^8 cell equivalents or ~1.5%) of an active, first-dimension HPLC fraction was loaded onto a column and eluted directly into the mass spectrometer with a linear, 17 minute gradient of 0-70% acetonitrile in 0.1% acetic acid. Full scan mass spectra, over a mass-to-charge (*m/z*) range 300 *m/z* 2500, were acquired at a rate of approximately 1 scan/second.

Mass Spectrometry/Mass Spectrometry (MS/MS) Data Acquisition. Mass spectrometry/mass spectrometry (MS/MS) data were acquired on a Finnigan LCQ quadrupole ion trap mass spectrometer (Finnigan Corp., San Jose, CA), equipped with a nano-HPLC micro-ESI source as described above. Typically, ~1.5 μL (corresponding to ~ 4.5 x 10^8 cell equivalents or ~3%) of an active, first-dimension HPLC fraction was loaded onto a column eluted directly into the mass spectrometer with a linear, 30 minute gradient of 0-30% acetonitrile in 0.1% acetic acid. Data dependent spectral acquisition (32) was performed as follows: A full scan mass spectrum (MS) was acquired over the range 300 *m/z* 2000. The instrument control computer then selected the top 5 most abundant ion species in the MS scan for subsequent MS/MS analysis over the next 5 scans. After acquiring MS/MS data on a particular ion species, its corresponding *m/z* value was excluded from consideration by the instrument control computer for a period equal to the observed chromatographic peak width (approximately 1.5 minutes for the data herein). This data acquisition procedure minimized redundancy and allowed MS/MS analysis on peptide

species whose abundances spanned a wide dynamic range. After acquisition, tandem mass spectral data were searched using SEQUEST (33), an algorithm that matches uninterpreted MS/MS spectra to theoretical spectra for peptides generated from user-specified databases. All data herein were searched against non-redundant (nr) protein databases compiled at the National Center for Biotechnology Information (NCBI). In addition, manual (e.g. de novo) interpretation of MS/MS spectra was performed. Peptide sequence information obtained in this manner was compared to sequences in the nr protein database using the MS-TAG algorithm (34). Candidate peptide sequences were subsequently confirmed by comparison of their MS/MS spectra acquired for synthetic analogs.

MHC Class I stabilization assays. Peptide-induced stabilization of HLA-A2.1 molecules on T2 cells was done as previously described (35). 2×10^5 T2 cells were incubated with 20 μg/ml of the indicated synthetic peptides in 3 μg/ml human B_2m (Calbiochem, La Jolla, CA) for 18-20 hours at room temperature. The cells were then stained with the HLA-A2.1-specific antibody, MA2.1, for 45 minutes, washed with FACS Buffer (PBS, 5% FBS, and 0.01% sodium azide), and stained with a secondary FITC-conjugated anti-IgG antibody (Biosource International, Camarillo, CA). The cells were fixed in 4% formaldehyde prior to flow cytometry analysis. The negative control consisted of T2 cells without peptide. The positive control consisted of T2 cells loaded with the Flu matrix peptide, GILGFVFTL. Flow cytometric analysis was done using a FACScan flow cytometer (Becton-Dickinson). Experimental results are depicted as X-Fold increase = (Mean Fluorescent Intensity of T2 cells loaded with peptide/Mean Fluorescent Intensity of T2 cells with no peptide). An X-Fold Increase of >1 indicates that the peptide binds to HLA-A2.1.

IFN-γ ELISPOT Assays. IFN-γ ELISPOT assays were done as previously described (36). Briefly, nitrocellulose plates (Millipore, Bedford, MA) were coated with the anti-IFN-γ capture mAb 1-D1K (MabTech, Stockholm, Sweden) overnight at 4^0C. For assays using dendritic cells as APCs, DCs were loaded with 10 μg of the indicated peptides for 2-6 hrs, and mixed with autologous T cells at a DC:T ratio of 1:10 for 20 hours at 37^0C. For assays using autologous PBMCs as APCs, PBMCs were irradiated at 3000 Rads, loaded with 10 μg of peptides for 4 hours, and mixed with autologous T cells at an APC:T ratio of 1:5 for 40 hours at 37^0C. The T cells were seeded at $3x10^3$ – $1x10^5$ cells/well. All assays were done in serum-free AIM-V medium (Gibco Life Technologies, Grand Island, NY). The plates were then washed in PBS + 0.1% Tween and stained with anti-IFN-γ mAb 7-B6-1 (Mabtech) for 2 hours at 37^0C. The plates were washed, and the avidin-peroxidase complex (Vectastain ABC Kit, Vector Laboratories) was added to the plates for 1 hour. The plates were then developed using AEC (Sigma) substrate, and spots were quantified microscopically with an inverted phase-contrast microscope (Carl Zeiss, Hallbergmoos, Germany) along with a computer-assisted image analysis system (KS ELISPOT). For HLA Class I blocking experiments, the W6/32 antibody was added to the APCs for 30-45 minutes prior to the incubation with the T cells.

T cell cultures. *1) Priming naive $CD8^+$ T cells from a healthy donor to cyclin B1 peptides in vitro.* Naïve $CD8^+$ T cells and *in vitro* generated dendritic cells were purified as previously described (27). 2×10^4 dendritic cells were loaded overnight with 10 μg/well peptide in 96-well U-bottom plates (Falcon, Franklin lakes, NJ) and mixed with 2×10^5 autologous naïve $CD8^+$ T cells the next day in the presence of 2 ng/ml IL-1β (R & D Systems, Minneapolis, MN), 20 U/ml

IL-2 (DuPont, Wilmington, DE), and 10 U/ml IL-4 (Schering Plough). Depending on growth kinetics, T cells were fed every 3-4 days with 10 U/ml IL-2 and 5 U/ml IL-4. T cells were restimulated every 7-10 days using peptide-loaded autologous macrophages.

2) Stimulating $CD8^+$ T cells from breast cancer and SCCHN patients with cyclin B1 peptides in vitro. PBMCs from cancer patients were X-irradiated at 3000 Rads, loaded with 10 μg of the indicated peptides for 2-4 hours, and mixed with autologous PBMCs in the presence of 20 U/ml IL-2 (DuPont). The T cell cultures were fed every 3-4 days with 10 U/ml IL-2, and restimulated every 10-12 days, if necessary, using peptide-loaded autologous irradiated PBMCs. All T cell cultures were grown in RPMI medium (ICN, Costa Mesa, CA) supplemented with 10% human AB sera (Gemini Products, Calabasas, CA), L-glutamine, and penicillin/streptomycin (Life Technologies).

Immunohistochemical staining of cyclin B1 in tumor cell lines and in tumor sections. For tumor cell lines, the cells were left to adhere overnight on poly-lysine charged slides (Fisher Scientific) in the presence of RPMI + 10% FBS (Cellgro®, Media Tech, Inc., Herndon, VA). The cells were then fixed for 15 minutes on ice with either 2% Triton-X or 50% Formalin/50% acetone, blocked with serum, and stained with the anti-cyclin B1 antibody, GNS-1 (BD-Pharmingen). The avidin-biotin peroxidase method was then applied according to manufacturer's instructions using the Vectastain ABC Elite™ staining kit (Vector Laboratories, Burlingame, CA). For SCCHN sections, formalin-fixed, paraffin-embedded tumor tissues were sectioned (3-5 μm), air-dried overnight at 37°C, deparaffinized and dehydrated and stained with the anti-human cyclin B1 antibody. The avidin-biotin peroxidase method was applied as above

according to the instructions supplied by the manufacturer (DAKO Corporation, Carpinteria, CA)

PCR amplification of the cyclin B1 gene fragment. Genomic DNA from two tumor cell lines (PCI-13, MS-A2) and PBLs from two normal donors was extracted, ethanol precipitated, and first amplified with PCR primers (P1) 5'-GTGTGCCCAAGAAGATGC-3' and (P3) 5'-AGTTGGTGTCCATTCACCATT-3' flanking the region encoding peptides P1-P6 (nucleotide region 1056-1085 in HeLa cylin B1 cDNA: ascension number M25753) under the following PCR conditions: an initial denaturation step for 3 minutes at 94^0C, followed by 35 cycles (30 seconds at 94^0C, 1 minute 55^0C, 30 seconds at 72^0C), and an elongation step for 7 minutes at 72^0C. The PCR products were gel purified, and a second nested-PCR reaction was carried out using primers P3 and P4 (5'-ATGCTGCAGCTGGTTGGTGTC-3') to ensure that the region of interest in the cyclin B1 gene was actually being amplified. The PCR products were then sent for DNA sequencing analysis.

Cloning of cyclin B1 cDNA fragment amplified by PCR. From the same cells as above total RNA was extracted with Trizol™ following the manufacturer's protocol (Gibco BRL), and reverse transcribed into cDNA using the GeneAmp® RNA PCR Kit (Perkin Elmer, Roche Molecular Systems, Inc., Branchburg, New Jersey). Total normal lung tissue RNA was purchased from Ambion®, Austin, Texas. PCR amplification was done using primers P1 and P3, and the PCR products were cloned into the pcDNA3.1/V5-His-TOPO® plasmid vector using the TA Cloning® Kit (Invitrogen Corporation, Carlsbad, CA). Transformants were screened for the

insert using PCR primers P3 and P4, and plasmids isolated from positive clones were sent for DNA sequencing.

DNA Sequence Analysis. DNA sequencing was done at the University of Pittsburgh DNA Sequencing Facility using the dideoxy-chain termination method (Perkin Elmer) with the specific cyclin B1 oligonucleotides P3 and P4 as primers.

Results

Identification of T cell stimulatory tumor-derived peptides. Peptides were acid-extracted from immunoaffinity purified HLA Class I molecules of an HLA-A*0201 epithelial tumor cell line, fractionated by RP-HPLC, and loaded onto dendritic cells to prime *in vitro* autologous naive $CD8^+$ T cells from a healthy donor. One analyzed RP-HPLC fraction whose peptides supported the growth of tumor-specific CTLs was analyzed by nano-HPLC micro ESI tandem mass spectrometry. Analysis of the resulting MS/MS data yielded 6 candidate peptide sequences that corresponded to the mass range expected for HLA Class I-associated peptides (700-1300 Da). The abundances of these candidates represented the majority of total ion current observed in the mass range of 700-1300 Da. Candidate peptide sequences were subsequently confirmed by comparison of their mass spectra acquired for synthetic analogs. All six peptides had related sequences, with four being 9 amino acids long, and two being 10 amino acids long (Table 1). The four 9-mers (P1-P4) were identical in the first eight amino acids and differed at the C-terminus, where the amino acids were valine (P1), methionine (P2), phenylalanine (P3), and cysteine (P4). The two 10-mers, P5 and P6, were identical to P2 and P3, respectively, except for an additional alanine at the C-terminus. When these sequences were entered into the protein database, they were found to be homologous to a human cyclin B1 sequence derived from HeLa cells. These sequences were also homologous to mouse and rat cyclin B1 (Table 1).

We synthesized peptides P1-P6 along with the homologous 9 and 10 residue HeLa sequences (CB9 and CB10) from the database and tested them for their ability to bind HLA-A2.1 using the T2 cell line and class I stabilization assay. Since leucine and isoleucine have identical masses and are not distinguished by low-energy MS/MS analysis, the peptides were synthesized with leucine at positions 4 and 7 to match leucine present at the same position in the HeLa cyclin

B1 sequence, as well as in the mouse and rat cyclin B1 sequences. All the peptides bound to HLA-A2.1, with various affinities, as measured by increases in mean fluorescent intensity in anti-HLA-A2.1 staining of peptide-loaded T2 cells. The HeLa-derived cyclin B1 peptides also bound to HLA-A2.1. Affinities of the HeLa-derived cyclin B1 peptides were higher than that of all tumor-derived peptides, except P6 (Table 1).

*$CD8^+$ T cells from an HLA-A*0201 healthy donor can be primed to synthetic cyclin B1 peptide P4.* Since these peptides were derived from a 1st dimension HPLC fraction that primed tumor-specific CTLs from a HLA-$A2.1^+$ donor, we sought to determine whether the cyclin B1 peptides were indeed responsible for this immunostimulatory activity by using them to prime T cells from another HLA-$A2.1^+$ donor. We again used naive $CD8^+$ T cells and autologous dendritic cells loaded with the individual synthetic peptides (P1-P6). No T cell responses were detected against the peptides in the absence of *in vitro* stimulation in this donor as well as another HLA-$A2.1^+$ donor (data not shown). However, after several rounds of restimulation, we detected antigen-specific IFN-γ secretion by $CD8^+$ T cells in response to P4, and not to other peptides (P1, P2, P5, P6) or HIV-POL (ILKEPGSHV), which is known to bind HLA-A2.1 and serves here as the negative control (Figure 1). We were also able to block the T cell response to P4 using the anti-Class I antibody, W6/32, suggesting that the antigen-specific responses were HLA Class I-restricted. However, the T cells that specifically recognized P4-loaded DCs were unable to kill the original tumor from which the peptides were derived (data not shown). This was not unexpected considering that these T cells were primed to high concentrations of peptide (50 μM), and are thus expected to be of low affinity and incapable of recognizing the comparatively lower levels of the same HLA-peptide complexes on the tumor.

HLA Class I-restricted memory T cell responses against cyclin B1 peptides in HLA-A*0201 *breast cancer patients.* We tested PBMCs from six breast cancer patients who had undergone surgery but no chemotherapy, for their ability to recognize the cyclin B1 peptides in an IFN-γ ELISPOT assay. Four out of the six HLA-$A2^+$ breast cancer patients tested exhibited secondary responses against one or more of the cyclin B1 peptides (Figure 2). Patient A exhibited strong HLA Class I-restricted secondary T cell responses to three of the three peptides tested, P4, CB9, and CB10, after only one *in vitro* stimulation. There was no recognition of the HIV-POL control peptide. Patient B appeared to have a weak secondary response to one of the three peptides tested, P1, and only after two *in vitro* stimulations. This patient was later found to be HLA-A*0206, suggesting that, if the P1 response is real, P1 may also bind to HLA-A*0206.

Most interestingly, we detected secondary responses in the absence of any *in vitro* stimulation. Patient C showed peptide-specific HLA Class I-restricted T cell responses to two of two peptides tested, P4 and CB9. Patient D showed strong HLA Class I-restricted T cell responses to P4 and lower responses against both the HIV-POL peptide and CB9. However, only CB9 response was blocked by the anti-MHC Class I antibody, confirming antigen-specificity. Patients E and F did not respond to either of the two peptides tested, P4 and CB9. We also did not detect responses to any peptides in an HLA-A*0201 negative patient (data not shown)

*HLA Class I-restricted memory T cell responses to cyclin B1 peptides in HLA-A*0201 SCCHN patients.* We also examined PBMCs from five HLA-A*0201 SCCHN patients for their ability to respond to the cyclin B1 peptides in an IFN-γ ELISPOT assay. We detected HLA Class I-

restricted T cell responses to one or more of the cyclin B1 peptides in four of the five patients tested (Figure 3). Patient A exhibited HLA Class I-restricted T cell responses to five of eight peptides after only one *in vitro* stimulation. For two of these peptides, P4 and CB9, we also detected peptide-specific T cells in the absence of any *in vitro* stimulation (data now shown).

Patient B exhibited HLA Class I-restricted T cell responses to three of the five peptides (P3, P4, CB9), and not to the other two (P1, P2). Patient C showed heightened T cell responses to all five peptides tested, but only responses against P2 and CB10 could be blocked with anti-Class I antibody. Patient D had the same heightened T cell response that appeared specific for three of the six peptides tested, P4, P5, and CB9. The fifth SCCHN patient failed to show a detectable response to any of the peptides even after three *in vitro* stimulations (data not shown).

Cyclin B1 protein is overexpressed in epithelial tumor cell lines. To understand the reason why cyclin B1 peptides would elicit T cell responses in cancer patients, we examined cyclin B1 expression by immunohistochemistry in the original tumor cell line MS-A2 from where they were first isolated and identified (Figure 4, Panels A and B). There was intense staining of cyclin B1 protein in the tumor cells, predominantly found in the cytoplasm. Panels C and D depict similar intense cytoplasmic staining of cyclin B1 in a human lung adenocarcinoma cell line 201T, also localized in the cytoplasm. No cyclin B1 staining was observed in normal cells, represented by primary cultures of human airway bronchoepithelial cells (Panel E).

Cyclin B1 protein is also overexpressed in SCCHN tumors. To ascertain that the intense staining of cyclin B1 observed in the tumor cell lines was not a result of a prolonged *in vitro* culture, we examined both a tumor cell line and tumor tissue sections obtained from the SCCHN patients

whom we had analyzed previously for cyclin B1-specific T cell responses. Figure 5, Panels A and B show intense cytoplasmic staining of cyclin B1 in the tumor cell line PCI-13. This cell line was derived from a tumor of the SCCHN Patient A described in Figure 3. Very high expression of cyclin B1 in the cell line correlates with strong cyclin B1-specific T cell responses observed in this patient. Intense cytoplasmic cyclin B1 staining was also observed in the tumor samples (Panels C-D; E-F) of two other patients who exhibited cyclin B1-specific T cell responses (Patients C and D respectively; Figure 3). No cyclin B1 staining was detected in the normal mucosa surrounding the tumor. The tumor seen in Panels G-H, showed weak and diffuse cyclin B1 staining that was not convincingly positive. Patient B from whom the tumor was derived did have cyclin B1-specific T cell responses (Figure 3). The same weak staining was seen in the tumor seen in Panels I and J derived from a patient who did not exhibit any HLA Class I-restricted T cell responses against the cyclin B1 peptides (data not shown).

Differences in the C-terminus of the cyclin B1 peptides are not the result of DNA or RNA mutations. Since cyclin B1 peptides P1-P6 that we isolated from MS-A2 tumor class I molecules differed from the HeLa sequence in the second and eighth amino acid and from each other in the C-terminal residues, we set out to examine if these differences were a result of mutations in the DNA or RNA. We sequenced the area in the genomic DNA of the cell line MS-A2 corresponding to the region encoding the peptides. Since the only human cyclin B1 sequence available in the database was from HeLa cells, we also sequenced the same region of genomic DNA from two normal donors, as well as from the SCCHN cell line PCI-13. The sequences were all identical in the region of interest (Table 2), ruling out mutations at the DNA level as the cause for generation of these differences in the cyclin B1 peptides. We next examined the RNA

by cloning and sequencing the corresponding cyclin B1 cDNA from normal lung tissue and MS tumor. Most of the MS sequences were identical, except for a thymine to adenine substitution in clone MS6.1, that would render an amino acid change from Glutamic acid (E) to Aspartic acid (D) (Table 2). This change, however, does not contribute to the sequences of P1-P6. The other sequences in the region of interest were identical, ruling out mutations at the RNA level as the cause for the generation of multiple cyclin B1 peptides.

Discussion

In this study, we report the identification of cyclin B1 as a shared epithelial tumor antigen using our recently described approach of tumor antigen discovery that utilizes dendritic cells as antigen-presenting cells to prime naive $CD8^+$ T cells against tumor-derived peptides (27). Although a variety of approaches have been used to identify HLA Class I-restricted tumor antigens, most depended on the availability of tumor-specific T cell lines or clones derived from cancer patients. Our approach employed T cells from healthy donors and applied the full repertoire of anti-tumor responses that can be generated in healthy, immunocompetent individuals to tumor antigens presented by professional APCs.

Cyclin B1 is an important molecule involved in the transition from G2 to M phase of the cell cycle (28). It associates with the active form of the cdc2 (cdk1) kinase in the cytoplasm, and translocates into the nucleus where it initiates chromosome condensation, destruction of the nuclear membrane, and assembly of the mitotic spindle. It then rapidly gets ubiquitinated and targeted to the proteasome for degradation (37). Anaphase is then initiated and the cell progresses to complete the cell cycle. Cyclin B1 is expressed only at certain points of the cell cycle, starting with the gradual accumulation of the protein at G1, to its peak at G2 where it acquires the threshold needed to initiate mitosis. Overexpression of cyclin B1 has been reported in a variety of tumors, i.e. breast, colon, prostate, oral, esophageal, and non-small cell lung cancers (38-43). We detected overexpression of cyclin B1 in a panel of SCCHN tumors that showed intense cyclin B1 staining in the tumor cells and not in the surrounding mucosa. This was also observed in adenocarcinomas of the lung and breast (data not shown). The overexpressed protein was found predominantly in the cytoplasm which is different from the nuclear localization usually found in normal dividing cells. Cyclin B1 overexpression in tumors

from some of the patients correlated with the presence of cyclin B1-specific memory T cell responses in their PBLs, suggesting that T cells in these SCCHN patients had been primed *in vivo* to cyclin B1 derived from their tumors. We hypothesize that the overexpression of cyclin B1 in the cytoplasm in these tumors and its degradation in the proteasome increases dramatically HLA Class I-cyclin B1 peptide complexes on the tumor making them specific targets for T cells. It would be interesting to examine in a larger number of patients if cyclin B1 overexpression in SCCHN tumors and the presence of cyclin B1-specific T cell responses might correlate with a better prognosis and increased survival.

Since these cyclin B1 peptides were originally isolated from a fraction that supported the growth of peptide-specific CTL that lysed the original tumor cells, we were surprised that the synthetic peptide-sensitized T cells were unable to recognize and kill the same tumor (data not shown). We believe that this discrepancy between T cells recognizing peptide-loaded targets versus tumor probably lies in the comparatively lower density of HLA-cyclin B1 peptide complexes on the tumor that are below the threshold necessary for recognition by the low-affinity T cells generated on synthetic peptides *in vitro*. We will attempt to expand cyclin B1 peptide specific T cell line from patients' T cells that have been primed *in vivo*. Our expectation is that, having been primed to physiological concentrations of antigen that we have not been able to mimic in vitro, those T cells will be able to recognize tumor cells.

We do not have data to show the precise mechanism that is responsible for the differences we see among the isolated peptides. One possibility we considered was the polymorphism in human cyclin B1 genes, similar to what has been reported for rat cyclin B1 (44). Very little work has been done on human cyclin B1 genes. Only one has been cloned and sequenced from the HeLa cell line and nothing is known about the degree of polymorphism of

cyclin B1 genes in that line. We have sequenced from normal and tumor cells the portion of the cyclin B1 gene that contains the region encoding the peptides. We observed differences in several nucleotides outside the region of interest (data now shown). However, no mutations or other differences were observed in our specific region of interest, thus ruling out changes at the gene level as the cause for multiple related cyclin B1 peptides. We also did not detect any differences at the RNA level, suggesting that the changes were most likely occurring at the translational level. A recent study has suggested that up to 30% of proteins in a cell are mistranslated or misfolded (DRiPs; defective ribosomal products) and quickly directed to the proteasome for degradation (45). This process may even be exaggerated in transformed cells. Since cyclin B1 also uses the ubiquitin-proteasome system for degradation (37), we propose that the cyclin B1 peptides that we identified were derived from overexpressed and mistranslated cyclin B1 protein accumulating in the cytoplasm of tumor cells.

To our knowledge, this is the first report of a human cyclin as a tumor antigen recognized by T cells. Although deregulation of the cell cycle is one of the hallmarks of human cancer, little attention has been given to exploring cyclins as targets of an immune response, with an exception of a brief report regarding the presence of antibody responses against cyclin B1 in hepatocellular carcinoma patients (46). Our work did not specifically target cyclin B1 molecules either, until peptides derived from this molecule were found to be targets of a T cell response. Pathologists have previously reported overexpression of various cyclins in certain cancers, such as overexpression of cyclin D1 and cyclin E in breast cancer (47), and cyclin A and B1 in melanomas (48), breast cancer (38, 49, 50), and in oral carcinomas (41). Studies in our lab have shown that in some tumors, G1 cyclins are found to be more abundant while in others the G2 cyclins predominate (data not shown). Their aberrant expression may also lead to presentation

of immunogenic peptides on the surface of tumors. While here we have presented data only on peptides derived from cyclin B1, we believe that the whole family of human cyclins could be candidate tumor antigens provided their expression in tumor cells differs significantly from their expression in normal cells.

Acknowledgments

The authors want to thank Joseph M. Pilewski and Joseph D. Latoche for helpful assistance with the immunohistochemical staining of the tumor cell lines. We also thank Robert Bast, MD Anderson, Houston, Texas, for the collection of PBMCs and tumor digests from breast cancer patients. We thank Elaine Elder, Tissue Bank Core Facility, for the collection of PBMCs from head and neck cancer patients. We also thank Nehad Alajez, Pam Beatty, and Vandana Kalia for helpful suggestions with the cloning and sequencing of the cyclin B1 gene. We also want to thank Daniel F. Graziano and Jessica C. Kettel for helpful assistance with the ELISPOT. We would also like to thank Joseph Ahearn for sharing his flow cytometer. This work is supported by DOD grant DAMD 17-9-1-7057 to H.K., NIH grant 2R37 A133993 to D.F.H and NIH grant 5PO1CA 73743 to O.J.F.

Figure Legends

Figure 1: HLA Class I-restricted T cell response of a healthy donor to cyclin B1 peptides. $CD8^+$ T cells generated in vitro by priming to synthetic cyclin B1 peptides were used in an IFN-γ ELISPOT assay after the 4th restimulation. Number of T cells per well is indicated in parenthesis.

Figure 2: HLA Class I-restricted T cell responses to cyclin B1 peptides in HLA-$A2^+$ breast cancer patients. PBMCs from breast cancer patients were tested for recognition of cyclin B1 peptides after one *in vitro* stimulation (A, B, E, F) or no *in vitro* stimulation (C, D) in an IFN-γ ELISPOT assay. Number of T cells per well is indicated in parenthesis.

Figure 3: HLA Class I-restricted T cell responses to cyclin B1 peptides in HLA-$A2.1^+$ SCCHN patients. PBMCs were tested for recognition of cyclin B1 peptides after one (A) or two *in vitro* stimulations (B, C, D) in an IFN-γ ELISPOT assay.

Figure 4: Cyclin B1 protein is overexpressed in epithelial tumor cells. (A) MS-A2 cells, magnification 20X. (B) MS-A2 cells, magnification 40X. (C) 201T cells, magnification 20X. (D) 201T cells, magnification 40X. (E) Human airway bronchoepithelial cells, magnification, 20X.

Figure 5: Cyclin B1 protein is overexpressed in SCCHN. Panels A and B, SCCHN cell Line PCI-13. Panels C-J, SCCHN tumor sections. Panels A, C, E, G and I, magnification, 10X. Panels B, D, F, H and J, magnification, 20X.

References

1. Brichard, V., A. Van Pel, T. Wolfel, C. Wolfel, E. De Plaen, B. Lethe, P. Coulie, and T. Boon. 1993. The tyrosinase gene codes for an antigen recognized by autologous cytolytic T lymphocytes on HLA-A2 melanomas. *J Exp Med* 178, no. 2:489-495.

2. Coulie, P.G., V. Brichard, A. Van Pel, T. Wolfel, J. Schneider, C. Traversari, S. Mattei, E. De Plaen, C. Lurquin, J.P. Szikora, and et al. 1994. A new gene coding for a differentiation antigen recognized by autologous cytolytic T lymphocytes on HLA-A2 melanomas [see comments]. *J Exp Med* 180, no. 1:35-42.

3. Hunt, D.F., H. Michel, T.A. Dickinson, J. Shabanowitz, A.L. Cox, K. Sakaguchi, E. Appella, H.M. Grey, and A. Sette. 1992. Peptides presented to the immune system by the murine class II major histocompatibility complex molecule I-Ad. *Science* 256, no. 5065:1817-1820.

4. Hunt, D.F., R.A. Henderson, J. Shabanowitz, K. Sakaguchi, H. Michel, N. Sevilir, A.L. Cox, E. Appella, and V.H. Engelhard. 1992. Characterization of peptides bound to the class I MHC molecule HLA-A2.1 by mass spectrometry [see comments]. *Science* 255, no. 5049:1261-1263.

5. Fisk, B., T.L. Blevins, J.T. Wharton, and C.G. Ioannides. 1995. Identification of an immunodominant peptide of HER-2/neu protooncogene recognized by ovarian tumor-specific cytotoxic T lymphocyte lines. *J. Exp. Med.* 181, no. 6:2109-2117.

6. Blake, J., J.V. Johnston, K.E. Hellstrom, H. Marquardt, and L. Chen. 1996. Use of combinatorial peptide libraries to construct functional mimics of tumor epitopes recognized by MHC class I-restricted cytolytic T lymphocytes. *J Exp Med* 184, no. 1:121-130.

7. Tureci, O., U. Sahin, and M. Pfreundschuh. 1997. Serological analysis of human tumor antigens: molecular definition and implications. *Molecular Medicine Today* 3, no. 8:342-349.

8. Henderson, R.A., and O.J. Finn. 1996. Human tumor antigens are ready to fly. *Adv. Immunol.* 62:217-256.

9. Traversari, C., P. van der Bruggen, I.F. Luescher, C. Lurquin, P. Chomez, A. Van Pel, E. De Plaen, A. Amar-Costesec, and T. Boon. 1992. A nonapeptide encoded by human gene MAGE-1 is recognized on HLA-A1 by cytolytic T lymphocytes directed against tumor antigen MZ2-E. *J Exp. Med* 176, no. 5:1453-1457.

10. Gaugler, B., B. Van den Eynde, P. van der Bruggen, P. Romero, J.J. Gaforio, E. De Plaen, B. Lethe, F. Brasseur, and T. Boon. 1994. Human gene MAGE-3 codes for an antigen recognized on a melanoma by autologous cytolytic T lymphocytes. *J. Exp. Med* 179, no. 3:921-930.

11. Boel, P., C. Wildmann, M.L. Sensi, R. Brasseur, J.C. Renauld, P. Coulie, T. Boon, and P. van der Bruggen. 1995. BAGE: a new gene encoding an antigen recognized on human melanomas by cytolytic T lymphocytes. *Immunity* 2, no. 2:167-175.

12. Van den Eynde, B., O. Peeters, O. De Backer, B. Gaugler, S. Lucas, and T. Boon. 1995. A new family of genes coding for an antigen recognized by autologous cytolytic T lymphocytes on a human melanoma. *J. Exp. Med* 182, no. 3:689-698.

13. Chen, Y.T., M.J. Scanlan, U. Sahin, O. Tureci, A.O. Gure, S. Tsang, B. Williamson, E. Stockert, M. Pfreundschuh, and L.J. Old. 1997. A testicular antigen aberrantly expressed in human cancers detected by autologous antibody screening. *Proc Natl Acad Sci U S A* 94, no. 5:1914-1918.

14. Kawakami, Y., S. Eliyahu, C. Jennings, K. Sakaguchi, X. Kang, S. Southwood, P.F. Robbins, A. Sette, E. Appella, and S.A. Rosenberg. 1995. Recognition of multiple epitopes in the human melanoma antigen gp100 by tumor-infiltrating T lymphocytes associated with in vivo tumor regression. *J Immunol* 154, no. 8:3961-3968.

15. Kawakami, Y., S. Eliyahu, C.H. Delgado, P.F. Robbins, K. Sakaguchi, E. Appella, J.R. Yannelli, G.J. Adema, T. Miki, and S.A. Rosenberg. 1994. Identification of a human melanoma antigen recognized by tumor- infiltrating lymphocytes associated with in vivo tumor rejection. *Proc Natl Acad Sci U S A* 91, no. 14:6458-6462.

16. Wolfel, T., M. Hauer, J. Schneider, M. Serrano, C. Wolfel, E. Klehmann-Hieb, E. De Plaen, T. Hankeln, K.H. Meyer zum Buschenfelde, and D. Beach. 1995. A p16INK4a-insensitive CDK4 mutant targeted by cytolytic T lymphocytes in a human melanoma. *Science* 269, no. 5228:1281-1284.

17. Robbins, P.F., M. El-Gamil, Y.F. Li, Y. Kawakami, D. Loftus, E. Appella, and S.A. Rosenberg. 1996. A mutated beta-catenin gene encodes a melanoma-specific antigen recognized by tumor infiltrating lymphocytes. *J Exp Med* 183, no. 3:1185-1192.

18. Wang, R.F., X. Wang, A.C. Atwood, S.L. Topalian, and S.A. Rosenberg. 1999. Cloning genes encoding MHC class II-restricted antigens: mutated CDC27 as a tumor antigen. *Science* 284, no. 5418:1351-1354.

19. Ikeda, H., B. Lethe, F. Lehmann, N. van Baren, J.F. Baurain, C. de Smet, H. Chambost, M. Vitale, A. Moretta, T. Boon, and P.G. Coulie. 1997. Characterization of an antigen that is recognized on a melanoma showing partial HLA loss by CTL expressing an NK inhibitory receptor. *Immunity* 6, no. 2:199-208.

20. Ropke, M., J. Hald, P. Guldberg, J. Zeuthen, L. Norgaard, L. Fugger, A. Svejgaard, S. Van der Burg, H.W. Nijman, C.J. Melief, and M.H. Claesson. 1996. Spontaneous human squamous cell carcinomas are killed by a human cytotoxic T lymphocyte clone recognizing a wild-type p53-derived peptide. *Proceedings of the National Academy of Sciences of the United States of America* 93, no. 25:14704-14707.

21. Ressing, M.E., A. Sette, R.M. Brandt, J. Ruppert, P.A. Wentworth, M. Hartman, C. Oseroff, H.M. Grey, C.J. Melief, and W.M. Kast. 1995. Human CTL epitopes encoded by human papillomavirus type 16 E6 and E7 identified through in vivo and in vitro immunogenicity studies of HLA- A*0201-binding peptides. *J Immunol* 154, no. 11:5934-5943.

22. Lennette, E.T., G. Winberg, M. Yadav, G. Enblad, and G. Klein. 1995. Antibodies to LMP2A/2B in EBV-carrying malignancies. *Eur J Cancer* 31A, no. 11:1875-1878.

23. Shievely, J., and J. Beatty. 1985. CEA related antigens: molecular, biological and clinical significance. *CRC Crit. Rev. Oncol. Hematol.* 2:355-399.

24. Wang, M.C., L.D. Papsider, M. Kuriyama, L.A. Valenzuela, G.P. Murphy, and T.M. Chu. 1981. Prostate antigen: a new potential marker for prostatic cancer. *Prostate* 2:89-96.

25. Disis, M.L., and M.A. Cheever. 1998. HER-2/neu oncogenic protein: issues in vaccine development. *Crit Rev Immunol* 18, no. 1-2:37-45.

26. Finn, O.J., K.R. Jerome, R.A. Henderson, G. Pecher, N. Domenech, J. Magarian-Blander, and S.M. Barratt-Boyes. 1995. MUC-1 epithelial tumor mucin-based immunity and cancer vaccines. *Immunological Reviews* 145:61-89.

27. Kao, H., A.A. Amoscato, P. Ciborowski, and O.J. Finn. 2001. A new strategy for tumor antigen discovery based on in vitro priming of naive T cells with dendritic cells. *Clinical Cancer Research*:in press.

28. King, R.W., P.K. Jackson, and M.W. Kirschner. 1994. Mitosis in transition [see comments]. *Cell* 79, no. 4:563-571.

29. Hiltbold, E.M., M.D. Alter, P. Ciborowski, and O.J. Finn. 1999. Presentation of MUC1 tumor antigen by class I MHC and CTL function correlate with the glycosylation state of the protein taken Up by dendritic cells. *Cell Immunol* 194, no. 2:143-149.

30. Yasumura, S., H. Hirabayashi, D.R. Schwartz, J.F. Toso, J.T. Johnson, R.B. Herberman, and T.L. Whiteside. 1993. Human cytotoxic T-cell lines with restricted specificity for squamous cell carcinoma of the head and neck. *Cancer Res* 53, no. 6:1461-1468.

31. Martin, S.E., J. Shabanowitz, D.F. Hunt, and J.A. Marto. 2000. Subfemtomole MS and MS/MS peptide sequence analysis using nano-HPLC micro-ESI fourier transform ion cyclotron resonance mass spectrometry. *Anal Chem* 72, no. 18:4266-4274.

32. Shabanowitz, J., R.E. Settlage, J.A. Marto, R.E. Christian, F.W. White, P.S. Russo, S.E. Martin, and D.F. Hunt. 2000. Sequencing the Primordial Soup. *In* Mass Spectrometry in Biology and Medicine. A.L. Burlingame, S.A. Carr and M.A. Baldwin, editors. Humana Press, Totowa, NJ. 163-177.

33. Eng, J.K., A.L. McCormack, and J.R. Yates. 1994. An approach to correlate tandem mass spectral data of peptides with amino acid sequences in a protein database. *J. Am. Soc. Mass. Spectrom.* 5:976-989.

34. Clauser, K.R., P. Baker, and A.L. Burlingame. 1999. Role of accurate mass measurement (+/- 10 ppm) in protein identification strategies employing MS or MS/MS and database searching. *Anal Chem* 71, no. 14:2871-2882.

35. Zeh, H.J., 3rd, G.H. Leder, M.T. Lotze, R.D. Salter, M. Tector, G. Stuber, S. Modrow, and W.J. Storkus. 1994. Flow-cytometric determination of peptide-class I complex formation. Identification of p53 peptides that bind to HLA-A2. *Hum Immunol* 39, no. 2:79-86.

36. Herr, W., J. Schneider, A.W. Lohse, K.H. Meyer zum Buschenfelde, and T. Wolfel. 1996. Detection and quantification of blood-derived CD8+ T lymphocytes secreting tumor necrosis factor alpha in response to HLA-A2.1-binding melanoma and viral peptide antigens. *J Immunol Methods* 191, no. 2:131-142.

37. Murray, A. 1995. Cyclin Ubiquitination: The destructive end of mitosis. *Cell* 81:149-152.

38. Kawamoto, H., H. Koizumi, and T. Uchikoshi. 1997. Expression of the G2-M checkpoint regulators cyclin B1 and cdc2 in nonmalignant and malignant human breast lesions: immunocytochemical and quantitative image analyses. *Am J Pathol* 150, no. 1:15-23.

39. Wang, A., N. Yoshimi, N. Ino, T. Tanaka, and H. Mori. 1997. Overexpression of cyclin B1 in human colorectal cancers. *J Cancer Res Clin Oncol* 123, no. 2:124-127.

40. Mashal, R.D., S. Lester, C. Corless, J.P. Richie, R. Chandra, K.J. Propert, and A. Dutta. 1996. Expression of cell cycle-regulated proteins in prostate cancer. *Cancer Research* 56:4159-4163.

41. Kushner, J., G. Bradley, B. Young, and R.C. Jordan. 1999. Aberrant expression of cyclin A and cyclin B1 proteins in oral carcinoma. *J Oral Pathol Med* 28, no. 2:77-81.

42. Murakami, H., M. Furihata, Y. Ohtsuki, and S. Ogoshi. 1999. Determination of the prognostic significance of cyclin B1 overexpression in patients with esophageal squamous cell carcinoma. *Virchows Arch* 434, no. 2:153-158.

43. Soria, J.C., S.J. Jang, F.R. Khuri, K. Hassan, D. Liu, W.K. Hong, and L. Mao. 2000. Overexpression of cyclin B1 in early-stage non-small cell lung cancer and its clinical implication. *Cancer Res* 60, no. 15:4000-4004.

44. Petit, J., M. Riviere, J. Szpirer, and C. Szpirer. 1999. High level of single-nucleotide polymorphism in the rat cyclin B1 gene. *Mamm Genome* 10, no. 6:635-637.

45. Schubert, U., L.C. Anton, J. Gibbs, C.C. Norbury, J.W. Yewdell, and J.R. Bennink. 2000. Rapid degradation of a large fraction of newly synthesized proteins by proteasomes. *Nature* 404:770-774.

46. Covini, G., E.K. Chan, M. Nishioka, S.A. Morshed, S.I. Reed, and E.M. Tan. 1997. Immune response to cyclin B1 in hepatocellular carcinoma. *Hepatology* 25, no. 1:75-80.

47. Steeg, P.S., and Q. Zhou. 1998. Cyclins and breast cancer. *Breast Cancer Research and Treatment* 52:17-28.

48. Tran, T.A., J.S. Ross, J.A. Carlson, and M.C. Mihm. 1998. Mitotic cyclins and cyclin-dependent kinases in melanocytic lesions. *Human Pathology* 29:1085-1090.

49. Keyomarsi, K., and A.B. Pardee. 1993. Redundant cyclin overexpression and gene amplification in breast cancer cells. *Proc. Natl. Acad. Sci.* 90:1112-1116.

50. Dutta, A., R. Chandra, L. Leiter, and S. Lester. 1995. Cyclins as markers of tumor proliferation: immunocytochemical studies in breast cancer. *Proc. Natl. Acad. Sci.* 92:5386-5390.

Table 1. Cyclin B1 sequences derived from the tumor and database bind to HLA-A2.1

Cyclin B1 peptides from the tumor	Sequence[a]	HLA-A2.1 Binding[b]
P1	AGYLMELCV	1.60
P2	AGYLMELCM	1.48
P3	AGYLMELCF	1.42
P4	AGYLMELCC	1.61
P5	AGYLMELCMA	1.58
P6	AGYLMELCFA	2.08
Cyclin B1 peptides from the database		
Human cyclin B1 (CB9)	AKYLMELTM	2.28
Human cyclin B1 (CB10)	AKYLMELTML	2.25
Mouse cyclin B1	AKYLMELSML	---
Rat cyclin B1	AKYLMELSML	---

[a] Tumor-derived peptides were sequenced by electrospray ionization tandem mass spectrometry, yielding six peptides (P1-P6) having high homology to human Hela cyclin B1 (ascension number: P14635), as well as mouse (ascension number: P24860) and rat cyclin B1 (ascension number: P30277).

[b] X-Fold increase = (Mean Fluorescent Intensity of T2 cells loaded with peptide/Mean Fluorescent Intensity of T2 cells with no peptide). An X-Fold Increase of >1 indicates that the peptide binds to HLA-A2.1. The positive control consisted of T2 cells loaded with the Flu matrix peptide (GILGFVFTL), which had an X-Fold Increase of 2.2.

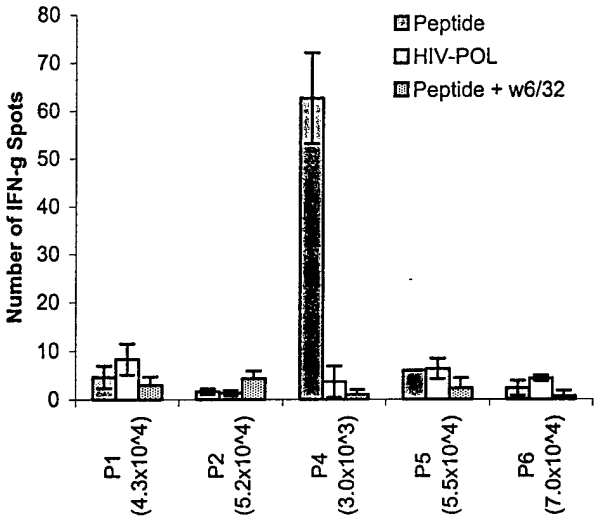
Number of IFN-g Spots
80
70
60
50
40
30
20
10
0
Peptide
HIV-POL
Peptide + w6/32
P1 (4.3x10^4)
P2 (5.2x10^4)
P4 (3.0x10^3)
P5 (5.5x10^4)
P6 (7.0x10^4)

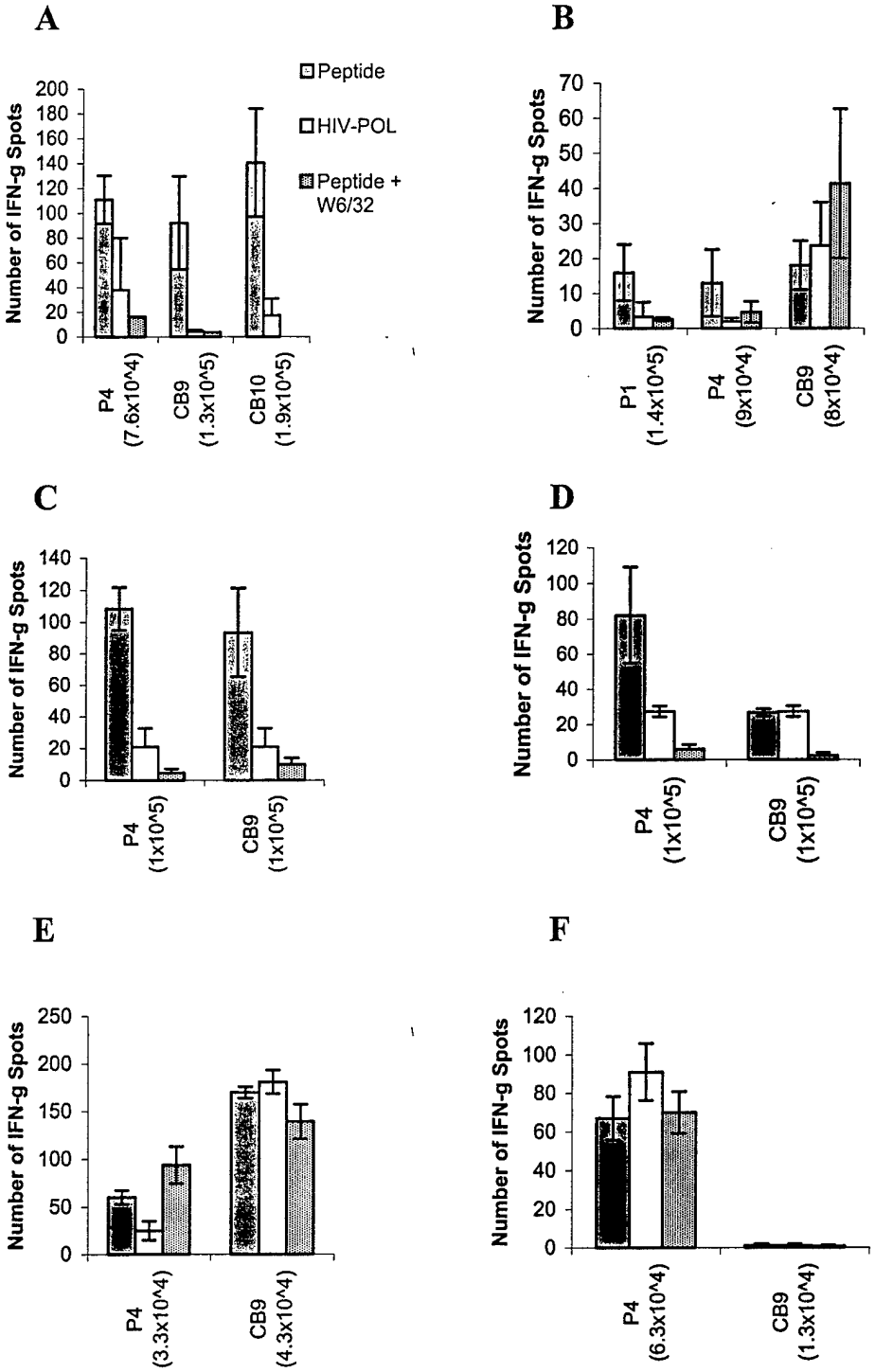
A
Peptide
HIV-POL
Peptide + W6/32
Number of IFN-g Spots
200
180
160
140
120
100
80
60
40
20
0
P4 (7.6x10^4)
CB9 (1.3x10^5)
CB10 (1.9x10^5)
B
Number of IFN-g Spots
70
60
50
40
30
20
10
0
P1 (1.4x10^5)
P4 (9x10^4)
CB9 (8x10^4)
C
Number of IFN-g Spots
140
120
100
80
60
40
20
0
P4 (1x10^5)
CB9 (1x10^5)
D
Number of IFN-g Spots
120
100
80
60
40
20
0
P4 (1x10^5)
CB9 (1x10^5)
E
Number of IFN-g Spots
250
200
150
100
50
0
P4 (3.3x10^4)
CB9 (4.3x10^4)
F
Number of IFN-g Spots
120
100
80
60
40
20
0
P4 (6.3x10^4)
CB9 (1.3x10^4)

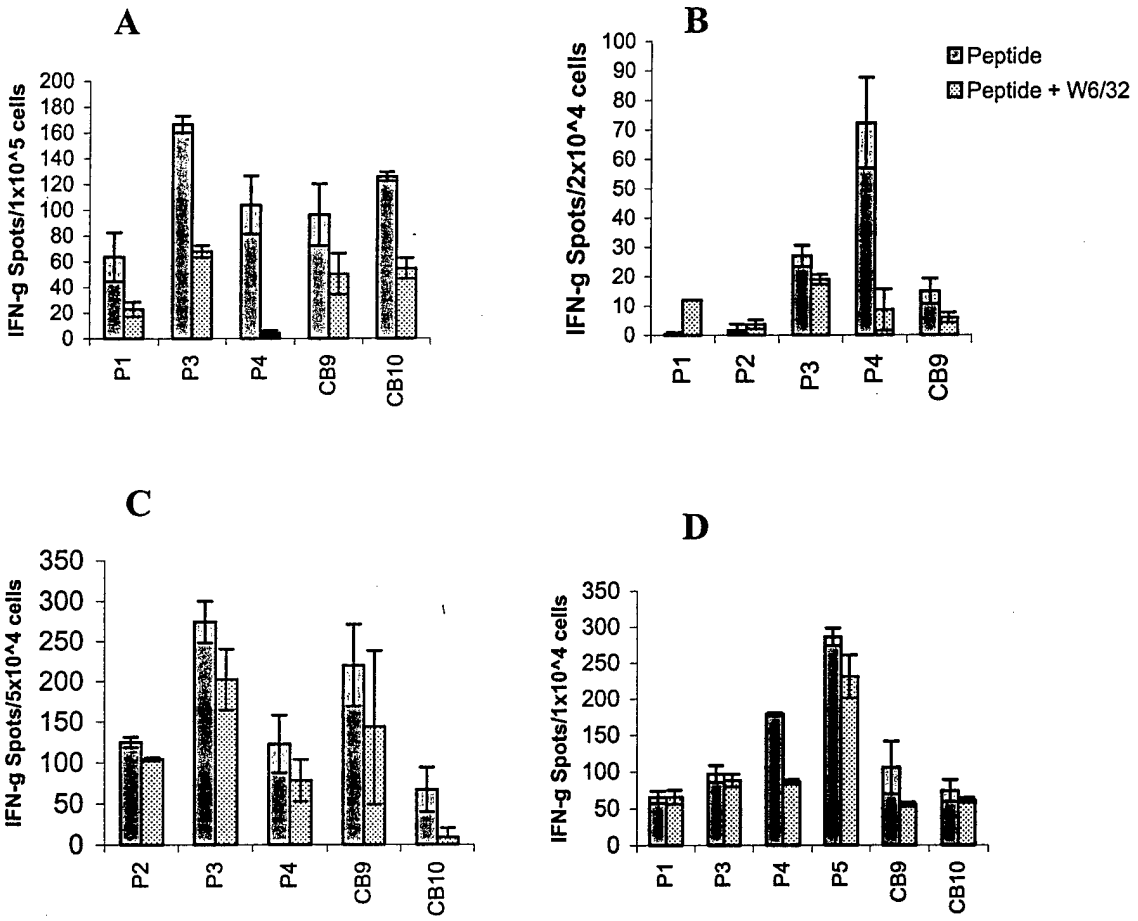
A
IFN-g Spots/1x10^5 cells
200
180
160
140
120
100
80
60
40
20
0
P1
P3
P4
CB9
CB10
B
IFN-g Spots/2x10^4 cells
100
90
80
70
60
50
40
30
20
10
0
P1
P2
P3
P4
CB9
Peptide
Peptide + W6/32
C
IFN-g Spots/5x10^4 cells
350
300
250
200
150
100
50
0
P2
P3
P4
CB9
CB10
D
IFN-g Spots/1x10^4 cells
350
300
250
200
150
100
50
0
P1
P3
P4
P5
CB9
CB10

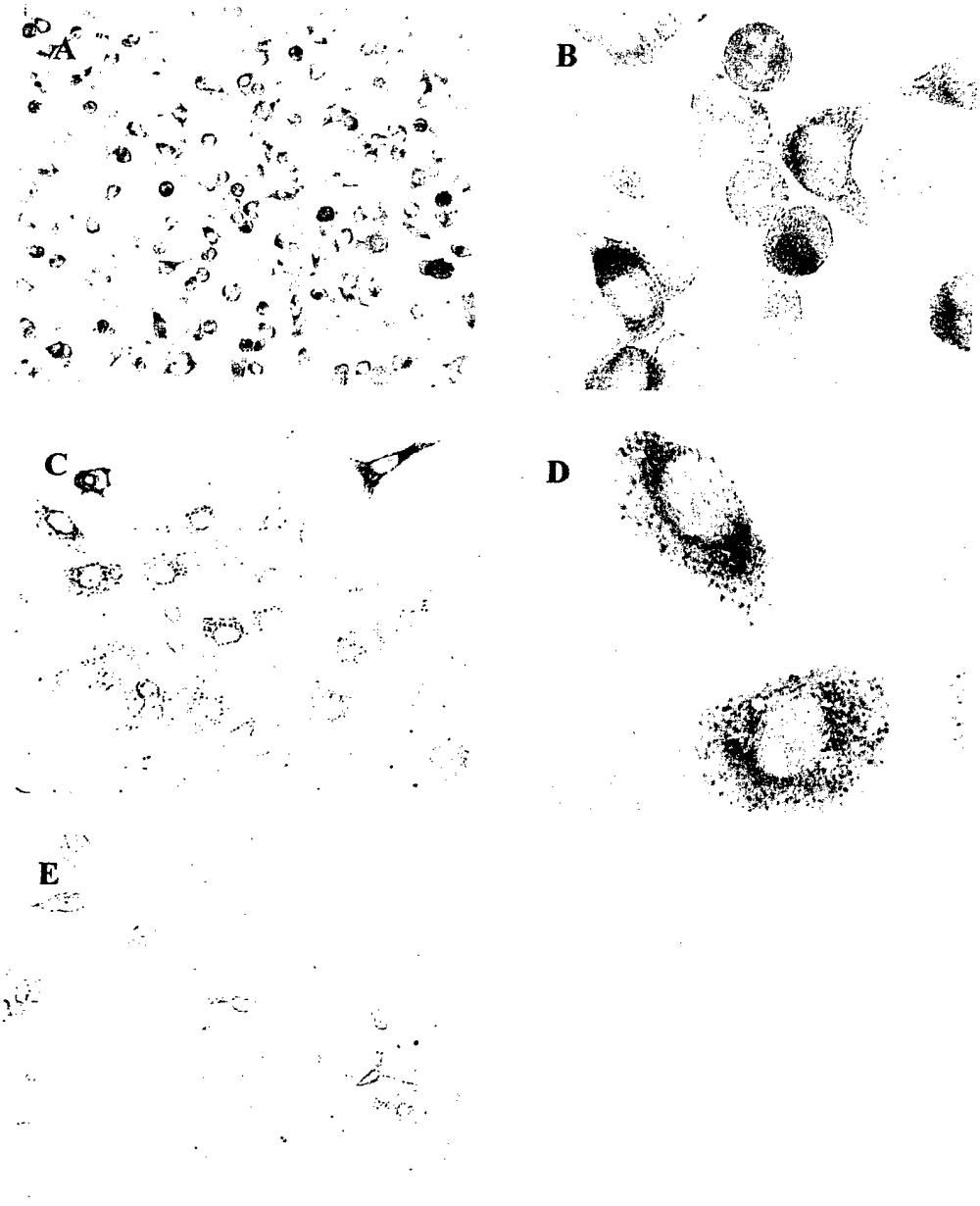
A
B
C
D
E

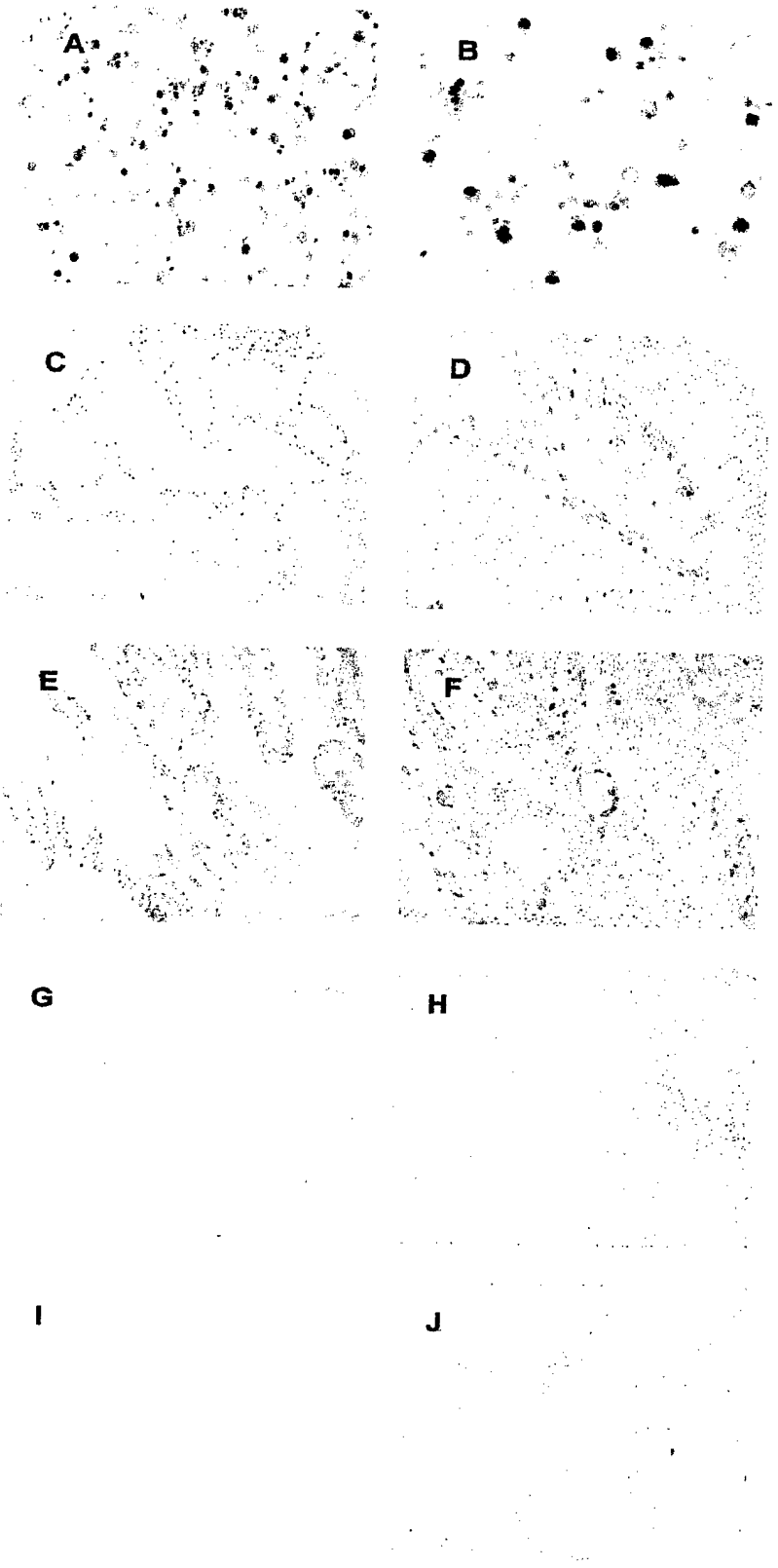
A
B
C
D
E
F
G
H
I
J

Table 2: Partial sequence alignment analysis of cyclin B1 DNA and cDNA in the region of interest.

A.

```
                                          A  K  Y  L  M  E  L  T  M  L
HeLa Cyclin B1 cDNA        TGATGTCGAGCAACATACTTTGGCCAAATACCTGATGGAACTAACTATGTTGGAC-TATGACATGGTGCA
Normal Cyclin B1 DNA (1)   ..........................................................-..........
Normal Cyclin B1 DNA (2)   ..........................................................-..........
MSA2 Cyclin B1 DNA         ....................A.....................................-..........
PCI13 Cyclin B1 DNA        ..........................................................A..........
```

B.

```
                                          A  K  Y  L  M  E  L  T  M  L
Normal Lung cDNA           TGATGTCGAGCAACATACTTTGGCCAAATACCTGATGGAACTAACTATGTTGGACTATGACATGGTGCA
HeLa Cyclin B1 cDNA        ............................................................
MS6.1-cDNA                 ..........................................T.................
MS6.2-cDNA                 ....................A.......................................
MS6.3-cDNA                 ....................A.......................................
MS6.4-cDNA                 ....................A.......................................
MS6.5-cDNA                 ....................................................
MS6.6-cDNA                 .-..................A.......................................
MS6.7-cDNA                 ....................N.......................................
MS6.9-cDNA                 ....................................................
MS6.10-cDNA                ....................A.......................................
```

These sequence data are available from GenBank under accession numbers AY027761-027774.

Psychology and Health, 2000, Vol. 15, pp. 881–891
Reprints available directly from the Publisher
Photocopying permitted by license only

THE EFFECTS OF STRESS ON DNA REPAIR CAPACITY

MICHAEL J. FORLENZA[1,*], JEAN J. LATIMER[2] and ANDREW BAUM[1]

[1]*Division of Behavioral Medicine and Oncology, University of Pittsburgh Cancer Institute, 3600 Forbes Ave, Suite 405, Pittsburgh, PA 15213*
[2]*University of Pittsburgh Department of Obstetrics, Gynecology, and Reproductive Sciences, Magee Women's Research Institute*

(Received 8 March, 2000; in final form 24 May, 2000)

Research has shown that lymphocytes of high-distress patients have reduced DNA repair relative to that of low-distress patients and healthy controls. Furthermore, deficits in repair are associated with an increased risk of cancer. Using and academic stress model, we hypothesized that students would exhibit lower levels of Nucleotide Excision Repair (NER) during a stressful exam period when compared to a lower stress period. Participants were 19 healthy graduate level students. NER was measured in lymphocytes using the unscheduled DNA synthesis (UDS) assay with slide autoradiography. Contrary to prediction, mean values for NER significantly *increased* during the higher stress period relative to the lower stress period controlling for background differences in repair. Furthermore, lymphocytes had significantly increased repair of endogenous damage during the higher stress period. Stress appears to directly increase DNA repair. Additionally, stress may increase DNA repair indirectly by increasing damage to DNA.

KEY WORDS: Psychological stress, academic stress, DNA repair, DNA damage, nucleotide excision repair.

Human DNA is constantly exposed to both endogenous (e.g., superoxide and hydroxyl radicals) and exogenous (e.g., ultraviolet radiation, X-rays, chemicals) genotoxic agents (Feigelson, Ross, Yu, Coetzee, Reichardt and Henderson, 1997). Unrepaired damage due to a reduction or loss of DNA repair leads to permanent somatic mutations and an accumulation of mutations within a single cell drives that cell towards malignancy and cancer (Hall and Johnson, 1996; Vogelstein and Kinzler, 1993). There are several DNA repair pathways organized according to the type of damage repaired or the mechanism of repair (Bohr, 1995; Friedberg, Walker and Siede, 1995). For example, oxidative damage is repaired by the Base Excision Repair (BER) pathway, which removes a single damaged base (Yu, Chen, Ford, Brackley and Glickman, 1999). Lesions induced by UV radiation are repaired by the Nucleotide Excision Repair (NER) pathway, which removes a long 22–30 bp patch of DNA (Yu *et al.*, 1999). BER, NER, and Double Strand Break (DSB) repair pathways repair lesions induced by ionizing radiation. (Yu *et al.*, 1999)

People who inherit DNA repair deficiency syndromes such as xeroderma pigmentosum (XP), Bloom's syndrome, ataxia telengiectasia (AT), or hereditary nonpolyposis colorectal cancer (HNPCC) are at increased risk for developing cancer (Setlow, 1978; Bonn, 1998).

*Corresponding Author. Tel.: (412) 647-0928; Fax (412) 647-1936; E-mail: mjfst36@imap.pitt.edu

For instance, people born with XP are prone to skin cancer because they have a mutation in an NER gene that prevents them from repairing damage caused by exposure to UV light (Bootsma *et al.*, 1995; Bonn, 1998). People with HNPCC have a mutation in a gene encoding for mismatch repair, a system involved in correcting replication errors (Jiricny, 1994).

The connection between DNA repair and cancer is not limited to people with inherited syndromes. DNA repair deficits (NER) in blood (PBL's) have been linked to sporadic cancers such as basal cell carcinoma (Wei, Matanoski, Farmer, Hedayati and Grossman, 1994), breast cancer (Kovacs, Stucki, Weber and Muller, 1986), lung cancer (Wei, Cheng, Hong and Spitz, 1996) and head and neck cancer (Cheng, Eicher, Guo, Hong, Spitz and Wei, 1998).

In addition, research has shown that increasing age, independent of antioxidant status, is associated with a decrease in oxidative repair and an increase in mutation in lymphocytes (Bootsma *et al.*, 1995). Aging was also associated with a decrease in the ability to repair UV damage and an increase in DNA mutability in both cultured skin and blood cells (Barnett and King, 1995). Finally, an age-dependent decline in DNA repair has been linked with increases in accumulated mutations in lymphocytes (Moriwaki, Ray, Tarone, Kraemer and Grossman, 1996). However, little work has focused on examining modifiable factors that contribute to the normal variation in DNA repair. Understanding these factors is important for understanding the complex process of carcinogenesis.

There is some evidence that stress can affect DNA repair. In a sample of nonpsychotic psychiatric inpatients, high-distress patients had reduced repair in lymphocytes (i.e., decreased nucleoid sedimentation rates) two hours and five hours after X-irradiation relative to low-distress patients and matched controls. In addition, repair rates in the psychiatric patients were reduced 5 hours post-irradiation compared with healthy controls (Kiecolt-Glaser, Stephens, Lipetz, Speicher and Glaser, 1985). This study provided the first evidence that stress altered DNA repair capacity in humans. If stress suppresses aspects of DNA repair, there may be important consequences for several aspects of cancer prevention and control.

Stress has also been shown to inhibit the repair of carcinogen-induced DNA damage in rats (Glaser, Thorn, Tarr, Kiecolt-Glaser and D'Ambrosio, 1985). Rats were given 50 parts per million (ppm) of dimethylnitrosamine (DMN; a carcinogen) in their drinking water for 16 days and were randomly assigned to a stress or no stress condition. The stress condition consisted of four 24-hr periods of rotational stress in their home cage. After 16 days, the stressed animals had significantly less spleenic methytransferase activity (an important DNA repair enzyme) than the nonstressed animals that had the same level of carcinogen exposure. This suggests that stress may moderate the effect of genotoxic exposures via alteration of DNA repair mechanisms.

The primary objective of this research was to evaluate the relationship between stress and repair of exogenously damaged DNA. Academic examinations are commonplace stressors that have been studied extensively. They are reliably associated with alterations in erythron variables (e.g., hematocrit, hemoglobin, mean corpuscular volume) (Maes, *et al.*, 1998), wound healing (Marucha, Kiecolt-Glaser and Favagehi, 1998), total serum protein (Van Hunsel *et al.*, 1998), serum immunoglobulins, complement, and acute phase proteins (Maes *et al.*, 1997), reactivation of latent Epstein-Barr Virus (Glaser, Pearl, Kiecolt-Glaser and Malarkey, 1994), and inhibition of radiation-induced apoptosis (Tomei, Kiecolt-Glaser, Kennedy and Glaser, 1990). These data suggest that an examination stress model may be a productive way of studying the effects of stress on DNA repair.

METHODS

This study was a prospective examination of perceived stress and DNA repair in 19 students during both a low stress (time 1) and higher stress period (time 2). The low stress period was scheduled within 2 days of returning from spring or summer break, and the higher stress period occurred during the week preceding final or board exams. The primary hypothesis, derived from Kiecolt-Glaser *et al.* (1985), was that students would exhibit lower levels of DNA repair in peripheral blood lymphocytes during the stressful exam period than during the (relatively) low stress period. This study was conducted after review and approval by the University of Pittsburgh Institutional Review Board.

Participants

Participants were healthy first and second-year students recruited from the University of Pittsburgh Medical School ($n=8$), Dental School ($n=4$), Law School ($n=4$), and School of Pharmacy ($n=3$). Exclusion criteria included smoking, personal history of cancer, and personal history of major psychiatric disorder. Subjects were paid $10 at the end of each session.

Procedure

Upon arrival at the testing site, the study and procedures were explained to the participants and informed consent was obtained. After the subjects completed background and perceived stress questionnaires, 30 ml of blood were drawn into three 10 ml green top tubes (Vacutainer Brand) by a trained phlebotomist or medical assistant. Subjects were then given written information about the time and date of their second appointment and were paid. Procedures for both the low and higher stress periods were similar.

Measures

Basic demographic information and family history of cancer were measured as background variables. In order to evaluate whether the higher stress period was perceived as more stressful, stress appraisal was measured on the Perceived Stress Scale (PSS), a 14-item self-report measure of the extent to which respondents feel their lives are unpredictable, uncontrollable, and overloaded (Cohen, 1986). The PSS demonstrates good internal consistency ($\alpha=.85$) (Cohen, Kamarck and Mermelstein, 1983).

NER was measured in peripheral blood lymphocytes using the unscheduled DNA synthesis (UDS) assay with autoradiography (Cleaver and Thomas, 1981). UDS is a robust functional assay that measures the amount of [^{3}-H]-thymidine incorporated into DNA after an exogenous dose of damaging UV-C light *in vitro*. This permits the quantitative measurement of overall genomic repair (both transcribed and untranscribed genes). The advantage of using a functional assay for NER is that the assay can examine the coordinated functioning of all of the gene products (approximately 30, 11 of which have been cloned) that operate in this repair pathway (Latimer, Hultner, Cleaver and Pedersen, 1996). Additionally, the autoradiographic procedure for UDS, as opposed to the scintillation counting method, allows for a clear-cut elimination through visual inspection of cells incorporating [^{3}-H]-thymidine that are in S-phase.

Blood Preparation

Blood samples were obtained from the participants via standard phlebotomy procedures. Peripheral blood lymphocytes (PBL) were isolated by Ficoll-Hypaque Gradient Centrifugation (Coligan, Kruisbeek, Margulies, Shevach and Strober, 1995). After the final wash, pellets were resuspended in media containing RPMI (Beckman TJ-6) supplemented with 10% autologous serum and 1% pen/strep (Gibco). Autologous serum was used because it contains relevant stress hormones (e.g., cortisol) or biological response modifiers characteristic of the person from whom the sample was obtained (Larcom and Smith, 1988; Larcom, Morris and Smith, 1990). These factors would not be present in samples incubated with fetal bovine sera. Aliquots were placed into culture on chamber slides coated with a diluted form of Matrigel (Collaborative Research, Inc.). This allowed the attachment of the PBLs to the slide (Latimer *et al.*, 1996; Latimer *et al.*, submitted), enabling autoradiographic analysis. Three chamber slides were prepared for each subject.

Assay Procedures

After 3 days in culture with autologous serum and without passaging, the PBL's were assayed for NER. One side of each slide was irradiated with UV-C light (254 nm at a mean fluence of $1.2\,J/m^{-2}s^{-1}\times12$ seconds for a total of $14\,J/m^2$) using a machine specifically built to deliver a reproducible dose of UV radiation (Steier and Cleaver, 1969). The unirradiated side of the slide served as an untreated control and reflected the rate of NER prior to exogenous damage. Immediately following irradiation, samples were cultured in labeling medium containing 10μCi ml [^{3}H]-methyl-thymidine (80Ci/mmol) (NEN Dupont) and allowed to repair for 2 hours at 37°C. The kinetics of UV repair is such that 2 hours of incubation are enough time to repair induced 6–4 photoproducts but not pyrimidine dimers (Latimer *et al.*, submitted). After 2 hours, the labeling medium was removed and replaced with a chasing medium containing non-radioactive thymidine (Sigma) allowing any residual radioactive thymidine to be removed from the intracellular nucleotide pools. The slides were then immersed in photographic emulsion (Kodak type NTB2), and allowed to develop for 11 to 15 days in complete darkness (Cleaver and Thomas, 1981). Tester slides with control cells (foreskin fibroblasts and MDA MB231) were used to assess the optimal time of exposure.

In addition to the peripheral blood lymphocytes, human foreskin fibroblasts were plated, irradiated, and labeled as described for the lymphocyte samples for each experiment. These cells have been documented to have the highest level of NER in mammals and have traditionally served as positive internal controls for the UDS assay (Latimer *et al.*, 1996; Latimer *et al.*, submitted). Normal foreskin fibroblasts have also traditionally been used as a standard in the clinical diagnosis of the classic NER disorder xeroderma pigmentosum, a recessively inherited deficiency in the repair of UV damage.

Determination of NER of exogenously damaged DNA. Following development of the slides, the nuclei were stained with Giemsa and the number of radiolabled grains over the nuclei of 88 non-S-phase cells per chamber was counted at 1000X magnification under oil-immersion. Local background counts for each microscopic field were subtracted from the grain counts of each nucleus as a correction. The average number of grains per nucleus for both the irradiated and unirradiated sides of the slide was then calculated. The final values for the mean number of grains per nucleus for each slide were calculated by

subtracting the corrected unirradiated mean grains per nucleus from the corrected irradiated means.

(corrected avg.#grains/ nucleus irradiated) –
(corrected avg. # grains/ nucleus unirradiated)
=average # of grains/ nucleus for each slide

Mean grain counts for each subject were determined by averaging the mean counts for each of the three slides. This represents the corrected average number of grains over the nuclei of at least 276 cells per subject. Results are expressed as a percentage of irradiated foreskin fibroblast repair, the positive standard of comparison for each experiment.

$$[(\text{Average \# grains/ nucleus lymphocytes}) / (\text{average \# grains/ nucleus FF})] \times 100$$

Normalizing the average number of grains per nucleus in lymphocytes to that of foreskin fibroblast, run in the same experiment, enables inter-assay comparisons and controls for inter-assay variation.

Determinations of NER of Endogenously Damaged DNA. Levels of repair of endogenous damage were calculated using the average number of grains per nucleus from the unirradiated side of the chamber slide. Mean grain counts for each subject were determined by averaging the mean counts for each of the three slides. Results are expressed as a percentage of irradiated foreskin fibroblast repair, the positive standard of comparison for each experiment. As previously stated, normalizing the average number of grains per nucleus in lymphocytes to that of foreskin fibroblasts, run in the same experiment, enables inter-assay comparisons and controls for inter-assay variation.

RESULTS

Demographics. Nineteen subjects completed the protocol at time 1. The mean age of the sample was 25.3 years (range = 19–35). The sample was 68% female ($n = 13$) and 84% of participants ($n = 16$) described themselves as Caucasian. Eighty-nine percent ($n = 17$) were single and never married. This sample consisted of students in a professional academic training program; all of them had completed at least 16 years of schooling. Sixty-three percent ($n = 12$) reported at least one family member with cancer. Demographic data are summarized in Table 1.

Fourteen of the nineteen subjects returned to provide data for time 2. Values for the demographic variables, PSS scores, and NER at time 1 did not differ significantly between those who completed both time points and those who did not complete the second assessment. The demographic characteristics of the sample did not change. All subsequent analyses were carried out using data from only those subjects who completed both assessments.

For the manipulation check, paired *t*-tests were performed on the measures of perceived stress. As expected, the students reported significantly higher levels of perceived stress just prior to exams (time 2) than after returning from a semester or spring break, $t(13) = -2.53$, $p < .05$, two-tailed.

DNA Repair. In order to test the primary hypothesis that DNA repair would be reduced during the examination period, mean values for NER were compared, again using a paired *t*-test. Contrary to our original hypothesis, mean values for NER during the examination period

Table 1 Sample demographic characteristics

Variable	*Mean (SD)*	*Frequency*	*%*
Age in years	25.3 (4.34)		
Gender			
Male		N = 6	31.6
Female		N = 13	68.4
Ethnicity			
African-American		N = 1	5.3
Asian		N = 1	5.3
Caucasian		N = 16	84.2
Other		N = 1	5.3
Marital Status			
Single		N = 17	89.5
Married		N = 1	5.3
Divorced		N = 1	5.3
Family History of Cancer			
Yes		N = 12	63.2
No		N = 7	36.8

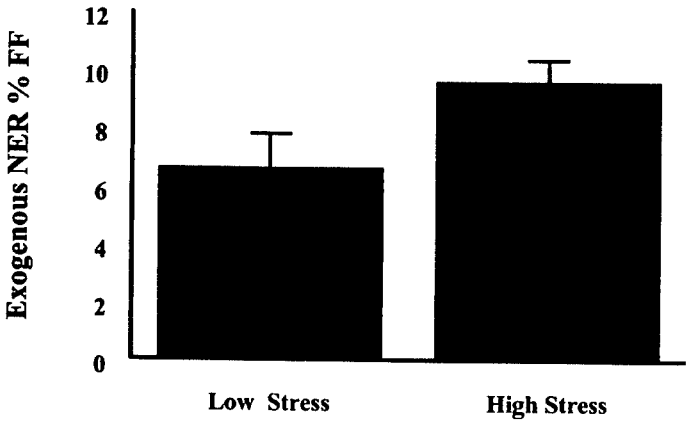

Figure 1 Repair of exogenously damaged DNA by stress period.
Note: Mean values for NER are significantly higher during the high stress period, $t(13) = -2.75$, $p < .05$.

($M = 9.58\%$, $SD = .79$) were significantly *greater* than mean values for NER during the low stress period ($M = 6.23\%$, $SD = 1.31$), $t(13) = -2.47$, $p < .05$ (see Figure 1). There were no differences in DNA repair at time 1 or time 2 as a function of gender or family history of cancer.

To examine the possibility that increased NER might be a function of endogenous DNA damage, secondary analyses with the NER values of the lymphocytes from the unirradiated side of the chamber slide were conducted. This allowed us to examine preirradiated levels of NER during the exam and non-exam periods. While this value is typically removed from the calculation of NER as a background control, it has previously been viewed as an index of DNA repair that may reflect pre-existing levels of DNA damage (Fischman, Pero and Kelly, 1996). The levels of NER during the exam period ($M = 67.78\%$ $SD = 25.19$) were almost twice that for the non-exam period ($M = 36.63\%$ $SD = 17.74$), $t(13) = -4.99$, $p < .001$, suggesting that stress may be damaging to DNA in a way that can be remediated by the NER pathway (see Figure 2).

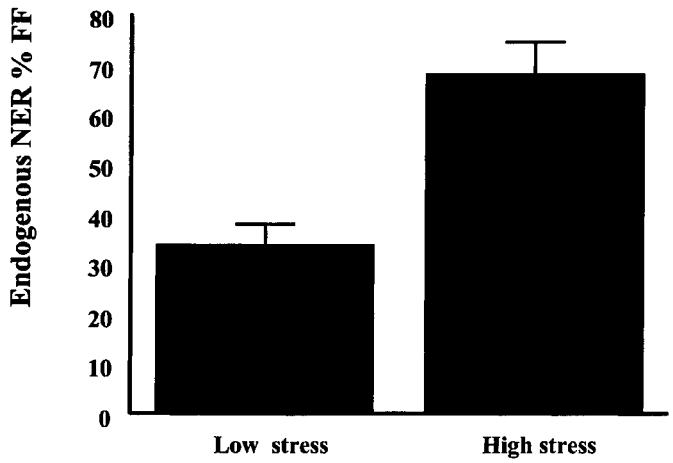

Figure 2 Repair of endogenously damaged DNA by stress period.
Note: Mean values for NER are significantly higher during the high stress period, $t\,(13) = 4.99$, $p < .001$.

DISCUSSION

This study tested the hypothesis that stress associated with academic examinations can inhibit the repair of exogenously damaged DNA. This hypothesis was examined by evaluating the NER capacity of peripheral blood lymphocytes from healthy, nonsmoking, graduate students during both a low and high stress period. Contrary to prediction, DNA repair increased significantly during the examination period and was independent of age, gender, and family history of cancer. Thus, stress may account for some of the non-age related variation in NER that has been reported previously (Setlow, 1983; Wei *et al.*, 1994; Grossman, 1997).

Additionally, stress may increase DNA repair indirectly by increasing damage to DNA. In other words, stress may have direct or indirect genotoxic effects that would require adaptive increases in DNA repair to keep the rate of mutation the same. We examined this possibility in secondary analyses with the NER values of the lymphocytes from the unirradiated side of the chamber slide. As noted previously, increased levels of NER prior to exogenously induced damage may reflect increases in endogenous DNA damage (Fischman, Pero and Kelly, 1996). The observed increase in unirradiated levels of NER during the high stress period lends support to the hypothesis that the higher levels of DNA repair observed during the high stress examination period were due at least in part, to greater DNA damage (see Figure 3).

These results are different from those reported by Kiecolt-Glaser *et al.* (1985) and the extensive dissimilarities in both the samples and the methods of these studies make comparison somewhat problematic. However, these differences may account for some discrepancies. Severity of stress is likely to be important, and the present study measured modest, transient stress in a sample of young, healthy, nonsmoking, community-dwelling students. Kiecolt-Glaser *et al.* (1985) measured more severe distress in psychiatric inpatients. Another important difference concerns the timing of the putative stressor. Exam related stress could be considered an acute or episodic event of a relatively fixed duration. In contrast, mental

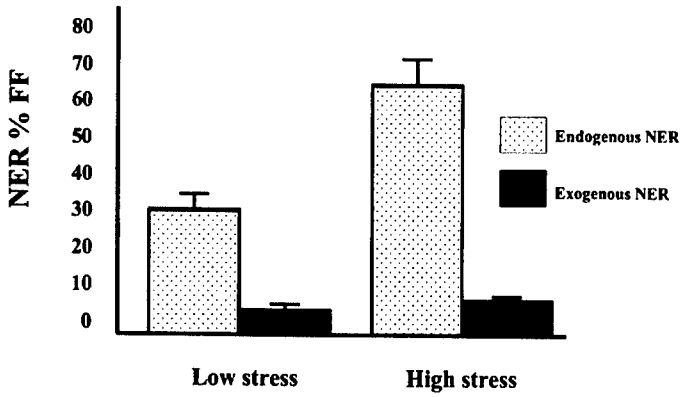

Figure 3 Repair of exogenously and endogenously damaged DNA by stress period.
Note: Mean values for NER of exogenously damaged DNA are significantly higher during the high stress period, $t(13) = -2.75, p < .05$.
Mean values for NER of endogenously damaged DNA are significantly higher during the high stress period, $t(13) = 4.99, p < .001$.

illness severe enough to warrant hospitalization is typically more chronic in nature. The differential effects of acute and chronic stress exposure on DNA repair are unknown.

Additionally, each study examined different repair systems. The present study looked at the NER of UV damaged DNA. UV light creates very specific types of lesions in DNA (i.e. 6–4 photoproducts and pyrimidine dimers). These lesions are remediated specifically though the NER pathway. In contrast, X-ray damage induces a much wider variety and severity of lesions (e.g., single and double strand breaks, oxidative damage) requiring the involvement of many different repair systems including NER. It is not clear how the mechanisms of UV and X-ray damage repair relate to each other.

Another difference concerns preparation of the cells prior to irradiation. We cultured our cells in media supplemented with autologous serum, not fetal bovine serum (FBS). Larcom, Morris and Smith (1990) report that autologous serum always yields higher values than FBS for UDS reasoning that the serum contains biological response modifiers that could affect cellular processes related to repair. This may also partially account for our higher values and the persistence of the stress effects across three days of culture.

Finally, our study allowed only two hours for repair of the DNA before removing the radioactive label. Kiecolt-Glaser *et al.* (1985) measured repair at 0, 2, and 5 hours. When compared with healthy blood donors, differences were not apparent until the repair process had gone on for 5 hours, with no difference in repair observed at two hours. The many differences in stress-related and DNA repair-related variables suggest that future studies will need to pay closer attention to the various methodological details in measurement of DNA damage and repair.

Our results also differ from those of Glaser *et al.* (1985). This is not surprising as there are differences in the DNA repair systems of rats and humans (Cleaver, Speakman and Volpe, 1995). For example, UDS in human cells is 5–10 fold higher than in rodent cells and excises more pyrimidine dimers (Layer and Cleaver, 1997). Additionally, rodents appear to repair damage in genomic regions that are actively transcribed while humans repair both transcribed and untranscribed regions (Layer and Cleaver, 1997). Finally, Glaser *et al.* (1985) did not measure NER, but the expression of spleenic methytransferase activity which functions as part of the Base Excision Repair (BER) pathway.

Despite the small size of our study sample, our findings are statistically significant. The within-subjects design provides more power than a between-subjects design with a similar sample size and is unprecedented in the DNA repair literature. Additionally, small sample size (and the resultant low power) often contributes to the inability to find significant differences that truly exist. Our significant result argues against this possibility. However, we do acknowledge that our small sample size is a limitation that argues for caution when generalizing these results. A larger more representative sample would increase variance and could yield different results.

A selection bias may also exist in our volunteer sample. However, the bias seems to have favored those students that were least stressed during exams. That is, the most distressed students did not participate because they did not want their blood drawn immediately prior to their exams. This made detection of a significant difference more difficult, not less. Despite this fact, the difference in repair was still significant.

A third variable other than stress may be responsible for the observed increase in repair. Changes in diet, exercise, sleep or some other unidentified variable may influence DNA repair. The lack of a control group does not allow us to evaluate these alternative hypotheses.

We have suggested that studying the relationship between stress and DNA repair could help explain variation in DNA repair capacity and the subsequent long-term cancer risk. This in turn may offer insight into discrepancies in the literature looking at stress and cancer. Previous research examining the effects of stress on cancer has often led to inconsistent and inconclusive results (Cassileth, 1996; Fox, 1995; Hilakivi-Clarke, Rowland, Clarke and Lippman, 1994; Garssen and Goodkin, 1999; McGee, Williams and Elwood, 1996; Spiegel and Kato, 1996). Methodological problems such as recall and reporting biases, inadequate timing of stress measurements and failure to account for strong biological (e.g., stage of tumor) or behavioral (e.g., smoking history) factors, have made drawing firm conclusions impossible. More importantly, efforts to link stress with the etiology of cancer have failed to identify the intrinsic genetic mechanisms that are affected by stress and that influence neoplastic growth. Research in this area is strengthened by focusing on potential biological mechanisms such as increases in DNA damage, alterations in the amount or rate of DNA repair, inhibition of apoptosis, increases in somatic mutations, and failures of immune surveillance.

Contrary to our hypothesis, we found that NER of exogenously damaged DNA was increased during a period of high stress in young healthy students. Furthermore, we found increases in levels of NER prior to irradiation suggesting as one possibility that stress may be causing an increase in endogenous DNA damage. There is a small literature supporting the relationship between stress and DNA damage in animals. Psychological stress has been shown to damage DNA at the molecular (Adachi, Kawamura and Takemoto, 1993) and chromosomal levels in rats (Fischman, 1989; Fischman, Pero and Kelly, 1996), but there are no such studies in humans. These findings suggest that damage studies directly measuring DNA adducts or excreted DNA damage products should be a priority in research on stress and carcinogenesis.

Acknowledgements

The authors would like to thank Dr. Gregory Miller and Dr. Steven Grant for their intellectual and creative input into the preparation of this manuscript. We would also like to thank Elena Kisin for running the UDS assay, and Laurie Hall and Trish Piatti for their expert assistance in blood collection.

References

Adachi, S., Kawamura, K. and Takemoto, K. (1993) Oxidative damage of nuclear DNA in liver of rats exposed to psychological stress. *Cancer Research*, **53**, 4153–4155.

Barnett, Y.A. and King, C.M. (1995) An investigation of antioxidant status, DNA repair capacity and mutation as a function of age in humans. *Mutation Research*, **338**, 115–128.

Bonn, D. (1998) How DNA-repair pathways may affect cancer risk. *Lancet*, **351** (9095), 42.

Bootsma, D., Weeda, G., Vermeulen, W., Van Vuure, H., Troelstra, C., Van Der Spek, P. and Hoeijmakers, J.H.J. (1995) Nucleotide excision repair syndromes: Molecular basis and clinical symptoms. *Philosophical Transactions of the Royal Society London*, **347**, 75–81.

Bohr, V. (1995) DNA repair fine structure and its relation to genomic instability. *Carcinogenesis*, **16**(12), 2885–2892.

Cassileth, B.R. (1996) Stress and the development of breast cancer. *Cancer*, **77**(6), 1015–1016.

Cheng, L., Eicher, S.A., Guo, Z., Hong, W.K., Spitz, M.R. and Wei, Q. (1998) Reduced DNA repair capacity in head and neck cancer patients. *Cancer Epidemiology Biomarkers Prevention*, **7**, 465–468.

Cleaver, J.E. and Thomas, G.H. (1981) Measurement of unscheduled synthesis by autoradiography. In: E.C. Friedberg and P.C. Hanawalt (Eds.), *DNA Repair: A Laboratory Manual of Research Procedures* (pp. 277–287). New York: Marcel Dekker.

Cleaver, J.E., Speakman, J.R. and Volpe, J.P. (1995) Nucleotide excision repair: variations associated with cancer development and speciation. *Cancer Surveys*, **25**, 125–142.

Cohen, S. (1986) Contrasting the hassles scale with the perceived stress scale: Who's really measuring appraised stress? *American Psychologist*, **41**(6), 716–718.

Cohen, S., Kamarck, T. and Mermelstein, R. (1983) A global measure of perceived stress. *Journal of Health and Social Behavior*, **24**, 385–396.

Coligan, J.E., Kruisbeek, A.M., Margulies, D.H., Shevach, E.M. and Strober, W. (Eds.) (1995) *Current Protocols in Immunology* (pp. 7.1.1–7.1.7). New York: John Wiley and Sons, Inc.

Feigelson, H.S., Ross, R.K., Yu, M.C., Coetzee, G.A., Reichardt, J.K.V. and Henderson, B.E. (1997) Genetic susceptibility to cancer form exogenous and endogenous exposures. *Journal of Cell Biochemistry*, **255**, 15–22.

Fischman, H. (1989) Sister chromatid exchanges induced by behavioral stress. *Loss, Grief and Care*, **3**(3–4), 203–213.

Fischman, H., Pero, R.W. and Kelly, D.D. (1996) Psychogenic stress induces chromosomal and DNA damage. *International Journal of Neuroscience*, **84**, 219–227.

Friedberg, E.C., Walker, G.C. and Siede, W. (1995) *DNA Repair and Mutagenesis*. Washington, DC: ASM Press.

Fox, B.H. (1995) The role of psychological factors in cancer incidence and prognosis. *Oncology*, **9**(3), 245–256.

Garssen, B. and Goodkin, K. (1999) On the role of immunological factors as mediators between psychosocial factors and cancer progression. *Psychiatry Research*, **85**, 51–61.

Glaser, R., Pearl, D.K., Kiecolt-Glaser, J.K. and Malarkey, W.B. (1994) Plasma cortisol levels and reactivation of latent herpes virus in response to examination stress. *Psychoneuroendocrinology*, **19**(8), 765–772.

Glaser, R., Thorn, B.E., Tarr, K.L., Kiecolt-Glaser, J. and D'Ambrosio, S.M. (1985) Effects of stress on methytransferase synthesis: An important DNA repair enzyme. *Health Psychology*, **4**(5), 403–415.

Grossman, L. (1997) Epidemiology of ultraviolet-DNA repair capacity and human cancer. *Environmental Health Perspectives*, **105**(supp. 4), 927–930.

Hall, M. and Johnson, R.T. (1996) The role of DNA repair in the prevention of cancer. *Molecular Aspects of Medicine*, **17**(3), 235–283.

Hilakivi-Clarke, L., Rowland, J., Clarke, R. and Lippman, M.E. (1994) Psychosocial factors in the development and progression of breast cancer. *Breast Cancer Research and Treatment*, **29**(2), 141–160.

Jiricny, J. (1994) Colon cancer and DNA repair: Have mismatches met their match? *Trends in Genetics*, **10**(5), 164–168.

Kiecolt-Glaser, J.K., Stephens, R.E., Lipetz, P.D., Speicher, C.E. and Glaser R. (1985) Distress and DNA repair in human lymphocytes. *Journal of Behavioral Medicine*, **8**(4), 311–320.

Kovacs, E., Stucki, D., Weber, W. and Muller, Hj. (1986) Impaired DNA repair-synthesis in lymphocytes of breast cancer patients. *European Journal of Cancer and Clinical Oncology*, **22**, 863–869.

Larcom, L.L., Morris, T.E. and Smith M.E. (1990) Factors which affect DNA repair in human lymphocytes. In: B.M. Sutherland and A.D. Woodhead (Eds.), *DNA Repair in Human Tissues* (263–276). New York: Plenum Press.

Larcom, L.L. and Smith, M.E. (1988) Quantitative assay for evaluation immunocompetence and DNA repair capacity. *Journal of the National Cancer Institute*, **80**(14), 1112–1118.

Latimer, J.J., Hultner, M.L., Cleaver, J.E. and Pedersen, R.A. (1996) Elevated DNA excision repair capacity in the extraembryonic mesoderm of the midgestation mouse embryo. *Experimental Cell Research*, **228**, 19–28.

Latimer, J.J, Nazir, T., Dimsdale, J., Kisin, E., Kanbour-Shakir, A. and Flowers, L. (under review) DNA repair capacity in normal breast and ovarian epithelium.

Layer, S.L. and Cleaver, J.E. (1997) Quantification of XPA gene expression levels in human and mouse cell lines by competitive RT-PCR. *Mutation Research*, **383**, 9–19.

Maes, M., Hendriks, D., Van Gastel, A., Demedts, P., Wauters, A., Neels, H., Janca, A. and Scharpe, S. (1997) Effects of psychological stress on serum immunoglobulin, complement and acute phase protein concentrations in normal volunteers. *Psychoneuroendocrinology*, **22**(6), 397–410.

Maes, M., Van Der Planken, M., Van Gastel, A., Bruyland, K., Van Hunsel, F., Neels, H., Hendriks, D., Wauters, A., Demedts, P., Janca, A. and Scharpe, S. (1998) Influence of academic examination stress on hematological measurements in subjectively healthy volunteers. *Psychiatry Research*, **80**(3), 201–212.

Marucha, P.T., Kiecolt-Glaser, J.K. and Favagehi, M. (1998) Mucosal wound healing is impaired by examination stress. *Psychosomatic Medicine*, **60**(3), 362–365.

McGee, R., Williams, S. and Elwood, M. (1996) Are life events related to the onset of breast cancer? *Psychological Medicine*, **26**(3), 441–448.

Moriwaki, Ray, Tarone, Kraemer and Grossman. (1996) The effect of donor age on the processing of UV-damaged DNA by cultured human cells: Reduced DNA repair capacity and increased DNA mutability. *Mutation Research*, **364**, 117–123.

Setlow, R.B. (1978) Repair deficient human disorders and cancer. *Nature*, **271**, 713–717.

Setlow, R.B. (1983) Variation in DNA repair among humans. In: C. Harris and H. Autrup (Eds.), *Human Carcinogenesis* (pp. 231–244). New York: Academic Press.

Spiegel, D. and Kato, P.M. (1996) Psychosocial influences on cancer incidence and progression. *Harvard Review of Psychiatry*, **4**, 10–26.

Steier, H. and Cleaver, J.E. (1969) Exposure chamber for quantitative ultraviolet photobiology. *Lab Practice*, **18**, 1295.

Tomei, L.D., Kiecolt-Glaser, J.K., Kennedy, S. and Glaser, R. (1990) Psychological stress and phorbol ester inhibition of radiation-induced apoptosis n human peripheral blood leukocytes. *Psychiatry Research*, **33**(1), 59–71.

Van Hunsel, F., Van Gastel, A., Neels, H., Wauters, A., Demedts, P., Bruyland, K., Demeester, I., Scharpe, S., Janca, A., Song, C. and Maes, M. (1998) The influence of psychological stress on total serum protein and patterns obtained in serum protein electrophoresis. *Psychological Medicine*, **28**(2), 301–309.

Vogelstein, B. and Kinzler, K. (1993) The multistep nature of cancer. *Trends in Genetics*, **9**(4), 138–141.

Wei, Q., Cheng, L., Hong, W.K. and Spitz, M.R. (1996) Reduced DNA repair capacity in lung cancer patients. *Cancer Research*, **56**, 4103–4107.

Wei, Q., Matanoski, G.M., Farmer, E.R., Hedayati, M.A. and Grossman, L. (1994) DNA repair related to multiple skin cancers and drug use. *Cancer Research*, **54**, 437–440.

Yu, Z., Chen. J., Ford, B.N., Brackley, M.E. and Glickman, B.W. (1999) Human DNA repair systems: An overview. *Environmental and Molecular Mutagenesis*, **33**, 3–20.

A New Strategy for Tumor Antigen Discovery Based on *in Vitro* Priming of Naïve T Cells with Dendritic Cells[1]

Henry Kao, Andrew A. Amoscato, Pawel Ciborowski, and Olivera J. Finn[2]

Immunology Graduate Program [H. K.], Department of Molecular Genetics and Biochemistry [H. K., P. C., O. J. F.], University of Pittsburgh Mass Spectrometry Facility, The University of Pittsburgh Center for Biotechnology and Bioengineering [A. A. A.], University of Pittsburgh School of Medicine, Pittsburgh, Pennsylvania 15261

Abstract

We describe a method for discovery of new tumor antigens that uses dendritic cells (DCs) as antigen-presenting cells to prime autologous naïve $CD4^+$ and $CD8^+$ T cells from healthy donors against tumor proteins and peptides. For the identification of HLA class I-restricted tumor antigens, peptides were extracted from tumor HLA class I molecules, fractionated by reverse phase-high performance liquid chromatography, and loaded onto *in vitro*-generated DCs to prime naïve $CD8^+$ T cells. Our results show that we were able to prime naïve $CD8^+$ T cells *in vitro* to several peptide fractions and generate specificity for the tumor. Electrospray ionization mass spectrometry was used to confirm that these fractions contained peptides derived from MHC class I molecules, and the primed $CD8^+$ T cells were used to further analyze the immunostimulatory peptide fractions. For the identification of HLA class II-restricted tumor antigens, we fractionated tumor protein extracts using reverse phase-high performance liquid chromatography and loaded individual fractions onto DCs to prime naïve $CD4^+$ T cells. Our results show that we were also able to prime naïve $CD4^+$ T cells to several protein fractions and generate specificity for the tumor. These results illustrate the potential of this method to identify new immunostimulatory MHC class I- and class II-restricted tumor antigens.

Introduction

Successful immunotherapy against tumors relies in part on the discovery of tumor-specific antigens that are able to stimulate effective immune responses in the host. Several approaches have been developed over the years for the identification of tumor antigens. The "genetic approach" uses tumor cDNA libraries transfected into target cells expressing appropriate HLA molecules (1, 2). The "peptide elution approach" uses peptides eluted from tumor HLA and loaded on target cells bearing the same HLA molecules (3, 4). The "reverse immunology approach" uses peptide sequences derived from already known oncogenes or other putative tumor-associated genes that contain desired HLA anchor motifs (5, 6). All of these approaches depend on the availability of tumor-specific T-cell lines or clones derived from cancer patients and used to recognize the new targets. Most recently, the SEREX approach has been used where tumor cDNA expression libraries are screened with sera from cancer patients (7). These approaches have led to the identification of a panel of tumor antigens, primarily in melanomas (8–15). Very few tumor-specific antigens have been described in epithelial tumors, the best known being the HER-2/neu-derived peptides (16) and the core peptides of the MUC-1 tandem repeat (17). In addition to the overall number of tumor antigens being small, there is a concern that they were all identified using an immune response from individuals with cancer that has clearly not been effective as a tumor rejection response. Therefore, we devised and tested a new antigen discovery system that seeks to determine not what a cancer patient recognizes on his/her tumor but rather what a healthy immune system recognizes as foreign among numerous peptides and proteins derived from tumor cells. Our approach is based on *in vitro* cultured DCs[3] that are used to prime autologous healthy naïve T cells.

DCs have been shown to be the most potent APCs in the immune system, expressing high levels of MHC molecules, costimulatory molecules, and adhesion molecules essential for T-cell activation (18). Furthermore, DCs are capable of inducing primary T-cell responses *in vitro* to both viruses and synthetic peptides (19–22), whereas other APCs can only stimulate previously sensitized T cells (23). DCs have been successfully used to prime naïve T cells *in vitro* against several known tumor antigens (24–30).

Studies have shown marked alterations in the signal-transduction molecules in the T cells of human cancer patients, such as alterations in expression of $p56^{lck}$ tyrosine kinase, T-cell receptor ζ-chain (31), and nuclear factor-κB p65 transcription factors (32). Therefore, in our approach we have used T cells from healthy donors. The results here illustrate the utility of this new approach for priming naïve $CD4^+$ and $CD8^+$ T cells against proteins and peptides isolated from a breast epithelial tumor cell line and presented by DCs grown *in vitro*, and generation of specificity for the tumor. This has led to the isolation of candidate HLA class I- and HLA class II-restricted epithelial tumor antigens.

[1] This work is supported by Department of Defense Grant DAMD 17-9-1-7057 (to H. K.) and NIH Grant 1PO1CA 73743 (to O. J. F.).

[2] To whom requests for reprints should be addressed, at University of Pittsburgh School of Medicine, Department of Molecular Genetics and Biochemistry, W1142 Biomedical Science Tower, Terrace and DeSoto Streets, Pittsburgh, PA 15261. Phone: (412) 648-9816; Fax: (412) 383-8859; E-mail: ojfinn@pitt.edu.

[3] The abbreviations used are: DC, dendritic cell; APC, antigen-presenting cell; RP-HPLC, reverse phase- high performance liquid chromatography; TFA, trifluoroacetic acid; ATCC, American Type Culture Collection; IL, interleukin.

Materials and Methods

Cell Lines

MS (A3, B7, B7, C7, C7; DR15, DQ6 homozygous) is a breast epithelial adenocarcinoma cell line derived from the metastasis of a breast cancer patient. This cell line does not express either MUC1 or HER-2/neu (data not shown), the two major epithelial tumor antigens. MS-A2 is the same cell line that we stably transfected with the HLA-A2.1 plasmid (33) using the calcium phosphate precipitation method (Stratagene, La Jolla, CA). The B-lymphoma cell line Raji (A3, B15, C7 homozygous; DR3, DR10, DQ1, DQ2) was purchased from the ATCC (Manassas, VA). The chronic myelogenous leukemia cell line K562 was also purchased from ATCC. The melanoma cell line Mel 624 (A2, A3, B7) was provided by Dr. S. A. Rosenberg (National Cancer Institute, Bethesda, MD). The lung tumor cell line, 201T (A10, A29, B15, B44), which we also transfected with the HLA-A2.1 plasmid (designated 201T-A2), was a kind gift from Dr. Jill Siegfried (University of Pittsburgh). Naïve $CD4^+$, $CD8^+$ T cells, DCs, and macrophages were derived from a leukophoresis product of a healthy platelet donor (A2, A29, B7, B44, C7, C7; DR15, DR7, DQ6, DQ2) obtained through the Central Blood Bank of Pittsburgh (Pittsburgh, PA).

Antibodies

Mouse antihuman HLA-DR (L243), CD3 (Leu-4), CD4 (Leu-3a), CD8 (Leu-2a), and CD56 (Leu-19) were purchased from Becton Dickinson (San Jose, CA). Mouse antihuman CD45RO (UCHL1) and CD20 were purchased from Dako (Carpinteria, CA). Goat antimouse IgG antibodies were obtained from Zymed Laboratories, Inc. (South San Francisco, CA). W6/32, a mouse antihuman MHC class I antibody, was produced by the W/632 hybridoma obtained from ATCC (Manassas, VA) and purified via a protein A-Sepharose column (Sigma Chemical Co., St. Louis, MO) in the laboratory.

Isolation of Tumor HLA Class I-bound Peptides

Isolation of HLA class I-associated peptides was similar to methods described previously (3, 34). MS-A2 tumor cells were grown in 10-chamber cell factories (Nalge Nunc, Naperville, IL) and expanded weekly until $>1.5 \times 10^{10}$ cells were obtained. The cells were washed three times in ice-cold PBS, pelleted, and stored at −80°C for later use. Detergent lysis buffer (1% 3-[(3-cholamidopropyl)dimethylamino]-1-propanesulfonate and a mixture of protease inhibitors (2 mM phenylmethylsulfonyl fluoride, 100 μM iodoacetamide, 5 μg/ml aprotinin, 10 μg/ml leupeptin, 10 μg/ml pepstatin A, 3 ng/ml EDTA, and 0.04% sodium azide; Sigma) were used to solubilize the cells at 4°C for 1 h. The cell lysate was spun at 100,000 × *g* for 1 h to remove insoluble proteins, and the supernatant was filtered through a 0.22 μm filter (Millipore, Bedford, MA) to further remove debris from the suspension. The supernatant was then passed through a protein A-Sepharose anti-class I (W6/32) column (Bio-Rad, Hercules, CA) overnight. The column was then washed 30 times sequentially with low salt (150 mM NaCl, 20 mM Tris, pH 8.0) buffer, high salt (1 M NaCl, 20 mM Tris, pH 8.0) buffer, and Tris buffer (20 mM Tris, pH 8.0). Class I molecules were then eluted from the column using 0.2 N acetic acid, and peptides were extracted from the class I molecules by boiling in 10% acetic acid for 5 min. The released peptides were further purified using 5-kDa cutoff microconcentrators (Amicon, Bedford, MA), vacuum centrifuged to reduce the volume, and frozen at −80°C.

HPLC

Fractionation of Peptide Extracts. The peptide extracts were fractionated by RP-HPLC on a Rainin HPLC separation system (Varian, Woburn, MA). The peptide extracts were concentrated to 150 μl via vacuum centrifugation and injected into a Brownlee Aquapore (Applied Systems, Inc., San Jose, CA) C_{18} column (column dimensions, 2.1 mm × 3 cm; pore size, 300 Å; particle size, 7 μm) on the HPLC. The peptides were eluted with a 65-min TFA/acetonitrile gradient [v/v 0–15% for 5 min, 15–60% for 50 min, and 60–100% for 10 min solvent B (60% acetonitrile in 0.085% TFA) in solvent A (deionized water in 0.1% TFA)] with a flow rate of 200 μl/min. Two hundred-μl fractions were collected at 1-min intervals, concentrated via vacuum centrifugation to 40 μl, and divided into four aliquots, three for the use in T-cell stimulation and 1 for mass spectrometry analysis.

Fractionation of Protein Extracts. MS tumor cells ($>1 \times 10^9$) were lysed in detergent buffer, spun at 100,000 × *g*, and then filtered using a 0.22 μm filter as above. The supernatant was dialyzed overnight in Tris-buffered saline (TBS; pH 7.2; Sigma) to remove detergent. The protein extract was concentrated by vacuum centrifugation, and one-tenth of the extract ($\sim 1 \times 10^8$ cell equivalents) was fractionated by RP-HPLC using a Phenomenex Jupiter C4 column (column dimensions, 4.6 mm × 150 mm; pore size, 300 Å; particle size, 7 μm; Torrence, CA). The proteins were eluted with a 60-min TFA/acetonitrile gradient [v/v 10–80% solvent B (100% acetonitrile in 0.1 TFA) in solvent A (deionized water in 0.1% TFA)] at a flow rate of 500 μl/min. Five hundred-μl fractions were collected at 1-min intervals, concentrated by vacuum centrifugation to 100 μl, and divided into four aliquots, three for the use in T-cell stimulation and one for protein content analysis.

Subfractionation of Protein Fractions. Twenty-five % of a specific protein fraction obtained from the primary fractionation was further subfractionated by RP-HPLC using a Phenomenex Jupiter C4 column (column dimensions, 4.6 mm × 150 mm; pore size, 300 Å; particle size, 7 μm; Torrence, CA). The proteins were eluted with a shallow 10-min TFA/acetonitrile gradient [v/v 55–62% solvent B (100% acetonitrile in 0.1 TFA) in solvent A (deionized water in 0.1% TFA)] at a flow rate of 500 μl/min, and fractions were collected at 1-min intervals. The subfractions were then further concentrated by vacuum centrifugation, with 33% of the material loaded onto a 15% SDS-PAGE gel and visualized using a silver stain analysis kit (Bio-Rad), and 33% was loaded onto macrophages and used in a proliferation assay (see below). All solvents were HPLC grade and were obtained from VWR Scientific Products (West Chester, PA).

Generation of DCs *in Vitro*

DCs were cultured *in vitro* for 7 days as described previously (28). Peripheral blood mononuclear cells from a healthy donor were isolated after centrifugation over Lymphocyte Sep-

aration Medium (Organon Teknika, Durham, NC) and washed extensively with PBS to eliminate residual platelets. The cells were plated in a T-75 flask for 2 h in serum-free AIM-V (Life Technologies, Inc., Grand Island, NY) medium, after which the nonadherent cells were removed and used as the source of naïve T cells (see below). The adherent cells were treated with 1000 units/ml granulocyte/macrophage-colony stimulating factor and 26 ng/ml IL-4 (Schering-Plough, Kenilworth, NJ) for 7 days in serum-free AIM-V (Life Technologies, Inc.) medium supplemented with 2 mM L-glutamine and penicillin/streptomycin. DCs were fed with additional medium and cytokines on day 4 of culture and purified on day 7 by negative selection of contaminating T, B, and NK cells. The cells were stained with anti-CD3, anti-CD19, and anti-CD56 antibodies for 45 min in cold PBS and washed in PBS supplemented with 5% human AB serum (Gemini Products, Calabasas, CA). Magnetic Dynal beads (Lake Success, NY) coated with goat antimouse IgG were then added to the cells for 45 min, and the contaminating cells were removed by magnetic separation. Flow cytometry analysis of the remaining cells showed that they were high HLA-DR$^+$ and B7–2$^+$.

Purification of Naïve CD8$^+$ and CD4$^+$ T Cells

Nonadherent cells obtained after plastic adherence for DC isolation was used as the source of naïve CD8$^+$ or naïve CD4$^+$ T cells. To purify naïve CD8$^+$ T cells, the cells were stained with anti-CD4, anti-CD20, anti-CD56, and anti-CD45RO antibodies for 45 min in cold PBS and washed in PBS with 5% HAB serum. Four 100-mm Petri dishes (Nunc LabTek, Naperville, IL) were precoated with 10 μg/ml goat antimouse IgG antibodies (Zymed) in 0.05 M Tris (pH 9.5) at room temperature for 1 h and washed with PBS. Cells were added to each plate and incubated at 4°C for 1 h. The nonadherent cells collected were the CD45RA$^+$CD8$^+$ T cells. The same procedure was used for purifying naïve CD4$^+$ T cells, except that anti-CD8 antibodies are used instead. All T-cell cultures were grown in RPMI 1640 (ICN, Costa Mesa, CA) supplemented with 10% human AB sera (Gemini Products), L-glutamine, and penicillin/streptomycin (Life Technologies, Inc.).

Priming Naïve CD8$^+$ T Cells to Tumor Peptides

To prime naïve CD8$^+$ T cells, 2×10^4 DCs were incubated for 2–4 h, first with 25% of each peptide containing RP-HPLC fraction (10 μl) and then overnight in the presence of 1000 units/ml tumor necrosis factor-α (Genzyme, Cambridge, MA) in 96-well, U-bottomed plates (Falcon, Franklin lakes, NJ). Autologous naïve CD8$^+$ T cells (2×10^5) were added the next day to the DCs in the presence of 2 ng/ml IL-1β (R&D Systems, Minneapolis, MN), 20 units/ml IL-2 (DuPont, Wilmington, DE), and 26 ng/ml IL-4 (Schering-Plough). The CD8$^+$ T-cell cultures were fed every 3–4 days with 10 units/ml IL-2 and 13 ng/ml IL-4, depending on growth kinetics. In addition, 10 ng/ml IL-7 (PharMingen, San Diego, CA) was included in the cytokine mixture after the second restimulation. The CD8$^+$ T-cell cultures were restimulated every 7–10 days using autologous macrophages (obtained by plastic adherence) loaded with the individual peptide fractions until the third restimulation, where autologous macrophages loaded with irradiated (12,000 rads) MS-A2 tumors (macrophages:tumor, 1: 5) were used as stimulators (T cells:loaded macrophages, 10:1).

Priming Naïve CD4$^+$ T Cells to Tumor Proteins

To prime naïve CD4$^+$ T cells, DCs were loaded with 25% of each protein fraction (~ 25 μl) and treated the same as described for CD8$^+$ T-cell priming above. The CD4$^+$ T-cell cultures were restimulated every 10–14 days using autologous macrophages loaded with the individual protein fractions (T cells:macrophages, 10:1) and fed every 4–5 days with 10 units/ml IL-2 and 13 ng/ml IL-4, depending on growth kinetics. Ten ng/ml IL-7 (PharMingen) were added to the CD4$^+$ T-cell cultures after the second restimulation. For the third restimulation, MS tumor was irradiated for 7 min (2.18 J/cm^2) using a Spectra Mini II UV-B irradiator (Daavlin, Bryan, OH) and loaded onto macrophages overnight (apoptotic tumor:macrophages, 5:1) that were used as stimulators (T cells:loaded macrophages, 10:1) the next day.

Cytotoxicity Assays

Target cells (1–2 × 10^6) were labeled with 50 μCi of $Na_2{}^{51}CrO_4$ (Amersham, Arlington Heights, IL) for 90 min at 37°C. The labeled cells were then washed three times and plated at 1×10^3 cells/well in a 96-well, V-bottomed plate (Costar, Cambridge, MA) with various numbers of effector T cells. In addition, a 50-fold excess of unlabeled K562 (5×10^4) was added to the wells for 15 min prior to the addition of T cells to prevent the detection of lymphokine-activated killer activity in the assay. The plates were centrifuged and incubated for 4 h at 37°C. All determinations were done in triplicate. Supernatants were harvested using a Skatron harvesting press (Skatron Instruments, Sterling, VA) and counted on a Cobra II series auto gamma counting system (Packard, Meriden, CT). Maximum release was obtained by adding 50 μl of 1% Triton X-100 to the labeled target cells. Spontaneous release was obtained by incubating the labeled cells in the absence of T cells. The percentage of specific lysis was calculated from the following formula: % specific lysis = 100 × (experimental release − spontaneous release)/(maximum release − spontaneous release). In blocking experiments, anti-MHC class I antibody (W6/32) was added to the labeled target cells for 30 min prior to the addition of the effector T cells.

Proliferation Assays

Autologous macrophages loaded with UV-induced apoptotic MS tumor cells (apoptotic tumor:macrophages, 5:1) were seeded in round-bottomed, 96-well microplates (Costar, Cambridge, MA) with primed T-cell cultures at a T cell:stimulator ratio of 20:1. For proliferation assays using tumor lysate, MS tumor cell lysate was generated as described above, and 1.75×10^8 cell equivalents were loaded onto 2×10^6 autologous macrophages for 2 h. T cells were added at a T cell:stimulator ratio of 10:1. For the proliferation assay using the subfraction 44, 33% of the subfraction was loaded onto 5×10^4 macrophages overnight and added to T cells with a T cell:stimulator ratio of 1:1 the next day. The wells were pulsed with [^{3}H]thymidine (Amersham, Life Science) for the last 18 h of the 5-day period, harvested by a Skatron semiautomatic cell harvester (Skatron Instruments), and counted on a Wallac 1205 beta plate scintillation counter (Gaithersburg, MD). The results are expressed as mean values of triplicate determinations.

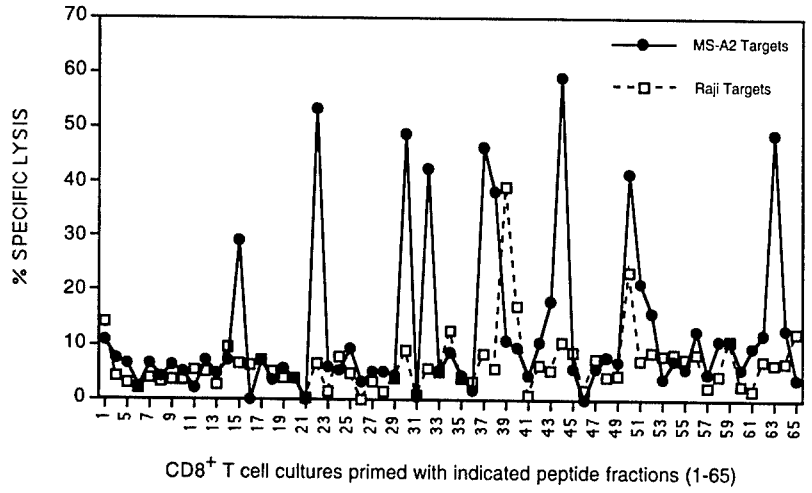

Fig. 1 Identification of 12 primed $CD8^+$ T-cell cultures that recognized the original tumor, MS-A2, from which the tumor peptides were derived. The primed T cells were tested after the fourth restimulation. The E:T ratio was 100:1. The Raji cell line (A3, B15, C7) was a control for alloreactivity.

Mass Spectrometry Analysis

Twenty-five % of the RP-HPLC peptide fraction was concentrated by vacuum centrifugation to near dryness and resuspended in 5 μl of 0.1 M acetic acid. One μl of this material was loaded onto a microcapillary C_{18} column (150 mm × 75 μm inside diameter) and eluted with a 20-min linear gradient [v/v 0–80% solvent B (0.1 M acetic acid in 100% acetonitrile) in solvent A (deionized water in 0.1 M acetic acid)]. Flow rates for the nanospray probe (186 nl/min) was achieved by coupling the Rainin HPLC system with an Accurate microflow processor (LC Packings, San Francisco, CA) for flow splitting. The nanospray probe was operated at a voltage differential of +3.2 keV. The source temperature was maintained at 30°C. Mass spectra were obtained by scanning from 300-1500 every 3 s and summing individual spectra on a Fisons Quattro II triple quadrupole mass spectrometer (Micromass, Inc., Loughborough, United Kingdom).

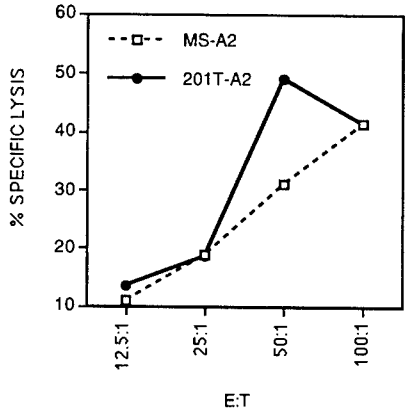

Fig. 2 $CD8^+$ T cells primed with peptide fraction 32 from MS-A2 tumor recognized a shared tumor antigen on a lung tumor cell line 201T-A2. $CD8^+$ T cells generated from priming to eluted peptides from fraction 32 were used in a CTL assay after the fifth restimulation.

Results

Identification of HPLC Fractions Containing Immunogenic Tumor Peptides. $CD8^+$ T-cell cultures were primed and restimulated with HPLC fractions as described in "Materials and Methods." Because of the low amount of peptide, later restimulations were done using macrophages loaded with irradiated MS-A2 tumor cells. Monitoring the $CD8^+$ T-cell cultures with an inverted microscope over four restimulations clearly showed that although there was T-cell proliferation in all wells, several of the $CD8^+$ T-cell cultures were expanding at a much higher rate, suggesting the presence of immunostimulatory peptides in the fractions used for priming in these wells. Most of the unstimulated $CD8^+$ T-cell cultures reached senescence after 8 weeks in culture.

Fig. 1 shows the result of one priming experiment in which after the fourth restimulation, we were able to test all of the T-cell cultures for their ability to recognize the original tumor, MS-A2, from which the peptides were derived. Of the 65 $CD8^+$ T-cell cultures primed on the individual peptide fractions, 12 (fractions 15, 22, 30, 32, 37, 38, 43, 44, 50, 51, 52, and 63) exhibited strong cytotoxicity against the tumor. Because the peripheral blood lymphocyte donor and the tumor were mismatched at the *HLA-A3* allele, we also used the Raji tumor cell line, which was matched only at the *HLA-A3* allele with the peripheral blood lymphocyte donor, to ensure that the cytotoxic $CD8^+$ T-cell cultures were not alloreactive. None of the cultures that killed MS-A2 tumor cells recognized the Raji targets.

The 12 cytotoxic $CD8^+$ T-cell cultures were also tested for their ability to recognize another epithelial adenocarcinoma, a lung tumor, 201T-A2, to look for shared tumor antigens. As shown in Fig. 2, a $CD8^+$ T-cell culture, primed with peptide fraction 32, recognized again the original tumor and also the lung tumor. Because the lung tumor and the breast tumor shared only the *HLA-A2.1* allele, this suggested that the peptide being recognized was a shared antigen restricted by HLA-A2.1.

To determine the extent of reproducibility of this approach, we repeated the acid extraction, peptide fractionation, and priming procedure. We decided to pool several consecutive HPLC fractions for two reasons: (*a*) to compensate for small shifts in fraction number between HPLC runs; and (*b*) to reduce the total number of T-cell cultures *in vitro*, making the approach less labor intensive. Naive $CD8^+$ T cells were primed on pooled

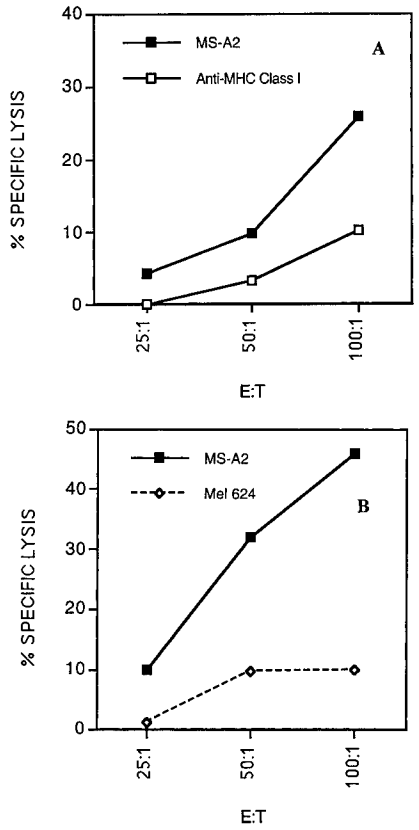

Fig. 3 $CD8^+$ T cells primed with pooled peptide fractions recognized the original tumor and were HLA class I-restricted. *A*, $CD8^+$ T cells primed with peptide fractions 41–46 recognized the original tumor, MS-A2, and were blocked by the anti-MHC class I antibody, W6/32. *B*, $CD8^+$ T cells primed with peptide fractions 61–65 recognized the original tumor (MS-A2) and not an HLA-matched tumor, Mel 624.

fractions that were composed of the immunostimulatory fractions identified earlier as well as flanking fractions. The patterns of T-cell stimulation and expansion induced by the pooled fractions were consistent with the patterns induced by the immunostimulatory fractions observed in the previous priming. An example is shown in Fig. 3, in which we primed $CD8^+$ T-cell cultures to pooled fractions 41–46 (Fig. 3*A*) and 61–65 (Fig. 3*B*), and generated specificity to the original tumor, MS-A2. This corresponded to immunostimulatory fraction 44 and fraction 63 from the previous run, respectively (Fig. 1). We also showed that $CD8^+$ T cells primed on pooled fractions 41–46 were blocked by the anti-MHC class I antibody, W6/32 (Fig. 3*A*). Furthermore, we showed that the specific antigen was present in the epithelial tumor and not in the perfectly HLA-matched melanoma Mel 624 (Fig. 3*B*).

To evaluate the content of these 12 immunostimulatory fractions, we analyzed them by electrospray ionization nanospray mass spectrometry. We obtained a panel of peptide species (Table 1) conforming to mass:charge ratios of 700-1300 daltons, indicative of HLA class I-binding peptides. These results showed that we were successful in extracting peptides from HLA class I molecules, and that there were immunostimulatory peptides in the HPLC fractions that were capable of stimulating naïve $CD8^+$ T cells to

Table 1 Mass spectrometry analyses of immunostimulatory peptide fractions[a]

Fraction no.	m/z[b]	Fraction no.	m/z
15	851.7, 879.8[c]	44	615.2, 1229.5, 942.3, 921.4, 1061.5
22	921.3, 1061.4	50	728.1, 949.2, 1256.5
30	717	51	949
32	717	52	949, 885.9
37	None	63	805.6
38	921.3		
43	949.2, 816		

[a] HPLC peptide fractions that tested positive in the CTL assay were analyzed by nanospray microcapillary HPLC mass spectrometry.
[b] Mass:charge ratio.
[c] Peptide mass:charge ratios (m/z) conforming to peptides that bind HLA class I molecules (700–1300 daltons) were considered candidates for tumor antigens.

proliferate and expand *in vitro*. We are in the process of sequencing these peptides, and thus far, we have identified a series of peptides that belong to a new tumor antigen.[4]

Identification of HPLC Fractions Containing Immunogenic Tumor Proteins. We have devised and tested a similar strategy to identify HLA class II-restricted tumor antigens by analyzing immunostimulatory properties of fractionated tumor proteins. $CD4^+$ T-cell cultures were primed and restimulated as described in "Materials and Methods." By the third restimulation, macrophages loaded with apoptotic MS tumor cells were used to stimulate the $CD4^+$ T-cell cultures. Similar to the $CD8^+$ T-cell cultures, observation of the $CD4^+$ T-cell cultures with an inverted microscope over five restimulations showed that not all of the $CD4^+$ T-cell cultures were growing equally well, suggesting that the $CD4^+$ T cells were responding to immunostimulatory proteins present in some of these fractions and not in others. Most of the unstimulated $CD4^+$ T-cell cultures reached senescence after 10 weeks in culture.

Fig. 4 shows the results of one priming experiment in which after the second restimulation, we tested all of the T-cell cultures for their ability to recognize the original tumor, MS, from which the proteins were obtained. Autologous macrophages were loaded with apoptotic tumor and used in a 5-day proliferation assay as stimulators of the primed $CD4^+$ T-cell cultures. Of the 52 $CD4^+$ T-cell cultures primed on the individual protein fractions, 14 (fractions 5, 10, 11, 12, 13, 22, 28, 35, 37, 38, 39, 40, 46, and 51) proliferated in response to macrophages loaded with apoptotic tumor. We also tested the $CD4^+$ T-cell cultures for cytotoxicity against the original tumor via a CTL assay. None of the T cells tested killed the original tumor (data not shown). Some of the positive $CD4^+$ T-cell cultures were also tested for their ability to recognize autologous macrophages loaded with tumor lysate. As shown in Fig. 5, $CD4^+$ T-cell

[4] Kao, H. Marto, J. A., Hoffman, T. K., Shabanowitz, J., Finkelstein, S. D., Whiteside, T. L., Hunt, D. F., Finn, O. J., manuscript in preparation.

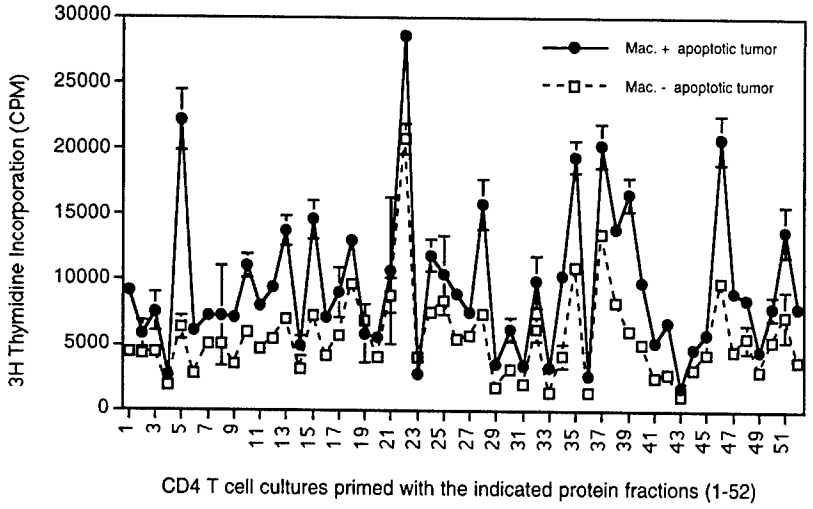

Fig. 4 Identification of 12 primed $CD4^+$ T-cell cultures that recognized the original tumor, MS, from which the proteins were obtained. The primed $CD4^+$ T cells were tested in a proliferation assay using macrophages loaded with UVB-induced apoptotic tumor (T cells:macrophages, 20:1) after the second restimulation. *Bars*, SD.

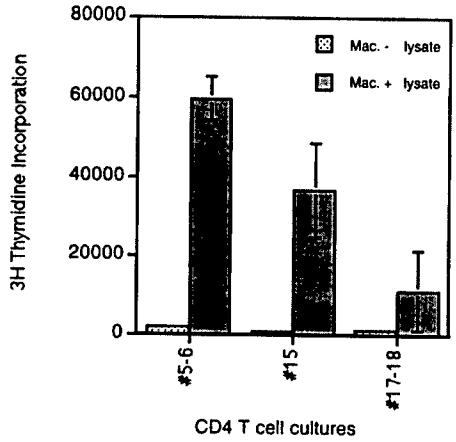

Fig. 5 $CD4^+$ T-cell cultures primed with protein fractions recognize autologous macrophages loaded with tumor lysate. Autologous macrophages (2×10^6) were loaded with $\sim 1.75 \times 10^8$ cell equivalents of tumor lysate for 2 h and used as stimulators of primed $CD4^+$ T-cell cultures in a proliferation assay. T-cell cultures were pooled as indicated. T cells were added at a T cell:macrophage ratio of 10:1. *Bars*, SD.

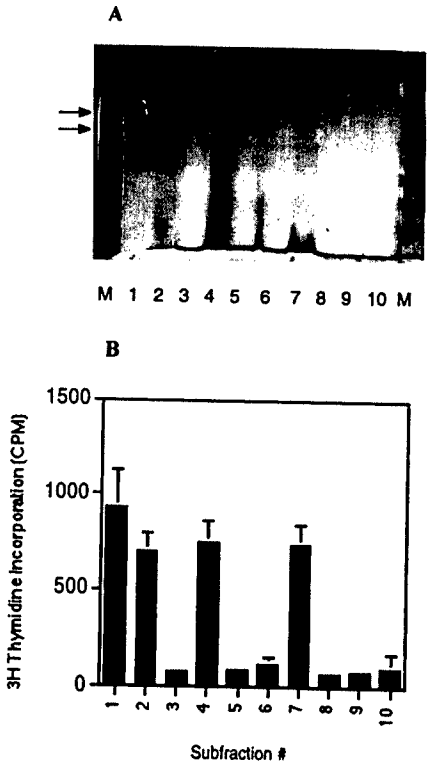

Fig. 6 SDS-PAGE and functional analysis of subfractions 44.1–44.10. Fraction 44 was subfractionated as described in "Materials and Methods," and 10 subfractions were collected. *A*, 33% of each HPLC subfraction (44.1–44.10) was resolved on a 15% SDS-PAGE gel and silver stained. *B*, 33% of each subfraction was loaded onto 5×10^4 macrophages overnight and added to T cells primed to fraction 44 with a T cell:stimulator ratio of 1:1 for a 5-day proliferation assay. *M*, molecular weight markers. *Bars*, SD.

cultures primed with protein fractions 5, 6, and 15 were able to proliferate to macrophages loaded with tumor lysate, consistent with results shown in Fig. 4.

To determine the content of the immunostimulatory protein fractions, we evaluated the protein fractions using SDS-PAGE and silver stain analysis. Because of a large number of proteins in each fraction, the fractions of interest were further subfractionated by RP-HPLC. An example is shown in Fig. 6, where we analyzed the immunostimulatory protein fraction 44 from the second HPLC run that corresponded to fraction 46 from the first run (Fig. 4), because of slight variations in HPLC fraction number between runs. From fraction 44, we derived 10 subfractions and analyzed them for protein content (Fig. 6*A*) and immunostimulatory capacity (Fig. 6*B*). We detected immunostimulatory capacity in 4 of the 10 subfractions (44.1, 44.2, 44.4, and 44.7). Silver stain analysis detected two prominent bands, one at 17 kDa, and the other at 19 kDa in fraction 44.4 (Fig. 6*A*). We are in the process of sequencing these bands, as well as determining the immunostimulatory proteins in the other HPLC fractions.

Discussion

We have devised and tested a new approach to tumor antigen discovery that uses DCs as APCs to prime naïve $CD4^+$ and $CD8^+$ T cells against tumor proteins and peptides. This approach has advantages over previous approaches in that it seeks to explore antitumor responses that can be generated in healthy, immunocompetent individuals to tumor antigens presented by professional APCs. This new approach eliminates the use of T cells from cancer patients and the use of tumor cells as APCs. Studies have shown that T cells in cancer patients may be defective, and tumor cells are poor APCs (35, 36). In addition, by using T cells from healthy donors, we are relying on a T-cell repertoire that has not been affected by the presence of the tumor.

We have used this approach in search of new epithelial tumor antigens that have been limiting to date, mainly because of the difficulty in generating tumor cell lines and consequently tumor-reactive T-cell lines (8). For the identification of HLA class I-restricted tumor antigens, we showed that we were able to prime naïve $CD8^+$ T cells to tumor peptides and generate specificity to the original tumor from which the peptides were derived. In some cases, the primed $CD8^+$ T cells also recognized another tumor of the same tissue type, suggesting the existence of shared tumor antigens. We also showed that we could reproduce the whole procedure, demonstrating that there were indeed tumor peptides present in similar fractions that conferred immunostimulatory capacity.

To determine the composition of immunostimulatory peptide fractions, we used electrospray ionization mass spectrometry to look for masses that would conform to what is expected of HLA class I-associated peptides that have mass:charge ratios between 700 and 1300 daltons. The advantages of using the mass spectrometer to identify HLA class I-associated peptides have been documented extensively (37). It offers high sensitivity for detection of small amounts of peptides. We were able to identify a panel of peptides that fit the criteria of HLA class I-binding peptides, suggesting that these immunostimulatory fractions contained peptides that could be MHC class I-restricted candidate tumor antigens. The identification and sequencing of these naturally processed peptides is currently ongoing. Fraction 50 (Fig. 1) has already yielded a new tumor antigen[4] not found by other approaches to date.

For the identification of HLA class II-restricted tumor antigens, we demonstrated that we were able to prime naïve $CD4^+$ T cells to fractionated tumor proteins and generate specificity against macrophages fed the original tumor, both in the apoptotic form and the tumor lysate form. Not surprisingly, SDS-PAGE and silver stain analysis of each of the positive protein fractions yielded an array of protein bands (data not shown), requiring further subfractionation and confirmation of immunostimulatory capacity. Subfractionation of one of these protein fractions yielded two predominant proteins of 17 kDa and 19 kDa, narrowing our search to two specific tumor antigen candidates. Investigations are currently under way in our laboratory to further subfractionate and sequence other positive protein fractions identified by *in vitro* priming of $CD4^+$ T cells.

Although we expect that this new approach will be capable of identifying numerous new tumor antigens, it is not without its disadvantages. As with all of the other methods used previously, it is very labor intensive. Furthermore, it is very dependent on the ability to grow and expand tumor peptide or tumor protein-specific T cells. In our experience, we have been able to generate only 3–5 $\times$ 10^6 $CD8^+$ and $CD4^+$ T cells/HPLC fraction, which severely limited the number of cytotoxicity and proliferation assays that could be done to evaluate their specificity. This problem is becoming less critical, however, with the advent of new functional assays that use very few T cells, such as ELISPOT (38). The technical complexities of using the mass spectrometer to detect and sequence peptides from these fractions could also be a daunting task, although we were moderately successful in identifying a panel of peptides at the 100 fmol level.

In summary, by devising a system that relies on healthy donors, we have used the full immune potential of the donor's T cells and DCs as reagents to screen for new tumor antigens, and we have detected a number of candidate tumor antigens that are being further characterized. Although we focused our search on epithelial tumor antigens, the strength of our approach is its universal applicability to all tumors, including those that do not readily grow *in vitro*. Although we have used a tumor cell line as a source of peptides and proteins, they can just as easily be derived from pieces of tumor removed at the time of surgery. In this approach, the peptides and proteins that are found to be immunostimulatory are already known to be naturally processed and presented, an important factor in the design of cancer vaccines.

Acknowledgments

We would like to thank Robert A. Henderson and Elizabeth M. Hiltbold for help at the beginning of this project. We would also like to thank Joseph Ahearn for sharing the flow cytometer and UV irradiator.

References

1. Brichard, V., Van Pel, A., Wolfel, T., Wolfel, C., De Plaen, E., Lethe, B., Coulie, P., and Boon, T. The *tyrosinase* gene codes for an antigen recognized by autologous cytolytic T lymphocytes on HLA-A2 melanomas. J. Exp. Med., *178:* 489–495, 1993.

2. Coulie, P. G., Brichard, V., Van Pel, A., Wolfel, T., Schneider, J., Traversari, C., Mattei, S., De Plaen, E., Lurquin, C., Szikora, J. P., *et al.* A new gene coding for a differentiation antigen recognized by autologous cytolytic T lymphocytes on HLA-A2 melanomas [see comments]. J. Exp. Med., *180:* 35–42, 1994.

3. Hunt, D. F., Henderson, R. A., Shabanowitz, J., Sakaguchi, K., Michel, H., Sevilir, N., Cox, A. L., Appella, E., and Engelhard, V. H. Characterization of peptides bound to the class I MHC molecule HLA-A2.1 by mass spectrometry [see comments]. Science (Washington DC), *255:* 1261–1263, 1992.

4. Hunt, D. F., Michel, H., Dickinson, T. A., Shabanowitz, J., Cox, A. L., Sakaguchi, K., Appella, E., Grey, H. M., and Sette, A. Peptides presented to the immune system by the murine class II major histocompatibility complex molecule I-Ad. Science (Washington DC), *256:* 1817–1820, 1992.

5. Fisk, B., Blevins, T. L., Wharton, J. T., and Ioannides, C. G. Identification of an immunodominant peptide of HER-2/*neu* protooncogene recognized by ovarian tumor-specific cytotoxic T lymphocyte lines. J. Exp. Med., *181:* 2109–2117, 1995.

6. Blake, J., Johnston, J. V., Hellstrom, K. E., Marquardt, H., and Chen, L. Use of combinatorial peptide libraries to construct functional mimics of tumor epitopes recognized by MHC class I-restricted cytolytic T lymphocytes. J. Exp. Med., *184:* 121–130, 1996.

7. Tureci, O., Sahin, U., and Pfreundschuh, M. Serological analysis of human tumor antigens: molecular definition and implications. Mol. Med. Today, *3:* 342–349, 1997.

8. Wang, R. F., and Rosenberg, S. A. Human tumor antigens for cancer vaccine development. Immunol. Rev., *170:* 85–100, 1999.

9. Traversari, C., van der Bruggen, P., Luescher, I. F., Lurquin, C., Chomez, P., Van Pel, A., De Plaen, E., Amar-Costesec, A., and Boon, T. A nonapeptide encoded by human gene *MAGE-1* is recognized on HLA-A1 by cytolytic T lymphocytes directed against tumor antigen MZ2-E. J. Exp. Med., *176:* 1453–1457, 1992.

10. van der Bruggen, P., Szikora, J. P., Boel, P., Wildmann, C., Somville, M., Sensi, M., and Boon, T. Autologous cytolytic T lymphocytes recognize a MAGE-1 nonapeptide on melanomas expressing HLA-Cw*1601. Eur. J. Immunol., *24:* 2134–2140, 1994.

11. Gaugler, B., Van den Eynde, B., van der Bruggen, P., Romero, P., Gaforio, J. J., De Plaen, E., Lethe, B., Brasseur, F., and Boon, T. Human gene *MAGE-3* codes for an antigen recognized on a melanoma by autologous cytolytic T lymphocytes. J. Exp. Med., *179:* 921–930, 1994.

12. van der Bruggen, P., Bastin, J., Gajewski, T., Coulie, P. G., Boel, P., De Smet, C., Traversari, C., Townsend, A., and Boon, T. A peptide encoded by human gene *MAGE-3* and presented by HLA-A2 induces cytolytic T lymphocytes that recognize tumor cells expressing MAGE-3. Eur. J. Immunol., *24:* 3038–3043, 1994.

13. Herman, J., van der Bruggen, P., Luescher, I. F., Mandruzzato, S., Romero, P., Thonnard, J., Fleischhauer, K., Boon, T., and Coulie, P. G. A peptide encoded by the human *MAGE3* gene and presented by HLA-B44 induces cytolytic T lymphocytes that recognize tumor cells expressing MAGE3. Immunogenetics, *43:* 377–383, 1996.

14. Boel, P., Wildmann, C., Sensi, M. L., Brasseur, R., Renauld, J. C., Coulie, P., Boon, T., and van der Bruggen, P. *BAGE*: a new gene encoding an antigen recognized on human melanomas by cytolytic T lymphocytes. Immunity, *2:* 167–175, 1995.

15. Van den Eynde, B., Peeters, O., De Backer, O., Gaugler, B., Lucas, S., and Boon, T. A new family of genes coding for an antigen recognized by autologous cytolytic T lymphocytes on a human melanoma. J. Exp. Med., *182:* 689–698, 1995.

16. Disis, M. L., and Cheever, M. A. HER-2/neu oncogenic protein: issues in vaccine development. Crit. Rev. Immunol., *18:* 37–45, 1998.

17. Barratt-Boyes, S. M. Making the most of mucin: a novel target for tumor immunotherapy. Cancer Immunol. Immunother., *43:* 142–151, 1996.

18. Banchereau, J., Briere, F., Caux, C., Davoust, J., Lebecque, S., Liu, Y. J., Pulendran, B., and Palucka, K. Immunobiology of dendritic cells. Annu. Rev. Immunol., *18:* 767–811, 2000.

19. Macatonia, S. E., Taylor, P. M., Knight, S. C., and Askonas, B. A. Primary stimulation by dendritic cells induces antiviral proliferative and cytotoxic T cell responses in vitro. J. Exp. Med., *169:* 1255–1264, 1989.

20. Macatonia, S. E., Patterson, S., and Knight, S. C. Primary proliferative and cytotoxic T-cell responses to HIV induced *in vitro* by human dendritic cells. Immunology, *74:* 399–406, 1991.

21. Mehta-Damani, A., Markowicz, S., and Engleman, E. G. Generation of antigen-specific CD8+ CTLs from naive precursors. J. Immunol., *153:* 996–1003, 1994.

22. Mehta-Damani, A., Markowicz, S., and Engleman, E. G. Generation of antigen-specific CD4+ T cell lines from naive precursors. Eur. J. Immunol., *25:* 1206–1211, 1995.

23. Steinman, R. M. The dendritic cell system and its role in immunogenicity. Annu. Rev. Immunol., *9:* 271–296, 1991.

24. Celis, E., Tsai, V., Crimi, C., DeMars, R., Wentworth, P. A., Chesnut, R. W., Grey, H. M., Sette, A., and Serra, H. M. Induction of anti-tumor cytotoxic T lymphocytes in normal humans using primary cultures and synthetic peptide epitopes. Proc. Natl. Acad. Sci., *91:* 2105–2109, 1994.

25. Tsai, V., Southwood, S., Sidney, J., Sakaguchi, K., Kawakami, Y., Appella, E., Sette, A., and Celis, E. Identification of subdominant CTL epitopes of the GP100 melanoma-associated tumor antigen by primary *in vitro* immunization with peptide-pulsed dendritic cells. J. Immunol., *158:* 1796–1802, 1997.

26. Kawashima, I., Hudson, S. J., Tsai, V., Southwood, S., Takesako, K., Appella, E., Sette, A., and Celis, E. The multi-epitope approach for immunotherapy for cancer: identification of several CTL epitopes from various tumor-associated antigens expressed on solid epithelial tumors. Hum. Immunol., *59:* 1–14, 1998.

27. Brossart, P., Stuhler, G., Flad, T., Stevanovic, S., Rammensee, H. G., Kanz, L., and Brugger, W. Her-2/neu-derived peptides are tumor-associated antigens expressed by human renal cell and colon carcinoma lines and are recognized by *in vitro* induced specific cytotoxic T lymphocytes. Cancer Res., *58:* 732–736, 1998.

28. Hiltbold, E. M., Ciborowski, P., and Finn, O. J. Naturally processed class II epitope from the tumor antigen MUC1 primes human CD4+ T cells. Cancer Res., *58:* 5066–5070, 1998.

29. Hiltbold, E. M., Alter, M. D., Ciborowski, P., and Finn, O. J. Presentation of MUC1 tumor antigen by class I MHC and CTL function correlate with the glycosylation state of the protein taken up by dendritic cells. Cell. Immunol., *194:* 143–149, 1999.

30. Chaux, P., Vantomme, V., Stroobant, V., Thielemans, K., Corthals, J., Luiten, R., Eggermont, A. M., Boon, T., and van der Bruggen, P. Identification of MAGE-3 epitopes presented by HLA-DR molecules to CD4(+) T lymphocytes [see comments]. J. Exp. Med., *189:* 767–778, 1999.

31. Finke, J. H., Zea, A. H., Stanley, J., Longo, D. L., Mizoguchi, H., Tubbs, R. R., Wiltrout, R. H., O'Shea, J. J., Kudoh, S., Klein, E., *et al.* Loss of T-cell receptor ζ chain and p56lck in T-cells infiltrating human renal cell carcinoma. Cancer Res., *53:* 5613–5616, 1993.

32. Finke, J., Ferrone, S., Frey, A., Mufson, A., and Ochoa, A. Where have all the T cells gone? Mechanisms of immune evasion by tumors. Immunol. Today, *20:* 158–160, 1999.

33. Vega, M. A., and Strominger, J. L. Constitutive endocytosis of HLA class I antigens requires a specific portion of the intracytoplasmic tail that shares structural features with other endocytosed molecules. Proc. Natl. Acad. Sci. USA, *86:* 2688–2692, 1989.

34. Henderson, R. A., Michel, H., Sakaguchi, K., Shabanowitz, J., Appella, E., Hunt, D. F., and Engelhard, V. H. HLA-A2.1-associated peptides from a mutant cell line: a second pathway of antigen presentation [see comments]. Science (Washington DC), *255:* 1264–1266, 1992.

35. Kiessling, R., Kono, K., Petersson, M., and Wasserman, K. Immunosuppression in human tumor-host interaction: role of cytokines and alterations in signal-transducing molecules. Springer Semin. Immunopathol., *18:* 227–242, 1996.

36. Ostrand-Rosenberg, S. Tumor immunotherapy: the tumor cell as an antigen-presenting cell. Curr. Opin. Immunol., *6:* 722–727, 1994.

37. Engelhard, V. H. Direct identification of tumor-associated peptide antigens. Springer Semin. Immunopathol., *18:* 171–183, 1996.

38. Herr, W., Schneider, J., Lohse, A. W., Meyer zum Buschenfelde, K. H., and Wolfel, T. Detection and quantification of blood-derived CD8+ T lymphocytes secreting tumor necrosis factor α in response to HLA-A2.1-binding melanoma and viral peptide antigens. J. Immunol. Methods, *191:* 131–142, 1996.

Protein Expression and Purification 22, 92–100 (2001)
doi:10.1006/prep.2001.1414, available online at http://www.idealibrary.com on IDEAL®

Recombinant Human Tumor Antigen MUC1 Expressed in Insect Cells: Structure and Immunogenicity

Melina Soares,* Franz-Georg Hanisch,† Olivera J. Finn,* and Pawel Ciborowski*,[1]

*Department of Molecular Genetics & Biochemistry, School of Medicine, University of Pittsburgh, Biomedical Science Tower, Room E 1240, Pittsburgh, Pennsylvania 15261; and †Institute of Biochemistry II, Faculty of Medicine, University of Cologne, Joseph-Stelzmann-Strasse 52, D-50931 Cologne, Germany

Received December 7, 2000, and in revised form January 13, 2001; published online May 7, 2001

MUC1, a member of the mucin family of molecules, is a transmembrane glycoprotein abundantly expressed on human ductal epithelial cells and tumors originating from those cells. MUC1 expressed by malignant cells is aberrantly O-glycosylated. Differences in O-glycosylation of the tandem repeat region of MUC1 make tumor and normal forms of this antigen immunologically distinct. The tumor-specific glycoform is, therefore, expected to be a good target for immunotherapy and a good immunogen for generation of antitumor immune responses. We have generated a renewable source of this glycoform by expressing MUC1 cDNA in Sf-9 insect cells using a baculovirus vector. This form of MUC1 (BV-MUC1) is O-glycosylated at a very low level, approximately 0.3% (w/w), and this is not due to the lack of appropriate glycosylotransferases in insect cells. Peptidyl GalNAc-transferases isolated from Sf-9 cells were able to glycosylate *in vitro* a synthetic MUC1 peptide as efficiently as the transferases isolated from human milk. Neither preparation of peptidyl GalNAc-transferases, however, was able to glycosylate BV-MUC1. This underglycosylated recombinant MUC1 mimics underglycosylated MUC1 on human tumor cells and could serve as an immunogen to stimulate responses that would recognize MUC1 on tumor cells. To test this we immunized mice with Sf-9 cells expressing BV-MUC1. Sera from immunized mice recognized MUC1 on human tumor cells. We also generated MUC1-specific T cells that proliferated in response to synthetic MUC1 peptide. © 2001 Academic Press

Key Words: **MUC1; glycosylation; baculovirus; immunization; recombinant.**

MUC1 glycoprotein is abundantly expressed on the apical surface of normal ductal epithelial cells. The tandem repeat region of MUC1 consists of conserved, 20-amino-acid-long polypeptide segments (Fig. 1) with five potential sites of O-glycosylation per each repeat (1). In normal epithelial cells, this region is O-glycosylated with long and branched oligosaccharides (2). In tumor cells originating from ductal epithelium, MUC1 is aberrantly glycosylated such that oligosaccharide chains are prematurely terminated with sialic acid (3). Changes in O-glycosylation lead to exposure of otherwise masked epitopes and make it possible to differentiate between normal and tumor-specific forms of MUC1 (4). This antigenic distinction has been explored when targeting MUC1 for immunotherapy (5).

Studies focused on MUC1 processing, presentation, and immunogenicity require large amounts of a tumor-specific form of this antigen. Tumor mucin can be obtained from tumor cells grown *in vitro* or ascites fluid obtained from cancer patients. Tumor cells grown *in vitro* give a very low yield of MUC1 after a very laborious purification procedure. Although ascites MUC1 is easier to purify, the soluble form of MUC1 is not full length and until recently it had not been well characterized (6). Previous efforts to produce recombinant MUC1 in *Escherichia coli* resulted in its rapid degradation by bacterial proteolytic enzymes (7). Expression of MUC1 in vaccinia virus resulted in almost complete deletion of its tandem repeat region through homologous recombination (8). This led us to try to express MUC1 in insect cells using a baculovirus vector. This system had several advantages. Insect cells are able to modify recombinant proteins posttranslationally similar to mammalian cells. Insect cells can also be grown in large numbers in roller bottles and do not require CO_2. The

[1] To whom correspondence and reprint requests should be addressed. Fax: (412) 383-8859. E-mail: pawelc@pitt.edu.

1046-5928/01 $35.00

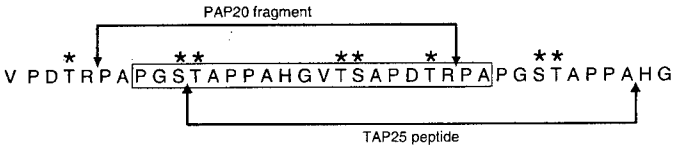

FIG. 1. Amino acid sequence of a fragment of the tandem repeat region of MUC1. Boxed sequence indicates one tandem repeat. PAP20 fragment is derived after clostripain digestion. TAP25 is the peptide used for *in vitro* glycosylation experiments. Potential sites of O-glycosylation are marked with asterisks.

yield of expressed protein is usually much higher than can be achieved in other mammalian systems.

We reported previously the initial characterization of the recombinant MUC1 (BV-MUC1) we obtained in Sf-9 insect cells. Using a panel of 56 anti-MUC1 monoclonal antibodies that recognize epitopes on variously glycosylated MUC1 molecules, we concluded that insect cells infected with the recombinant baculovirus produced several forms of MUC1 glycoprotein with electrophoretic mobility and antibody reactivity typical of molecules that have either a low or a high level of O-glycosylation (9). In order to select a form that most closely resembles human tumor MUC1, we undertook a more detailed analysis of BV-MUC1, including sequencing of the O-linked oligosaccharides and the tandem repeat peptide. Contrary to the results of the antibody analysis, quantitative analysis of O-linked oligosaccharides showed that all of BV-MUC1 was severely underglycosylated. This was not due to the deletion of the tandem repeat region. The recombinant molecule was full length and the tandem repeat peptide sequence was intact in terms of its many glycosylation sites. Underglycosylation was also not due to the absence of peptidyl *N*-acetyl-D-galactosamine (GalNAc)[2]-transferases in Sf-9 cells. While we can at the moment only speculate why insect cells do not glycosylate MUC1, we show that this underglycosylated molecule is a very good candidate for use as an immunogen. Immunization of mice with Sf-9 cells expressing recombinant MUC1 generated MUC1-specific antibodies that recognize MUC1$^+$ human tumor cells. MUC1-specific T cell responses were also generated.

EXPERIMENTAL PROCEDURES

Materials. Anti-MUC1 monoclonal antibody VU-4H5 was obtained from culture supernatant of a hybridoma generously provided by Dr. J. Hilgers (Department of Obstetrics and Gynecology, Academisch Ziekenhuis, Vrije Universiteit, Amsterdam, The Netherlands) and grown in our laboratory. The D2SC1 cell line was a generous gift from Dr. P. Ricciardi-Castagnoli (University of Milan, Bicoca, Italy). D2SC1-MUC1 was obtained by transduction of the original D2SC1 cells with the MFG-MUC1 retroviral vector encoding 22 tandem repeats of the MUC1 cDNA (10).

Expression and purity of BV-MUC1. Recombinant MUC1 was expressed in Sf-9 insect cells as previously described (9). Briefly, a *Hin*dIII cassette containing 3.2-kb cDNA-coding full-length MUC1 molecule with 22 tandem repeats was inserted into pBlueBacIII transfer vector (Invitrogen, San Diego, CA). Insect cells were transfected with a mixture of pBlueBacIII-MUC1 recombinant transfer vector, linearized baculovirus genomic DNA (AcMNPV from Invitrogen) and Insecticin liposomes (Invitrogen). Double recombinant virus, occ$^-$, LacZ$^+$, was selected by plaque assay, amplified, and further tested for purity of double-recombined virus by two rounds of end-point dilution as described by O'Reilly *et al.* (11). Viral stock was prepared by amplification and titration of the purified recombinant baculovirus.

BV-MUC1 was purified from Sf-9 insect cells infected with the recombinant baculovirus. Sf-9 cells were grown in roller bottles and infected at the density of approximately 1.5×10^6 cells/ml, 300 ml/flask. Additional 50 ml of fresh medium was added twice, 24 and 48 h after infection. Average number of cells harvested after 72 h postinfection was approximately 4.5×10^8. The cells were washed twice with PBS, and lysed in 25 ml of 0.5% octyl glucoside in Tris–HCl, buffer, pH 6.5 for 1 h with rocking, at room temperature. The cell lysate was first spun in Sorvall (Newtown, CT) tabletop centrifuge at 2000 rpm to remove major particles and then ultracentrifuged for 1 h at 35,000 rpm in SW 41Ti rotor (Beckman Instruments Inc., Fullerton, CA). Clear supernatant (2.5 ml) was loaded onto Sephacryl S-300 (Pharmacia Biotech, Uppsala, Sweden) column (i.d. 4.6 mm, 120 cm) equilibrated with 50 mM Tris–HCl buffer, pH 6.5, containing 100 mM NaCl. The column was calibrated with a mixture of molecular sieving standard proteins (Bio-Rad Laboratories, Inc., Hercules, CA) consisting of the following: thyroglobulin (670 kDa), γ-globulin (158 kDa), ovalbumin (44 kDa), myoglobin (17 kDa), and cyanocobalamine (1.35 kDa). Fractions containing BV-MUC1, as determined by Western blot using anti-MUC1 antibodies, were pooled, dialyzed against water, and lyophilized. Final purification step was preparative isopycnic centrifugation in CsCl density gradient for 72 h at 10°C in a SW41Ti rotor (Beckman Instruments Inc.) at 35,000 rpm.

Southern blot analysis of the recombinant baculovirus DNA. The presence and correct size of MUC1-cDNA inserted into the recombinant baculovirus genome was

[2] Abbreviations used: GalNAc, *N*-acetyl-D-galactosamine; PBS, phosphate-buffered saline; DIG, digoxigenin; TFA, trifluoroacetic acid; GC-EIMS, gas chromatography/electron impact mass spectrometry; DMSO, dimethyl sulfoxide; MALDI-(TOF)-MS, matrix-assisted laser desorption (time of flight) mass spectrometry; DTT, dithiothreitol; RP-HPLC, reversed -phase high-performance liquid chromatography; PSD, postsource decay; GlcNAc, *N*-acetyl-D-glucosamine; ELISA, enzyme-linked immunosorbent assay; APC, antigen-presenting cells; CHO, Chinese hamster ovary.

verified by Southern blot analysis. Random DIG-labeled primers were prepared using a *Hin*dIII fragment excised from the original vector pDKOF-MUC1 (8) as a template. Viral genomic DNA was isolated according to the protocol described in "Baculovirus Expression Vectors: A Laboratory Manual" (11). Samples of genomic DNA obtained from wild-type AcMNPV and recombinant virus were digested with *Hin*dIII, electrophoresed on 0.8% agarose gel, transferred onto ImmobilonP (Millipore, Inc., Bedford, MA) membrane, and probed with DIG-labeled primers. Hybridization and detection were performed according to protocols provided by Boehringer Mannheim Co. (Indianapolis, IN).

Monosaccharide analysis. BV-MUC1 was quantitated by weighing the sample dried overnight in a desiccator under vacuum in the presence of KOH and P_2O_5 for monosaccharide quantitation. It was resuspended in dH_2O at a final concentration of 1 mg/ml and stored frozen. Aliquots of MUC1 from frozen stock used for further tests were placed into glass tubes and dried again in desiccator under vacuum in the presence of KOH and P_2O_5.

BV-MUC1 samples were hydrolyzed during a 2-h incubation with 2 M TFA at 121°C. The samples were resuspended in 1 M ammonium hydroxide containing sodium borohydride (10mg/ml) and subjected to reduction during overnight incubation at 4°C. After the reduction step, borohydride was removed and alditols were O-acetylated by the addition of acetic acid anhydride and pyridine in 1:1 ratio and heated for 20 min. at 121°C. The samples were again dried under a stream of nitrogen and dissolved in chloroform. Acetylated alditols of monosaccharides were analyzed by gas chromatography/electron impact mass spectrometry (GC-EIMS) analysis (MD800, Fisons, Manchester, England) on 15-m DB5 capillary column heated from 50 to 250°C (7.5°C/min). The alditol acetates were registered by monitoring the total ion current and single ions at *m/z* 145, 217, 289, and 361 (hexose and pentose) or at *m/z* 144, 216, 288, and 360 (*N*-acetylhexosamine). To analyze the relative contents of monosaccharides we used erythritol as an internal standard.

The O-linked oligosaccharides were liberated from BV-MUC1 by methylation/β-elimination. Briefly, dry sample was solubilized in DMSO (200 μl) and treated under argon with a mixture of methyliodide (100 μl) and fine suspension of NaOH in DMSO (200 μl). The reaction was carried out for 16 h at room temperature. The reaction mixture was then extracted with chloroform–water and methylated oligosaccharides were analyzed by GC-EIMS and matrix-assisted laser desorption (time of flight) mass spectrometry (MALDI-(TOF)-MS).

Clostripain digestion. Purified BV-MUC1 was digested with clostripain (Promega, Madison, WI) to obtain 20-mer peptide fragments (PAP 20) from the tandem repeat region. Prior to proteolytic digestion, clostripain was activated for 3 h at room temperature in the presence of 5 mM DTT and 1 mM Ca–acetate. BV-MUC1 was resuspended in 10 ml of 25 mM sodium–phosphate buffer, pH 7.5, containing 5 mM DTT and 0.2 mM Ca–acetate, and mixed with activated clostripain. Reaction mixture was incubated for 18 h at 37°C. Digestion was terminated by adding 10 mM EDTA and the digest was subjected to fractionation on reversed -phase high-performance liquid chromatography (RP-HPLC) on microbore C18 column (Beckman Instruments Inc.). The flow rate during separation was 0.3 ml/min and 1-min fractions of 300 μl were collected. Selected fractions were analyzed for the presence of peptides by MALDI-MS, and major signals were subsequently sequenced by postsource decay matrix-assisted laser desorption mass spectrometry (PSD-MALDI-MS).

MALDI-MS. The matrix HCCA (α-cyano-4-hydroxycinnamic acid; saturated solution in acetonitrile/0.1% trifluoroacetic acid, 2:1) was mixed on the target 1:1 by volume with 0.5 μl sample in 0.1% TFA and air-dried. Reflectron and PSD mass spectrometric analyses were performed on a Bruker Reflex III instrument (Bruker Daltonik, Bremen, Germany) using a pulsed laser beam (nitrogen laser, λ = 337 nm). Residual gas pressure was at 0.8×10^7 mbar. Ion spectra were recorded in the positive mode. Acceleration and reflector voltages were set to 28.5 and 30 kV, respectively. The molecular parent ion was isolated with a pulsed field by deflection of all other ions. Complete PSD fragment ion spectra were obtained by stepwise, reducing the reflector voltage to produce overlapping mass ranges and combination of the spectral sections as described previously (12).

In vitro glycosylation. Peptidyl GalNAc-transferases were isolated either from Sf-9 insect cells or from human milk as described previously (6, 13).

A synthetic peptide, TAP25 (13), representing one full tandem repeat and five additional amino acids, containing six potential sites of glycosylation (see Fig. 1 for the sequence), was used a substrate. The reaction mixture consisted of 50 μg (22 nmol) of the substrate, 5 μl of cosubstrate UDP-GalNAc (300 μM final concentration) and 25 μl of the preparation of peptidyl GalNAc-transferases isolated either from Sf-9 cells or from milk. The reaction was carried out for 40 h at 37°C. After the first 24 h another portion of cosubstrate (5 μl) and enzyme (25 μl) was added. Reaction was eventually terminated with 20 mM tetraborate buffer, pH 9.2, containing 1 mM EDTA. Samples were filtered through Centriprep 10 (Amicon Inc., Beverly, MA) filter with 10,000-Da cutoff. The filtrate was subjected to RP-HPLC according to the protocol described previously

(14). *In vitro* glycosylation of purified BV-MUC1 using [^{3}H]UDP-GalNAc as a cosubstrate was performed as described previously (6).

Antigen preparation and immunizations. Sf-9 cells transfected with the recombinant virus and expressing MUC1 on the cell surface were washed three times with PBS, irradiated at 12,000 rads, and stored in sterile PBS at 4°C. Expression of MUC1 on these cells was tested by flow cytometry after staining with anti-MUC1 monoclonal antibodies followed by secondary anti-mouse FITC conjugated antibody. Flow cytometry analysis showed no changes in the levels of MUC1 on these cells during prolonged storage at 4°C (data not shown). Irradiated nontransfected Sf-9 cells were used for control immunizations. Mice received doses of 10^6 cells/mouse iv at days 1, 14, and 90. Mice were sacrificed 7 days following the last dose.

MUC1-specific ELISA and flow cytometry. Serum was collected from mice by tail bleeds. MUC1-specific antibody titers were determined as previously described by Kotera *et al.* (15). Briefly, 96-well Immunlon-4 plates (Dynex Technologies, Inc., Chantilly, VA) were coated with the 140-amino-acid MUC1 peptide representing seven tandem repeats (10 μg/ml) overnight at 4°C. The plates were blocked with 10% BSA in PBS at room temperature for 1 h. The plates were incubated with the indicated serum dilutions for 1 h at room temperature followed by a 1-h incubation with anti-mouse, horseradish peroxidase-conjugated secondary antibodies (Sigma, St. Louis, MO) using OPD (Sigma) as a substrate. Reactivity was expressed as absorbance at 490nm.

Tumor cells expressing and not expressing MUC1 were grown in vented tissue culture flasks, harvested, washed, and resuspended in 5% BSA in PBS at the concentration of 2×10^6/ml. One-hundred-microliter aliquots of cell suspensions were added U-bottom 96-well plates, mixed with either mouse serum or anti-MUC1 antibody, and incubated at 4°C for 30 min. After three washes with 5% BSA in PBS, the cells were incubated for an additional 30 min at 4°C with FITC-conjugated anti-mouse antibodies. Cells were then washed three times, fixed with 1% paraformaldehyde, and analyzed in a Becton Dickinson (Bedford, MA) FACScalibur using CellQuest software.

Proliferation assay. Splenocytes (2×10^6) harvested from mice 1 week after the last boost were restimulated *in vitro* at 1:10 ratio with Sf-9 cells (irradiated at 12,000 rads, ^{137}Cs source) in a 24-well plate. After 7 days in culture, the effector cells were harvested and used in chromium release and proliferation assays. Five-day proliferation assays were done using 2×10^4 effector cells and variable numbers of stimulator cells (irradiated at 6000 rads). Proliferation was determined following an 18-h incubation with [^{3}H]thymidine as described previously (16).

RESULTS

Purification of the recombinant MUC1 (BV-MUC1). Sf-9 insect cells infected with the recombinant virus produced a full-length MUC1 and incorporated it into the cell membrane. Negligible amounts of MUC1 were found in culture supernatant. In designing the purification procedure of this glycoprotein we took advantage of two general characteristics of mucins. First, mucins usually elute from molecular sieving chromatography columns in the void volume. Second, average density of glycoproteins is higher than not glycosylated proteins. Under slightly acidic conditions and in the presence of 100 mM NaCl, MUC1 was eluted from 120-cm-long Sephacryl S-300 column as a single peak at the volume corresponding to the elution volume of thyroglobulin (670 kDa). The majority of proteins originating from insect cells were eluted at higher volumes. The next step of purification was preparative isopycnic ultracentrifugation in CsCl density gradient. The average density of the purified BV-MUC1 corresponded to 1.35 g/ml of CsCl. The purity of BV-MUC1 preparations was evaluated by silver staining and Western blot analysis. Western blot analysis showed a single band that corresponded to a single band detected by silver staining after loading a 1000 ng of BV-MUC1 preparation per lane. Considering 50 ng of protein the amount needed for detection by silver staining, our BV-MUC1 preparation was not less than 95% pure. Total amount of BV-MUC1 purified from one roller-bottle culture of 4.5×10^8 infected Sf-9 cells was approximately 2.5 mg.

Sf-9 cells do not efficiently glycosylate recombinant MUC1 in vivo. The putative O-linked glycans on BV-MUC1 were analyzed at the mono- and oligosaccharide levels by using several approaches. To identify and quantify the monosaccharide components of mucin glycans, BV-MUC1 was methanolyzed or hydrolyzed to yield the respective methylglycosides or free sugars (Table 1). Both methods yielded similar results, which

TABLE 1

Monosaccharide Composition Analysis of Glycans on BV-MUC1

	Amounts in μg per 100 μg of mucin					
BV-MUC1	Fuc	Man	Gal	GlcNAc	GalNAc	NeuAc
Methanolysis	—	0.13	0.05	0.09	0.02	—
Hydrolysis (HCl)	n.d.	n.d.	n.d.	0.86	0.26	n.d.

Note. n.d., not detectable under the conditions used; —, no traces found.

showed that the contents of hexoses and hexosamines on BV-MUC1 reached about 0.3% by weight. In addition to L-fucose, the hexoses D-mannose, D-galactose, and the hexosamines GalNAc and *N*-acetyl-D-glucosamine (GlcNAc) were detected in low or only trace amounts. Sialic acid was not found even at trace levels. To make sure that the amounts of hexosamines had not been underestimated by using mild condition for sugar liberation, the analyses were repeated by hydrolysis in 4 M HCl. Only hexosamines can be quantitatively assessed by this method, since deoxyhexoses and hexoses are largely destroyed. Under these more drastic conditions, the content of hexosamines on BV-MUC1 was found to be higher, but comparable to the low levels measured after methanolysis (Table 1). On liberation of oligosaccharides by methylation/β-elimination, the sample derived from BV-MUC1 did not reveal any presence of methylated glycans, neither by measurement in GC/MS (mono- to trisaccharide range) nor in MALDI-MS (data not shown).

One possible explanation would have been lack of glycosylation sites due to deletion of tandem repeat sequence from the inserted cDNA in the recombinant baculovirus. Such deletion has been previously reported for recombinant vaccinia virus carrying MUC1 cDNA (17). To examine whether the recombinant baculovirus maintained MUC1 cDNA insert intact, we performed Southern blot analysis of *Hin*dIII-digested viral genomic DNA. One sample was recombinant viral DNA isolated after first purification of the recombinant baculovirus and the other one was DNA isolated from the recombinant baculovirus after at least 15 passages. Figure 2 shows that the size of the inserted cDNA remained unchanged regardless of numerous passages.

In summary, on calculating the average glycosylation of BV-MUC1, there is less than one glycan residue per one tandem repeat. Hence, this recombinant form can be regarded as substantially underglycosylated.

Amino acid sequence analysis of tandem repeat peptides generated by clostripain digestion of BV-MUC1. Clostripain, an Arg-C proteinase, can be used to cleave Arg-Pro peptide bonds within the tandem repeat region, to generate single repeat PAP20 peptides of the consensus sequence PAPGSTAPPAHGVTSAPDTR (see Fig. 1) for mass spectrometric analysis. Clostripain digestion of the tandem repeat region of MUC1 is possible only in the absence of extended O-linked oligosaccharides thus we used this strategy to address two questions: (i) what percentage of tandem repeats are singly glycosylated with GalNAc and (ii) does the recombinant form of MUC1 have other posttranslational modifications.

We used two preparations of BV-MUC1 for clostripain digestion. One preparation was chemically deglycosylated using TFMSA; the other one was untreated. These two preparations were digested with clostripain for 18 h at 37°C and subsequently subjected to fractionation by RP-HPLC on a microbore C18 column. A 140-mer synthetic peptide representing seven nonmodified tandem repeats was used as a positive control. RP-HPLC profiles showed that both preparations of the recombinant MUC1 were equally well digested by clostripain, as was the positive control (data not shown). This result indicated that recombinant BV-MUC1 was not glycosylated to an extent that would prevent clostripain digestion. Mass spectrometric analysis of individual HPLC fractions showed that nonglycosylated PAP20 peptide generated by digestion of the 140-mer synthetic peptide was eluted with 25% of acetonitrile. We analyzed by MALDI-TOF all RP-HPLC fractions eluted within 23 to 33% gradient of acetonitrile. The predominant species that we found in 0.5-ml fractions within that range of acetonitrile was the 1887-Da peptide corresponding to the nonmodified PAP20 fragment of MUC1. This species was further sequenced by PSD-MALDI to confirm its identity with the PAP20 peptide sequence (Table 2). We have also found that the protein core of the recombinant MUC1 has modifications in amino acid sequence in some, but not in all PAP20 fragments. Specifically, we found a species at *m/z* 1944 with one glycine insertion and one at *m/z* 2056 with a proline–glycine insertion (Table 2). We did not find any species, however, with masses corresponding to mono-, di-, or triglycosylated PAP20 fragments. We also did not find any PAP20 fragments with other possible posttranslational modifications, e.g., phosphorylation, acetylation, and methylation. This result indicates that the tandem repeat region of the recombinant BV-MUC1 is not glycosylated and is not posttranslationally modified in any other way.

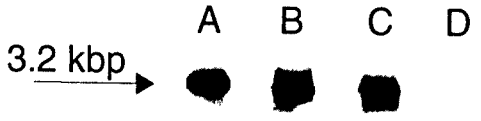

FIG. 2. Southern blot analysis of the MUC1-22TR cDNA insert in the recombinant baculovirus genome. (A) The original MUC1-22TR cDNA *Hin*dIII cassette. This fragment was used to make DIG-labeled random primers. (B) The fragment obtained by *Hin*dIII digestion of viral DNA from the first viral stock obtained after purification of the recombinant virus. (C) The fragment obtained after *Hin*dIII digestion from viral DNA obtained after at least 15 passages of the recombinant virus. (D) *Hin*dIII digest of the wild-type baculovirus genomic DNA used to make the recombinant virus.

Recombinant MUC1 is not a substrate for peptidyl GalNAc-transferases from either Sf-9 cells or human milk. To understand the reasons for such low level of glycosylation of recombinant MUC1 by Sf-9 cells, we isolated peptidyl GalNAc-transferases from insect cell lysate and performed *in vitro* glycosylation experiments. We also used a preparation of peptidyl GalNAc-transferases from human milk, containing T1 and T 2

TABLE 2

PSD-MALDI-Mass Spectrometry of Clostripain Fragments from BV-MUC1 and the Derived Amino Acid Sequences (Inserted Amino Acids Are Bolded)

A.	y- or b-series ions registered for signals with molecular mass at *m/z*		
	1887	1944	2056
	169 (b2)	n.r.	n.r.
	242	242	242
	266 (b3)	266	266
	276 (y2)	276	276
	294	294	294
	323 (b4)	232	232
	325	325	325
	—	332	—
	—	—	337
	343	—	—
	—	—	362
	376	375	375
	396	396	396
	404	403	403
	411 (b5)	—	—
	415	414	414
	461	460	460
	472	471	471
	488	(490)	487
	511 (b6)	—	—
	—	514	514
	532	—	—
	555	554	554
	560	559	559
	583 (b7)	582	582
	647 (y6)	646	646
	652	?	—
	661	?	661
	679 (b8)	?	680
	—	?	707
	722	?	722
	748 (y7)	747	747
	777 (b9)	—	—
	819	818	818
	848 (y8, b10)	847	847
	903 (y9)	903 (b11)	903
	985 (b11)	985	—(?)
	1030	1030	1030
	1041 (y10, b12)	1041 (b12)	1041
	1113 (y11)	—	—
	1142 (b13)	—	—
	—	—	1192
	1209 (y12)	1209	1209 (b14)
	1243 (b14)	—	—
	1289	1289	1289
	1306 (y13)	1306	1306
	—	1362 (y14)	—
	—	1376	1376
	1378 (y14)	—	—
	1400 (b16)	1399	—
	—	1432 (y15)	—
	—	—	1444
	—	1455 (b17)	—
	—	—	1476 (y15)
	1478 (y15)	—	—
	—	—	1495 (b17)
	1498 (b17)	—	—
	—	—	1539
	1564 (y16)	—	1564
	1613 (b18)	1612	1612
	1621 (y17)	—	—
	—	1669 (b19)	—
	1712 (b19)	—	—
	1718 (y18)	—	—
	—	1776 (y19)	—
	—	—	1770 (b20)
	1788 (y19)	—	—
	1888	—	1887

B. Amino acid sequences of signals at *m/z*

1887	PAPGSTAPPAHGVTSAPDTR
1944	PAPGSTA **G** PPAHGVTSAPDTR
2056	PAPGSTA **PA** PPAHGVTSAPDTR

Note. —, not present.

enzymes. Recombinant MUC1 or a synthetic 25-amino-acid, TAP25 peptide (see Fig. 1) representing 1.25 tandem repeats, were used as substrates. TAP25 contains six potential sites of O-glycosylation. UDP-GalNAc was used as a cosubstrate to glycosylate the synthetic peptide and [^{3}H]UDP-GalNAc was used as a cosubstrate to glycosylate the recombinant MUC1. Table 3 shows that peptidyl GalNAc-transferases isolated from Sf-9 cells glycosylated the synthetic peptide at two of six potential sites and produced mono- and di-glycosylated species. Within the same time, human milk peptidyl GalNAc-transferases produced mono-, di-, and triglycosylated species utilizing the synthetic peptide as a substrate. The same preparations of peptidyl GalNAc-transferases from Sf-9 cells and human milk were used to incorporate [^{3}H]UDP-GalNAc into BV-MUC1. Neither of these preparations glycosylated the recombinant molecule (data not shown).

Immune responses elicited by BV-MUC1$^+$ Sf-9 cells. We immunized mice with MUC1$^+$ Sf-9 cells as an immunogen. We expected whole cells to be more efficiently taken up by APC and to stimulate the APC better than soluble BV MUC1. MUC1-specific antibody responses were measured using a synthetic peptide representing seven tandem repeats of MUC1 as an antigen in ELISA assay. As shown in Fig. 3, both isotypes of MUC1-specific antibodies, IgM and IgG, were generated in immunized mice. The end point titers of these antibodies were comparable, 1:160 for IgM isotype and 1:320 for IgG isotype. These titers are in turn comparable to previously reported titers obtained by vaccination of BALB/c mice with recombinant vaccinia virus expressing MUC1 (18).

To prove that BV-MUC1 mimics the human tumor

TABLE 3

Yield (in %) of *in Vitro* Glycosylation of a TAP25 Synthetic Peptide by Preparation of Peptidyl GalNAc Transferases Isolated from Human Milk (HM) or Sf-9 Insect Cells

GalNAc-transferases	Substrate not glycosylated	Monoglycosylated	Diglycosylated	Triglycosylated
HM-GalNAc-T	45.6	9.1	41.3	4.0
Sf-9-GalNAc-T	75.6	11.0	13.4	0

MUC1, we tested anti-MUC1 antibodies elicited against MUC1$^+$ Sf-9 cells for their ability to recognize MUC1$^+$ human tumor cells. MS is a MUC1-negative human adenocarcinoma cell line that we transfected with MUC1 cDNA to generate MS-MUC1 cells. Figure 4 shows that a monoclonal antibody VU-4H5, that recognizes the tumor associated form of MUC1, stains the MS-MUC1 cells (Fig. 4D) but not the parental control cells, MS (Fig. 4B). Two pools of sera (five mice in each pool) from two independent immunizations with Sf-9 cells expressing MUC1, and one pool of sera from five mice immunized with control Sf-9 cells, were tested. Positive staining of MS-MUC1 cells was observed with sera from mice immunized with Sf-9 cells expressing MUC1 (Fig. 4C). These sera did not stain MS cells which were MUC1 negative (Fig. 4A). Sera from mice immunized with Sf-9 cells only did not stain either of the cells.

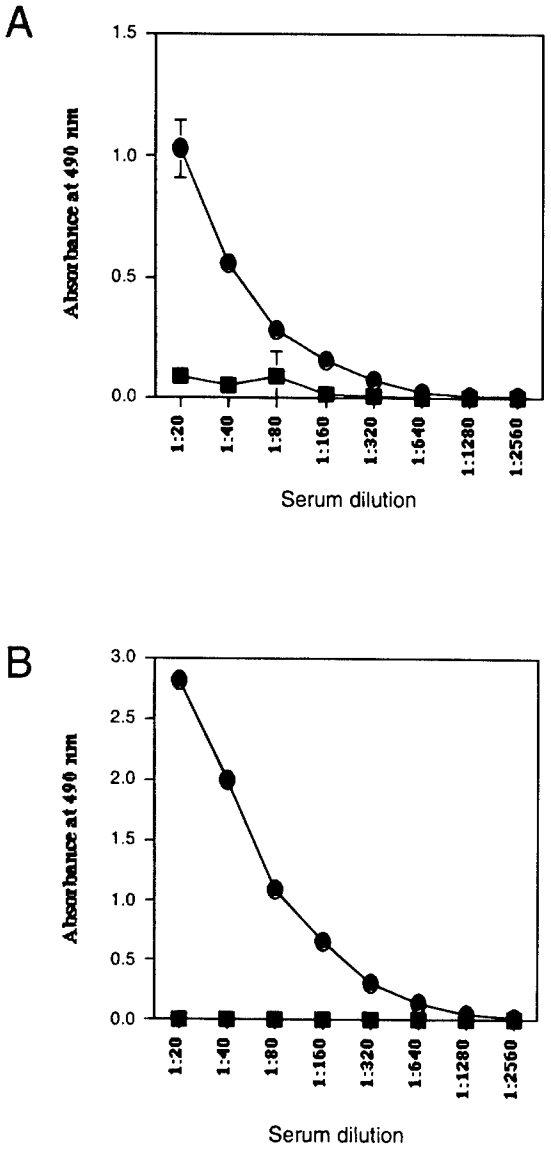

FIG. 3. Antibodies induced in mice immunized with Sf-9 cells expressing (closed circles) and nonexpressing (closed boxes) MUC1. (A) IgM and (B) IgG antibodies were detected by ELISA.

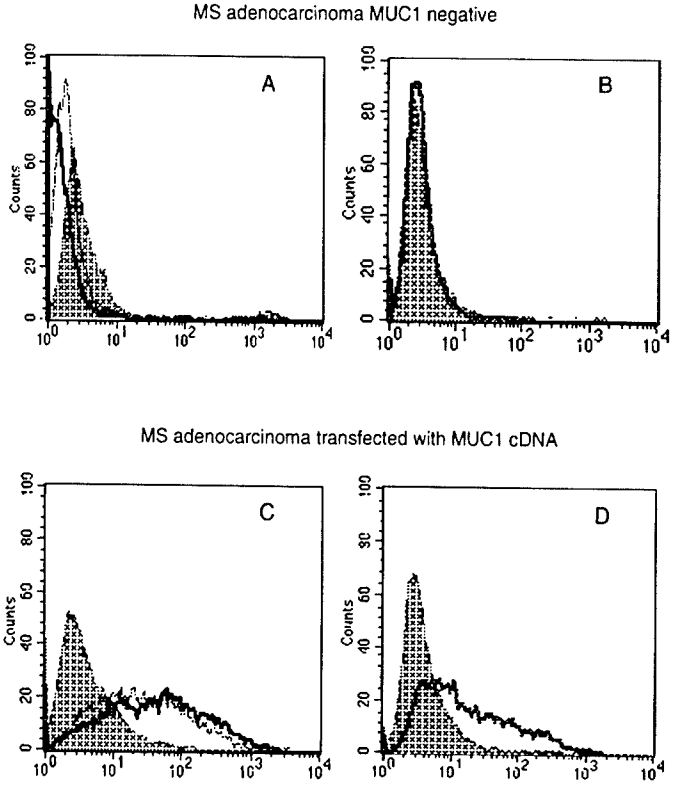

FIG. 4. Flow cytometry analysis of sera from immunized mice for reactivity with MUC1 expressed on human tumor cells. Shaded areas represent either preimmune mouse serum (A and C) or isotype control antibody (B and D). In A and C, solid and dotted lines represent staining with pooled immune sera from two independent immunizations. In B and D, solid line represents staining with VU-4H5 monoclonal antibody that recognizes tumor specific form of MUC1.

Splenocytes from immunized mice were also tested for their ability to proliferate in response to mouse APC expressing MUC1. D2SC1 cell line is a murine dendritic cell line that we transduced with MUC1 cDNA and it now expresses this antigen on the cell surface (D2SC1-MUC1). Figure 5 shows that two of three immunized mice have a detectable increase in proliferation in response to D2SC-MUC1 compared to control D2SC1 stimulator cells.

We also evaluated whether MUC1$^+$ Sf-9 cells were capable of eliciting a MUC1-specific cytotoxic T cell response as well, but we did not observe significant specific cytotoxicity in spleens from immunized mice (data not shown).

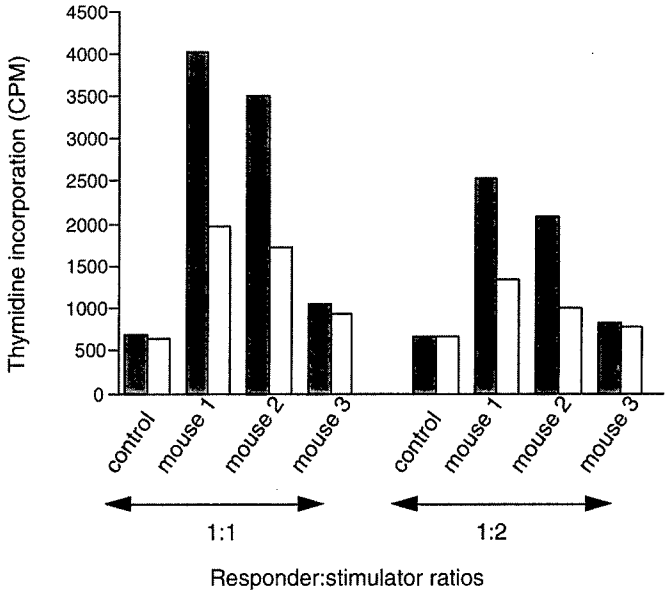

FIG. 5. MUC1-specific T cell proliferation of spleen cells from mice immunized with MUC1+ Sf-9 cells (mouse 1, 2, and 3) or MUC1-Sf-9 cells (control) in response to D2SC1-MUC1 (closed bars) or D2SC1 (open bars) stimulator cells.

DISCUSSION

We have developed an efficient, three steps purification system for purifying MUC1 glycoprotein produced by Sf-9 cells infected with the recombinant baculovirus. The fact that insect cells incorporate recombinant MUC1 into the cell membrane allowed us to remove easily all contaminating proteins from culture medium by simple washing of the cells in PBS. On the other hand, the yield of membrane integrated MUC1 was lower because extraction with octyl-glucoside or other detergents such as Chaps and deoxycholate was not complete. We were unable to determine the exact yield of purification and express it as a percentage of recovery because MUC1 does not have an activity that can be measured using a substrate and ELISA method is not quantitative because of the multiplicity of epitopes (22 per one BV-MUC1 molecule) that might not be equally accessible to antibody. Nevertheless, we could be certain of its purity and thus we could determine by weight the amount of purified recombinant product we obtained.

We present in this study the quantitative analysis of saccharides O-linked to the tandem repeat region of the recombinant MUC1 and the immunogenic properties of this antigen. Our results show that the recombinant product containing 22 tandem repeats was O-glycosylated at the level of less than one GalNAc residue per one tandem repeat. This is substantially lower O-glycosylation compared to preparations of MUC1 obtained from other sources (19, 20) and agrees with previously reported lack of reactivity of the recombinant MUC1 expressed in insect cells with several lectins (21). Based on the previous reports on O-glycosylation of other mammalian proteins expressed in insect cells, we expected MUC1 to be glycosylated to the levels comparable to native MUC1. For example, rIFN-α2 expressed in Sf-9 cells was O-glycosylated at the same position as natural human IFN-α2 (22), indicating that the recombinant product was properly processed and routed through the compartments within insect cells that are important for O-glycosylation. Moreover, insects themselves make intestinal mucin similar in structure and function to mucins made by vertebrates. It is organized in repetitive regions rich in proline with multiple threonine residues as potential sites of O-glycosylation (23, 24). Thomsen *et al.* reported lower level of O-glycosylation of recombinant pseudorabies virus glycoprotein gp50 expressed in Sf-9 cells compared to mammalian CHO and Vero cells (25). However, the difference was in the level of Galβ1-3GalNAc disaccharide residues on this recombinant product as a result of lower level of β1-3Gal-transferase in insect cells. The levels of peptidyl GalNAc transferases were comparable in these three cell lines (25). The recombinant product that we obtained, however, had the tandem repeat region almost completely devoid of saccharidic residues providing rich source of tumor-specific, uncovered -Pro-Asn-Thr-Arg-Pro- cryptic epitope.

To explore the reasons for this unexpected low number of GalNAc residues incorporated into recombinant MUC1, we tested whether peptidyl GalNAc-transferases in Sf-9 cells specifically fail to glycosylate the tandem repeat of MUC1 because of their different substrate specificity compared to mammalian peptidyl GalNAc transferases. Strikingly, neither peptidyl GalNAc-transferase isolated from Sf-9 cells nor T1 and T2 peptidyl GalNAc transferases isolated from human milk were able to glycosylate the recombinant MUC1 protein (BV-MUC1). Based on these results we hypothesize that a specific tertiary structure of MUC1 is critical for effective glycosylation of the tandem repeat region. Conformations necessary for effective glycosylation that are attained by

MUC1 made in human epithelial cells may not be attained by MUC1 made in insect cells. If our hypothesis is correct, this would further suggest that the tertiary structure of MUC1 in epithelial cells is created in an ordered fashion, e.g., with the help from specific mammalian chaperons that are not present in insect cells.

The inability of insect cells to glycosylate BV-MUC1 has yielded a recombinant product that may be especially useful for eliciting immune responses against underglycosylated MUC1 on human tumor cells. The results of our first immunization attempt showed that Sf-9 cells expressing BV-MUC1 serve as efficient immunogens in Balb/c mice eliciting antibodies that cross-react with human tumors. We are currently exploring the immunogenic potential of various vaccine preparations based on soluble BV-MUC1. We have already reported that dendritic cells take up and efficiently process this antigen for presentation to T cells (16).

ACKNOWLEDGMENTS

This work was supported in part by NIH Grant 5PO1 CA73743 and NIH Grant 5RO1 CA56103 to O.J.F., DFG Grants Ha2092/4-2 and Ha2092/4-4 to F-G.H., and Alexander von Humboldt Foundation Scholarship to P.C.

REFERENCES

1. Gendler, S. J., and Spicer, A. P. (1995) Epithelial cell mucins. *Annu. Rev. Pysiol.* **57,** 607–634.
2. Lloyd, K. O., Burchell, J., Kudryshov, V., Yin, B. W. T., and Taylor-Papadimitriou, J. (1996) Comparison of O-linked carbohydrate chains in MUC-1 mucin from normal breast epithelial cell lines and breast carcinoma lines. *J. Biol. Chem.* **271,** 33325–33334.
3. Brockhausen, I., Yang, J. M., Burchell, J., Whitehouse, C., and Taylor-Papadimitriou, J. (1995) Mechanisms underlying aberrant glycosylation of MUC1 mucin in breast cancer cells. *Eur. J. Biochem.* **233,** 607–617.
4. Burchell, J., Gendler, S., Taylor-Papadimitriou, J., Girling, A., Lewis, R., Millis, R., and Lamport, D. (1987) Development and characterization of breast cancer reactive monoclonal antibodies directed to the core protein of the human milk mucin. *Cancer Res.* **47,** 5476–5482.
5. Soares, M., and Finn, O. J. (2001) MUC1 mucin as a target for immunotherapy of cancer *in* "Cancer Immunology, Immunology in Medicine Series" (Rees, R., and Robbins, A., Eds.), in press, Kluwer, Dordrecht.
6. Beatty, P., Hanisch, F.-G., Beer Stolz, D., Finn, O. J., and Ciborowski, P. (2001) Biochemical characterization of the soluble form of tumor antigen MUC1 isolated from sera and ascites fluid of breast and pancreatic cancer patients. *Clin. Cancer Res.*, **7,** 781s–787s.
7. Dolby, N., Dombrowski, K. E., and Wright, S. E. (1999) Design and expression of synthetic mucin gene fragment in *Escherichia coli. Protein Express. Purif.* **15,** 146–154.
8. Jerome, K. R., Bu, D., and Finn, O. J. (1992) Expression of tumor associated epitopes on Epstein–Barr virus-immortalized B-cells and Burkitt's lymphomas transfected with epithelial mucin complementary DNA. *Cancer Res.* **52,** 5985–5990.
9. Ciborowski, P., and Finn, O. J. (1995) Recombinant epithelial cell mucin (MUC-1) expressed in baculovirus resembles antigenically tumor associated mucin, target for cancer immunotherapy. *Biomed. Pep. Prot. Nucleic Acids* **1,** 193–198.
10. Henderson, R. A., Konitsky, W. M., Barratt-Boyes, S. M., Soares, M., Robbins, P. D., and Finn, O. J. (1998) Retroviral expression of MUC-1 human tumor antigen with intact repeat structure and capacity to elicit immunity *in vivo. J. Immunol.* **21,** 247–256.
11. O'Reilly, D. R., Miller, L. K., and Luckow, V. A. (1994) Titering virus stock *in* Baculovirus Expression Vectors—A Laboratory Manual, pp. 130–134, Oxford Univ. Press, New York/Oxford.
12. Muller, S., Goletz, S., Packer, N., Gooley, A., Lawson, A. M., and Hanisch, F.-G. (1997) Localization of O-glycosylation sites on glycopeptide fragments from lactation-associated MUC1. *J. Biol. Chem.* **272,** 24780–24793.
13. Stadie, T. R. E., Chai, W., Lawson, A. M., Byfield, G. H., and Hanisch, F.-G. (1995) Studies on the order and site specificity of GalNAc transfer to MUC1 tandem repeats by UDP-GalNAc:polypeptide N-acetylgalactosylaminyltransferase from milk or mammary carcinoma cells. *Eur. J. Biochem.* **229,** 140–147.
14. Hanisch, F.-G., Müller, S., Hassan, H., Clausen, H., Zachara, N., Gooley, A. A., Paulsen, H., Alving, K., and Peter-Katalinic, J. (1999) Dynamic epigenetic regulation of initial O-glycosylation by UDP-N-acetylgalactosamine: peptide N-acetylgalactosaminyltransferases. *J. Biol. Chem.* **274,** 9946–9954.
15. Kotera, Y., Fontenot, J. D., Pecher, G., Metzgar, R. S., and Finn, O. J. (1994) Humoral immunity against a tandem repeat epitope of human mucin MUC-1 in sera from breast, pancreatic, and colon cancer patients. *Cancer Res.* **54,** 2856–2860.
16. Hiltbold, E. M., Vlad, A. M., Ciborowski, P., Watkins, S. C., and Finn, O. J. (2000) Mechanism of unresponsiveness to circulating tumor antigen MUC1 is a block in intracellular sorting and processing by dendritic cells. *J. Immunol.* **165,** 3730–3741.
17. Bu, D., Domenech, N., Lewis, J., Taylor-Papadimitriou, J., and Finn, O. J. (1993) Recombinant vaccinia mucin vector: *In vitro* analysis of expression of tumor-associated epitopes for antibody and human cytotoxic T-cell recognition. *J. Immunol.* **14,** 127–135.
18. Acres, B. R., Hareuveni, M., Balloul, J.-M., and Kieny, M.-P. (1993) Vaccinia virus MUC1 immunization of mice: Immune response and protection against the growth of murine tumors bearing the MUC1 antigen. *J. Immunother.* **14,** 136–143.
19. Hanisch, F.-G., Uhlenbruck, G., Peter-Katalinic, J., Egge, H., Dabrowski, J., and Dabrowski, U. (1989) Structures of neutral O-linked polylactosaminglycans on human skim milk mucins. *J. Biol. Chem.* **264,** 872–883.
20. Hanisch, F.-G., Stadie, T. R. E., Deutzman, F., and Peter-Katalinic, J. (1996) MUC1 glycoforms in breast cancer: Cell line T47D as a model for carcinoma-associated alterations of O-glycosylation. *Eur. J. Biochem.* **236,** 318–327.
21. Hu, P., and Wright, S. E. (1998) Recombinant breast carcinoma-associated mucins expressed in a baculovirus system contain a tumor specific epitope. *Immunotechnology* **4,** 97–105.
22. Sugyiama, K., Ahorn, H., Maurer-Fogy, I., and Voss, T. (1993) Expression of human interferon-α in Sf-9 cells: Characterization of O-linked glycosylation and protein heterogeneities. *Eur. J. Biochem.* **217,** 921–927.
23. Wang, P., and Granados, R. R. (1997) Molecular cloning and sequencing of a novel invertebrate intestinal mucin cDNA. *J. Biol. Chem.* **272,** 16663–16669.
24. Wang, P., and Granados, R. R. (1997) An intestinal mucin is the target substrate for a baculovirus enhancin. *Proc. Natl. Acad. Sci. USA* **94,** 6977–6982.
25. Thomsen, D. R., Post, L. E., and Elhammer, A. P. (1990) Structure of O-glycosidically linked oligosaccharides synthesized by the insect cell line Sf-9. *J. Cell. Biochem.* **43,** 67–79.

Three Different Vaccines Based on the 140-Amino Acid MUC1 Peptide with Seven Tandemly Repeated Tumor-Specific Epitopes Elicit Distinct Immune Effector Mechanisms in Wild-Type Versus MUC1-Transgenic Mice with Different Potential for Tumor Rejection[1]

M. Melina Soares,* Vinay Mehta,† and Olivera J. Finn[2]*

Low-frequency CTL and low-titer IgM responses against tumor-associated Ag MUC1 are present in cancer patients but do not prevent cancer growth. Boosting MUC1-specific immunity with vaccines, especially effector mechanisms responsible for tumor rejection, is an important goal. We studied immunogenicity, tumor rejection potential, and safety of three vaccines: 1) MUC1 peptide admixed with murine GM-CSF as an adjuvant; 2) MUC1 peptide admixed with adjuvant SB-AS2; and 3) MUC1 peptide-pulsed dendritic cells (DC). We examined the qualitative and quantitative differences in humoral and T cell-mediated MUC1-specific immunity elicited in human MUC1-transgenic (Tg) mice compared with wild-type (WT) mice. Adjuvant-based vaccines induced MUC1-specific Abs but failed to stimulate MUC1-specific T cells. MUC1 peptide with GM-CSF induced IgG1 and IgG2b in WT mice but only IgM in MUC1-Tg mice. MUC1 peptide with SB-AS2 induced high-titer IgG1, IgG2b, and IgG3 Abs in both WT and MUC1-Tg mice. Induction of IgG responses was T cell independent and did not have any effect on tumor growth. MUC1 peptide-loaded DC induced only T cell immunity. If injected together with soluble peptide, the DC vaccine also triggered Ab production. Importantly, the DC vaccine elicited tumor rejection responses in both WT and MUC1-Tg mice. These responses correlated with the induction of MUC1-specific $CD4^+$ and $CD8^+$ T cells in WT mice, but only $CD8^+$ T cells in MUC1-Tg mice. Even though MUC1-specific $CD4^+$ T cell tolerance was not broken, the capacity of MUC1-Tg mice to reject tumor was not compromised. *The Journal of Immunology,* **2001, 166: 6555–6563.**

Human mucin MUC1 is a transmembrane glycoprotein normally expressed on the apical surface of ductal epithelial cells (1). It also is one of the few well-characterized tumor Ags found to be aberrantly expressed on a wide variety of ductal adenocarcinomas, including those of the breast, pancreas, lung, colon, ovaries, and prostate (reviewed in Ref. 2). MUC1 on normal tissues is heavily glycosylated with branched sugar chains extending out from the protein backbone (3–5). However, on tumors, MUC1 is highly overexpressed, loses polarization, and is severely underglycosylated with oligosaccharides that are mostly linear and shorter because of premature termination of glycosylation (6–9). Underglycosylation and loss of polarization of tumor-associated MUC1 make it accessible to effector mechanisms such as Abs and T cells and recognizable by the immune system.

Analyses of immune responses in cancer patients with various adenocarcinomas have revealed the presence of low-titer anti-MUC1 Abs (10–15) and of low-frequency MUC1-specific CTL (16–20). No MUC1-specific Th cell responses have been reported to date. Taking into consideration the pivotal role that Th cells have in regulating both humoral and cellular responses, we have proposed that the lack of MUC1-specific $CD4^+$ Th cells in patients is responsible for their inability to generate stronger immune responses and overcome the disease. Our group reported that dendritic cells (DC)[3] can endocytose the aberrantly glycosylated circulating form of MUC1 that is shed from tumor cells but are unable to efficiently process and present it to either MHC class I- or MHC class II-restricted T cells (21, 22). This could account, in part, for the lack of MUC1-specific Th cells, low Ab titer of predominantly IgM isotype, and low CTL frequency. MUC1-specific Th cell responses can be generated in vitro by priming $CD4^+$ T cells on DC loaded with the unglycosylated synthetic MUC1 peptide that is efficiently processed and presented (23). High concentrations of peptide needed to elicit these responses suggest that in addition to inefficient Ag processing, $CD4^+$ T cell tolerance, especially of the high affinity T cells, also could contribute to the lack of MUC1-specific Th cells in vivo. In the studies we report here, we have addressed in a Tg mouse model the extent and consequences of MUC1-specific Th cell tolerance by testing several vaccination protocols for their ability to induce MUC1-specific immunity and cause tumor rejection.

Efforts already are underway by multiple groups to use MUC1-based immunotherapy in cancer patients (24–27). These are predicated on studies done primarily in conventional mice (28–40).

*Immunology Program and Department of Molecular Genetics and Biochemistry, University of Pittsburgh School of Medicine, Pittsburgh PA 15261; and †Biology Department, Washington and Jefferson College, Washington, PA 15301

Received for publication January 18, 2001. Accepted for publication March 21, 2001.

The costs of publication of this article were defrayed in part by the payment of page charges. This article must therefore be hereby marked *advertisement* in accordance with 18 U.S.C. Section 1734 solely to indicate this fact.

[1] This work was supported by National Institutes of Health Grant 5RO1 CA56103 (to O.J.F.) and Department of Defense Training Grant DAMD 17-99-1-9352 (to M.M.S.). Animal purchase and maintenance were supported in part by a grant to O.J.F. from an anonymous donor.

[2] Address correspondence and reprint requests to Dr. Olivera J. Finn, Department of Molecular Genetics and Biochemistry, W1142 Biomedical Science Tower, University of Pittsburgh, Pittsburgh PA 15261. E-mail address: ojfinn@pitt.edu

[3] Abbreviations used in this paper: DC, dendritic cell; Tg, transgenic, ELISPOT, enzyme-linked immunospot; LN, lymph node, ADCC, Ab-dependent cellular cytotoxicity.

0022-1767/01/$02.00

Human MUC1 is a very strong immunogen in the mouse, and these studies do not provide a realistic evaluation of its immunogenic or immunotherapeutic potential. Furthermore, as these studies sidestep the issues of tolerance and autoimmunity, they provide very little information about the relevance of MUC1-specific responses for tumor rejection or their safety in cancer patients. We have reported a number of studies conducted in a more relevant chimpanzee model where MUC1 is highly homologous to human MUC1 (41–43), and they have shown that the anti-MUC1 immune responses generated did not cause autoimmunity. However, the lack of a tumor model in the chimpanzee did not allow evaluation of the role of these responses in tumor rejection.

Recently, efforts have been directed toward developing mice transgenic (Tg) for a variety of human tumor Ags such as Her 2/Neu and carcinoembryonic Ag. Such Tg mouse models have made it possible to test immunotherapeutic strategies within the context of tolerance and autoimmunity (44–50). More recently, MUC1-Tg mice have become available, and several groups have started to address some of the above questions in this model (51–55). We have used this model to analyze MUC1-specific immune responses that can be elicited in MUC1-Tg mice compared with WT mice. We were interested especially in knowing whether the reported Th cell tolerance in these mice (51, 53) could be broken by different vaccines based on a synthetic 140-aa MUC1 peptide containing multiple tandemly repeated tumor-specific epitopes. Another important question we addressed was whether a strong tumor rejection response, if elicited, would result in autoimmunity. Our results show that two vaccines combining MUC1 peptide with adjuvants induced only humoral responses. MUC1 peptide admixed with murine GM-CSF as an adjuvant induced IgM Abs in both WT and MUC1-Tg mice, but the switch to IgG Abs occurred only in WT mice. In contrast, MUC1 peptide admixed with the adjuvant SB-AS2 induced high-titer IgG Abs in both WT and MUC1-Tg mice. We discovered that these humoral responses were T cell independent in both MUC1-Tg and WT mice and did not result in tumor rejection. We found that the cytokines necessary for isotype switching, and in particular IFN-γ, were contributed by activated NK cells and other non-T cells. The vaccine composed of MUC1 peptide-pulsed DC elicited T cell immunity and effective tumor rejection response in both WT and MUC1-Tg mice even though it was unable to break $CD4^+$ T cell tolerance in MUC1-Tg mice. The effector cells in these mice were MUC1-specific $CD8^+$ T cells that produced IFN-γ.

Materials and Methods

Animals

MUC1-Tg mice (4–6 wk old) on a C57BL/6 background were purchased from Mayo Clinic, (Scottsdale, AZ), and conventional C57BL/6 mice were obtained from The Jackson Laboratory (Bar Harbor, ME). All experimental animals were housed at the University of Pittsburgh Cancer Institute Animal Facility (Pittsburgh, PA) under standard pathogen-free conditions.

Antigens

The 140-aa synthetic MUC1 peptide used for immunization corresponds to seven tandem repeats of a 20-aa sequence from the extracellular tandem repeat domain of MUC1. The amino acid sequence of one repeat is GVT SAPDTRPAPGSTAPPAH. The peptide was synthesized on a Chemtech 200 machine with *N*-(9-fluorenyl)methoxycarbonyl chemistry and purified by HPLC in the University of Pittsburgh Cancer Institute Peptide Facility. In some in vitro assays, a 100-aa MUC1 synthetic peptide corresponding to five tandem repeats was used instead of the 140-aa MUC1 peptide.

Vaccines and immunization protocols

Three different immunization protocols were tested in vivo. Mice were immunized with: 1) synthetic MUC1 peptide (100 μg/mouse) coadministered with soluble murine GM-CSF (2 μg/mouse; a generous gift from Immunex, Seattle, WA) injected s.c.; 2) synthetic MUC1 peptide (100 μg/mouse) coadministered with SB-AS2 (50 μl/mouse; a generous gift of SmithKline Beecham Biologicals, Rixensart, Belgium) injected i.m.; or 3) murine DC prepulsed with 20 μg/ml of synthetic MUC1 peptide in AIM-V medium (Life Technologies, Grand Island, NY) overnight ($2–5 \times 10^4$ DC/mouse injected s.c.). SB-AS2 is an oil-in-water emulsion containing 3-deacylated-monophosphoryl lipid A, a detoxified form of lipid A, and purified fraction number 21 of Quillaria saponaria, known as Quil A (56, 57). The DC were generated as described previously (58), the major modification being that they were grown in serum-free medium. Briefly, they were differentiated in vitro from bone marrow precursors with murine GM-CSF (10 ng/ml) and murine IL-4 (10 ng/ml) in AIM-V medium for 7 days. On day 7, the DC were purified on a Nycoprep gradient (Nycomed, Oslo, Norway), pulsed overnight with peptide in Teflon vials, and washed before vaccination. For the DC vaccine containing soluble peptide, soluble MUC1 peptide was added to the washed peptide-pulsed DC at a final concentration of 100 μg/mouse before vaccination. The mice were immunized once and boosted twice at 3-wk intervals in the right hind flank.

MUC1-specific ELISA

Ten days after the last boost, blood samples were collected by tail bleeding, and the serum was tested for the presence of MUC1-specific Abs with a MUC1-specific ELISA (10) with a few modifications. Briefly, 96-well Immulon 4 plates (Dynatech, Chantilly, VA) were coated at room temperature overnight with 10 μg/ml of 100-aa MUC1 peptide in PBS. The plates were washed three times with PBS and incubated with serial dilutions of the immune serum for 1 h at room temperature. After three washes with PBS/0.1% Tween 20, the plates were incubated with goat anti-mouse peroxidase-conjugated secondary Abs for 1 h at room temperature. The goat anti-mouse-IgM and -IgG secondary Abs were obtained from Sigma (St. Louis, MO). The goat anti-mouse-IgG1,-IgG2b, and -IgG3 Abs were obtained from Southern Biotechnology Associates (Birmingham, AL). The plates were washed three times with PBS/0.1% Tween 20 and then incubated with the substrate *O*-phenylenediamine dihydrochloride tablets (Sigma) for 1 h. The reaction was stopped with 2.5 M sulfuric acid, and the absorbance was measured at 490 nm.

IFN-γ enzyme-linked immunospot (ELISPOT) assay

Lymph node (LN) cells were mixed with peptide-pulsed bone marrow-derived DC (at a ratio of 10:1) in MultiScreen 96-well filtration plates (Millipore, Bedford, MA) precoated with the anti-IFN-γ capture Ab (BD PharMingen, San Jose, CA). The plates were incubated for 40 h at 37°C. After three washes with PBS/0.1% Tween 20, the plates were incubated with 2 μg/well of biotin-labeled anti-IFN-γ Ab (BD PharMingen) at 37°C. The plates were washed, and spots developed with the Elite Vectastain ABC Kit (Vector Laboratories, Burlingame, CA). For blocking studies, anti-CD4, anti-CD8, or isotype control Abs (BD PharMingen) were added to the wells at a final concentration of 2.5 μg/ml.

Intracellular cytokine detection assay

To analyze the T cells, bone marrow-derived DC were prepulsed with MUC1 synthetic peptide and used to stimulate LN cells at a 1:10 stimulator:responder cell ratio. Responder cells stimulated with DC alone served as the negative controls. After 30 h, PMA (20 ng/ml), ionomycin (1 μM), and monensin (3 μM) were added to the cultures for 6 h. The cells were washed twice in FACS buffer (5% FBS and 0.01% sodium azide in 1× PBS) and then stained for surface markers with anti-CD3 PERCP and anti-CD8 FITC. To analyze NK cells, LN cells and splenocytes were harvested from mice injected 24 h earlier with SB-AS2 adjuvant. The cells were stimulated in vitro with PMA (20 ng/ml), ionomycin (1 μM), and monensin (3 μM) for 4 h and then stained for surface markers with anti-NK, anti-CD16, or anti-NK1.1-FITC-conjugated Abs.

Intracellular staining for IFN-γ was conducted according to a previously described protocol (59) with a few modifications. After surface staining, the cells were washed three times with FACS buffer and then fixed in a final concentration of 2% paraformaldehyde for 30 min at 4°C. The cells were permeabilized with 0.1% saponin in FACS buffer and stained with labeled anti-IFN-PE Ab. All of the Abs used in FACS assays were obtained from BD PharMingen. After a 1-h incubation at 4°C, the cells were washed and fixed in 1% paraformaldehyde solution. The samples were read on a FACSCalibur (Becton Dickinson, San Jose, CA) and the data analyzed with the CellQuest data analysis program (Becton Dickinson, San Jose, CA). A fold increase >2 over the control is considered to be significant.

Human MUC1 expression on the mouse tumor and tumor challenge

The T cell lymphoma line RMA on a C57BL6 background was transfected by electroporation with the pR/CMV-MUC1 plasmid containing full-length MUC1 cDNA with 42 tandem repeats (42). Stable transfectants were selected by using G418 (Life Technologies) and further cloned by limiting dilution. Anti-MUC1 Abs 3C6 and 4H5 (generous gifts from Jo Hilgers, Free University, Amsterdam, The Netherlands), were used to confirm cell surface expression of MUC1. Transfected RMA clones were incubated for 1 h at 4°C with anti-MUC1 Abs, washed, and then incubated with goat anti-mouse PE-conjugated secondary Ab (Biosource, Camarillo, CA) for 1 h at 4°C. The cells were washed and then fixed with a final concentration of 1% paraformaldehyde. The samples were read on a FACSCalibur (Becton Dickinson) and the data analyzed using the CellQuest data analysis program (Becton Dickinson). The RMA-MUC1 cell line that was derived maintains long-term stable expression of MUC1 in vitro and in vivo and has been used in tumor challenge experiments.

Ten days after the last boost, the mice were anesthetized with Metofane (Schering-Plough Animal Health, Omaha, NE) and 5×10^4 RMA-MUC1 cells injected s.c. in the shaved right hind flank. Tumor growth was monitored every 2–3 days and tumor size determined with calipers. Mice were sacrificed when the tumor size reached 2 cm in diameter.

Statistical analysis

The statistical significance of our results was calculated in a Student unpaired t test. The two-tailed p values were determined with the statistical program INSTAT version 2.03 GraphPad Software (San Diego, California). Values of $p < 0.05$ were considered significant.

Results

Differential induction of MUC1-specific Ig isotypes in WT and MUC1-Tg mice

Cytokines produced by Th cells have been implicated in inducing switching from IgM to other Ab isotypes (60–62). Hence, we were interested in the quantitative as well as qualitative differences in the humoral responses elicited by different MUC1 peptide-based vaccines, not only as a direct reflection of the B cell response, but also as an indirect reflection of the Th cell response in WT vs MUC1-Tg mice. Table I is a summary of anti-MUC1 Abs detected in the sera of immunized mice from various groups 10 days after the last boost. Sera from unimmunized mice were used as controls. When MUC1 peptide was administered with GM-CSF as an adjuvant, the vaccine induced IgM and moderate IgG1 and IgG2b Ab responses in conventional mice but only IgM Ab in MUC1-Tg mice. Ab responses elicited by vaccination with MUC1 peptide with SB-AS2 adjuvant were very different. Strong IgG1, IgG2b, and IgG3 responses were induced in both WT and MUC1-Tg mice. In C57BL/6 mice, the IgG2a gene is deleted (63), and thus this isotype was not measured here. Even though of very high titer in both strains, IgG responses in MUC1-Tg mice were nevertheless 10-fold lower in end-point titer compared with WT mice. Low- to moderate-titer IgM and no IgG Ab responses were detected in WT and MUC1-Tg mice immunized with peptide-pulsed DC (Table I). This was expected, as the peptide-pulsed DC were washed before injection, and, hence, there was little soluble peptide available to activate the B cells. Addition of soluble peptide to the peptide-pulsed DC vaccine induced high-titer IgG1 and moderate IgG2b (Table I), an isotype profile similar to that elicited by MUC1 peptide admixed with GM-CSF.

DC vaccine activates $CD4^+$ T cells in WT mice but not in MUC1-Tg mice

The ability of the two adjuvant-based vaccines to elicit multiple IgG isotypes suggested that MUC1-specific $CD4^+$ T cells were being stimulated. The differences that were seen between the WT and MUC1-Tg mice suggested that the $CD4^+$, MUC1-specific T cells were impaired in Tg mice but could be efficiently activated depending on the immunization protocol, MUC1 plus SB-AS2 in this case appearing to be a better vaccine than MUC1 plus GM-CSF. Because IFN-γ plays an important role in isotype switching and in particular in switching to IgG3, we expected to find Ag-specific, IFN-γ-producing Th cells, especially in mice where we detected MUC1-specific IgG3 Ab. Contrary to our expectations, we were not able to detect any such cells in mice immunized with adjuvant-based vaccines. The peptide-pulsed DC vaccine was the only one capable of inducing IFN-γ-producing T cells in WT (Fig. 1*A*) as well as in MUC1-Tg mice (Fig. 1*B*). These cells were MUC1-specific, as stimulation with DC in the absence of MUC1 peptide resulted in a significantly lower number of background spots in the ELISPOT assay. The number of IFN-γ-producing T cells was ~5-fold higher in WT mice compared with MUC1-Tg mice. More importantly, in WT mice, blocking with either anti-CD4 or anti-CD8 Abs resulted in a significant decrease in the total number of IFN-γ spots, indicating that both $CD4^+$ and $CD8^+$ cells contributed to MUC1-specific IFN-γ production (Fig. 1*A*). However, in MUC1-Tg mice, blocking with anti-CD8 Ab eliminated almost all IFN-γ production, whereas blocking with anti-CD4 Ab had no significant effect (Fig. 1*B*). The ELISPOT data were confirmed with the intracellular cytokine assay in which we could directly evaluate the phenotype of IFN-γ-producing cells. As seen in Table II, only $CD8^+$ T cells from MUC1-Tg mice immunized with peptide-pulsed DC were capable of producing IFN-γ in response to MUC1 peptide. Moreover, when cultured for 2 days in the presence of MUC1 peptide, the percentage $CD8^+$ T cells increased from 20% in the starting population to 66%, showing Ag-specific proliferation of $CD8^+$ cells. In vitro, these cells remain cytokine producing, without any measurable CTL activity. After in

Table I. *MUC1-specific Abs elicited in WT and MUC1-Tg mice*

Vaccine Group[a]	Mice	IgM	IgG1	IgG2b	IgG3
Control	WT	–	–	–	–
	MUC1-Tg	–	–	–	–
Peptide + GM-CSF	WT	640	640	640	–
		1280	1280	1280	
		1280	1280	1280	
		1280			
	MUC1-Tg	320	–	–	–
		1280			
		–			
		–			
Peptide + SB-AS2	WT	>1280	10^5	10^4	10^3
		>1280	10^5	10^4	10^3
		>1280	10^5	10^4	10^3
		>1280	10^5	10^4	10^3
	MUC1-Tg	>1280[b]	10^4	10^2	10^2
			10^5	10^2	10^2
			10^5	10^3	10^2
			10^5	10^3	10^2
Peptide-pulsed DC	WT	640[b]	–[c]	–	–
	MUC1-Tg	1280	–	–	–
		1280			
		1280			
		1280			
Pulsed DC + soluble peptide	WT	640	>1280	320	–
		1280	>1280	1280	
		1280	>1280	1280	
		1280	>1280	1280	

[a] Results are expressed as end point titers of sera from individual mice (three to four per vaccine group).
[b] Pooled serum from four mice per vaccine group.
[c] Indicative of zero absorbance at 490 nm in the ELISA.

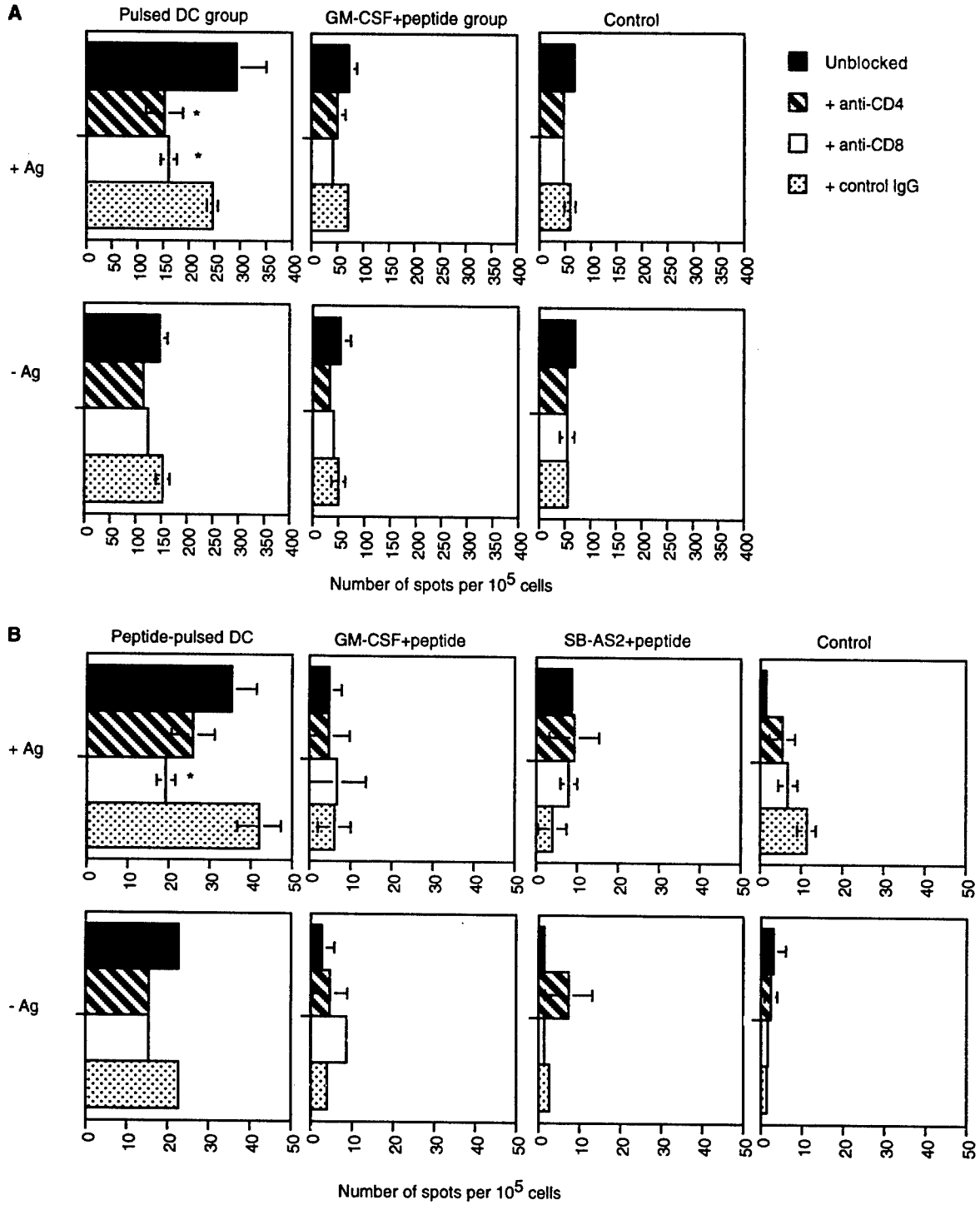

FIGURE 1. Cytokine production by MUC1-specific T cells from immunized WT (*A*) and MUC1-Tg (*B*) mice. ELISPOT assays were conducted with LN cells from immunized and control mice stimulated for 40 h with MUC1 peptide-pulsed (+Ag) or no peptide (−Ag) control DC. The LN cells were pooled from four mice per group. Anti-CD4 or anti-CD8 Abs were added to the T cells before the addition of the DC to the cultures for the duration of the assay. *, The only statistically significant differences: *A*, anti-CD4, $p = 0.02$; anti-CD8 $p = 0.01$; *B*, anti-CD8, $p = 0.01$.

vitro stimulation, we were able to detect on occasion very low MUC1-specific CTL activity in bulk LN cells from WT and MUC1-Tg mice immunized with the peptide-pulsed DC vaccine (data not shown), but these results were not always reproducible. CTL activity was never detected in bulk LN or spleen cells from mice immunized with adjuvant-based vaccines (data not shown).

Efforts to detect IL-4-producing Th cells were unsuccessful because of the difficulty of detecting Ag-specific IL-4 production in either the ELISPOT or the intracellular cytokine assay in the murine system.

Adjuvant-activated non-T Cells are a source of IFN-γ required for MUC1-specific IgG3 induction

To identify the source of the IFN-γ responsible for isotype switching and in particular to IFN-dependent IgG3 in mice immunized with the MUC1 peptide admixed with the SB-AS2 adjuvant, we

Table II. *Detection of intracellular IFN-γ in LN T cells from immunized MUC1-Tg mice following 2 days in vitro culture*[a]

Vaccine Group	+/– Peptide	IFN-γ$^+$		CD3$^+$	
		CD4$^+$	CD8$^+$	CD4$^+$	CD8$^+$
Peptide-pulsed DC	+	0	15.9	34	66
	–	8.4	5.7	80	20
Peptide + GM-CSF	+	2	2.2	72	18
	–	2.4	5	67	33
Peptide + SB-AS2	+	5.9	2.7	79	21
	–	5.2	6.8	65	35
Control	+	6.2	6.2	73	17
	–	8	4	77	23

[a] Numbers are expressed as a percentage of CD3$^+$ cells. The assays were carried out using pooled LN cells from four mice per vaccine group.

injected WT mice with SB-AS2 alone and 24 h later analyzed their spleen and draining LN for production of IFN-γ by non-T cells. SB-AS2 induced a 2- to 3-fold increase in the percentage of NK$^+$ or NK1.1$^+$ cells in the spleen, compared with untreated mice (Fig. 2*A*). This increase in the percentage of NK cells was unique to the spleen because no such difference was observed in LN from SB-AS2-treated and untreated control mice. In addition to the overall increase in cell number, we also saw an increase in the percentage of IFN-γ-producing NK$^+$ and NK1.1$^+$ cells in the spleen and not in the LN (Fig. 2*B*). There was no difference in the percentage of CD16$^+$ cells in either the spleen or LN in response to SB-AS2, as would be expected because CD16 is a marker found on a variety of cells other than NK cells, such as macrophages, B cells, and DC (Fig. 2*A*). However, the percentage of CD16$^+$ cells that produced IFN-γ in response to SB-AS2, was greatly increased in the spleen and not in the LN (Fig. 2*B*). Addition of MUC1 peptide to the adjuvant does not change the above results, as indicated by the induction of an IgG3 Ab response by the MUC1 peptide admixed with SB-AS2 vaccine in the absence of a T cell source of IFN-γ (Table I).

DC-based vaccine leads to tumor-free survival in both WT and MUC1-Tg mice

The mouse tumor cell line RMA was transfected with human MUC1 cDNA and, as seen in Fig. 3, epitopes present on both glycosylated normal MUC1 (recognized by Ab 3C6), as well as on underglycosylated tumor MUC1 (recognized by Ab 4H5) are expressed on the transfected RMA MUC1 tumor cells. RMA MUC1 grows well as a s.c. solid tumor, and we determined in preliminary experiments that injection of 5×10^4 tumor cells resulted in 80% tumor take in 18 days (data not shown).

All mice were challenged 10 days after the last immunization with RMA-MUC1 tumor cells injected s.c., and tumor growth was monitored up to 60 days. By day 30, ~60% of unimmunized control WT and MUC1-Tg mice were sacrificed because their tumors reached a size of 2 cm. WT and MUC1-Tg mice that had been immunized with MUC1 peptide admixed with either GM-CSF or SB-AS2 also had to be sacrificed because they failed to reject the tumors (Fig. 4). Before concluding that the humoral response alone was not being effective against this MUC1-expressing tumor, it was important to determine whether the Abs elicited by the synthetic MUC1 peptide-based vaccines that recognized the immunizing peptide in the ELISA were also capable of recognizing the native MUC1 molecule on the RMA-MUC1 tumor. We stained RMA-MUC1 cells with a 1:100 dilution of immune serum from mice immunized with MUC1 peptide admixed with SB-AS2 and could clearly show MUC1 protein-specific immune reactivity (Fig. 5). This confirmed that MUC1 peptide and adjuvant-based vaccines did induce Abs capable of recognizing the tumor, but that recognition did not result in tumor rejection.

Only the MUC1 peptide-pulsed DC vaccine resulted in an impressive tumor rejection in both WT and MUC1-Tg mice. Ninety percent of immunized mice were completely tumor free up to 60 days after tumor challenge (Fig. 4). The survival curves were comparable between the WT and MUC1-Tg mice, even though in WT mice the vaccine had elicited CD4$^+$ as well as CD8$^+$ MUC1-specific T cells, but only CD8$^+$ MUC1-specific T cells in MUC1-Tg mice.

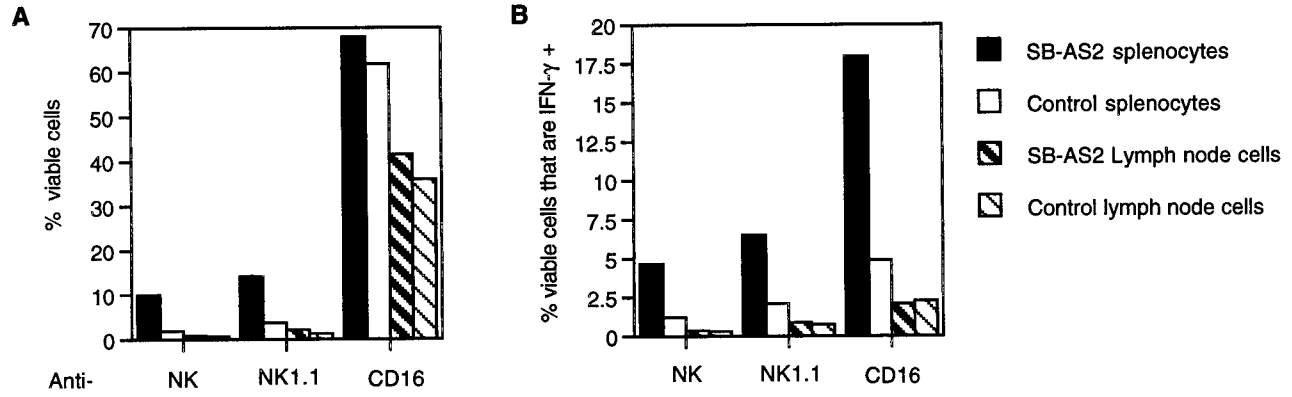

FIGURE 2. Non-T cells (*A*) and IFN-γ production by non-T cells (*B*) in spleens of SB-AS2-injected mice. Splenocytes and LN cells from uninjected mice were used as controls.

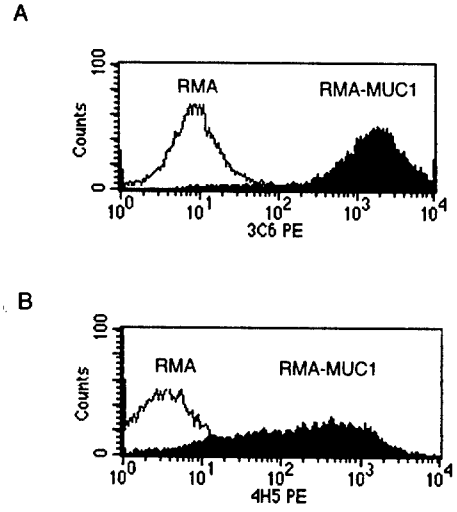

FIGURE 3. MUC1 expression on RMA-MUC1 tumor cells. Ab 3C6 (*A*) recognizes MUC1 irrespective of its glycosylation state, while 4H5 (*B*) recognizes only the underglycosylated (tumor) form of MUC1.

MUC1-expressing tissues, lung, pancreas, liver, and kidney, were harvested from MUC1-Tg mice after immunization and/or after tumor rejection to investigate whether the immune responses elicited by vaccination alone or also boosted through tumor rejection would show reactivity against normal tissues. As signs for autoimmunity, we looked by hematoxylin and eosin staining for mononuclear infiltrates in the tissues, especially around the $MUC1^+$ ducts, as well as evidence of tissue destruction. We saw no difference in the appearance of these tissues between immunized and control mice (data not shown), concluding that the MUC1-specific immune response that was strong enough to cause tumor rejection did not cause autoimmune damage to normal $MUC1^+$ tissues.

Discussion

We chose the long MUC1 synthetic peptide as the immunogen because of our previous studies that showed that this peptide is efficiently processed and presented by APCs such as DC (21, 22). In addition, studies in vitro with human T cells as responders have

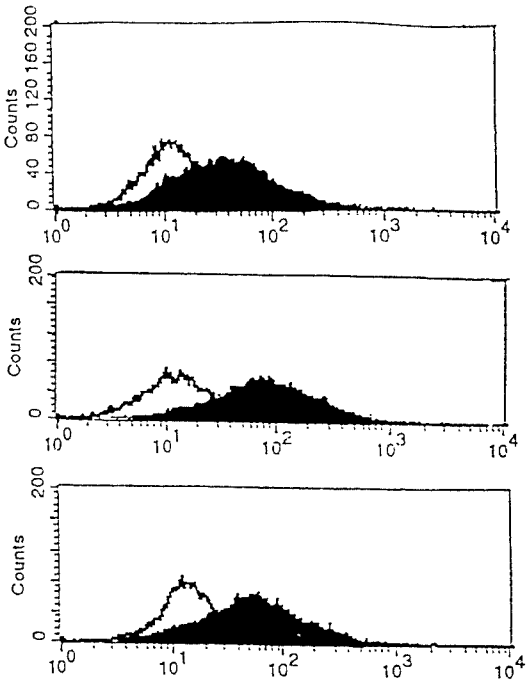

FIGURE 5. Recognition of MUC1 on the surface of RMA MUC1 tumor cells by sera of mice immunized with MUC1 peptide admixed with SB-AS2 adjuvant. Staining of RMA-MUC1 (filled peak) and RMA (unfilled peak) with sera used at 1:100 dilution. Data from three different mice are shown.

shown that DC pulsed with this form of MUC1 can prime both $CD8^+$ and $CD4^+$ T cells (21, 23). Our experiments demonstrate important differences in immune responses that can be elicited by the same tumor Ag administered in different vaccine formulations. As we expected, we saw additional differences in response to these vaccines between MUC1-Tg and WT mice. Thus, we saw that MUC1 peptide vaccine with GM-CSF adjuvant induces IgG responses only in conventional mice, and primarily those that do not depend on IFN-γ. The vaccine with SB-AS2 as adjuvant induces IgG responses in both conventional and MUC1-Tg mice, including the IFN-γ dependent isotype IgG3. It is important to note that the

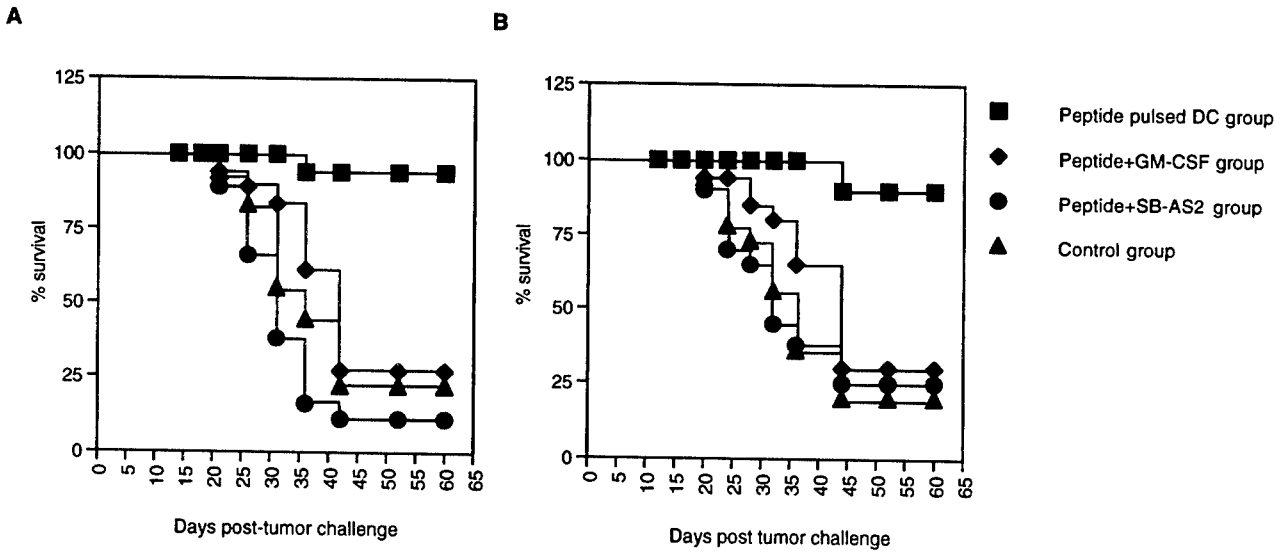

FIGURE 4. Potential for tumor rejection in mice immunized with the three different vaccines. *A*, WT mice. *B*, MUC1-Tg mice. Mice were injected three times, 3 wk apart. Ten days after the last boost, the mice were challenged s.c. with tumor. Unimmunized mice served as the control group. The results are from 20–35 mice per vaccine group. The data are representative of two independent experiments.

titer of IgG Abs elicited in MUC1-Tg mice was 10-fold lower than in WT mice. Inasmuch as there was no Th cell activation in either the WT or the MUC1-Tg mice, these results support previous reports that MUC1-Tg mice display some level of B cell tolerance (64, 65).

We correctly hypothesized that the lack of an Ab response in WT and MUC1-Tg mice immunized with peptide-pulsed DC was attributable to the absence of sufficient concentrations of soluble peptide that could simultaneously activate B cells. An IgG response was elicited when soluble peptide was added to the DC vaccine. Even though, to the extent that we have been able to evaluate in this particular tumor model, Abs did not play an important role, this is unlikely to be a common observation. In most cases, the most comprehensive immune response will likely be the most effective, and vaccines based on DC that have already processed the Ag will require additional soluble Ag to elicit both cellular and humoral immune responses.

IFN-γ is the cytokine responsible for up-regulating IgG3 isotype Ab in mice (62, 66). It is interesting to note that the DC vaccine with added soluble peptide was unable to induce IgG3 Abs in WT mice even though it was capable of inducing $CD4^+$ IFN-γ-producing cells in these mice. This suggests to us that the quantities of IFN-γ produced by these T cells were not sufficient to cause the switch to IgG3. Previous reports have suggested that Th cell-independent IgG3 can be induced by IFN-γ produced by NK cells (62, 67). We were able to confirm that SB-AS2, the adjuvant in the vaccine that elicited MUC1-specific IgG3, when administered alone increased the total number of NK cells and the number of NK cells producing IFN-γ in the spleen. The MUC1 peptide composed of five identical 20-aa repeats is a multivalent Ag that binds to B cell receptors and cross-links them sufficiently to activate the B cell. These activated B cells then can use IFN-γ produced in their vicinity by activated NK cells to switch their Ab production from IgM to other isotypes, in particular IgG3. These results show yet again the importance of including in vaccine preparations adjuvants that are capable of stimulating the components of the innate immune system, major producers of important cytokines (68). Although the SB-AS2-based vaccine did not induce MUC1-specific T cells in our model system, recent work has shown that immunization of E7-Tg mice and control wild-type mice with recombinant HPV 16 E7 protein coadministered with SB-AS2 as an adjuvant elicits E7-specific T cell responses (69).

Based on previous publications (53, 64), we expected to find signs of tolerance of MUC1-specific $CD4^+$ T cells in MUC1-Tg mice, but we were surprised that we could not overcome it with the DC-based vaccine. The same MUC1 peptide loaded onto human DC can prime human MUC1-specific $CD4^+$ T cell responses in vitro (23). We have also shown that it is possible to induce $CD4^+$ T cell responses in chimpanzees with the same MUC1 peptide admixed with *Leishmania* initiation factor as an adjuvant (42). We also have seen $CD4^+$ T cell proliferation in response to MUC1 peptide in patients vaccinated with this peptide (unpublished data). $CD4^+$ T cell tolerance in the MUC1-Tg mice appears to be more profound than in humans and may be a peculiarity of this particular Tg model.

MUC1-specific Abs of three different isotypes, IgG1, IgG2b, and IgG3, elicited by the adjuvant-based vaccines, could not provide protection against subsequent tumor challenge. It was previously reported that passive transfer of polyclonal sera containing MUC1-specific IgG1 Abs could not protect against another tumor, B16 melanoma transfected with MUC1 (65). Previous work investigating the role of Abs in tumor immunity against SV40-transformed cells suggested that Ab-dependent cellular cytotoxicity (ADCC) is an important protective mechanism against virus-induced tumors. Abs of the IgG2a isotype are thought to represent the principal element of ADCC mediated via their interaction with type II FcR (70). By working in C57BL/6 mice that lack the gene for IgG2a, we were unable to test the effect of this isotype that works primarily through ADCC. Cellular immunity clearly plays an important role in the rejection of $MUC1^+$ tumors in C57BL/6 mice, and Abs alone are ineffective. However, Abs may complement the cellular responses by contributing to the prevention of the metastatic spread of the tumor, an issue that was not addressed to date and that we are currently exploring.

Approximately 90% of the mice immunized with the DC vaccine rejected the RMA-MUC1 tumor, and in the case of MUC1-Tg mice, apparently through MUC1-specific $CD8^+$ T cells as the only effector mechanism. These T cells, as far as we were able to determine, were primarily IFN-γ producers, rather than CTL. It is possible that the function we measured in vitro does not correspond to their more comprehensive in vivo function, which might also include CTL activity. Alternatively, these cells may have destroyed the tumor cells through noncytolytic mechanisms that were first reported to operate in viral systems (71–73) and more recently in tumor rejection as well (74). It has been reported that bacterial CpG-DNA up-regulates costimulatory molecules and stimulates DC to produce IL-12, thereby "licensing" them to activate $CD8^+$ T cell responses in a Th cell-independent fashion (75). Thus, it is possible that in our study, the MUC1-peptide-pulsed DC that were generated in vitro were sufficiently activated to prime MUC1-specific $CD8^+$ T cells in a Th cell-independent fashion. The MUC1-specific T cells that caused tumor rejection did not infiltrate into or show destruction of normal MUC1-expressing tissues such as pancreas, kidney, and lung. However, we know that binding of MUC1 peptides from the tandem repeat region to $H\text{-}2K^b$ and D^b, C57BL6 MHC-class I alleles, is of such low affinity that we have never been able to detect it with the standard class I stabilization assay (unpublished data). In agreement with those observations, we also have never been able to generate class I-restricted CTL to the MUC1 tandem repeat region in C57BL6 mice. Thus, low-level expression of MUC1 in normal cells and low-affinity binding of MUC1 tandem repeat-derived peptides to $H\text{-}2^b$ alleles may account for the lack of recognition of normal tissues by MUC1-specific T cells. For that reason, we are now repeating immunizations and tumor rejections studies in double-Tg mice that not only express human MUC1, but also human HLA-A11 allele, known to be a restricting element for MUC1 specific CTL (17).

Acknowledgments

We thank Dr. Simon Barratt-Boyes for transfecting and cloning the RMA-MUC1 cell line. We also thank Dr. Joseph Ahearn and Jeanine Navratil for the use of the FACSCalibur.

References

1. Gendler, S. J., and A. P. Spicer. 1995. Epithelial mucin genes. *Annu. Rev. Physiol. 57:607.*
2. Soares, M. M., and O. J. Finn. MUC1 mucin as a target for immunotherapy of cancer. In *Cancer Immunology, Immunology in Medicine Series.* R. Rees and A. Robbins, eds. Kluver Academic Publishers. *In press.*
3. Hanisch, F. G., T. R. Stadie, F. Deutzmann, and J. Peter-Katalinic. 1996. MUC1 glycoforms in breast cancer cell line T47D as a model for carcinoma-associated alterations of *O*-glycosylation. *Eur. J. Biochem. 236:318.*
4. Lancaster, C. A., N. Peat, T. Duhig, D. Wilson, J. Taylor-Papadimitriou, and S. J. Gendler. 1990. Structure and expression of the human polymorphic epithelial mucin gene: an expressed VNTR unit. *Biochem. Biophys. Res. Commun. 173:1019.*
5. Muller, S., S. Goletz, N. Packer, A. Gooley, A. M. Lawson, and F. G. Hanisch. 1997. Localization of *O*-glycosylation sites on glycopeptide fragments from lactation-associated MUC1: all putative sites within the tandem repeat are glycosylation targets in vivo. *J. Biol. Chem. 272:24780.*
6. Brockhausen, I., J. M. Yang, J. Burchell, C. Whitehouse, and J. Taylor-Papadimitriou. 1995. Mechanisms underlying aberrant glycosylation of MUC1 mucin in breast cells. *Eur. J. Biochem. 233:607.*

7. Nishimori, I., F. Perini, K. P. Mountjoy, S. D. Sanderson, N. Johnson, R. L. Cerny, M. L. Gross, J. D. Fontenot, and M. A. Hollingsworth. 1994. *N*-acetylgalactosamine glycosylation of MUC1 tandem repeat peptides by pancreatic tumor cell extracts. *Cancer Res. 54:3738.*
8. Seregni, E., C. Botti, S. Massaron, C. Lombardo, A. Capobianco, A. Bogni, and E. Bombardieri. 1997. Structure, function and gene expression of epithelial mucins. *Tumor 83:625.*
9. Stadie, T. R., W. Chai, A. M. Lawson, P. G. Byfield, and F. G. Hanisch. 1995. Studies on the order and site specificity of GalNAc transfer to MUC1 tandem repeats by UDP-GalNAc: polypeptide *N*-acetylgalactosaminyltransferase from milk or mammary carcinoma cells. *Eur. J. Biochem. 229:140.*
10. Kotera, Y., J. D. Fontenot, G. Pecher, R. S. Metzgar, and O. J. Finn. 1994. Humoral immunity against a tandem repeat epitope of human mucin MUC-1 in sera from breast, pancreatic, and colon cancer patients. *Cancer Res. 54:2856.*
11. Petrarca, C., B. Casalino, S. von Mensdorff-Pouilly, A. Rughetti, H. Rahimi, G. Scambia, J. Hilgers, L. Frati, and M. Nuti. 1999. Isolation of MUC1-primed B lymphocytes from tumour-draining lymph nodes by immunomagnetic beads. *Cancer Immunol. Immunother. 47:272.*
12. Richards, E. R., P. L. Devine, R. J. Quin., J. D. Fontenot., B. G. Ward, and M. A. McGuckin. 1998. Antibodies reactive with the protein core of MUC1 mucin are present in ovarian cancer patients and healthy women. *Cancer Immunol. Immunother. 46:245.*
13. Rughetti, A., V. Turchi, C. A. Ghetti, G. Scambia, P. B. Panici, G. Roncucci, S. Mancuso, L. Frati, and M. Nuti. 1993. Human B-cell immune response to the polymorphic epithelial mucin. *Cancer Res. 53:2457.*
14. von Mensdorff-Pouilly, S., M. M. Gourevitch, P. Kenemans, A. A. Verstraeten, S. V. Litvinov, G. J. van Kamp, S. Meijer, J. Vermorken, and J. Hilgers. 1996. Humoral immune response to polymorphic epithelial mucin (MUC-1) in patients with benign and malignant breast tumour. *Eur. J. Cancer. 32A:1325.*
15. von Mensdorff-Pouilly, S., C. Vennegoor, and J. Hilgers. 2000. Detection of humoral immune responses to mucins. *Methods Mol. Bio. 125:495.*
16. Brossart, P., K. S. Heinrich, G. Stuhler, L. Behnke, V. L. Reichardt, S. Stevanovic, A. Muhm, H. G. Rammensee, L. Kanz, and W. Brugger. 1999. Identification of HLA-A2-restricted T-cell epitopes derived from the MUC1 tumor antigen for broadly applicable vaccine therapies. *Blood 93:4309.*
17. Domenech, N., R. A. Henderson, and O. J. Finn. 1995. Identification of an HLA-A11-restricted epitope from the tandem repeat domain of the epithelial tumor antigen mucin. *J. Immunol. 155:4766.*
18. Jerome, K. R., D. L. Barnd, K. M. Bendt, C. M. Boye, J. Taylor-Papadimitriou, I. F. McKenzie, R. C. Bast Jr., and O. J. Finn. 1991. Cytotoxic T-lymphocytes derived from patients with breast adenocarcinoma recognize an epitope present on the protein core of a mucin molecule preferentially expressed by malignant cells. *Cancer Res. 51:2908.*
19. Jerome, K. R., N. Domenech, and O. J. Finn. 1993. Tumor-specific cytotoxic T cell clones from patients with breast and pancreatic adenocarcinoma recognize EBV-immortalized B cells transfected with polymorphic epithelial mucin complementary DNA. *J. Immunol. 151:1654.*
20. McKolanis, J. R., and O. J. Finn. 2000. Analysis of the frequency of MHC-unrestricted MUC1-specific cytotoxic T-cells in peripheral blood by limiting dilution assay. *Methods Mol. Bio. 125:463.*
21. Hiltbold, E. M., M. D. Alter, P. Ciborowski, and O. J. Finn. 1999. Presentation of MUC1 tumor antigen by class I MHC and CTL function correlate with the glycosylation state of the protein taken up by dendritic cells. *Cell. Immunol. 194:143.*
22. Hiltbold, E. M., A. M. Vlad, P. Ciborowski, S. C. Watkins, and O. J. Finn. 2000. The mechanism of unresponsiveness to circulating tumor antigen MUC1 is a block in intracellular sorting and processing by dendritic cells. *J. Immunol. 165: 3730.*
23. Hiltbold, E. M., P. Ciborowski, and O. J. Finn. 1998. Naturally processed class II epitope from the tumor antigen MUC1 primes human $CD4^+$ T cells. *Cancer Res. 58:5066.*
24. Goydos, J. S., E. Elder, T. L. Whiteside, O. J. Finn, and M. T. Lotze. 1996. A phase I trial of a synthetic mucin peptide vaccine: induction of specific immune reactivity in patients with adenocarcinoma. *J. Surgical Res. 63:298.*
25. Longenecker, B. M., M. Reddish, R. Koganty, and G. D. MacLean. 1993. Immune responses of mice and human breast cancer patients following immunization with synthetic sialyl-Tn conjugated to KLH plus detox adjuvant. *Ann. NY Acad. Sci. 690:276.*
26. Scholl, S., B. Acres, C. Schatz, M. P. Kieny, J. M. Balloul, A. Vincent-Salomon, L. Deneux, E. Tartour, H. Fridman, and P. Pouillart. 1997. The polymorphic epithelial mucin (MUC1): a phase I clinical trial testing the tolerance and immunogenecity of a vaccinia virus-MUC1-IL-2 construct in breast cancer. *Breast Cancer Res. Treat. 46:67.*
27. Karanikas, V., L. A. Hwang, J. Pearson, C. S. Ong, V. Apostolopoulos, H. Vaughan, P. X. Xing, G. Jamieson, G. Pietersz, B. Tait, R. et al. 1997. Antibody and T cell responses of patients with adenocarcinoma immunized with mannan-MUC1 fusion protein. *J. Clin. Investigation. 100:2783.*
28. Acres, R. B., M. Hareuveni, J. M. Balloul, and M. P. Kieny. 1993. Vaccinia virus MUC1 immunization of mice: immune response and protection against the growth of murine tumors bearing the MUC1 antigen. *J. Immunother. 14:136.*
29. Akagi, J., J. W. Hodge, J. P. McLaughlin, L. Gritz, G. Mazzara, D. Kufe, J. Schlom, and J. A. Kantor. 1997. Therapeutic antitumor response after immunization with an admixture of recombinant vaccinia viruses expressing a modified MUC1 gene and the murine T-cell costimulatory molecule B7. *J. Immunother. 20:38.*
30. Apostolopoulos, V., G. A. Pietersz, B. E. Loveland, M. S. Sandrin, and I. F. McKenzie. 1995. Oxidative/reductive conjugation of mannan to antigen selects for T1 or T2 immune responses. *Proc. Natl. Acad. Sci. USA 92:10128.*
31. Apostolopoulos, V., G. A. Pietersz, P. X. Xing, C. J. Lees, M. Michael, J. Bishop, and I. F. McKenzie. 1995. The immunogenicity of MUC1 peptides and fusion protein. *Cancer Lett. 90:21.*
32. Apostolopoulos, V., G. A. Pietersz, and I. F. McKenzie. 1996. Cell-mediated immune responses to MUC1 fusion protein coupled to mannan. *Vaccine 14:930.*
33. Apostolopoulos, V., V. Popovski, and I. F. McKenzie. 1998. Cyclophosphamide enhances the CTL precursor frequency in mice immunized with MUC1-mannan fusion protein (M-FP). *J. Immunother. 21:109.*
34. Ding, L., E. N. Lalani, M. Reddish, R. Koganty, T. Wong, J. Samuel, M. B. Yacyshyn, A. Meikle, P. Y. Fung, J. Taylor-Papadimitriou, and B. Longenecker. 1993. Immunogenicity of synthetic peptides related to the core peptide sequence encoded by the human MUC1 mucin gene: effect of immunization on the growth of murine mammary adenocarcinoma cells transfected with the human MUC1 gene. *Cancer Immunol. Immunother. 36:9.*
35. Gong, J., D. Chen, M. Kashiwabam, and D. Kufe. 1997. Induction of antitumor activity by immunization with fusions of dendritic and carcinoma cells. *Nature Med. 3:558.*
36. Graham, R. A., J. M. Burchell, P. Beverley, and J. Taylor-Papadimitriou. 1996. Intramuscular immunisation with MUC1 cDNA can protect C57 mice challenged with MUC1-expressing syngeneic mouse tumour cells. *Intl. J. Cancer. 65:664.*
37. Henningsson, C. M., S. Selvaraj, G. D. MacLean, M. R. Suresh, A. A. Noujaim, and B. M. Longenecker. 1987. T cell recognition of a tumor-associated glycoprotein and its synthetic carbohydrate epitopes: stimulation of anticancer T cell immunity in vivo. *Cancer Immunol. Immunother. 25:231.*
38. Kieber-Emmons, T., P. Luo, J.Qiu, T. Y. Chang, M. Blaszczyk-Thurin, and Z. Steplewski. 1999. Vaccination with carbohydrate peptide mimotopes promotes anti-tumor responses. *Nat. Biotech. 17:660.*
39. Newman, K. D., D. L. Sosnowski, G. S. Kwon, and J. Samuel. 1998. Delivery of MUC1 mucin peptide by poly(D,L-lactic-co-glycolic acid) microspheres induces type 1 T helper immune responses. *J. Pharm. Sci. 87:1421.*
40. Samuel, J., W. A. Budzynski, M. A. Reddish, L. Ding., G. L. Zimmermann, M. J. Krantz, R. R. Koganty, and B. M. Longenecker. 1998. Immunogenicity and antitumor activity of a liposomal MUC1 peptide-based vaccine. *Intl. J. Cancer. 75:295.*
41. Barratt-Boyes, S. M., H. Kao, and O. J. Finn. 1998. Chimpanzee dendritic cells derived in vitro from blood monocytes and pulsed with antigen elicit specific immune responses in vivo. *J. Immunother. 21:142.*
42. Barratt-Boyes, S. M., A. Vlad, and O. J. Finn. 1999. Immunization of chimpanzees with tumor antigen MUC1 mucin tandem repeat peptide elicits both helper and cytotoxic T-cell responses. *Clin. Cancer Res. 5:1918.*
43. Pecher, G., and O. J. Finn. 1996. Induction of cellular immunity in chimpanzees to human tumor-associated antigen mucin by vaccination with MUC-1 cDNA-transfected Epstein-Barr virus-immortalized autologous B cells. *Proc. Natl. Acad. Sci. USA 93:1699.*
44. Clarke, P., J. Mann, J. F. Simpson, K. Rickard-Dickson and F. J. Primus. 1998. Mice transgenic for human carcinoembryonic antigen as a model for immunotherapy. *Cancer Res. 58:1469.*
45. Kass, E., J. Schlom, J. Thompson, F. Guadagni, P. Graziano, and J. W. Greiner. 1999. Induction of protective host immunity to carcinoembryonic antigen (CEA), a self-antigen in CEA transgenic mice, by immunizing with a recombinant vaccinia-CEA virus. *Cancer Res. 59:676.*
46. Mizobata, S., K. Tompkins, J. F. Simpson, Y. Shyr, and F. J. Primus. 2000. Induction of cytotoxic T cells and their antitumor activity in mice transgenic for carcinoembryonic antigen. *Cancer Immunol. Immunother. 49:285.*
47. Xu, X., P. Clarke, G. Szalai, J. E. Shively, L. E. Williams, Y. Shyr, E. Shi, and F. J. Primus. 2000. Targeting and therapy of carcinoembryonic antigen-expressing tumors in transgenic mice with an antibody-interleukin 2 fusion protein. *Cancer Res. 60:4475.*
48. Boggio, K., G. Nicoletti, E. Di Carlo, F. Cavallo, L. Landuzzi, C. Melani, M. Giovarelli, I. Rossi, P. Nanni, C. De Giovanni, et al. 1998. Interleukin 12-mediated prevention of spontaneous mammary adenocarcinomas in two lines of Her-2/neu transgenic mice. *J. Exp. Med. 188:589.*
49. Esserman, L. J., T. Lopez, R. Montes, L. N. Bald, B. M. Fendly, and M. J. Campbell. 1999. Vaccination with the extracellular domain of p185neu prevents mammary tumor development in neu transgenic mice. *Cancer Immunol. Immunother. 47:337.*
50. Reilly, R. T., M. B. Gottlieb, A. M. Ercolini, J. P. Machiels, C. E. Kane, F. I. Okoye, W. J. Muller, K. H. Dixon, and E. M. Jaffee. 2000. HER-2/neu is a tumor rejection target in tolerized HER-2/neu transgenic mice. *Cancer Res. 60: 3569.*
51. Carr-Brendel, V., D. Markovic, K. Ferrer, M. Smith, J. Taylor-Papadimitriou, J., and E. P. Cohen. 2000. Immunity to murine breast cancer cells modified to express MUC-1, a human breast cancer antigen, in transgenic mice tolerant to human MUC-1. *Cancer Res. 60:2435.*
52. Gong, J., D. Chen, L. Kashiwaba, Y. Li, L. Chen, H. Takeuchi, H. Qu, G. J. Rowse, S. J. Gendler, and D. Kufe. 1998. Reversal of tolerance to human MUC1 antigen in MUC1 transgenic mice immunized with fusions of dendritic and carcinoma cells. *Proc. Natl. Acad. Sci. USA 95:6279.*
53. Rowse, G. J., R. M. Tempero, M. L. VanLith, M. A. Hollingsworth, and S. J. Gendler. 1998. Tolerance and immunity to MUC1 in a human MUC1 transgenic murine model. *Cancer Res. 58:315.*
54. Smith, M., J. M. Burchell, R. Graham, E. P. Cohen, and J. Taylor-Papadimitriou. 1999. Expression of B7.1 in a MUC1-expressing mouse mammary epithelial

tumour cell line inhibits tumorigenicity but does not induce autoimmunity in MUC1 transgenic mice. *Immunol. 97:648.*
55. Tempero, R. M., M. L. VanLith, K. Morikane, G. J. Rowse, S. J. Gendler, and M. A. Hollingsworth. 1998. $CD4^+$ lymphocytes provide MUC1-specific tumor immunity in vivo that is undetectable in vitro and is absent in MUC1 transgenic mice. *J. Immunol. 161:5500.*
56. Ling, I. T., S. A. Ogun, P. Momin, R. L. Richards, N. Garcon, J. Cohen, W. R. Ballou, and A. A. Holder. 1997. Immunization against the murine malaria parasite *Plasmodium yoelii* using a recombinant protein with adjuvants developed for clinical use. *Vaccine 15:1562.*
57. Stoute, J. A., M. Slaoui, D. G. Heppner, P. Momin, K. E. Kester, P. Desmons, B. T. Wellde, N. Garcon, U. Krzych, and M. Marchand. 1997. A preliminary evaluation of a recombinant circumsporozoite protein vaccine against *Plasmodium falciparum* malaria: RTS, S malaria vaccine evaluation. *New Eng. J. Med. 336:86.*
58. Mayordomo, J. I., T. Zorina, W. J. Storkus, L. Zitvogel, C. Celluzzi, L. D. Falo, C. J. Melief, S. T. Ildstad, W. M. Kast, A. B. Deleo, et al. 1995. Bone marrow-derived dendritic cells pulsed with synthetic tumour peptides elicit protective and therapeutic antitumour immunity. *Nature Med. 1:1297.*
59. Prussin, C., and D. D. Metcalfe. 1995. Detection of intracytoplasmic cytokine using flow cytometry and directly conjugated anti-cytokine antibodies. *J. Immunol. Methods 188:117.*
60. Isakson, P. C., E. Pure, E. S. Vitetta, and P. H. Krammer. 1982. T cell-derived B cell differentiation factor(s): effect on the isotype switch of murine B cells. *J. Exp. Med. 155:734.*
61. McIntyre, T. M., D. R. Klinman, P. Rothman, M. Lugo, J. R. Dasch, J. J. Mond, and C. M. Snapper. 1993. Transforming growth factor β 1 selectivity stimulates immunoglobulin G2b secretion by lipopolysaccharide-activated murine B cells. *J. Exp. Med. 177:1031.*
62. Snapper, C. M., T. M. McIntyre, R. Mandler, L. M. Pecanha, F. D. Finkelman, A. Lees, and J. J. Mond. 1992. Induction of IgG3 secretion by interferon γ: a model for T cell-independent class switching in response to T cell-independent type 2 antigens. *J. Exp. Med. 175:1367.*
63. Martin, R. M., and A. M. Lew. 1998. Is IgG2a a good Th1 marker in mice? *Immunol. Today 19:49.*
64. Acres, B., V. Apostolopoulos, J. M. Balloul, D. Wreschner, P. X. Xing, D. Ali-Hadji, N. Bizouarne, M. P. Kieny, and I. F. McKenzie. 2000. MUC1-specific immune responses in human MUC1 transgenic mice immunized with various human MUC1 vaccines. *Cancer Immunol. Immunother. 48:588.*
65. Tempero, R. M., G. J. Rowse, S. J. Gendler, and M. A. Hollingsworth. 1999. Passively transferred anti-MUC1 antibodies cause neither autoimmune disorders nor immunity against transplanted tumors in MUC1 transgenic mice. *Intl. J. Cancer. 80:595.*
66. Wilder, J. A., C. Y. Koh, and D. Yuan. 1996. The role of NK cells during in vivo antigen-specific antibody responses. *J. Immunol. 156:146.*
67. Koh, C. Y., and D. Yuan. 1997. The effect of NK cell activation by tumor cells on antigen-specific antibody responses. *J. Immunol. 159:4745.*
68. Orange, J. S., and C. A. Biron. 1996. Characterization of early IL-12, IFN-$\alpha\beta$, and TNF effects on antiviral state and NK cell responses during murine cytomegalovirus infection. *J. Immunol. 156:4746.*
69. Gerard, C. M., N. Baudson, K. Kraemer, C. Ledent, Y. Paterson, Z. K. Pan, D. Pardoll, and C. Bruck. 2001. Recombinant HPV16 E7 protein as a model antigen to study the vaccine potential in control and E7 transgenic mice. *Clin. Cancer Res. 7:838s.*
70. Bright, R. K., M. H. Shearer, and R. C. Kennedy. 1994. Immunization of BALB/c mice with recombinant simian virus 40 large tumor antigen induces antibody-dependent cell-mediated cytotoxicity against simian virus 40-transformed cells: an antibody-based mechanism for tumor immunity. *J. Immunol. 153:2064.*
71. Guidotti, L. G., P. Borrow, A. Brown, H. McClary, R. Koch, and F. V. Chisari. 1999. Noncytopathic clearance of lymphocytic choriomeningitis virus from the hepatocyte. *J. Exp. Med. 189:1555.*
72. Guidotti, L. G., R. Rochford, J. Chung, M. Shapiro, R. Purcell, and F. V. Chisari. 1999. Viral clearance without destruction of infected cells during acute HBV infection. *Science 284:825.*
73. Liu, T., K. M. Khanna, X. Chen, D. J. Fink, and R. L. Hendricks. 2000. $CD8^+$ T cells can block herpes simplex virus type 1 (HSV-1) reactivation from latency in sensory neurons. *J. Exp. Med. 191:1459.*
74. Peng, L., J. C. Krauss, G. E. Plautz, S. Mukai, S. Shu, and P. A. Cohen. 2000. T cell-mediated tumor rejection displays diverse dependence upon perforin and IFN-γ mechanisms that cannot be predicted from in vitro T cell characteristics. *J. Immunol. 165:7116.*
75. Sparwasser, T., R. M. Vabulas, B. Villmow, G. B. Lipford, and H. Wagner. 2000. Bacterial CpG-DNA activates dendritic cells in vivo: T helper cell-independent cytotoxic T cell responses to soluble proteins. *Eur. J. Immunol. 30:3591.*

Psychosocial influences on cancer progression: alternative cellular and molecular mechanisms

Michael J. Forlenza and Andrew Baum

Considerable interest in the biobehavioural pathways linking stress and cancer as well as the identification of modifiable risk factors has increased research examining psychological adjustment, biological responses, and cancer outcomes. Although most of this work has focused on how stress affects processes such as immune surveillance that govern survival of tumors, less attention has been directed at how stress contributes to somatic mutation and genomic instability. Progress in this area may be facilitated by considering how stress affects events that modulate development and accumulation of somatic mutations in addition to those affecting survival of tumor cells. It is possible that a sharper focus on other relevant biological processes such as increases in DNA damage, alterations in DNA repair, and inhibition of apoptosis, may explain more of the variance in disease outcomes. Curr Opin Psychiatry 13:639–645.

Division of Behavioural Medicine & Oncology, University of Pittsburgh Cancer Institute, Pittsburgh, USA

Correspondence to Michael Forlenza, MS, Division of Behavioural Medicine & Oncology, University of Pittsburgh Cancer Institute, 3600 Forbes Ave, Suite 405, Pittsburgh, PA 15213, USA
Tel: (412) 647-0928; Fax: (412) 647-1936; e-mail: mjfst36@imap.pitt.edu

Current Opinion in Psychiatry 2000, 13:639–645

Abbreviations

8-OH-dG	8-hydroxy-2'-deoxyguanosine
BCC	basal cell carcinoma
ELISA	enzyme-linked immunosorbent assay
GPA	glycophorin A
HPLC	High Performance Liquid Chromatography
HPRT	hypoxanthine-guanine phosphoribosyltranferase
IL-2	interleukin-2
NCI	National Cancer Institute
NER	nucleotide excision repair
NK	natural killer
NKCA	natural killer cytotoxic activity
OFR	oxygen free radicals
POMS	profile of mood states
RBC	red blood cell
rIL-2	recombinant interleukin-2
rINF-γ	recombinant interferon gamma
SEER	surveillance, epidemiology, and end results
TAA	tumor associated antigens
TPA	12-o tetradeconoyl-phorbol-13-acetate
XP	xeroderma pigmentosum

0951-7367

Introduction

Cancer is the second leading cause of death in the United States [1]. More than 1.2 million people were diagnosed with cancer in 1998 and more than 500 000 people died of it, based on National Cancer Institute (NCI) Surveillance, Epidemiology, and End Results (SEER) data [2]. Men living in the United States have a one in two lifetime risk of developing cancer and women's lifetime risk is one in three [2]. Similarly, the estimated number of new cancer cases in member states of the European Union was more than 1.3 million and the number of deaths was about 900 000 [3]. Although cancer death rates in the US have declined nearly three percent between 1991 and 1995 [2], cancer remains a serious and stressful disease.

Considerable interest in the biobehavioural pathways linking stress and cancer as well as the identification of modifiable risk factors has increased research examining psychological adjustment, biological responses, and cancer outcomes. However, research examining the effects of psychosocial variables such as stress or depression on the etiology or progression of cancer continues to report mixed effects [4-9]. Efforts to identify specific mechanisms underlying or affecting cancer course have met with limited success. Most of this work has focused on how stress affects processes such as immune surveillance that govern survival of tumors. Less attention has been directed at how stress contributes to somatic mutation and genomic instability. Progress in this area may be facilitated by considering how stress affects events that modulate development and accumulation of somatic mutations in addition to those affecting survival of tumor cells. It is possible that a sharper focus on other relevant biological processes such as increases in DNA damage, alterations in DNA repair, and inhibition of apoptosis, may explain more of the variance in disease outcomes. This review considers a growing body of literature that bears on presumed mediators of psychosocial modulation of cancer course and research on cellular and subcellular aspects of stress.

To understand how psychosocial factors influence the etiology or progression of cancer, researchers need to examine psychosocial influences on basic mechanisms of mutagenesis and carcinogenesis. While we acknowledge the strong impact of various health-related behaviors on cancer (e.g. smoking, diet, sedentary lifestyle), review of health behaviors and their contribution to cancer are beyond the scope of this review. We begin with immune

surveillance because it has been the primary model of stress and cancer modulation over the past 10–20 years.

Immune surveillance

The concept of immune surveillance against neoplastic growth dates back to the early part of the twentieth century and is based on the idea that various components of the immune system are responsible for host defense against the emergence and growth of tumor cells [10]. The theory generally suggested that the immune system was capable of recognizing tumor cells, and initiating a specific cytotoxic response against them. Host resistance against neoplasia was thought to be T-cell dependent and since tumor cells reliably expressed recognizable tumor associated antigens (TAA), immune defenses against tumor cells should resemble responses to viral infection. The implication of this theory was that immunosuppression was associated with, and should precede, the development of tumors [10].

Although there is some evidence that is consistent with the immune surveillance hypothesis, particularly in animal models, most research in humans suggests that the hypothesis has major limitations. For example, it is not clear that all tumors express TAA or at what point in the transformation process these antigens emerge. Additionally, tumors may shed these TAA or actively suppress numerous immune cells [11]. Finally, systemic immunosuppression is not reliably related to tumor development and malignancy, especially the more common cancers of the breast, colon, and lung [7].

Because of these and other difficulties, the immune surveillance hypothesis has undergone significant revision. The focus on T-cells as primary effector cells has been de-emphasized in favor of a stronger role for natural killer (NK) cells because of their ability to non-specifically recognize and lyse tumor cells *in vitro*, especially blood-borne tumors [12]. This, together with increasingly clear evidence that stress affects NK trafficking and cytotoxic capacity independent of cancer [13], has led to the development of biobehavioural models of cancer [14-16]. These models suggest that psychosocial factors such as chronic stress, depression, or lack of social support contribute to cancer initiation or progression by suppressing NK cell numbers or lytic function. These theories further suggest that much of the variance in these relationships is modifiable and that psychosocial interventions aimed at providing education and support should reduce distress and corresponding suppression of NK activity. However, as will be discussed, evidence of restorative effects of psychosocial interventions is mixed [17••].

While there is convincing evidence for the role of NK cells in host resistance to tumors in animals, fewer studies show a clear role for NK in host resistance against tumors in humans [18]. Although NK cells can lyse allogenic tumor cell lines without prior sensitization, they are unable to lyse freshly isolated autologous tumor cells unless cultured with interleukin-2 (IL-2) [18]. Additionally, although there is evidence that NK cytotoxic activity (NKCA) is reduced in certain tumors [18], it is not known if this is the cause or the result of tumor burden. Tumors may themselves produce local suppression factors that may disrupt NK function [11].

Several correlational studies have examined the effects of psychosocial variables on NK number and function in cancer patients and data are consistent with the NK surveillance hypothesis. For example, Levy *et al.* [19] found that 51% of the variance in NKCA in breast cancer patients was accounted for by psychological adjustment, lack of social support, and fatigue. Additionally, breast cancer patients' perceptions of social support and how actively they sought social support significantly predicted NKCA [20]. Baseline NKCA predicted greater spread to axillary lymph nodes and better NKCA at follow-up predicted disease-free survival [21]. Andersen *et al.* [22] found that intrusive and avoidant thoughts about cancer negatively predicted NKCA and that intrusive thoughts negatively predicted NK response to recombinant interferon gamma (rINF-γ). Surprisingly, the majority of subjects did not show an NK response to recombinant interleukin-2 (rIL-2). Tajima *et al.* [23] report a significantly lower absolute number of NK in patients compared to controls, that NKCA was reduced in patients compared to controls, and that untreated or relapsed patients had lower NKCA than patients off treatment. These studies provide moderate but consistent evidence that psychological factors such as stress influence NK activity in cancer patients and that these alterations in NK activity are related to important disease processes.

The most compelling data concerning the role of immune surveillance in cancer patients comes from a randomized clinical trial of a six-week structured psychoeducational intervention for malignant melanoma patients [24]. Following the intervention, patients exhibited significant improvement in NKCA at six-month follow-up and higher NKCA at baseline was related to lower recurrence rates [25]. Unfortunately, these findings are not representative of the intervention literature as a whole. A recent meta-analysis reviewed evidence for psychological modulation of immune responses in humans from studies of psychosocial interventions and concluded that interventions have a relatively modest effect on immunity [17]. Moreover, the meta-analysis revealed no evidence to support the assertion that interventions can stimulate beneficial immune changes in medical populations. The authors

suggest that powerful biological forces (e.g. treatment protocols) may overwhelm immune changes induced by the intervention [17]. Additionally, it is not clear whether these changes in immune system activity are of sufficient magnitude for cancer to develop or progress [26].

DNA damage

The immune system and its supportive function can be thought of as affecting the likelihood that cells with somatic mutations survive, accumulate, and eventually induce tumor growth. However, another important level of analysis is subcellular and relates to whether stress affects the likelihood of DNA damage, somatic mutation, and genomic instability. Damage to DNA from oxygen free radicals (OFR) is perhaps the most common form of DNA damage [27] and is not only important in tumor initiation but is also prominent in all phases of tumor promotion and disease progression [28,29]. However, current biobehavioural models of cancer stress fail to account for oxidative damage as a plausible mechanism linking psychosocial variables and cancer. OFR result from exposure to pollution or ionizing radiation and are generated as by-products of inflammation and normal oxygen metabolism [29]. OFR damage DNA by attacking either its nucleotide residues or sugar backbone. OFR also damage other cellular components, such as lipids and proteins, that produce reactive intermediaries, which in turn, form mutagenic adducts with DNA [30].

Research suggests that oxidative damage to DNA (i.e. alteration of the coding sequence or functional properties of DNA) plays a role in mutagenesis and increases risk for developing cancer [28,29,31]. Research has demonstrated that unrepaired or misrepaired oxidative lesions are mutagenic and cause miscoding [32], single strand breaks, and induction of microsatellite instability [33]. The mutations induced by many of these lesions are commonly observed in mutated oncogenes and tumor suppressor genes [34••]. Oxidative lesions may also cause deletions, double strand breaks, chromosomal aberrations, micronuclei formation, damage to histones, aberrant signal transduction, and altered gene expression [35]. Additionally, oxidative lesions are mitogenic, which increases the probability of mutation through an increased number of replication cycles [31]. These observations suggest that increasing oxidative damage figures prominently in the etiology of many cancers [34••].

The reported five- to seven-fold interindividual differences in excreted oxidative damage products suggest that there may be modifiable sources of OFR [29]. Stress has been shown to damage DNA at the molecular [36] and chromosomal levels in rats [37,38] and Irie *et al.* [39] recently demonstrated that renal levels of 8-hydroxy-2′-deoxyguanosine (8-OH-dG), a common biomarker of oxidatively damaged DNA, could be classically conditioned using a conditioned taste aversion paradigm. In one of the few studies examining psychological variables and oxidative damage in humans, Irie *et al.* [40] found that levels of 8-OH-dG were negatively related to the Tension-Anxiety and Depression-Dejection scales of the Profile of Mood States (POMS) in males, but positively related to Depression-Dejection scores in women. Further, 8-OH-dG levels were increased in subjects who experienced the loss of a close family member within the previous three years when compared to those without a similar loss experience. These data suggest that oxidative damage may be related to mood and suggest that there may be sex differences in the generation of oxidative lesions. Finally, Forlenza *et al.* [41] found increased levels of DNA repair prior to exogenous damage suggesting that stress increased endogenous damage to DNA.

It is possible to directly measure oxidative lesions with a variety of assay systems in both urine and blood [42,43]. Blood measures of oxidative damage provide information on steady state levels of oxidative adducts to DNA and urine measures reflect the rate of damage [29]. Common assay techniques include High Performance Liquid Chromatography (HPLC) with electrochemical detection and enzyme-linked immunosorbent assay (ELISA) with monoclonal antibodies to oxidative lesions such as 8-hydroxyguanine. Measurement of biomarkers of oxidative damage can be a valuable tool for behavioral medicine and other biobehavioural studies of the impact of stress, adjustment, and other psychological variables in cancer onset as well as the impact of psychosocial interventions on disease progression.

DNA repair

If damage to DNA is not repaired prior to replication, resulting errors can become fixed in the genome and give rise to somatic mutations. Fortunately, mammalian cells have evolved mechanisms to recognize and repair many forms of damage to DNA. There are multiple repair pathways each specializing in the repair of a specific type of damage. For example, mismatch repair acts as a post-replication 'spell-checker' and fixes errors made by DNA polymerase during replication. Base excision repair focuses on single damaged bases and nucleotide excision repair (NER) targets a large variety of bulky lesions including pyrimidine dimers, DNA cross-links, and 6-4 photoproducts [44].

Nucleotide excision repair (NER) is a multi-step process that removes a broad array of DNA lesions including UV and chemical damage [45]. Proteins from at least 30 genes are necessary to complete the repair process, eleven of which have been cloned. Although all of the details have not yet been worked out, there are five basic

steps involved in the NER pathway: recognition of DNA alteration or damage, incision of 27–29 bp of DNA around the lesion, excision of the damaged portion, re-polymerization of the correct sequence, and finally, ligation of the DNA strands [29].

Previous studies have shown that there is a substantial amount of variability in DNA repair capacity [46]. Wei *et al.* [47] reported that the distribution of DNA repair capacity in the peripheral T-lymphocytes of their subjects was approximately normal with a five-fold variation among individuals. Given this large amount of variability, it is reasonable to examine psychosocial variables that might explain differences in rates of repair.

There is also evidence that DNA repair is associated with cancer. People with recessively-inherited DNA deficits are cancer-prone and studies suggest that unrepaired DNA damage has high carcinogenic potential [48]. For example, individuals born with xeroderma pigmentosum (XP) are extremely prone to cancerous skin lesions (carcinoma and melanoma) because they are unable to repair damage caused by exposure to UV light. Studies show that XP patients show a mutation in the genes coding for overall genomic repair and suggest that failure in overall repair is associated with cancer formation [45].

Wei *et al.*, [47] found that repair in lymphocytes was reduced in patients with basal cell carcinoma (BCC) and Grossman [49] found an age-dependent decline in DNA repair that was associated with an increase in accumulated mutations in lymphocytes. Kovacs *et al.* [50] found decreased DNA repair synthesis in the lymphocytes of women with invasive breast cancer and Pero *et al.* showed decreased repair synthesis in the mononuclear leukocytes of patients with adenomatous polyps [51] and colorectal cancer [52]. Further, Pero *et al.* [52] found that those individuals who were genetically predisposed to colorectal cancer also had decreased rates of unscheduled DNA repair synthesis compared to healthy controls.

Psychological stress has been associated with altered repair of damaged DNA in both humans [41,53,54] and rats [55]. However, the direction of the change in repair seems dependent on a number of factors such as the severity and chronicity of the stressor. For example, Kiecolt-Glaser *et al.* [53] found that the lymphocytes drawn from high-distress psychiatric inpatients exhibited poorer repair than did the lymphocytes of low-distress patients. However, Forlenza *et al.* [41], and Cohen *et al.* [54] found increases in DNA repair in lymphocytes from healthy students during a stressful exam period. It is likely that the duration and intensity of distress in these later studies were less than in the inpatient sample studied by Kiecolt-Glaser *et al.* [53]. Both Forlenza *et al.*, [41] and Cohen *et al.* [54] measured modest, transient stress in a sample of young, healthy, non-smoking, community-dwelling students while Kiecolt-Glaser *et al.* [53] measured more severe distress in psychiatric inpatients, half of whom smoked. Another important difference concerns the timing of the putative stressor. Exam related stress could be considered an acute or episodic event of a relatively fixed duration. In contrast, mental illness severe enough to warrant hospitalization is typically more chronic in nature. The differential effects of acute and chronic stress exposure on DNA repair are unknown.

Apoptosis

Apoptosis is a highly organized process of programmed cell death. Initiation of apoptosis results in the discarding of unwanted (i.e. extra), damaged, and atypical (i.e. neoplastic) cells and can be induced by various physiologic and pathologic stimuli such as UV light, ionizing radiation, dietary carcinogens, and high levels of glucocorticoids [56]. Apoptosis is an active process that is structured and sequential and can be considered an important response to extensive DNA damage [57]. It requires energy for the transcription and translation of specific genes and can be distinguished from necrosis (pathologic death of cells).

Apoptosis is of vital importance in the protection against cancer. In response to extensive DNA damage, levels of the tumor suppressor protein p53 increase, arresting the cell cycle in G1 phase and allowing relevant DNA repair mechanisms to operate. If repair is unsuccessful, p53 levels continue to increase, inducing apoptosis by several mechanisms [58]. Mutations in the p53 gene are exceedingly common and are reported to occur in 55% to 70% of human cancers [59]. Loss of functional p53 correlates with tumor aggressiveness and people with inherited defects in p53 develop cancer at a high rate [60].

Many assay systems are available for measurement of apoptosis, including gel electrophoresis and ELISA [61], flow cytometry and laser scanning cytometry [62,63], and various morphological and biochemical methods [64]. Measurement of apoptosis and related processes can be an important tool in biobehavioural studies of the impact of stress, adjustment, and other psychological variables in cancer progression.

Data examining the effects of stress on apoptosis are equivocal. Tomei *et al.* [65] reported that psychological stress associated with medical student exam stress inhibited radiation-induced apoptosis in peripheral blood lymphocytes when treated with a tumor-promoting phorbol ester (12-o tetradeconoyl-phorbol-13-acetate) (TPA). In contrast, Yin *et al.* [66] and Tarcic *et al.* [67]

showed that chronic restraint stress in rats induced apoptosis in splenocytes and thymocytes, respectively. As with the data reported for DNA repair, discrepancies are likely to be explained by the methods and model systems used.

Psychosocial alteration of apoptosis could have significant impact on tumor progression through several mechanisms. If apoptosis of damaged cells is inhibited, an important mechanism protecting against neoplasia is lost. However, if apoptosis is induced or enhanced by psychological variables, there may be significant loss of immunosurveillance (due to loss of lymphocytes). Future work needs to clarify these important issues.

Somatic mutation

As previously discussed, when somatic cells receive DNA damage and this damage is unrepaired prior to cell replication, the damage becomes fixed in that cell's genome, leading to somatic mutation. What is important to remember here is that for somatic mutation to occur, there must be failures in multiple protective systems designed to prevent the survival of the mutation. Despite these elaborate and overlapping systems of protection, mutations do occur and the accumulation of mutations in somatic cells is thought to be the molecular basis for cancer [68].

For cells to become neoplastic, specific mutations must occur in specific genetic mechanisms. The first of these mechanisms concerns mutations in putative oncogenes. These genes involve regulation of cell growth and replication. Mutational activation of these genes most often leads to overexpression, unregulated expression, or inappropriate expression of the gene product causing an uncontrolled stimulation of cell growth [69]. The second genetic mechanism of mutation in cancer involves loss or inactivation of a series of genes termed tumor suppressor genes. Both copies of these suppressor genes must be inactivated for the cell to exhibit loss of tumor suppression. Because inactivation of tumor suppression involves loss of function mutations, the spectrum of events capable of inducing these mutations is much greater than those leading to activation of oncogenes. This makes loss of tumor suppression a more common event.

Since somatic mutation is the *de facto* final common pathway to tumor initiation and progression, understanding the impact of psychosocial variables on the accumulation of somatic mutation is of great importance. Although measurement of in-vivo somatic mutation has become relatively commonplace in genetic toxicology and biodosimetry studies, quantitation of background mutation frequency in biobehavioural oncology is lacking. There are currently several reliable assay systems capable of measuring somatic mutation in various hematopoietic tissues and each system has several advantages and disadvantages [69]. For example, the glycophorin A (GPA) assay is a rapid and relatively inexpensive procedure that measures mutation in red blood cell (RBC) surface antigens resulting from in-vivo allele loss at the GPA locus. The assay is performed using immunolabelling and flow cytometric procedures on a small sample of blood and provides data on a wide range of mutation mechanisms. A major limitation of this assay is that only 50% of the population has the appropriate blood type for the assay to be performed. In contrast, the hypoxanthine-guanine phosphoribosyltranferase (HPRT) assay is a lymphocyte-based assay that is applicable to the entire population. In addition to providing quantitative data regarding mutation, this assay allows for the molecular analysis of mutated cells. However, the HPRT assay is expensive and labor intensive, making it less suitable for larger, population-based studies.

Research suggests that the mutation frequency as determined by HPRT may vary more than 10-fold in a healthy, unexposed population [70]. While some of this variance may be accounted for by genetic differences in antioxidant scavenging systems and DNA repair systems, additional variance may be explained by the influence of psychosocial variables on these processes. Although several studies have examined the effects of behavioural lifestyle factors such as smoking and diet on mutation frequency [71,72], there are currently no studies evaluating the effects of psychological variables on somatic mutation. This may prove to be an important line of research if it could be demonstrated that variables such as stress directly influence in-vivo mutational frequencies. These effects on mutation would need to be independent of their influence on health behaviors such as smoking, diet, or physical activity.

Summary

This review focused on biobehavioural pathways linking psychosocial factors with cancer and suggested promising areas of investigation for behavioural researchers interested in understanding the role of psychosocial factors in cancer etiology and progression. Research shows that there is considerable variance in the functioning of each of these pathways and preliminary evidence suggests that psychological factors may explain some of this variance. Furthermore, research suggests that people with alterations in these processes (i.e. increased DNA damage, alterations in DNA repair, failures of apoptosis) are at increased risk for cancer.

However, the reviewed research demonstrates that the effects of psychosocial factors on the mechanisms of carcinogenesis are likely to be complex. Stressors vary

Figure 1. A biobehavioural model of cancer initiation and progression

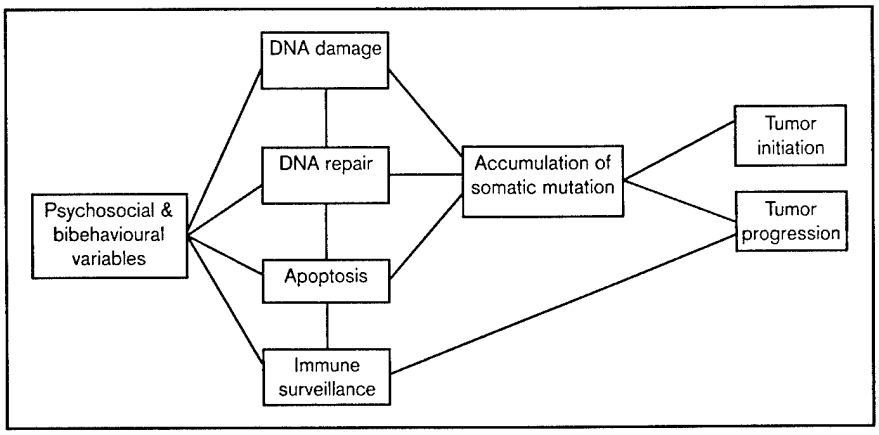

with regard to their intensity and duration and it is likely that these variables will in turn moderate the impact of stress exposure on cancer processes. Moreover, it is likely that these carcinogenic processes interact with each other. For example, if stress increases oxidative stress, antioxidant systems should protect the DNA from damage. If antioxidant systems are suppressed or overwhelmed, the ensuing damage to DNA will initiate repair mechanisms. If DNA repairs fail, apoptosis in the damaged cell begins. If apoptosis is inhibited, somatic mutations accumulate leading to tumor initiation and promotion. This leaves immune surveillance which can be inhibited by chronic stress, as the last line of defense (see Fig. 1). In this way, small perturbations in one pathway will initiate a cascade of responses.

It is clear that much work remains to be done. Because of the inherent difficulties involved in studying the influence of psychosocial variables on clinical endpoints in cancer, research may progress by focusing on processes relevant to carcinogenesis. Furthermore, it will be important to understand how various psychosocial variables interact with these processes simultaneously and how these interactions ultimately influence cancer risk.

References and recommended reading

Papers of particular interest, published within the annual period of review, have been highlighted as:

- • of special interest
- •• of outstanding interest

1 Garfinkel L. Cancer Statistics and Trends. In: Murphy GP, Lawrence W Jr, Lenhard RE Jr, (editors). American Cancer Society Textbook of Clinical Oncology. USA: American Cancer Society; 1995. Second Edition pp.1–9.

2 American Cancer Society, Inc. Cancer Facts & Figures.1998.

3 Black RJ, Bray F, Ferlay J, Parkin DM. Cancer incidence and mortality in the European Union: Cancer registry data and estimates of national incidences for 1990. Eur J Cancer 1997; 33(7):1075–1107.

4 Cassileth BR. Stress and the development of breast cancer. Cancer 1996; 77(6):1015–1016.

5 Fox BH. The role of psychological factors in cancer incidence and prognosis. Oncology 1995; 9(3):245–256.

6 Hilakivi-Clarke L, Rowland J, Clarke R, Lippman ME. Psychosocial factors in the development and progression of breast cancer. Breast Cancer Res Treat 1994; 29(2):141–160.

7 Garssen B, Goodkin K. On the role of immunological factors as mediators between psychosocial factors and cancer progression. Psychiatry Res 1999; 85:51–61.

8 McGee R, Williams S, Elwood M. Are life events related to the onset of breast cancer? Psychol Med 1996; 26(3):441–447.

9 Spiegel D, Kato PM. Psychosocial influences on cancer incidence and progression. Harvard Rev of Psychiatr 1996; 4:10–26.

10 Herberman RB. Principles of Tumor Immunology. In: Murphy GP, Lawrence W Jr, Lenhard RE Jr, (editors). American Cancer Society Textbook of Clinical Oncology. USA: American Cancer Society; 1995. Second Edition pp.1–9.

11 Somers S, Guillou PJ. Tumor cell strategies for escaping immune control: Implications for psychoimmunotherapy. In: Lewis CE, O'Sullivan C, Barraclough J, (editors). The Psychoimmunology of Cancer: Mind and body in the fight for survival. Oxford: Oxford Medical Publishing 1994. pp. 385–416.

12 Whiteside TJ, Herberman RB. The role of natural killer cells in immune surveillance of cancer. Curr Opin Immunol 1995; 7:704–710.

13 Herbert TB, Cohen S. Stress and immunity in humans: A meta-analytic review. Psychosom Med 1993; 55:364–379.

14 Levy SM, Wise BD. Psychosocial risk factors, natural immunity, and cancer progression. Curr Psychol: Res & Rev 1987; 6(3):229–243.

15 Andersen BL, Kiecolt-Glaser JK, Glaser R. A biobehavioural model of cancer stress and disease course. Am Psychol 1994; 49(5):389–404.

16 Spiegel D, Sephton SE, Terr AI, Stites DP. Effects of psychosocial treatment in prolonging cancer survival may be mediated by neuroimmune pathways. Ann Ny Acad Sci 1998; 840:674–683.

17 •• Miller GE, Cohen S. Psychological Interventions and the immune system: A meta-analytic review and critique. Health Psychol (in press).
This is an excellent quantitative review concerning the effects of psychological interventions on numerous indices of immune function.

18 Brittenden J, Heys SD, Ross J, Eremin O. Natural killer cells and cancer. Cancer 1996; 77(7):1226–1243.

19 Levy SM, Herberman RB, Maluish AM *et al.* Prognostic risk assessment in primary breast cancer by behavioural and immunological parameters. Health Psychol 1985; 4(2):99–113.

20 Levy SM, Herberman RB, Whiteside *et al.* Perceived social support and tumor estrogen/progesterone receptor status as predictors of natural killer cell activity in breast cancer patients. Psychosom Med 1990; 52(1):73–85.

21 Levy SM, Herberman RB, Lippman M *et al.* Immunological and psychological predictors of disease recurrence in patients with early-stage breast cancer. Behav Med 1991; 17(2):67–75.

22 Andersen BL, Farrar WB, Golden-Kreutz D *et al.* Stress and immune responses after surgical treatment for regional breast cancer. J Natl Cancer Inst 1998; 90(1):30–36.

23 Tajima F, Kawatani T, Endo A, Kawasaki H. Natural killer cell activity and cytokine production as prognostic factors in adult acute leukemia. Leukemia 1996; 10:478–482.

24 Fawzy FI, Kemeny ME, Fawzy NW *et al.* A structured psychiatric intervention for cancer patients: Changes over time in immunological measures. Arch Gen Psychiatry 1990; 47:729–735.

25 Fawzy FI, Fawzy NW, Hyun CS *et al.* Malignant melanoma: effects of an early structured psychiatric intervention, coping, and affective state on recurrence and survival 6 years later. Arch Gen Psychiatry 1993; 50:681–689.

26 Cohen S, Rabin BS. Psychologic Stress, immunity, and cancer. J Natl Cancer Inst 1998; 90(1):3–4.

27 Bohr V. DNA repair fine structure and its relation to genomic instability. Carcinogenesis 1995; 16(12):2885–2892.

28 Dreher D, Junod AF. Role of oxygen free radicals in cancer development. Eur J Cancer 1996; 32A(1):30–38.

29 Loft S, Poulsen HE. Cancer risk and oxidative DNA damage in man. J Mol Med 1996; 74:297–312.

30 Floyd RA. The role of 8-hydroxyguanine in carcinogenesis. Carcinogenesis 1990; 11(9): 1447–1450.

31 Ames BN, Shigenaga MK, Gold LS. DNA lesions, inducible DNA repair, and cell division: Three key factors in mutagenesis and carcinogenesis. Environ Health Perspect 1993; 101(5):35–44.

32 Cheng KC, Cahill DS, Kasai H *et al.* 8-hydroxyguanine, an abundant form of oxidative DNA damage, cause G—T and A—C substitutions. J Biol Chem 1991; 267(1):166–172.

33 Jackson AL, Chen R., Loeb LA. Induction of microsatellite instability of oxidative DNA damage. Proc Natl Acad Sci USA 1998; 95:12468–12473.

34 •• Marnett LJ. Oxyradicals and DNA damage. Carcinogenesis 2000; 21(3):361–370.

In-depth description of the role of oxygen free radicals in DNA damage.

35 Simic MG. DNA markers of oxidative processes in vivo: Relevance to carcinogenesis and anticarcinogenesis. Cancer Res 1994 (Suppl.) 54:1918s–1923s.

36 Adachi S, Kawamura K, Takemoto K. Oxidative damage of nuclear DNA in liver of rats exposed to psychological stress. Cancer Res 1993; 53:4153–4155.

37 Fischman H. Sister chromatid exchanges induced by behavioural stress. Loss, Grief, and Care 1989; 3(34):203–213.

38 Fischman H, Pero RW, Kelly DD. Psychogenic stress induces chromosomal and DNA damage. Int J Neurosci 1996; 84:219–227.

39 Irie M, Asami S, Nagata S *et al.* Classical conditioning of oxidative DNA damage in rats. Neuroscience Letters 2000; 288:13–16.

40 Irie M, Asami S, Nagata S *et al.* Psychological mediation of a type of oxidative damage, 8-hydroxydeoxyguanosine, in peripheral blood lymphocytes of non-smoking and non-drinking workers. (under review).

41 Forlenza MJ, Latimer JJ, Baum A. The effects of stress on DNA repair capacity. Psychol Health. (in press).

42 Wiseman H, Kaur H, Halliwell B. DNA damage and cancer: Measurement and mechanism. Cancer Lett 1995; 93:113–120.

43 Shigenaga MK, Ames BN. Assays for 8-hydroxy-2'deoxyguanosine: A biomarker of in vivo oxidative DNA damage. Free Radic Biol Med 1991; 10:211–216.

44 Snow ET. The role of DNA repair in development. Reprod Toxicol 1997; 11(23):353–365.

45 Bootsma D, Hoeijmakers JHJ. DNA repair: Engagement with transcription. (news: comment). Nature 1993; 363:114–115.

46 Setlow RB. Variation in DNA repair among humans. In: Harris C, Autrup H, (editors). Human Carcinogenesis. New York: Academic Press; 1983. pp. 231–244.

47 Wei Q, Matanoski GM, Farmer ER *et al.* DNA repair related to multiple skin cancers and drug use. Cancer Res 1994; 54:437–440.

48 Setlow RB. Repair deficient human disorders and cancer. Nature 1978; 271:713–717.

49 Grossman L. Epidemiology of ultraviolet-DNA repair capacity and human cancer. Environ Health Perspect 1997; 105(4):927–930.

50 Kovacs E, Stucki D, Weber W, Muller HJ. Impaired DNA repair synthesis in lymphocytes of breast cancer patients. Eur J Cancer Clin Oncol 1986; 22:863–869.

51 Pero RW, Miller DG, Lipkin M *et al.* Reduced capacity for DNA synthesis in patients with or genetically predisposed to colorectal cancer. J Natl Cancer Inst 1983; 70(5):867–875.

52 Pero RW, Ritchie M, Winawer SJ *et al.* Unscheduled DNA synthesis in mononuclear leukocytes from patients with colorectal polyps. Cancer Res 1985; 45:3388–3391.

53 Kiecolt-Glaser JK, Stephens RE, Lipetz PD *et al.* Distress and DNA repair in human lymphocytes. J Behav Med 1985; 8(4):311–320.

54 Cohen L, Marshall GD, Cheng L *et al.* DNA repair capacity in healthy medical students during and after exam stress. Behav Med (in press)

55 Glaser R, Thorn BE, Tarr KL *et al.* Effects of stress on methyltransferase synthesis: An important DNA repair enzyme. Health Psychol 1985; 4(5):403–412.

56 Dixon S, Soriano B, Lush R. *et al.* Apoptosis: Its role in the development of malignancies and its potential as a novel therapeutic agent. Ann Pharmacother 1997; 31:76–82.

57 Evan G, Littlewood T. A matter of life and cell death. Science 1998; 281(5381):1317–1322.

58 Hetts SW. To die or not to die: An overview of apoptosis and its role in disease. J Am Med Assoc 1998; 279(4):300–307.

59 Levine AJ. The cellular gatekeeper for growth and division. Cell 1997; 88:323-331. p53

60 Fisher DE. Apoptosis in cancer therapy: crossing the threshold. Cell 1994; 78:539–542.

61 Allen RT, Hunter WJ 3rd, Agrawal DK. Morphological and biochemical characterization and analysis of apoptosis. J Pharmacol Toxicol Methods 1997; 37(4):215–228.

62 Gorczyca W. Cytometric analyses to distinguish cell death processes. Endocrine-Related Cancer 1999; 6(1):17–19.

63 Bedner E, Li X, Gorczyca W *et al.* Analysis of Apoptosis by laser scanning cytometry. Cytometry 1999; 35(3):181–195.

64 Loo DT, Rillema JR. Measurement of cell death. Methods Cell Biol 1998; 57:251–64.

65 Tomei LD, Kiecolt-Glaser JK, Kennedy S, Glaser R. Psychological stress and phorbol ester inhibition of radiation-induced apoptosis in human peripheral blood leukocytes. Psychiatric Res 1990; 33:59–71.

66 Yin D, Tuthill D, Mufson RA., Shi Yufang. Chronic restraint stress promotes lymphocyte apoptosis by modulating CD95 expression. J Exp Med 2000; 191(8):1423–1428.

67 Tarcic N, Ovadia H, Weiss D, Weidenfeld J. Restraint stress-induced thymic involution and cell apoptosis are dependent on endogenous glucocorticoids. J Neuroimmunol 1998; 82(1):40–46.

68 Vogelstein B, Kinzler K. The multistep nature of cancer. Trends Genet 1993; 9(4):138–141.

69 Grant SG, Jensen RH. Use of hematopoietic cells and markers for the detection and quantitation of human in vivo somatic mutation. In: Garratty G, (editor). Immunobiology of Transfusion Medicine. Marcel Dekker: New York; 1993. pp. 299-323.

70 Podlutsky A, Hou S, Nyberg F *et al.* Influence of smoking and donor age on the spectrum of in vivo mutation at the HPRT-locus in T lymphocytes of healthy adults. Mutat Res 1999; 431:325–339.

71 Curry J, Karnaoukhova L, Guenette GC, Glickman BW. Influence of sex, smoking, and age on HPRT mutation frequencies and spectra. Genetics 1999; 152:1065–1077.

72 Barnett YA, Warnock CA, Gillespie ES *et al.* Effect of dietary intake and lifestyle factors on in vivo mutant frequency at the HPRT gene locus in healthy subjects. Mutat Res 1999; 431:305–315.

Correspondence

Aging, Immunity, and Cancer

To the Editor: Understanding and clarifying relationships among aging, immune senescence, and cancer are important for researchers interested in cancer prevention and control, especially as our population ages. The recent review by Burns and Leventhal[1] is a step in the right direction. However, there seem to be a number of conceptual issues related to immune surveillance and immunosenescence that need clarification, particularly with regard to the emergence and development of cancer. Further, behavioral variables that may confound the correlations between aging and cancer are not considered as alternative explanations. There are other alternative perspectives on the role of immune surveillance against neoplasia as well as other possible mechanisms underlying the associations between aging and cancer.

As correctly asserted by Burns and Leventhal, tumors arise from the clonal expansion of cells that have accumulated numerous somatic mutations in important regulatory genes. Subsequent to these mutations, the cells acquire behaviors that render them independent of stimulatory growth factors and insensitive to growth inhibitory signals.[2] Additionally, they may acquire other characteristics such as the capacity to evade apoptosis, to initiate and sustain the process of angiogenesis, to replicate without limit, and to invade tissue and metastasis.[2] Importantly, mutations may occur in any order, and mutated cells may or may not progress to a metastatic phenotype. All of these processes are internal to the cell nucleus, and it is currently unclear how or when components of the immune system might recognize these processes.

Although there is evidence that is consistent with the immune surveillance hypothesis, primarily in animal models, there are no unambiguous data suggesting that immune surveillance is a meaningful mechanism in the protection of humans from spontaneous neoplastic disease. The theory of immune surveillance assumes tumors express specific tumor-associated antigens (TAAs), that the TAAs are recognizable by components of the immune system, and that the TAAs stimulate an immune response. Expression of TAAs is assumed to reflect processes of somatic mutation and therefore identify self-cells as altered. However, it is not clear that all tumors reliably express TAAs or at what point in the transformation process these antigens emerge. Additionally, tumors show significant heterogeneity with regard to expressed antigens, and each tumor will express unique antigens that are different from other identically induced tumors.[3] Tumor cells do not necessarily illicit an immune response.[4] Further, even if transformed cells express TAAs, the mechanisms by which the immune system (eg, NK cells) might recognize them are currently unknown. Finally, tumors may escape a fully functioning immune system through several mechanisms such as downregulation of MHC-1 expression, suppression of immune response by tumor-secreted products, and induction of suppressor T cells, among others.[3] Based on these facts, it is premature to postulate that age-related immunosenescence leads to cancer.

The underlying model assumed by Burns and Leventhal is mediational; that is, the effects of aging on cancer incidence or progression are mediated through immunosenescence. This suggests that tumor survival and metastases result in older people from age-related failures of the immune system to recognize or adequately control tumor cells. For mediational models to be valid, there are several relationships that must hold true. First, aging should be reliably associated with declines in measures of immune function. It seems clear from the reviewed research that there is likely a decline in both enumerative and functional measures of immunity in older people. However, many host-related factors other than aging (eg, important health-related behaviors such as smoking, excessive alcohol consumption, lack of physical activity and poor fitness levels, sleep disturbance, and diet) can influence measures of immunity in older individuals.[5] Many medications commonly taken by older people may also interact with components of the immune system, and psychological factors such as stress, anxiety, and depression have been shown to reliably alter immune measures.[6] While these relationships hold true for people of all ages, older people may be subject to differential exposure. Unless these factors are controlled, the relationship between aging and immune senescence in humans will not be clear.

There must also be clear associations between measures of immunity and cancer. Examining evidence from individuals with systemic immunodeficiency syndromes or who are pharmacologically immunosuppressed may prove illustrative. Systemic immunosuppression is not reliably related to tumor development and malignancy, especially the more common cancers of the breast, colon, and lung.[7] While people with advanced HIV disease suffer from the emergence of malignancies, they rarely develop common cancers of the lung, breast, prostate, or colon. Rather, they develop Kaposi's sarcoma, a defining feature of clinical AIDS rarely diagnosed in non-AIDS populations. Cancer incidence in transplant patients who are pharmacologically immunosuppressed ranges from 4% to 18% with an average of only 6%.[8] Further, these malignancies are predominantly leukemias and lymphomas, that is, cancers of the immune system itself. These likely result from ingestion of immunosuppressive agents that are themselves mutagenic. Finally, a common feature of these cancers is their association with specific viral infections such as human herpes virus.[9] While it is likely that the immune system recognizes and combats tumors of viral origin, it is probable

that this results from recognition of virally infected cells rather than tumor cells per se. These data argue against a significant role for the immune system in the emergence of the more common cancers.

Since somatic mutation is the de facto final common pathway to tumor initiation and progression, it is possible that a sharper focus on other relevant biological processes involved in carcinogenesis, such as alterations in DNA damage and repair, may explain more of the variance in accumulation of somatic mutation and disease outcomes.[10] For example, data suggest that there is an age-related decline in repair of damaged DNA and that this decline is related to an increase in the accumulation of somatic mutation.[11,12] Additionally, the declining fidelity of DNA repair with age may underlie both cancer and immunosenescence.[13] This seems a promising area of research that will potentially explain the mechanisms whereby aging is related to cancer.

Michael J. Forlenza, MS
Behavioral Medicine and Oncology
University of Pittsburgh Cancer Institute

References

1. Burns EA, Leventhal EA. Aging, immunity, and cancer. *Cancer Control.* 2000;7;513-522.
2. Hanahan D, Weinberg RA. The hallmarks of cancer. *Cell.* 2000;100:57-70.
3. Shu S, Plautz GE, Krauss JC, et al. Tumor immunology. *JAMA.* 1997;278:1972-1981.
4. Hermans IF, Daish A, Yang J, et al. Antigen expressed on tumor cells fails to elicit an immune response, even in the presence of increased numbers of tumor-specific cytotoxic T lymphocytes. *Cancer Res.* 1998;57:3909-3917.
5. Ader R, Felton DL, Cohen N, eds. *Psychoneuroimmunology.* San Diego, Calif: Academic Press; 2001.
6. Cohen S, Herbert T. Health psychology: psychological factors and physical disease from the perspective of human psychoneuroimmunology. *Annu Rev Psychol.* 1997;47:113-142.
7. Garssen B, Goodkin K. On the role of immunological factors as mediators between psychosocial factors and cancer progression. *Psychiatry Res.* 1999;85;51-61.
8. Penn I. Neoplastic complications of transplantation. *Semin Respir Infect.* 1993; 8:233-239.
9. Beral V, Newton R. Overview of the epidemiology of immunodeficiency-associated cancers. *J Natl Cancer Inst Monogr.* 1998;23:1-6.
10. Forlenza MJ, Baum A. Psychosocial influences on cancer progression: alternative cellular and molecular mechanisms. *Curr Opin Psychiatry.* 2000;13:639-645.
11. Grossman L. Epidemiology of ultraviolet-DNA repair capacity and human cancer. *Environ Health Perspect.* 1997;105 (suppl 4);927-930.
12. Barnett YA, King CM. An investigation of antioxidant status, DNA repair capacity and mutation as a function of age in humans. *Mutat Res.* 1995;338:115-128.
13. Gennery AR, Cant AJ, Jeggo PA. Immunodeficiency associated with DNA repair defects. *Clin Exp Immunol.* 2000;121:1-7.

In Reply: Michael Forlenza's letter raises two issues: one targeting our proposal that immunosenescence is a possible pathway for the relationship of age and cancer, and the second that immune dysfunction is related to cancer. We will respond first to the two questions he raised regarding the first of these issues, ie, that immunosenescence is a pathway for cancer. First, he indicates that aging must be reliably associated with a decline in immune function for this hypothesis to hold. Second, assuming that immune function declines with age, as Mr Forlenza appears to accept, we cannot assume it is responsible for the age-related increase in cancers unless we can rule out alternative causes of immune decline that are associated with aging. As examples, he includes health behaviors (eg, smoking, excessive alcohol consumption, and lack of physical activity), psychological factors (eg, as stress, anxiety, and depression), and medication for treating other noncancer, age-related conditions. All of these factors can reduce immune surveillance and may be responsible for the increase in cancer with advancing age. At least two points can be made about these suggestions. While several of these factors (eg, smoking) are implicated in cancer causation, reviews of the literature suggest that many of these risky behaviors decline with advancing age (eg, smoking), and many health-improving behaviors increase with age; exercise is a critical exception to the latter. It is also widely reported that psychological distress declines with advancing age. For example, the percentage of major depressive disorders declines to less than 1% of the older population in community-based studies.[1] Thus, though we agree with Mr Forlenza on the importance of statistical controls for such factors, we suggest that the evidence is not overly supportive for these suggested alternatives.

The second — and more important — issue is whether these health risk and health promotion behaviors should be seen as "alternatives" to the hypothesis that immunosenescence is linked to aging and therefore to declines in surveillance for cancer, or whether these factors should be considered as links between age and immunosenescence. As we have suggested elsewhere, there are good reasons not to treat age as a "causal" variable; it is the variables and processes linked to age that have causal status.[2] Time (ie, age) is a marker of the *opportunity* for both harmful and helpful processes to influence health, cognition, affective status, physical performance, economic status, and social relationships. The hypothesis that age is a marker for immunosenescence and therefore declines in surveillance for cancer opens the door for examining the processes affecting immune decline on the one hand and those linking this decline to cancer on the other.

The second issue concerns the link of immune competence to cancer. In

the first of his three points, he states "...there is no unambiguous data suggesting that immune surveillance is a meaningful mechanism in the protection of humans from spontaneous neoplastic disease." He cites several findings supporting this ambiguity, such as the difficulty of immune recognition of heterogeneous antigens expressed by cancer cells, that some tumor cells do not express antigens and therefore fail to elicit an immune response, and indicates that the mechanisms by which NK cells recognize tumor associated antigens is unknown. His second similar point concerns the rarity of com mon cancers of the lung, breast, prostate, etc, in pharmacologically immunosuppressed persons and in persons immunosuppressed from advanced AIDS. The tumors seen in these cases are of the immune system itself and tumors of viral origin. Finally, he reviews what is likely the complex life history of a cancer from somatic mutations through the production of growth factors, the evasion of apoptosis and angiogenesis, to metastasis, and he suggests there is little evidence that the immune system can recognize or modulate the various regulatory failures that take place in this process. Mr Forlenza's point is that investigators should look elsewhere to account for the correlation of age with cancer. Specifically, age-related alterations in DNA damage and repair may account for both cancer and declines in immune competence.

Although Mr Forlenza's hypothesis is indeed interesting, it does not preclude the role of immune surveillance in the control of some cancers. It appears that the vast majority of cancer- related mutations are environmentally induced, and some (but not all) by agents that the immune system is designed to detect. Perhaps additional scrutiny should be given to detectable antecedents in tumors other than Kaposi's sarcoma. Given that animal studies find that immune enhancement slows or destroys tumors while suppression encourages proliferation and death, there may be good reason to examine which types of cancer are associated with immunosenescence and which are not and to ask whether the latter type are cancers that evade immune detection throughout the life span while the former do not.

In summary, Mr Forlenza raises interesting questions that may clarify the nature of the relationship between age-related immune decline and cancers. Much work will be needed to determine whether these pathways will provide productive lines for research. Though we find this second set of issues interesting, we feel it necessary to raise a cautionary note. Specifically, it is tempting to argue that the accrual of DNA damage and incomplete repair are the answers to the aging-cancer issue and occur independently of immune function. This is a reductionist view that downplays the role of the vast number of exogenous viral and chemical events that do indeed lead to DNA damage but also trigger immune mechanisms of defense. This includes the factors identified in the first issue. Some exogenous agents causing DNA damage may leave markers for immune attack, while others may not. If so, it will be the age-related increases in those selected tumors that will be causally linked to immunosenescence.

Edith A. Burns, MD
Section of Geriatrics
Department of Medicine
Medical College of Wisconsin

References

1. Lebowitz BD, Pearson JL, Schneider LS, et al. Diagnosis and treatment of depression in late life: Consensus statement update. *JAMA.* 1997;278:1186-1190.
2. Leventhal H, Leventhal EA, Diefenbach M, et al. Illness, stress and differential emotions over the lifespan. *Annu Rev Gerontol.* 1997;17:138-184.

Requirements for Letters

We encourage comments from readers on topics published in *Cancer Control.* Letters are published at the discrition of the editor and may be edited for space. Signed statements of authorship criteria and and responsibility, financial disclosure, copyright transfer, and acknowledgment are required for publication. Mail letters to Editor, *Cancer Control* Journal of the Moffitt Cancer Center, 12902 Magnolia Drive, Tampa, FL 33612; fax to (813) 903-4950; or e-mail to ccjournal@moffitt.usf.edu.